CENTRAL RESEARCH LIBRARY
DOCUMENT COLLECTION

[redacted]

[redacted]

MARTIN MARIETTA ENERGY SYSTEMS LIBRARIES
3 4456 0349526 0

ORNL-1554
Progress
8A

DECLASSIFIED
CLASSIFICATION CHANGED TO:
BY AUTHORITY OF: TID-1149
BY: Va Burnette 10/28/57

LABORATORY RECORDS
1954

HOMOGENEOUS REACTOR PROJECT

QUARTERLY PROGRESS REPORT

FOR PERIOD ENDING MARCH 31, 1953

CENTRAL RESEARCH LIBRARY
DOCUMENT COLLECTION
LIBRARY LOAN COPY
DO NOT TRANSFER TO ANOTHER PERSON
If you wish someone else to see this document, send in name with document and the library will arrange a loan.

OAK RIDGE NATIONAL LABORATORY
OPERATED BY
CARBIDE AND CARBON CHEMICALS COMPANY
A DIVISION OF UNION CARBIDE AND CARBON CORPORATION
UCC
POST OFFICE BOX P
OAK RIDGE, TENNESSEE

[redacted]

[redacted]

[redacted]

ORNL-1554

This document consists of 148 pages.
Copy 8 of 207 copies. Series A.

Contract No. W-7405-eng-26

HOMOGENEOUS REACTOR PROJECT
QUARTERLY PROGRESS REPORT
For Period Ending March 31, 1953

Project Director - J. A. Swartout
Engineering - C. E. Winters
Chemistry - S. C. Lind, C. H. Secoy
Corrosion - E. G. Bohlmann
Chemical Technology - F. L. Culler, F. R. Bruce
Compiled by W. E. Thompson

DATE ISSUED

JUN 25 1953

OAK RIDGE NATIONAL LABORATORY
Operated by
CARBIDE AND CARBON CHEMICALS COMPANY
A Division of Union Carbide and Carbon Corporation
Post Office Box P
Oak Ridge, Tennessee

[redacted]

MARTIN MARIETTA ENERGY SYSTEMS LIBRARIES
3 4456 0349526 0

[redacted]

INTERNAL DISTRIBUTION

1. C. Center
2. Bio y Library
3. Heal Physics Library
4. Metal y Library
5-6. Reactor perimental Engine g Library
7-8. Central R arch Library
9-18. Central Fil
19. R. E. Aven
20. S. E. Beall
21. W. B. Berggren
22. E. P. Blizard
23. E. G. Bohlmann
24. G. E. Boyd
25. W. M. Breazeale (Con tant)
26. R. C. Briant
27. R. B. Briggs
28. F. R. Bruce
29. A. D. Callihan
30. D. W. Cardwell
31. G. H. Cartledge
32. G. H. Clewett
33. T. E. Cole
34. D. D. Cowen
35. F. L. Culler
36. J. S. Culver
37. L. B. Emlet (Y-12)
38. J. L. English
39. D. E. Ferguson
40. W. R. Gall
41. J. P. Gill
42. R. J. Goldste
43. C. B. Grahar
44. J. C. Grie
45. W. D. Har
46. C. S. Ha ill
47. P. N. benreich
48. C. G. eisig
49. A. laender
50. A. S. House der
51. W. B. Hume (K-25)
52. G. R. Je ns (C&CCC, South Charle on)
53. G. H. nks
54. C. P. Keim
55. M. Kelley
56. E. King
57. A. S. Kitzes
58. E. Larson
59. S. C. Lind
60. R. S. Livingston
61. R. N. Lyon
62. W. L. Marshall
63. H. F. McDuffie
64. J. R. McWherter
65. E. C. Miller
66. K. Z. Morgan
67. E. J. Murphy
68. L. R. Quarles
69. P. M. Reyling
70. W. L. Ross
71. J. P. Sanders
72. H. C. Savage
73. C. H. Secoy
74. C. L. Segaser
75. E. D. Shipley
76. A. H. Snell
77. Spiewak
78. D. Susano
79. J. Swartout
80. E. Taylor
81. W. E. hompson
82. M. Tob s
83. S. Visn
84. W. P. Wa r
85. A. M. Wei rg
86. T. A. Welto
87. E. P. Wigner (Consultant)

[redacted]

[redacted]

[redacted]

88. C. E. Winters
89. F. C. VonderLage
[illegible]. F. C. Zapp
91. P. C. Zmola
92. G. C. Williams
[illegible]. J. C. Wilson

EXTERNAL DISTRIBUTI

94. A Plant Representative, Burbank
95. Al lant Representative, Seattle
96. ANP roject Office, Fort Worth
97-107. Argo National Laboratory
108. Armed rces Special Weapons P ject (Sandia)
109-113. Atomic rgy Commission, Was gton
114. Bechtel poration
115. Battelle orial Institute
116-118. Brookhaven tional Labora y
119. Bureau of Sh
120-121. California Re rch and elopment Company
122-127. Carbide and Ca n Chem ls Company (Y-12 Plant)
128. Chicago Patent up
129. Chief of Naval R ar
130. Commonwealth Edis pany
131. Department of the - Op-362
132. Detroit Edison Comp
133-136. duPont Company, Au
137. duPont Company, Wi in n
138. Foster Wheeler Co orat n
139-141. General Electric ompany NPP)
142-145. General Electri ompany, chland
146. Hanford Operati s Office
147-154. Idaho Operatio Office (1 y to Phillips Petroleum Company)
155. Iowa State Co ege
156-159. Knolls Atomic ower Laboratory
160-161. Los Alamos S entific Laborator
162. Massachuset Institute of Techn gy (Kaufmann)
163. Monsanto C mical Company
164. Mound Lab tory
165. National visory Committee for Aero tics, Cleveland
166. National dvisory Committee for Aeron ics, Washington
167. Naval R earch Laboratory
168-169. New Yo Operations Office
170-171. North erican Aviation, Inc.
172. Nucle Development Associates, Inc.
173. Pate Branch, Washington

[redacted]

[redacted]

[redacted]

[redacted]

174. Pi[illegible]r Service and Eng[illegible]ring Company
175. Powerp[illegible] Laborator[illegible]ADC)
176. Rand Corp[illegible]ion
177. San Francisco [illegible]tions Office
178. Savannah Rive[illegible]tions Office, Augusta
179. USAF Reside[illegible] East[illegible]tford
180. U. S. Nav[illegible]adiologic[illegible]efense Laboratory
181-182. Univers[illegible] of California [illegible]tion Laboratory, Berkeley
183-184. Unive[illegible]ty of California Radi[illegible]n Laboratory, Livermore
185. Vit[illegible] Corporation of America
186. W[illegible]er Kidde Nuclear Laboratories, [illegible]
187-192. [illegible]stinghouse Electric Corporation
193-207. [illegible]echnical Information Service, Oak Ridge

[redacted]

[redacted]

Reports pr[illegible]ously issued in [illegible]is series are as follows:

ORNL-527	[illegible]Date Issu[illegible], December 28, 1949
ORNL-630	[illegible]iod E[illegible]ing February 28, 1950
ORNL-730	F[illegible]ibi[illegible]ty Report - Date Issued, July 6, 1950
ORNL-826	Per[illegible]nding August 31, 1950
ORNL-925	Peri[illegible]nding November 30, 1950
ORNL-990	Peri[illegible]ing February 28, 1951
ORNL-1057	Pe[illegible]d En[illegible]g May 15, 1951
ORNL-1121	Pe[illegible]od Endi[illegible]August 15, 1951
ORNL-1221	P[illegible]iod Ending [illegible]ember 15, 1951
ORNL-1280	[illegible]eriod Ending M[illegible] 15, 1952
ORNL-1318	[illegible]eriod Ending Jul[illegible] 1952
ORNL-1424	Period Ending Octob[illegible], 1952
ORNL-1478	Period Ending January [illegible] 1953

[redacted]

[redacted]

[redacted]

[redacted]

SUMMARY

PART I
HOMOGENEOUS REACTOR EXPERIMENT

Reactor operation was resumed in February, and on February 24 a successful run was made at design conditions of power (1000 kw), temperature (230°C), and pressure (1000 psi). With the completion of this run, the original objectives for building the HRE were successfully fulfilled. Reactor stability and response to reactivity adjustments were excellent. Decomposition gas ($2H_2 + O_2$) at the 1000-kw level was measured as approximately 10 scfm, which corresponds to a *G* value of 1.4. The reappearance of chloride during the power run and an apparent increase in corrosion rate made it necessary to reprocess the fuel charge to remove the chloride contaminant by precipitation as silver chloride.

A spare electric boiler was installed for pressurization of the fuel, and the control circuits were modified after a review of the operational safety of the reactor. Operation was resumed at the end of the quarter.

PART II
BOILING REACTOR STUDIES

Graphs have been developed to permit rapid estimation of the plutonium production rates and the conditions required for criticality in single-region homogeneous boiling reactors. The UO_2SO_4-D_2O solution system and the UO_3-D_2O slurry system are presented in separate sets of curves.

An apparatus has been completed for measuring the effect of supersaturation with hydrogen on the nucleation of bubbles by fission fragments in superheated water. Design has been completed for the equipment for determining the minimum oxygen requirement for stabilization of the UO_2SO_4-H_2O-stainless steel system at temperatures of 250°C and below.

Electrically heated volume-boiling experiments in a 6-in.-square system have been conducted. In these experiments, depths of up to 3 ft and specific powers of up to 12 kw/liter were used. The results appear to corroborate a previously derived relationship between specific power and solution density.

A 6-ft tank has been erected for the study of vapor release from larger systems. In this tank, air is bubbled through the liquid to simulate boiling. In preliminary tests, density decreases up to 0.3 have been obtained. The Babcock and Wilcox Co. has been approached for assistance in developing vapor release devices.

PART III
GENERAL HOMOGENEOUS REACTOR STUDIES

Intermediate-Scale Homogeneous Reactor Design

The Intermediate-Scale Homogeneous Reactor is conceived of as a 50-megawatt, two-region converter. Uranyl sulfate solution containing approximately 5 g of uranium per liter of D_2O solution is pumped through the core. Surrounding the core is a blanket of thorium oxide slurry or thorium oxide pellets in D_2O. The core is 4 ft in diameter, and it is separated from the blanket by

[redacted]

[redacted]

a 1/8- to 1/4-in.-thick stainless steel shell. The blanket is 2 ft thick, and it is contained in an 8-ft-dia pressure vessel. Both the core and the blanket operate at a pressure of 1000 psia and a temperature of 250°C.

The present concept of the ISHR was described in some detail in the previous quarterly report; design data and a simplified flow sheet were presented. Flow sheet and component design studies are in progress in an effort to refine the design. Many of these studies are not sufficiently advanced to be reported at this time; so the design remains essentially as described previously. Results of the more advanced studies are reported.

Engineering Development

A pear-shaped, slug flow type of core has been selected for ISHR because of relative ease of fabrication, favorable flow distribution, and low fluid pressure losses. Small-scale tests are essentially complete and full-scale tests are planned.

The installation of an 8-ft, rotational flow type of core in the 48,000-gpm water-circulating facility is essentially complete. A limited number of tests will be made to confirm the predicted pressure loss in this core before a full-scale, slug-flow, ISHR core is installed in the circulating system.

Small-scale tests of gas separators that use 70°F water have shown the following: (1) either vanes or a volute may be used to establish a stable vortex in a pipe, and either may be used to recover a reasonable fraction of the rotational energy at the outlet; (2) pressure losses in these systems are relatively low; (3) gas separation is adequate if a small vortex is used, and efficient separation is difficult to attain if a large vortex is used. Further developmental work is being done that will lead to the operation of a full-scale experiment.

Preliminary operation of the small-scale, catalytic-recombiner testing facility, at low and high pressures, has resulted in confirmation of previous data and an indication of increased reactivity at elevated pressures. Further tests will be conducted to investigate alternate recombiners and to study the effects of pressure, gas concentration, deuterium vs. hydrogen, iodine, and traces of uranyl sulfate. Sufficient information has been accumulated to permit the design of a "packed-bed" recombiner, and there is considerable assurance that operation will be successful.

A gas circulator which utilizes a special pump impeller and a water-lubricated canned-rotor motor appears to be feasible for use in the recombiner system. It can be designed and fabricated by manufacturers who are now supplying canned-rotor pumps.

Fatigue tests and stress analysis of a pulsafeeder pump diaphragm indicate, tentatively, that the diaphragms will operate indefinitely if no dirt is allowed to enter the diaphragm chamber. Further stress and metallurgical analyses are needed before this indication can be considered as conclusive.

A Stellite piston and cylinder pump was tested in low-temperature, low-pressure fuel, and the results were favorable. If a satisfactory seal can

[redacted]

[redacted]

be developed for the drive shaft of this pump, it will be a promising alternate for the pulsafeeder pump.

Discussion of tentative ORNL heat exchanger designs with prospective manufacturers has emphasized a number of problems which must be solved. No insurmountable problems are evident.

The installation of a 4000-gpm stainless steel loop has been started, and a completion date of August 1 has been predicted.

Completion of the fabrication, in ORNL shops, of two small pumps is expected March 23, 1953. Delivery of five small pumps, which were ordered from Allis-Chalmers, is expected to start in June 1953.

A drawing of the proposed in-pile loop, which utilizes a copper catalyst, is presented. Completion of development of the first loop is anticipated in August 1953.

A UO_3 slurry has been circulated at room temperature through a simulated "let-down" valve and exchanger. Some settling difficulties caused by inadequate circulation were evident in a simulated dump tank. Further developmental work has been deferred because of the urgency of other work.

Corrosion

A loop which operated approximately 2100 hr at 250°C with uranyl sulfate solution containing 300 g of uranium per liter has been sectioned. The straight sections of pipe were in good condition, and there was no pitting. The areas of localized attack were confined to regions of high turbulence.

A loop designed to test the effect on corrosion of gas bubbles in the solution and an all-titanium loop have been completed and put into operation.

No precipitation of UO_3 from dilute uranyl sulfate solutions (5 to 15 g of uranium per liter) at 250°C has been observed when 25 eq. % excess sulfuric acid is present. The added sulfuric acid does not materially increase corrosion at concentration levels of 5 and 15 g of uranium per liter in the case of sulfate, but it substantially increases the corrosion at a uranyl sulfate concentration level of 40 g of uranium per liter. Similar results have been obtained with the addition of HF to UO_2F_2 solutions containing 5 g of uranium per liter at 250°C; higher-concentration solutions will also be investigated.

Previously observed hydrolytic precipitation of appreciable percentages of $CuSO_4$ in UO_2SO_4 solutions has been confirmed. Again, the addition of excess sulfuric acid prevented such precipitation.

Additional results on pin and coupon specimens under a variety of conditions are summarized. Tentative explanations for some of the anomalous results previously obtained are discussed, but it is obvious that some factors are still uncontrolled.

Some thorium dioxide pellets were exposed to a uranyl sulfate solution (5 g of uranium per liter) that was at 250°C and flowing at about 3 fps; no serious attack occurred.

Static test results on corrosion of synthetic gems and spinels, as well as results on crevice and stress corrosion of type 347 stainless steel, are reported. No stress corrosion was obtained, but definite signs of crevice corrosion were observed under some conditions. Tests on titanium in

[redacted]

[redacted]

uranyl sulfate solutions at 95°C indicated the absence of stress and crevice corrosion.

Design and planning for an in-pile loop have continued. Construction of mockups of some of the loop components for out-of-pile tests has been started.

Metallurgy

Several groups of corrosion test pins have been prepared for the dynamic corrosion loop testing program and are now being tested. The pins include a wide variety of base metals and were prepared by various metallurgical techniques, including heat treating, surface conditioning, mechanical working, and joining.

In the experimental welding of heavy plates of stainless and other steels, sound crack-free welds have been produced by using a combination of heliarc welding for the initial passes and coated electrode welding for the filler passes. Samples of the welds and base metal are now being subjected to physical and corrosion tests. This work will continue, and a larger variety of base metals will be tested.

The investigation of the properties of titanium that are pertinent to homogeneous reactor application continues. One of the more promising aspects of the work thus far is that it is difficult to effect any appreciable increase of hydrogen (and consequent temperature-sensitive brittleness) in commercial-purity titanium under simulated service conditions or under even more drastic conditions, such as cathodic treatment in acid solution at ambient temperature. This work is continuing, and various modifications of surface preparation, cold working, and chemical treatment of the samples are being investigated. Additional work is in progress to test the possibility of decomposing supersaturated solutions of hydrogen in titanium under reactor radiation. Impact specimens have been prepared by arc melting and working selected high-purity titanium sponge in an effort to obtain a material for testing which is initially less susceptible to low-temperature notch embrittlement than is commercial-purity titanium. If this work is successful, it will not be necessary to use the far more expensive crystal-bar titanium which is definitely known to have favorable low-temperature impact behavior.

Aqueous Solution and Radiation Chemistry

Experiments on the effect of reactor radiation on the static corrosion of type 347 stainless steel indicate that radiation does increase the corrosion rate when the partial pressure of oxygen is high and that it probably has some effect when the oxygen content is low. The initial corrosion rate (for several weeks) appears to be linear with the square root of time. The dependence of the corrosion rate on fission density remains uncertain.

Studies of the stability of the pertechnetate ion, TcO_4^-, which is of interest as a possible corrosion inhibitor, show that under reactor radiation or gamma radiation, in the absence of hydrogen, either there is no reduction or there exists a steady-state level of reduced technetium that is below the limits of detection. In the presence of hydrogen, a brown,

[redacted]

[redacted]

colloidal material, presumably TcO_2, is produced, with an initial yield of approximately 2.4 eq. of technetium per 100 ev absorbed.

Continued studies on the mechanism of the hydrogen-oxygen recombination reaction in solutions indicate that even though the uncomplexed copper ion is very active catalytically, there exists some other species which is more active.

An indirect method for measuring the solubility of hydrogen in uranyl sulfate solutions by means of an application of hydrogen-oxygen recombination kinetics has been developed. Preliminary tests substantiated the feasibility of the method, and apparatus specifically designed for this purpose is being built.

Investigations of phase equilibria in the system UO_3-SO_3-H_2O have continued, and some observations in the uranyl dichromate-water system and in systems involving $CuSO_4$, UO_2SO_4, H_2SO_4, and H_2O are reported. Work on the solubility of UO_3 in dilute uranyl sulfate solutions at 175°C has been completed. The mole ratio, U-to-SO_4, drops very sharply below unity at uranium concentrations less than approximately 0.01 molar. Hydrolytic precipitation of both copper and uranium occurs in low concentration solutions of these cations at 250°C unless specified amounts of free acid are added. The required amounts of acid for selected concentrations of copper and uranyl ion are reported.

A single experiment to determine the distribution of fission-product activity between the heavy uranium-rich and the light water-rich phases in the miscibility gap of the uranyl sulfate-water system indicates that the activity is largely associated with the uranium-rich phase. This suggests the possible utilization of uranyl sulfate as a scavenger for decontamination.

Additional vapor-pressure data for aqueous uranyl sulfate solutions have been obtained. This work will be completed with measurements at one additional concentration, and a terminal report will be written.

Experiments are in progress to determine the feasibility of additions of measured amounts of sulfur dioxide and oxygen to the in-pile loop to effect a condition equivalent to adding sulfuric acid. Results to date indicate that the uranyl ion is not reduced by sulfur dioxide and that the oxidation of the sulfur dioxide is complete and fairly rapid under the conditions of the experiment.

Slurry Chemistry

Work has continued on the investigation of the preparation of pure anhydrous UO_3, on a kilogram scale, by the thermal decomposition of ammonium uranyl carbonate. The oxides produced by this method yielded less than 10 ppm of soluble uranium on hydration to $UO_3 \cdot H_2O$ in water at 250°C at a slurry concentration of 250 g of uranium per liter.

A study of the temperature-crystal structure relationship of $UO_3 \cdot H_2O$ has been carried out. The transition temperature for the conversion of rods to platelets was found to occur at around 200°C. A summary of $UO_3 \cdot H_2O$ crystallography is included.

The preparation of UO_2CO_3 slurries, by the reaction of CO_2 with UO_3, and

[redacted]

the properties of the slurries have been investigated. Reactions at room temperature have been found to produce better slurries than those carried out at 200 to 250°C. It was found that a partial pressure of less than 500 psi of CO_2 would be sufficient to chemically stabilize a pure UO_2CO_3 slurry at 250°C.

Studies on thorium blanket systems have been started.

An experiment on the effect of reactor irradiation on a slurry of enriched $UO_3 \cdot H_2O$ platelets showed a high rate of gas production ($G_{250°C}$ = 0.4) and a high steady-state pressure. Considerable degradation of the particles to fragments and fines occurred. As much as 72% of the total solids (300 mg of uranium as oxide) plated on the interior surfaces of the radiation bomb.

Physical Studies of Slurries

Slurries of the $UO_3 \cdot H_2O$-H_2O system have been found to be stable while circulating at temperatures up to 200°C. Above 200°C, a change in crystal form causes plating of the solids on the walls of parts of the system and the loss of uranium from the circulating material. Efforts are being directed toward finding both chemical and mechanical means of preventing the plating.

Thorium oxide slurries were found, in general, to be too abrasive for circulation in stainless steel. Progress has been made in finding softer forms of thorium oxide and other suitable forms of thorium.

A simplified method of evaluating plutonium-producing single-core reactors has been developed and applied to boiling reactors containing UO_2SO_4-D_2O solution and UO_3-D_2O slurries.

Data have been obtained from which power removal from some types of boiling reactors can be estimated.

Chemical Processing

Chemical processing studies have been devoted to developing a method for removing fission products and corrosion products from the fuel of an aqueous, homogeneous, thermal, breeder reactor and to assisting in the development of a suitable thorium blanket material.

Two general methods for processing dilute uranyl sulfate solution fuel have been evaluated. Complete decontamination of the fuel by solvent extraction was found to be an unsatisfactory method of processing because of high cost and high losses; however, adsorption appears to be an economically attractive method for removing impurities. The cost of the adsorption method of processing may be as low as 0.3 to 0.5 mil per kwh of electricity produced. Both inorganic adsorbents and organic ion-exchange resins are being considered for this type of process.

In studies conducted by the Vitro Corp. for the HRP, calcium fluoride has been found to be a highly effective material for removing rare earth fission products from a dilute uranyl sulfate solution. Recent studies here have shown that this removal of rare earths is due to a metathesis in which rare earths replace calcium in the solid phase. Therefore the feasibility of using calcium fluoride depends on the solubility of calcium sulfate in

[redacted]

the fuel solution at 250°C. This solubility is being determined.

Thorium oxide pellets are stable in both water and 0.02 *M* UO_2SO_4 solution at 250°C. These pellets are subject to abrasion against one another; however, the rate of abrasion depends on the smoothness of the pellet surface, and the abrasion is negligible for pellets having no obvious surface imperfections.

A satisfactory rate of dissolution was obtained for unirradiated thorium oxide pellets in 60% nitric acid containing 0.1 *M* fluoride as a catalyst.

[redacted]

[redacted]

CONTENTS

	PAGE
SUMMARY	vii
PART I. HOMOGENEOUS REACTOR EXPERIMENT	
STATUS OF THE HRE	3
Reactor Operation	3
Experiment at 200 Kilowatts and Reduced Pressure	4
High Power Operation	7
HRE Off-Gas Pump	14
PART II. BOILING REACTOR RESEARCH	
BOILING REACTOR RESEARCH	19
Criticality Requirements and Plutonium Production of Bare, Homogeneous Reactor	19
Nucleation by Fission Fragments	20
Stability of Boiling UO_2SO_4 Solution in Stainless Steel	20
Power Removal from Boiling Reactors	22
Teapot Mockup	27
PART III. GENERAL HOMOGENEOUS REACTOR STUDIES	
INTERMEDIATE-SCALE HOMOGENEOUS REACTOR DESIGN	31
Internal Recombination Catalyst	31
Evaporation of D_2O in the Gas Separator	31
Cooling-Tower Reactor	32
ENGINEERING DEVELOPMENT	34
Core and Gas Separator Development	34
ISHR core	34
Eight-foot rotational-flow model	36
Pipe-line gas separators	36
Recombiner Development	39
Gas Circulator for ISHR Recombiner System	40
Pulsafeeder Pump Tests	41
Stellite Piston Pump Tests	41
Test Loop for 4000-gpm Pump	41
ISHR Heat Exchanger	41
Small Canned-Rotor Pump Development	42
Conversion of the HRE Mockup to Operate with Uranium Oxide Slurry	42
CORROSION	43
Pump Loop Operation and Maintenance	43
Loop Test Results	49

[redacted]

[redacted]

Small-Scale, Dynamic Corrosion Test Program 65
In-Pile Loop 66
Static Corrosion Studies 69

METALLURGY 80
Service and Miscellaneous Work 80
Radiation Damage Studies 81
Welding of Type 347 Stainless Steel 82
Brittle Fracture of Titanium 83
Titanium for Valve Trim 83
Properties of Titanium 83
Zirconium-Titanium Alloys 86

AQUEOUS SOLUTION AND RADIATION CHEMISTRY 87
Static Corrosion Tests with Radiation 87
The Mechanism of the Hydrogen-Oxygen Recombination Reaction in Solutions 89
Solubility of Hydrogen at High Temperatures and Pressures in Solutions of Uranyl Sulfate 96
Description of Filtration Apparatus Used for Aqueous Solubility Determinations Above 100°C 99
Solubility of UO_3 in Aqueous UO_2SO_4 at 175°C 101
Phase Diagram for the UO_3-SO_3-H_2O System at 25°C 101
Solubility of Uranium Trioxide in Uranyl Fluoride Solutions at 25 and 100°C 101
Equilibration Times for Uranium Trioxide in Uranyl Sulfate Solutions 101
Exploratory Phase Investigations of Systems Involving $CuSO_4$, UO_2SO_4, H_2SO_4, and H_2O at Uranium Concentrations Below 30 g per Liter 102
Comment on the System Uranyl Dichromate-Water 105
An Apparatus for Phase-Stability Studies and Corrosion Tests on 2-ml Solution Volumes 106
Extension of Two-Liquid Phase Studies of UO_2SO_4 108
Oxidation of Sulfur Dioxide in Uranyl Sulfate Solution 108
Chemistry of Corrosion 109
Vapor Pressures of Aqueous Uranyl Sulfate Solutions 109

SLURRY CHEMISTRY 110
Uranium Trioxide Chemistry 110
Chemistry of UO_2CO_3 114
Thorium Chemistry 118
Uranyl Oxide Slurry Irradiations 118

PHYSICAL STUDIES OF SLURRIES 120
Thorium Slurries 120

[redacted]

[redacted]

Uranium Slurry Loops 122
Critical Experiments 124

CHEMICAL PROCESSING 125
Fuel Processing 125
Thorium Oxide Pellet Studies 129
Dissolution of Thorium Oxide Pellets 130

[redacted]

Part I

HOMOGENEOUS REACTOR EXPERIMENT

HRP QUARTERLY PROGRESS REPORT

STATUS OF THE HRE

S. E. Beall, Section Chief
S. Visner, Experimental Physics Group Leader
J. J. Hairston J. W. Hill, Jr. T. H. Thomas
Operations Group Leaders
D. I. Eissenberg W. C. Keller S. I. Kaplan
V. K. Pare' J. L. Redford P. M. Wood
Reactor Engineers
T. E. Haynes G. H. Johnstone
A. L. Johnson W. B. Krick
Technicians

REACTOR OPERATION

At the beginning of this report period, the Homogeneous Reactor Experiment was out of service for repairs and decontamination made necessary by a fuel spill from a differential-pressure cell in the oxygen-gas-measuring apparatus. A completely new system for fuel oxygenation was completed and tested early in January. The reactor was restarted on January 5 and operated at 125°C, 1000 psi, and 50 kw for 16 hours. Experiments conducted during this time provided the information that the reactor system was leak tight and that the reactor was self-stabilizing; that is, the negative temperature coefficient was sufficiently effective to overcome small suddenly imposed reactivity changes and to level the reactor power without resorting to the standard control mechanisms. Failure of the electric boiler which provides 1500-lb steam for the fuel pressurizer made discontinuance of operation necessary. The boiler is located in the reflector compartment of the shield and is near the location of the recent fuel leak. Its confined position and high radiation level (2 r/hr) made the repair job a difficult one. Although successful repair was accomplished, it was decided to spend additional shutdown time to install a spare electric boiler outside the reactor shield so that uninterrupted reactor operation could continue if another failure of the inside boiler occurred.

While these repairs were in progress, a routine fuel analysis indicated the presence of sufficient chloride ion concentration (80 ppm at the operating uranium concentration of 40 g/kg) to cause excessive corrosion of the type 347 stainless steel piping in the fuel system. Plans were made to remove the chloride by an electrolytic method, which involved collection of the chloride on a silver electrode mounted in an opening at the fuel-sampling device. However, after several days of experimentation in which it was demonstrated that insufficient electrode surface was available in the limited space of the sample cavity, a method of precipitation with silver sulfate was adopted. To accomplish removal of the chloride by precipitation as AgCl, it was necessary to install a 12-liter, steam-jacketed, reaction vessel and a sintered stainless steel filter between the inner and outer fuel storage tanks so that the highly active fuel could be processed without removal from the reactor system. The fuel was treated in 6-liter batches with sufficient silver sulfate to precipitate the chloride and was boiled for 20 min to coagulate the precipitate. After cooling to room temperature, the

batches were filtered and transferred to the dump tanks inside the reactor shield. The source of the chloride was a liquid-level manometer, which contained Merriam red oil, as a fluid, and was connected to the outer storage tanks. This manometer was used to obtain information for fuel inventories, and on one occasion approximately 50 ml of oil was accidentally discharged into the fuel tanks. Subsequent experimentation showed that the oil (65% mono-chloronapthalene) could be expected to decompose at 200°C in the presence of the uranyl sulfate fuel solution and that the 50 ml was a sufficient quantity to account for about twice the amount of chloride found in the fuel.

In the course of the shutdown and in preparation for operation at higher power levels, the reactor instrumentation and the control circuitry were reviewed[1] for operational safety according to the reactor characteristics known at that time, which included experimental data on the temperature coefficient of reactivity and the effectiveness of rods and reflector, as well as information concerning the mechanical, chemical, and hydraulic behavior of the system. The main problems arose from the effectiveness of the safety rod and reflector having been shown to be much less and the temperature coefficient considerably larger than originally calculated. Thus, a decrease in temperature from 250 to 160°C is sufficient to override the effectiveness of the reflector. Feasibility studies of the HRE have indicated, however, that the reactor can withstand, without the aid of external safety systems, large increases in reactivity because of the large negative temperature coefficient of reactivity. A step increase in reactivity of 2% or the introduction of a linear rise in reactivity of 0.05 %/sec would lead to a power surge with a peak of about 10^5 kw and a peak pressure of less than that required to burst the core. In a reactor system completely tested and shielded, this should lead to no difficulties. The fundamental philosophy was adopted, however, that because of the absence, at the time, of experimental confirmation of the predictions on the kinetic behavior of the HRE and because of the possibility that unforeseen occurrences might lead to instabilities, the reactor power should be continually under the control of the operator so that unplanned power excursions could be prevented.

Several revisions were made in the reactor interlock control system and in the operating procedure to minimize the occurrence of reactivity changes greater than the capacity of the available safety system. In essence, the revisions were made to protect the reactor from the possibilities of excessive cooling and excessive concentrations of the fuel in the core.

On February 16, operation was resumed by circulating the fuel at 200°C and at a concentration of 20 g of uranium per kilogram of solution. It was determined by chemical analysis that no additional chloride had appeared after a 12-hr period. The reactor was operated at low power again on February 18 and 19, and on February 20 the power level was increased to 50 kw.

EXPERIMENT AT 200 KILOWATTS AND REDUCED PRESSURE

On February 21, the reactor power was increased to 200 kw at a temperature of 140°C and a pressure of 500 psi. The main purpose of operation at this level was to obtain information while the reactor was at low power and low pressure on its stability in the presence of gas production at a volume rate corresponding to 1000-kw operation at high pressure. The volume rate of gas production is proportional to the

[1] S. Visner, *Nuclear Safety of the HRE*, ORNL CF-53-2-76 (Feb. 10, 1953).

excess pressure, that is, the difference between the total pressure and the vapor pressure of the solution. At 500-psig total pressure, which corresponded to 20% of the full power volume gas rate, oscillations in power were observed that had an amplitude of 12% and a frequency of 0.08/sec that led to reactor periods as short as 15 sec with the power remaining constant, as shown in Fig. 1. The total pressure was then reduced to 330 psig, which yielded a volume gas rate of approximately 30% of that corresponding to full power operation. The amplitude of the oscillations then approached 15% and reactor periods as short as 12 sec were observed.

The power oscillations were directly associated with the operation of the let-down valve. At design conditions, this valve automatically controls the discharge of excess liquid and gas from the core to the low pressure system to maintain a constant level of fuel in the pressurizer above the core. Under the conditions of the test, however, the let-down valve cycled between closed and partly open positions with the same frequency as that of the observed power oscillations. When the valve closed, the gas vortex apparently started growing inside the reactor core and thus decreased the reactivity and the reactor power. When the valve opened, the gas volume in the core decreased and thus increased the reactivity and power.

An analysis of the power behavior was made by representing the power by a constant term and the first two terms of a Fourier Series:

$$P = P_0 + \Delta P_1 \cos \omega t - \Delta P_2 \cos 2\omega t \ , \quad (1)$$

with

$$\omega = 0.46 \ ,$$
$$P_0 = 200 \text{ kw} \ ,$$
$$\Delta P_1 = 20 \text{ kw} \ ,$$
$$\Delta P_2 = 7.5 \text{ kw} \ .$$

The kinetic equations describing the system are

$$\tau P = \left[\delta(t) - \beta - b \int_0^t (P - P_0)\, d\xi\right] P + \sum_i P_i \quad (2)$$

and

$$\mu_i P_i = -P_i + \beta_i P \ , \quad (3)$$

where

τ = prompt neutron generation time, 0.8×10^{-5} sec,

β_i = fraction of neutrons which are delayed, associated with mean life, τ_i,[2]

$\delta(t)$ = externally applied reactivity change,

b = ratio of the temperature coefficient of reactivity to the heat capacity of the system, 4.6×10^{-6} k_{eff}/megawatt·sec,

P = reactor power, kw,

P_i = fission power induced by the delayed neutrons of the ith group.

Substituting Eq. 1 into Eq. 3 and integrating yields

$$P_i = \beta_i P_0 + \frac{\beta_i \Delta P_1}{\sqrt{1 + \omega^2 \tau_i^2}} \cos\left[\omega t - \tan^{-1} \omega \tau_i\right] - \frac{\beta_i \Delta P_2}{\sqrt{1 + 4\omega^2 \tau_i^2}} \cos\left[2\omega t - \tan^{-1} 2\omega \tau_i\right] \ , \quad (4)$$

where the transient term containing the factor e^{-t/τ_i} has been neglected. Then, substituting Eqs. 1 and 4 in Eq. 2 gives

[2] H. T. Williams, *Photoneutrons in the HRE*, ORNL CF-51-12-122 (Dec. 19, 1951).

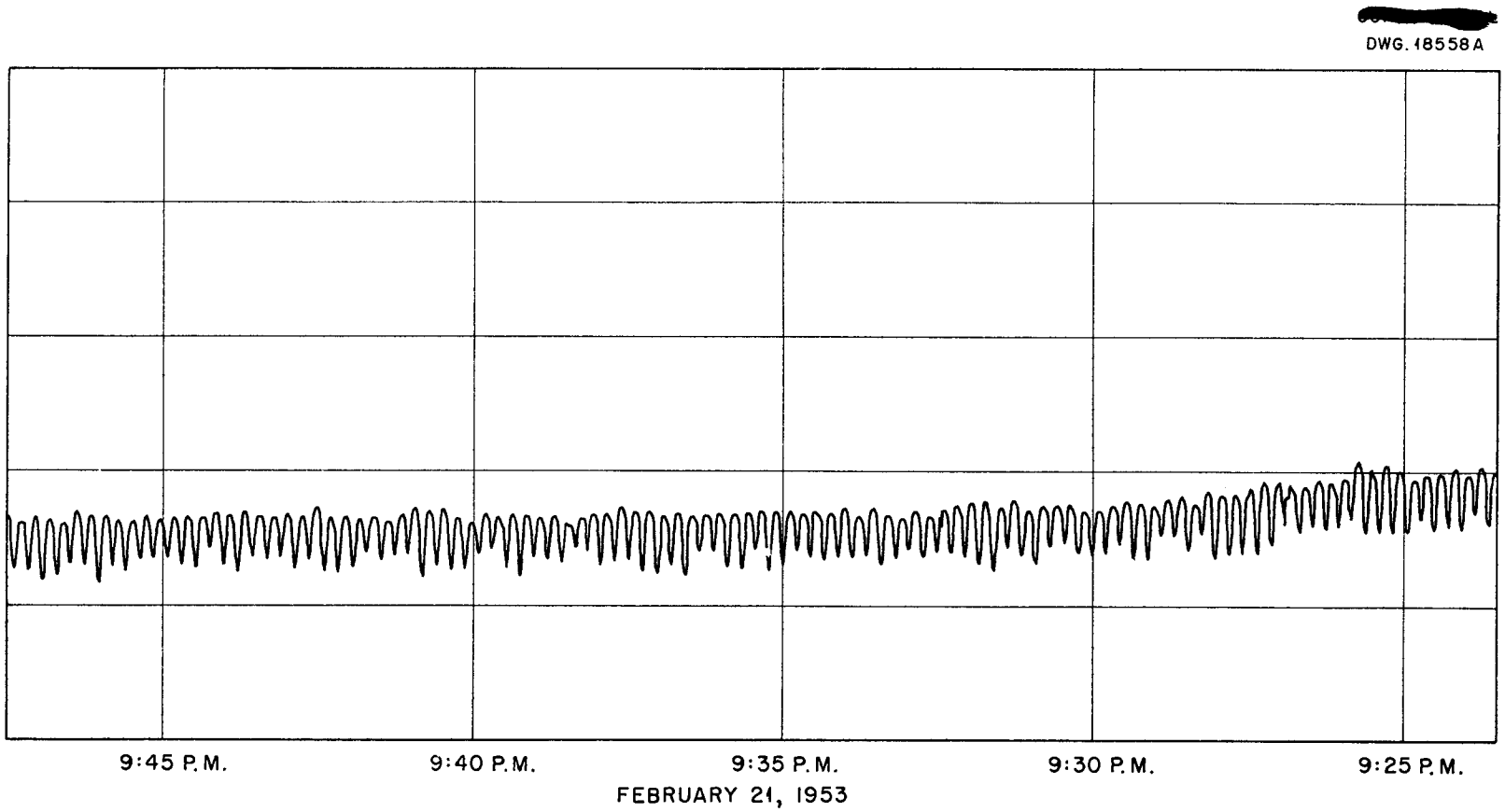

Fig. 1. HRE Operation at 200 kw, 400 psi, and 140°C on February 21, 1953.

$$\delta(t) = \frac{b\,\Delta P_i}{\omega} \sin \omega t - \frac{b\,\Delta P_2}{2\omega} \sin 2\omega t$$

$$+ \frac{\beta\,\Delta P_1 \cos \omega t - \beta\,\Delta P_2 \cos 2\omega t - \tau\omega\,\Delta P_1 \sin \omega t + 2\tau\omega\,\Delta P_2 \sin 2\omega t}{P_0 + \Delta P_1 \cos \omega t - \Delta P_2 \cos 2\omega t}$$

$$- \Delta P_1 \sum_i \frac{\beta_i}{\sqrt{1 + \omega^2 \tau_i^2}} \cos\left[\omega t - \tan^{-1} \omega\tau_i\right]$$

$$- \Delta P_2 \sum_i \frac{\beta_i}{\sqrt{1 + 4\omega^2 \tau_i^2}} \cos\left[2\omega t - \tan^{-1} 2\omega\tau_i\right] \quad . \quad (5)$$

Further simplification is obtained by neglecting the oscillatory terms in the denominator and combining the trigonometric functions of the same frequency. The final result, after substituting numerical values, is, in units of per cent k_{eff},

$$\delta(t) = 0.052 \cos(\omega t - 0.03) - 0.019 \cos(2\omega t + 0.11) \quad . \quad (6)$$

The amplitude of the reactivity change resulting from the variation in gas volume in the core is approximately 0.05% k_{eff}, or a total change in reactivity of 0.1% every 6 seconds.

A heat balance was made on the system, and it was confirmed that the reactor was operating at a power of 208 kw. The primary means of heat removal was the discharge of steam from the main heat exchanger through a throttle valve to the turbine condenser.

HIGH POWER OPERATION

High power operation of the HRE was attained at 1:08 AM, February 24, with the steam output driving a turbogenerator unit. Within the next 30 min, the reactor power was raised to 1000 kw at an electrical output of approximately 160 kw. The important physical criteria of successful operation were met with respect to reactor stability in the presence of gas production and a power density of 20 kw/liter, air activity in the stack, handling of the decomposition gases, and adequacy of the concrete shield around the reactor. The events related to the attainment of full power are summarized here from the log entries recorded during the experiment. A plot of the power level, core inlet and outlet temperatures, and steam temperature is shown in Fig. 2.

Approach to 1000-kw Power

February 23, 1953

7:40 PM Reactor critical at 50 kw, 200°C, and 1000 psig.

9:05 Power increased by withdrawing steam to the condenser.

9:48 Reactor power leveled off in the vicinity of 200 kw.

The following observations were made.

Monitrons: All readings on low scale.

Stack activity: Four times breathing tolerance. It is expected that there is a further dilution of perhaps a thousand-fold as the gas discharges from the stack.

Heat balance: 220-kw reactor power.

Gas recombiners: 2.4 cfm STP of H_2 and O_2.

Shield: Fast-neutron radiation above tolerance outside the instrument thimbles. Additional concrete blocks stacked about these locations reduced the radiation to a safe value.

Stability: Amplitude of power oscillations 2%. Reactor periods as short as 50 sec were observed.

10:30 PM Power increased by increasing the heat withdrawal from the heat exchanger.

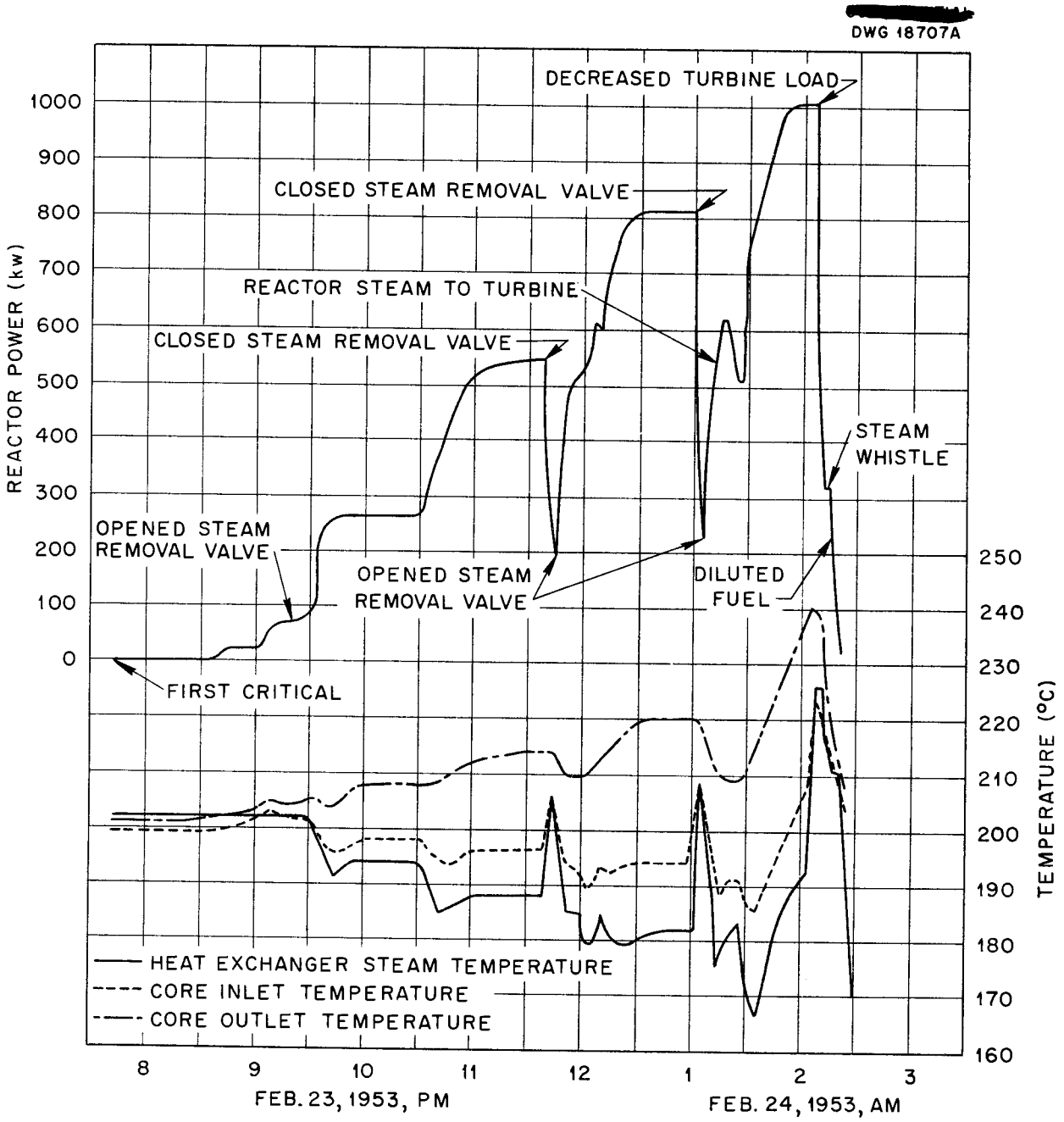

Fig. 2. Initial Operation of the HRE at Full Power.

10:50 Power leveled off at approximately 500 kw.

The following observations were made.

Monitrons: All on high scale. The ventilator monitron located at roof of building was reading off-scale. The high readings of monitrons were attributed to the high background in the building because of radiation from the charcoal beds which adsorb the fission gases. The beds are located about 100 ft east of the reactor building. The radiation level at the fence east of reactor building, 30 ft from absorbers, was 5 r/hr.

Heat balance: Reactor power level (500 kw) confirmed.

Gas recombiners: 5.2 scfm of gas.

Shield: Radiation through shield appeared below tolerance.

Stack activity: Ten times breathing tolerance.

Stability: Amplitude of power oscillations 3%. Reactor periods as short as 40 sec were observed.

11:40 PM An experiment was performed to test the stability of the reactor to changes in heat withdrawal rate. The steam removal valve was closed first and the power was observed to decay, as shown in Fig. 3, from about 500 to 200 kw. The steam valve was then opened, within 2 sec, to its previous position. The difference between the heat withdrawal rate of 500 kw and the power production of 200 kw is equivalent to introducing reactivity into the reactor at the rate of 0.17% k_{eff}/sec. As expected, the reactor power rose to its new equilibrium value with a relaxation time of approximately 90 sec.

February 24

12:08 AM Power increased by increasing heat withdrawal. *The reactor was controlled during the previous 3 1/2 hr solely by power withdrawal, without the other reactor controls, such as rods, reflector level, and concentration, being used.*

12:18 Reactor power leveled off at approximately 800 kw.

The following observations were made.

Heat balance: Reactor power level established at 810 kw.

Stack activity: About 3 times breathing tolerance.

Radiation levels: 8.7 r/hr at fence near charcoal bed; 10 mr/hr in the control room.

Stability: Oscillation amplitude 8%. Reactor periods as short as 15 sec were observed.

12:30 Decision made that sufficient steam was being generated to direct the reactor output steam to the turbine.

12:40 Turbine being warmed up with plant steam. Power removal from reactor was decreased in order to have the full condenser capacity available for warming up the turbine.

1:02 Turbine synchronized with TVA network. The generator was then motoring on the TVA line with plant steam turned off.

1:05 Reactor power increased by withdrawing steam to the condenser (Fig. 4).

1:08 Power level of 500 kw reached. The steam was directed to turbine and the governor control opened. An electrical output of 70 kw was immediately attained.

1:12 Reactor power at 600 kw. Reactor power was varied by changing governor setting.

1:16 Electrical load of reactor and building switched to the generator output so that the building electrical requirement of about 70 kw was supplied by the reactor.

1:25 Turbine, carrying the building load, resynchronized with TVA.

1:45 Reactor power at 1000 kw; electrical output 160 kw. Excess electrical power being delivered to ORNL network. Figure 5 shows the reactor power and temperature behavior at that time.

2:05 Power decreased by turning down governor control.

2:30 Fuel solution diluted with condensate and the reactor shutdown.

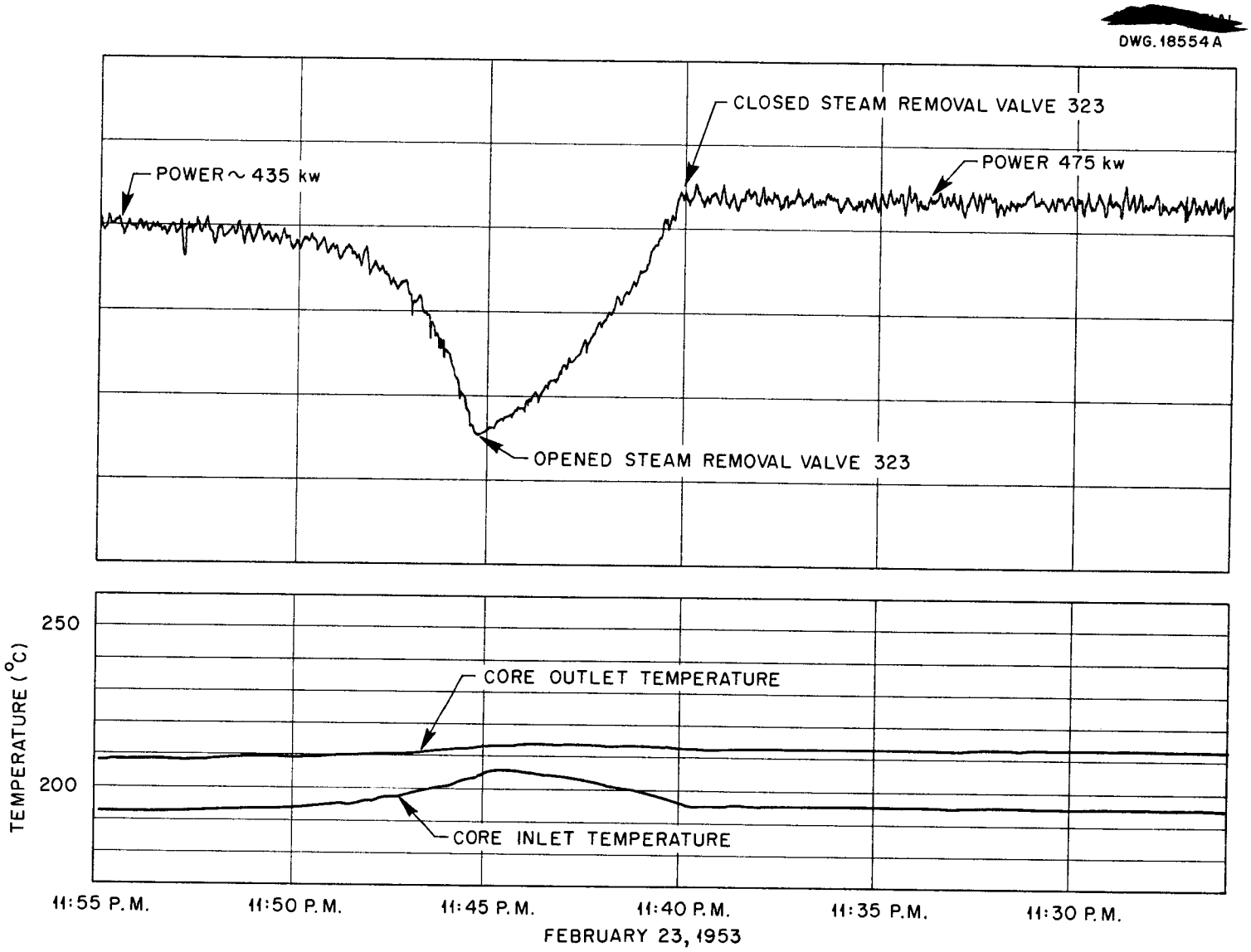

Fig. 3. HRE Operation at 1000 psi and 200°C on February 23, 1953.

[redacted]

DWG. 18557A

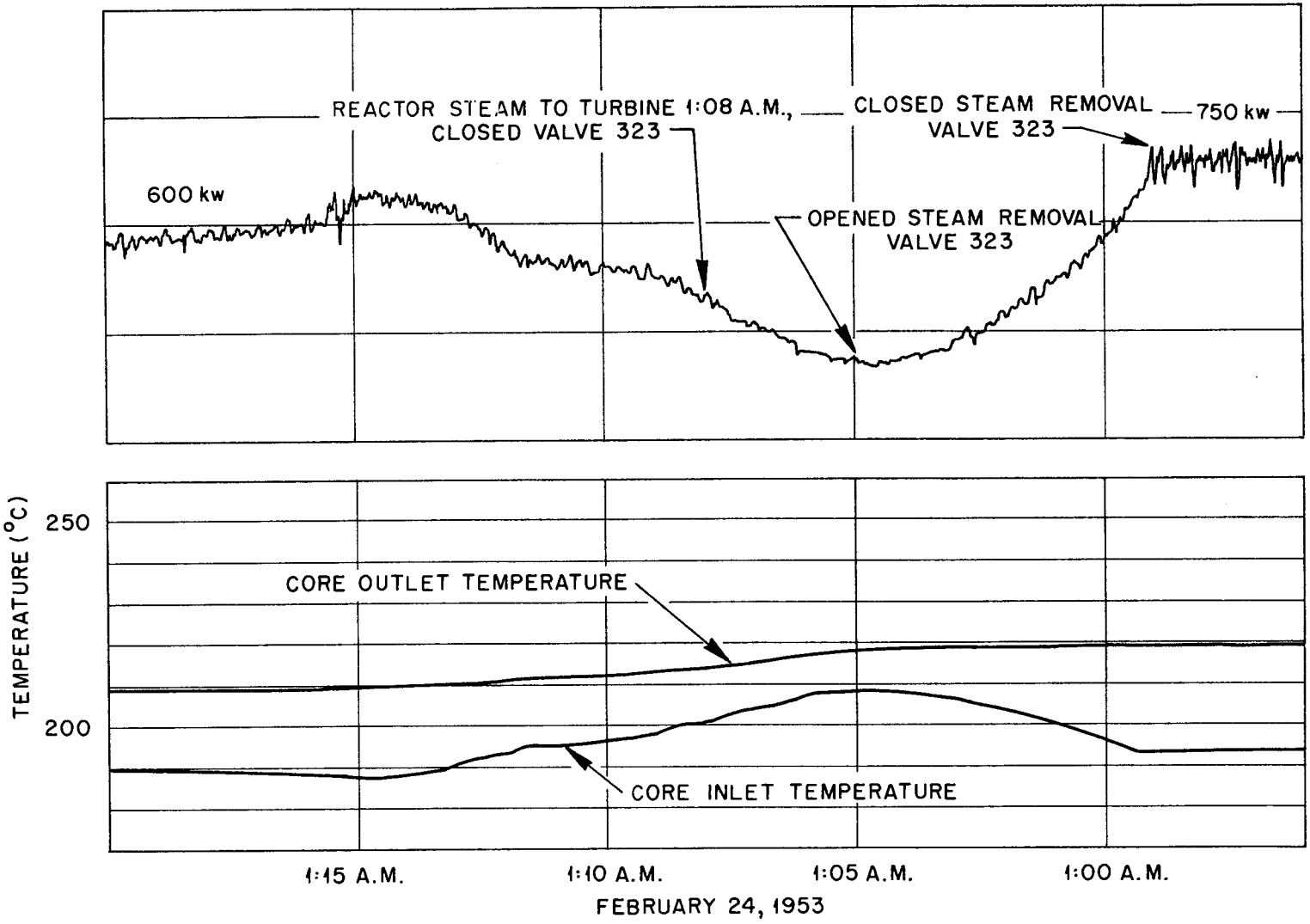

Fig. 4. HRE Operation at 1000 psi and 200°C on February 24, 1953.

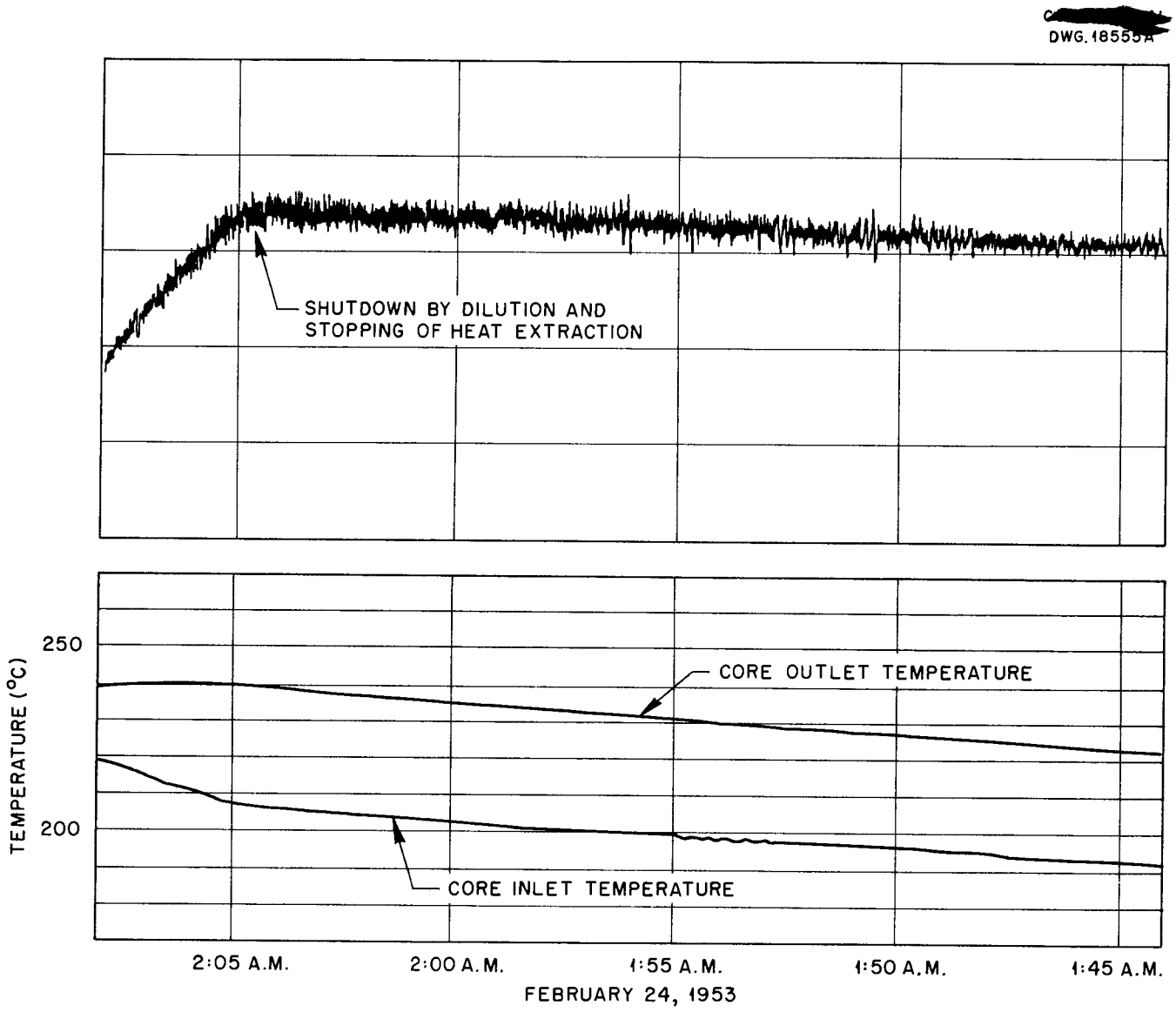

Fig. 5. HRE Operation at 1000 kw, 1000 psi, and 200°C on February 24, 1953.

Reactor Off-Gas and Recombiner System. The rate of dissociation of the water of the fuel solution while the reactor was at high power was determined by measuring the rate of heat removal from the gas recombiners at steady state, since this is a measure of the recombination rate of the hydrogen and oxygen. The results obtained during the initial high power run on February 23 and 24 are shown in Fig. 6, where a straight line was drawn through the data. From this information, the value of 1.4 was obtained for the *G* value, that is, the number of water molecules dissociated per 100 ev.

The charcoal beds for adsorbing the fission-product gases appeared to function satisfactorily, as evidenced by the fact that there was no indication of excessive activity in the stack to which the beds discharge.

Analyses of fuel samples removed during the 1000-kw run indicated that the chloride ion had reappeared to the extent of approximately 30 ppm and that the corrosion rate of the system, based on the nickel concentration in the fuel, had increased from 0.3 to 1.0 mpy to 3 to 8 mpy. The higher corrosion rate might be attributed to the chloride content of the fuel, to radiation effects, or to the erosive action of gas bubbles circulating at the high power level. It was considered necessary to eliminate the chloride, which was assumed to have come from outer-dump-tank manometer oil. The fuel was retreated with silver sulfate, as described previously, and the chloride content was again reduced to 1 ppm.

While the fuel processing was in progress, activity was discovered in the condensate on the steam side of the main fuel heat exchanger, and it was thought that a fuel leak had developed in one of the heat exchanger tubes. However, subsequent testing

[redacted]

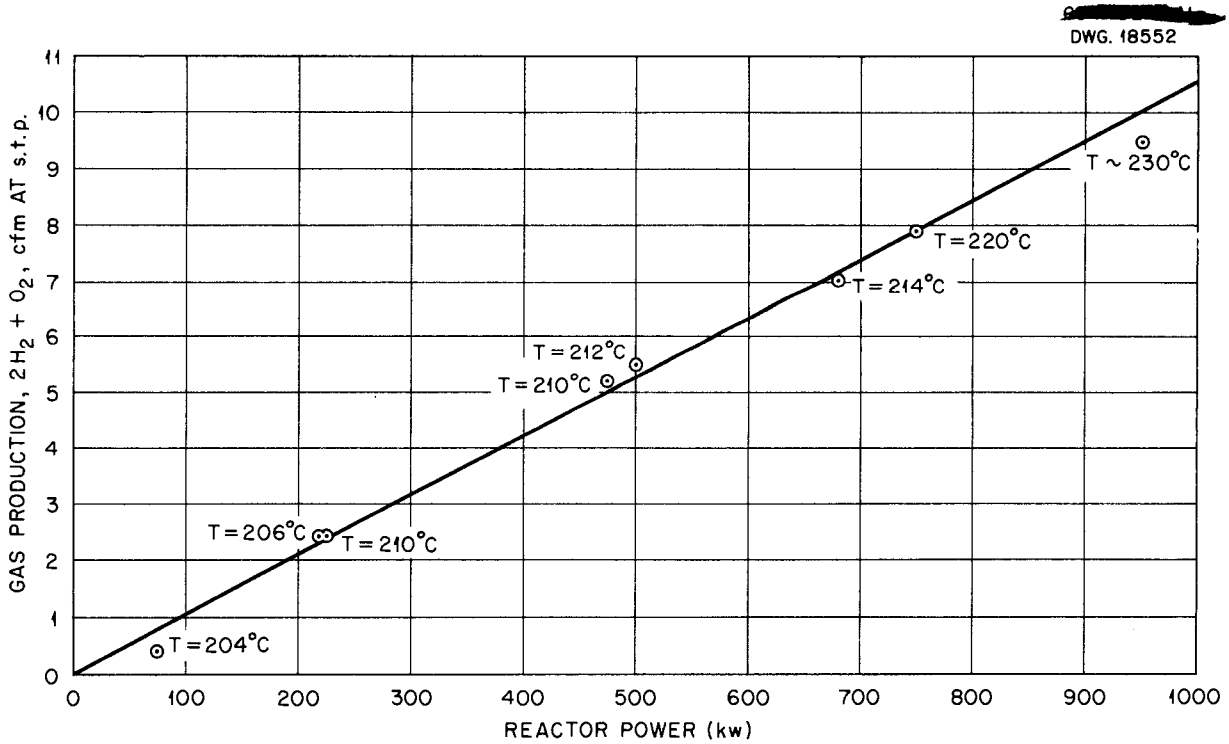

Fig. 6. Gas Production in the HRE on the First Run at Full Power, February 23-24, 1953.

of the exchanger proved this assumption to be erroneous. Further investigation indicated that a quantity of highly active liquid from the waste storage tank had leaked back through the blow-down valve of the heat exchanger and had contaminated the steam condensate system. The activity did not reappear when reactor operation was resumed.

The purpose of the period of operation beginning March 16 was to determine the cause of the sudden increase in corrosion indicated during the 200- to 1000-kw run. The plan was to run the reactor at zero power for sufficient time to determine the rate of corrosion and chloride content in the absence of radiation and then to add the radiation variable by increasing the reactor power first to 10 kw and then to 1000 kw. Over a period of 5 days of continuous operation, the corrosion rate, as indicated by the concentration of nickel ion in the fuel, was found to be approximately 8 mpy, irrespective of the reactor power level. The cause for this apparent increase in corrosion rate as compared with that experienced prior to the appearance of the chloride ion is being studied.

In the course of this operating period, the reactor was started from a subcritical condition at 200°C by concentrating the fuel to a value sufficient to make the reactor supercritical on a 10- to 20-sec period. At this point, concentration was stopped and the reactor level permitted to rise until the slight excess reactivity was overcome by the temperature coefficient because sufficient heat had been generated to raise the operating temperature. The reactor leveled itself at approximately 10 kw and continued to operate steadily without a mechanical control having been touched. The power level was then increased in the usual manner, that is, by withdrawing steam, to the normal level of 1000 kw. During this run, it was proved that the source of the oscillations described earlier in this report was, as suspected, the gas-liquid let-down valve, and by increasing the output of the pulsafeeder feed pump, the valve was made to throttle instead of operating with an intermittent open-close action. This change reduced the amplitude of the oscillations to 2% and made operation at higher power levels possible. For a period of 1 hr the reactor level was maintained at 1200 to 1500 kw and 195-kw electrical output without difficulty. This period of operation provided good evidence that a homogeneous system of the HRE type can be operated at power densities of at least 30 kw/liter without difficulty from nuclear instabilities.

HRE OFF-GAS PUMP

R. H. Chapman

A leak in the fuel gas condenser in the low-pressure fuel system in the HRE permits radioactive gases to escape if the low-pressure system is operated at greater than atmospheric pressure. At the present time, subatmospheric pressure is maintained by a mechanical vacuum pump in the line between the charcoal beds and the stack. Use of this pump is not satisfactory because the resistance of the charcoal beds to the flow of gas is high. The pressure in the beds must be reduced far below atmospheric pressure to achieve the desired pressure in the fuel system. Since the capacity of the charcoal to adsorb fission-product gases is greatly reduced at low pressure, it is doubtful whether the HRE could operate under existing conditions for long periods at high power without discharging prohibitive amounts of radioactive gas.

A gas pump has been designed to be installed between the low-pressure fuel system and the charcoal beds to overcome the present difficulty. Because the specific activity of the

gas is high, the pump is required to be absolutely leak proof. The design flow rate is approximately 0.5 cfm, and the specified suction and discharge pressures are 10 and 45 psia, respectively. No commercial pumps were found which could meet all the specifications, and therefore a reciprocating pump with a mercury piston and a gas seal was chosen as the basis for design.

The pump assembly consists of two 6-in.-dia cylinders and a 3-gpm rotary gear pump, connected as shown in Fig. 7. The lower chamber of each cylinder contains oil and mercury; the upper chamber is the gas-pumping cylinder. As oil is forced into the lower chamber by the gear pump, mercury is displaced into the upper chamber to compress the gas to a pressure high enough for it to flow into the discharge line. Mercury-sealed, ball check valves are used in both the suction and discharge lines. A high, theoretical, volumetric efficiency is achieved by allowing the mercury to flow out through the discharge valve before reversing the flow. This also provides a supply of mercury to both valves for sealing. Flow is reversed by reversing the direction of rotation of the gear pump on a signal from probes in the discharge valve chamber. A safety probe is provided in each suction chamber to reverse the pump if there is leakage past the check. A probe is also provided in each cylinder to reverse the pump if the mercury level gets too low.

The valves, as shown by Fig. 7, employ 3/4-in.-dia balls which float partially submerged in mercury. In the suction valve, the mercury acts as a liquid spring to keep the ball seated. The gas entering must bubble through a very small head of mercury before it enters the pump chamber. On the discharge stroke, the mercury, in addition to keeping the suction check seated, acts as a gas seal. The discharge check will trap a small amount of mercury for a gas seal on the downstream side of the ball at the start of each suction stroke.

The pump will be installed on a concrete pad adjoining the stack at the southeast corner of Building 7500. Concrete blocks and lead bricks are to be stacked around the installation, as needed, for shielding. Traps are provided on both the upstream and downstream sides of the pump for use if all safety measures fail. Each trap has sufficient volume to hold the entire amount of mercury and oil from both cylinders. The traps, which will be in the existing off-gas line, will be buried under several feet of earth.

The pump is presently being assembled. Upon completion, extensive testing is planned to demonstrate the reliability of the pump.

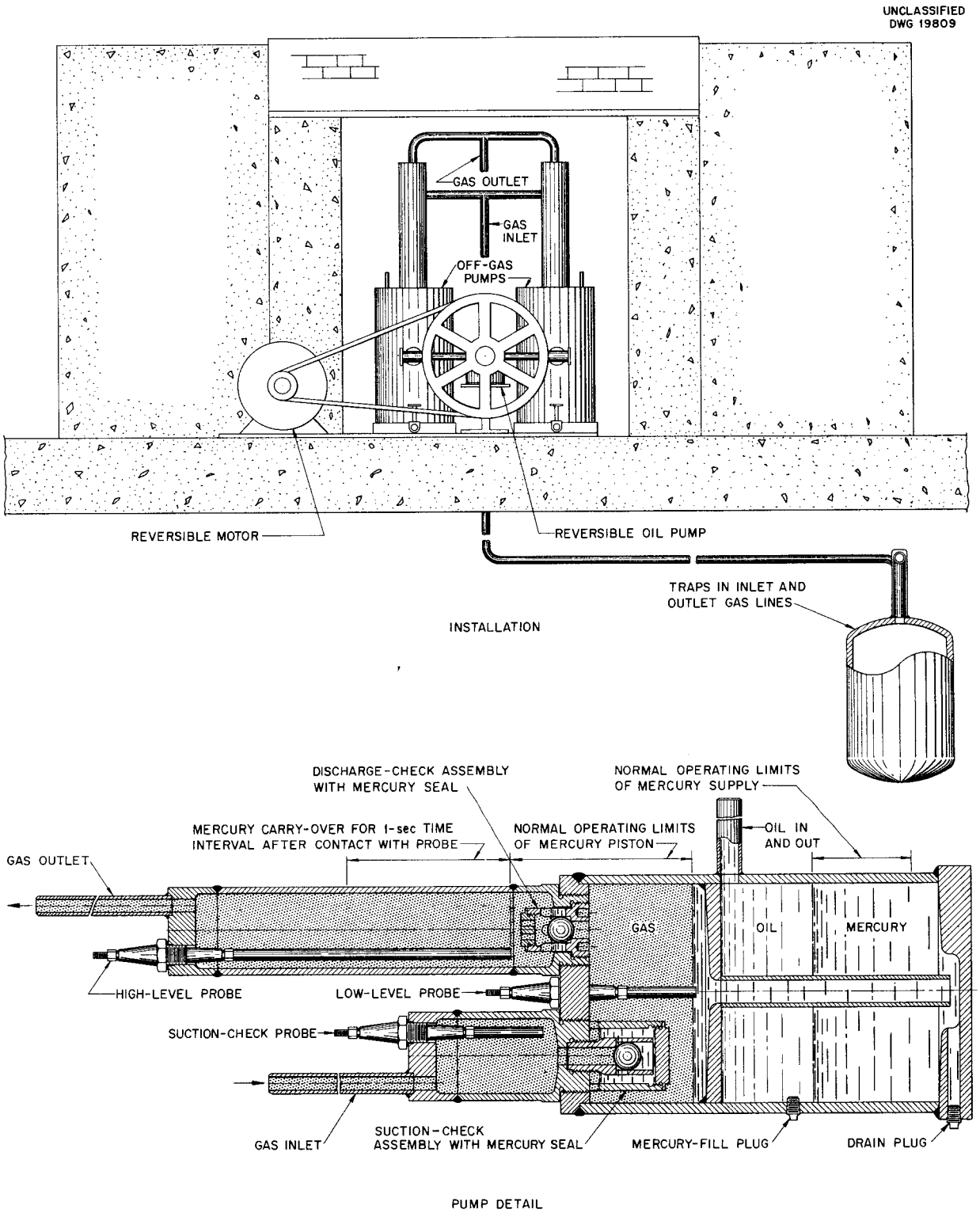

Fig. 7. HRE Off-Gas Pump.

Part II

BOILING REACTOR RESEARCH

BOILING REACTOR RESEARCH

R. N. Lyon, Section Chief

CRITICALITY REQUIREMENTS AND PLUTONIUM PRODUCTION OF BARE, HOMOGENEOUS REACTORS

P. R. Kasten

Criticality conditions and plutonium production rates in single-region homogeneous reactors have been calculated as a function of fuel enrichment, moderator ratio, and vapor fraction at 250°C for two fuel systems: (1) UO_2SO_4-D_2O solution and (2) UO_3-D_2O slurry. The geometry, temperature, and vapor fraction parameters can be combined into one term, the ratio of geometric buckling to the square of the fluid density, $(B/\rho)^2$, which is only a function of moderator ratio and enrichment. The results are shown in Fig. 8, in which $(B/\rho)^2$ is given as a function of moderator ratio, β, for various fuel enrichments.

With the aid of Fig. 8, the plutonium production rate can be calculated as a function of β from

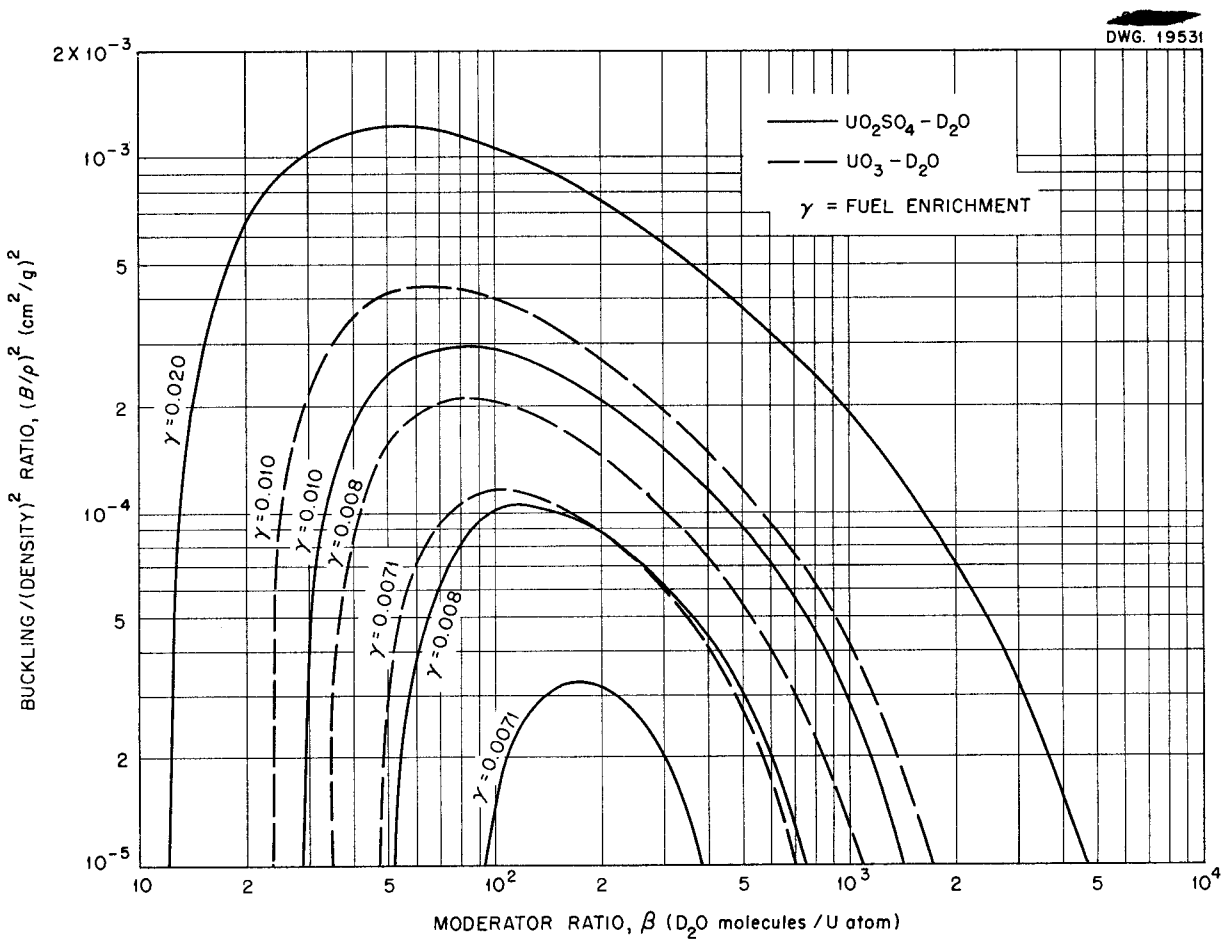

Fig. 8. Ratio of Geometric Buckling to the Square of the Fluid Density vs. Moderator Ratio for Homogeneous Reactors.

$$PPR = \frac{2.5\,(1-p)}{1+\left(\frac{B}{\rho}\right)^2 \tau_0 \rho_0} + \frac{1-\alpha}{\alpha}\,5.138 \times 10^{-3}\,, \qquad (1)$$

where

PPR = plutonium production rate, atoms/fission,

τ_0 = effective Fermi age at fluid density ρ_0,

α = fuel enrichment,

p = resonance escape probability.

Figure 9 gives β and $(B/\rho)^2$, for several enrichments, as a function of plutonium production rate. In this case, β is essentially the same for both fuel systems.

The neutron losses in sulfur, as expected, have a marked effect on the plutonium production rate. For example, a 15-ft-dia reactor with 0% vapor fraction and 1% enriched fuel gives a plutonium production rate of 1.18 for the UO_3 fuel, as compared with 1.00 for the UO_2-SO_4 fuel.

The calculations are accurate to within a 3% error caused by temperature variations in the range 250 ± 25°C. The values of p[1] and F used in the calculations are given in Figs. 10 and 11,[2] which present the resonance escape probability and fraction of fluid occupied by moderator as functions of β. The calculations and results are being reported by Kasten.[3]

NUCLEATION BY FISSION FRAGMENTS

R. J. Goldstein

The apparatus for determining the effect of supersaturation with hydrogen on the nucleation of bubbles by fission fragments in slightly superheated aqueous solutions of enriched uranyl sulfate has been completed, and measurements will be undertaken in the near future.

Preliminary experiments with the equipment and with small glass ampoules have been performed on relatively gas-free (preboiled) samples. These experiments indicated that fission fragments will form vapor nuclei at approximately 130.7 and 135.3°C for total pressures of 746 and 1000 mm Hg, respectively, in an aqueous uranyl sulfate solution (~27 g of U^{235} per kg of solution). In addition, finely drawn ampoules containing water and an aqueous solution of a boron compound have been superheated more than 100°C at atmospheric pressure in the absence of radiation. These samples will be used to study the effect of various radiations on nucleation in an effort to understand the mechanisms involved.

Some qualitative observations on the superheating of water and aqueous solutions in the absence of radiation have also been made in the course of this study:

1. In general, the smaller the inner diameter of the ampoule, the greater is the attainable superheat.
2. As also found by other experimenters,[4] exposing the ampoule to the atmosphere for some time after it is drawn and before it is filled with liquid seems to lower the maximum superheat.
3. Ampoules in which the liquid is nucleated and then allowed to condense, without allowing air to contact the inner heated surface, will ebullate at much lower temperatures on subsequent reheating.

STABILITY OF BOILING UO_2SO_4 SOLUTION IN STAINLESS STEEL

C. G. Lawson

The motivation and approach for the study of the stability of boiling

(1) Values obtained from P. N. Haubenreich and R. B. Briggs, private communication.

(2) M. Tobias and P. N. Haubenreich, *Critical Calculations for Half-Filled ISHR Sphere*, ORNL CF-52-5-230 (May 16, 1952).

(3) P. R. Kasten, *Criticality Requirements and Plutonium Production of Bare Homogeneous Reactors*, ORNL CF-53-3-108 (in press).

(4) F. B. Kenrick, C. S. Gilbert, and K. L. Wismer, *J. Phys. Chem.* 28, 1297 (1924).

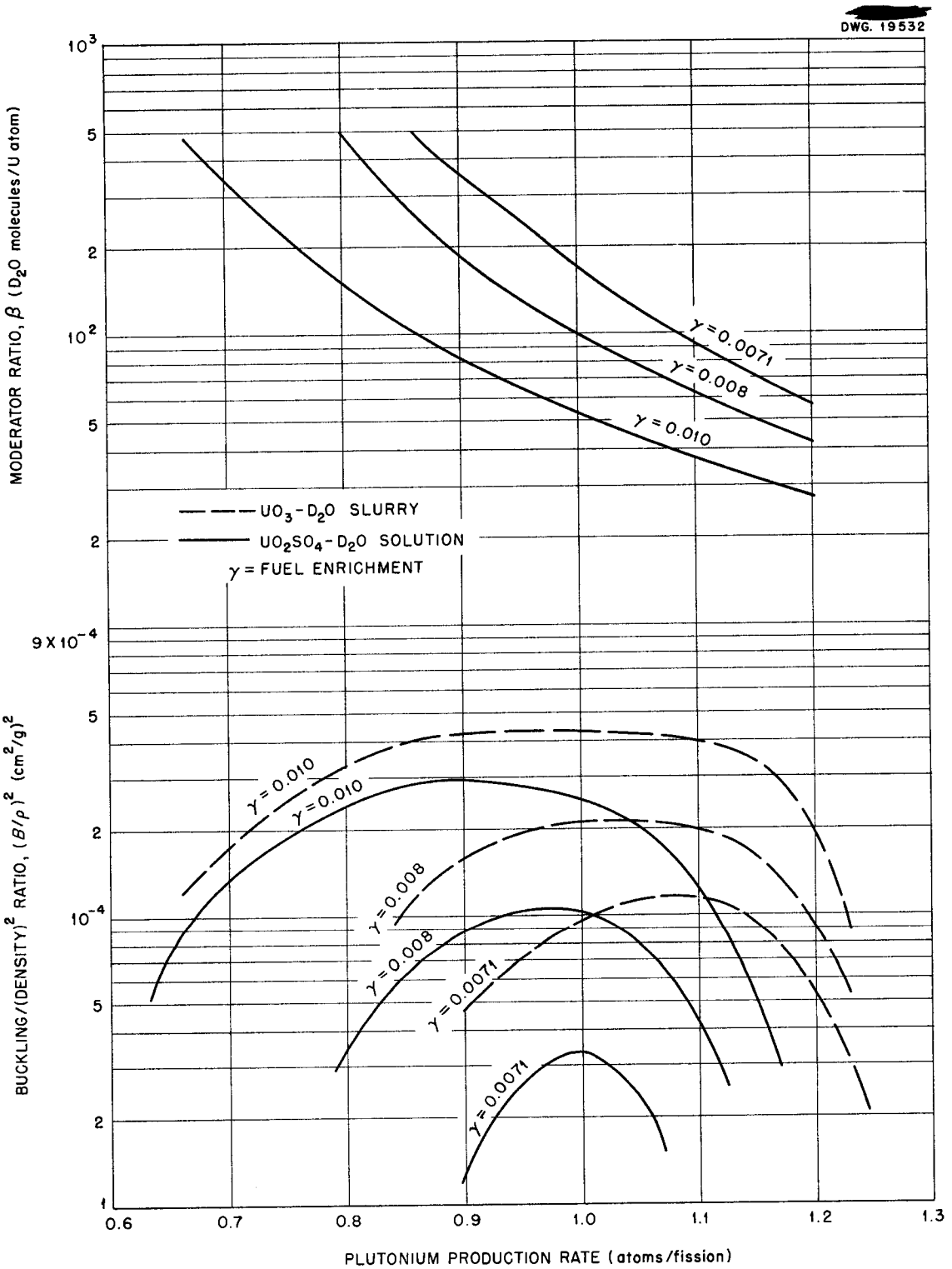

Fig. 9. Moderator Ratio and Ratio of Geometric Buckling to the Square of the Fluid Density as Functions of the Plutonium Production Rate.

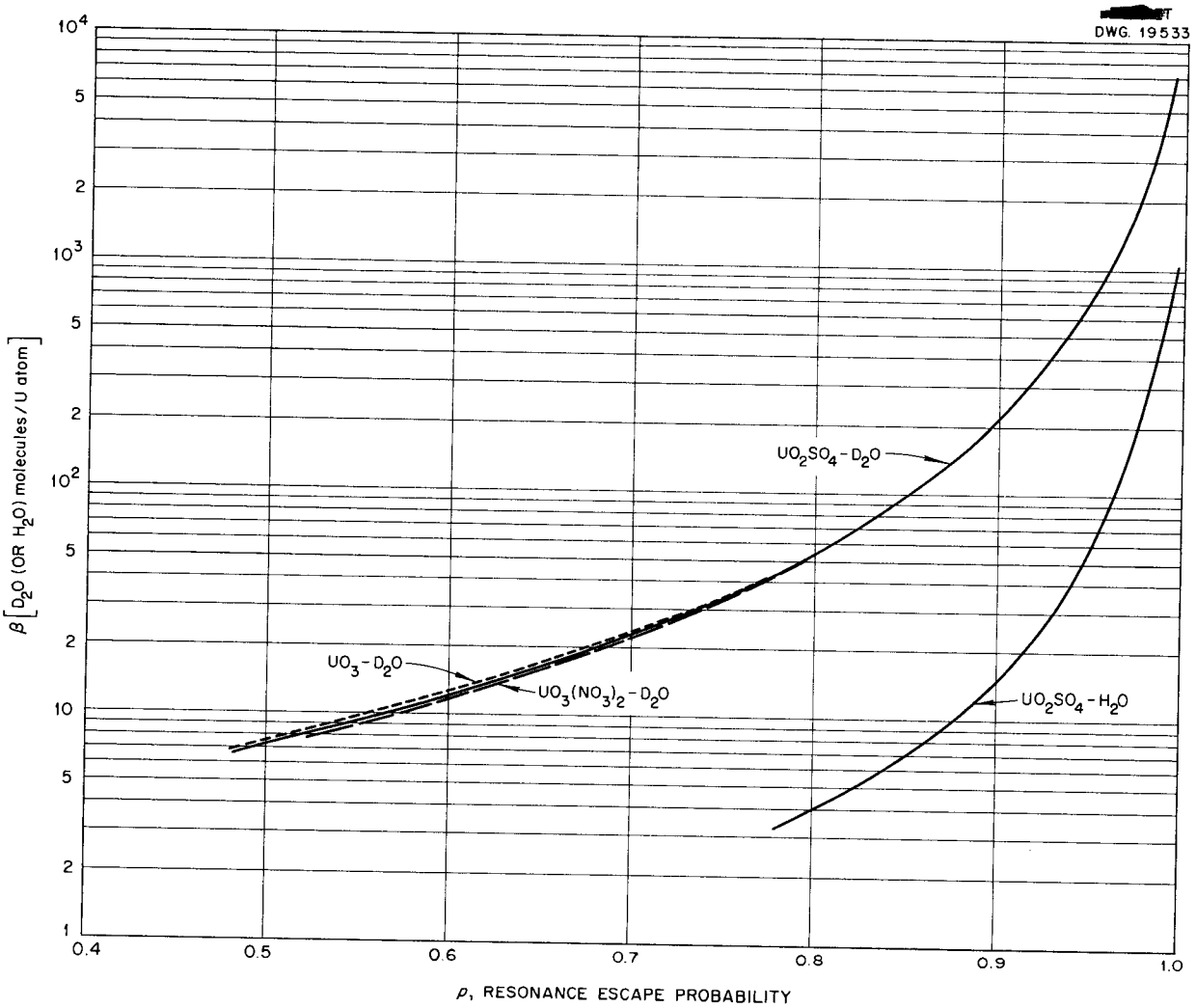

Fig. 10. Resonance Escape Probability for Uranium-Aqueous Systems.

uranyl sulfate solution in stainless steel were described in the last quarterly report.[5] Equipment design was completed and construction was started during this quarter.

POWER REMOVAL FROM BOILING REACTORS

W. S. Brown M. Richardson
H. A. MacColl P. C. Zmola

Power removal from boiling, aqueous, homogeneous systems depends in large measure upon the size of the unit. For small units (on the order of 2 ft in height), the predominant mechanism for energy removal is natural vapor rise through the bulk of the liquid. In large units (10 or 20 ft in height), natural convection, or circulation of the liquid-vapor mixture resulting from density differences in the core, is superposed on the natural vapor rise mechanism; for some arrangements, natural convection appears to be the predominant mechanism for energy removal. In addition, the existence of a free surface, particularly for

[5] R. N. Lyon *et al.*, *HRP Quar. Prog. Rep. Jan. 1, 1953*, ORNL-1478, p. 11.

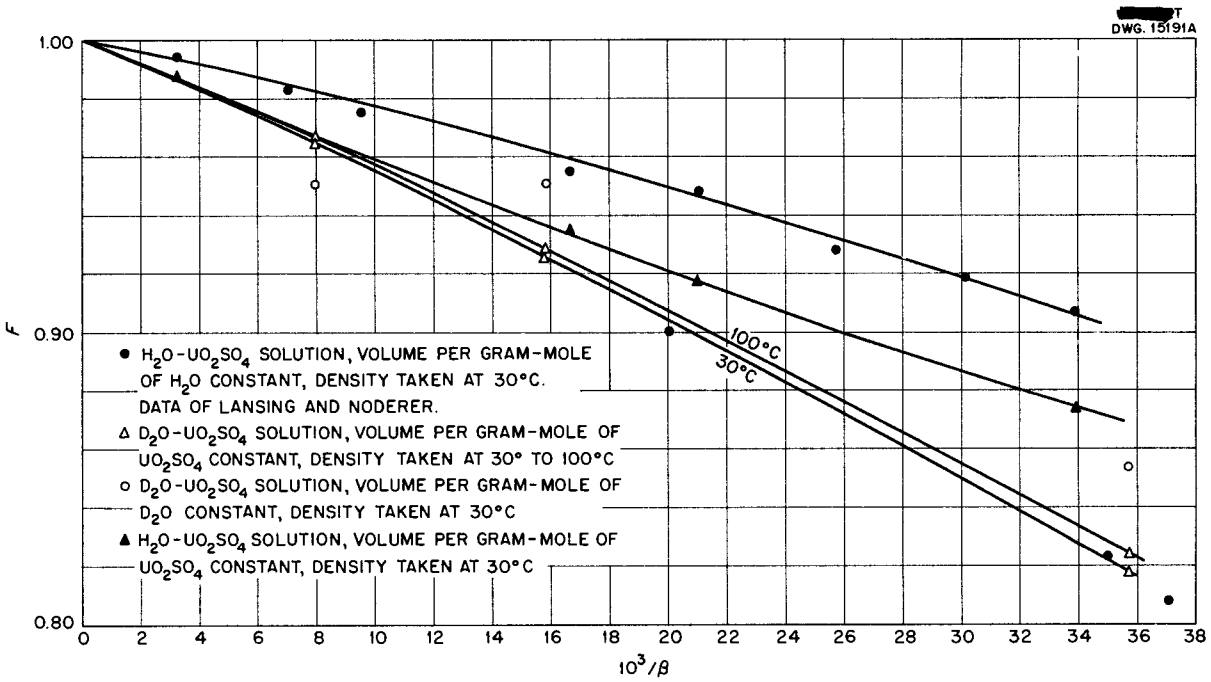

Fig. 11. Calculation of F vs. $10^3/\beta$ by Various Methods.

large units, may limit the power as a result of unsatisfactory vapor disengagement (splashing) at the top surface. These problems have been discussed to some extent in previous quarterly reports.

At present, effort is being directed toward obtaining information on

1. the specific power attainable in small electrical-resistance-heated volume boiling systems as a function of the mean density decrease and density distribution,
2. the influence of natural circulation and gas disengagement at the free surface in a mockup of a large-scale system in which air is bubbled into a 6-ft-dia tank filled with water,
3. the need for controlled vapor-separation devices in large-size units.

Volume Boiling in Small Systems. The apparatus has a test section 4 ft high and 6 in. square in which dilute acid and salt solutions are boiled by electrical-resistance heating of the liquid. The electrodes form two sides of the test section; the other sides are of Lucite. Vapor leaving the top is condensed and returned to the test section.

The mean fluid density is determined from measurements of the boiling liquid level. A vertical density distribution was obtained by measuring the attenuation of a collimated gamma beam through the fluid. A Lauritsen electroscope was used as the detector. The source was iridium which had been irradiated in the ORNL graphite reactor. The mounting of both the source and the detector permitted a traverse of the entire height of the test section. Glass-enclosed thermocouples were used to measure the vertical temperature distribution in the fluid.

The apparatus has been operated over a range of boiling liquid depths of from 2 to 36 in. and at total power levels of from 1 to 50 kw, which

resulted in specific power levels of from 0.3 to 12 kw/liter. The highest specific power corresponds to the lowest liquid levels. For liquid levels greater than 15 in., the maximum specific power attained was 2.75 kw/liter. A recent change in the power supply will make it possible to operate at a total power of 100 kw.

Photographs of volume boiling in the test section at 0.65 and 2.05 kw/liter are shown in Figs. 12 and 13. The sharp horizontal line indicates the nonboiling liquid level. Representative curves of the vapor fraction as a function of the vertical height in the boiling liquid, y/Y, are given in Fig. 14 for specific powers of 1.2 and 2.75 kw/liter. The vertical temperature profile is shown in Fig. 15.

An expression for the attainable specific power as a function of the mean density decrease and liquid height in a natural vapor rise system, obtained for a simple analytical model, has been reported previously:[6]

$$P = 0.04 \left(1 - \frac{\rho_{avg}}{\rho_l}\right)\left(\frac{1}{Y}\right)^{2/3}\left(\frac{h_{fg}}{U_{fg}}\right)^{2/3}\left(\frac{h_b \Delta}{f_D}\right)^{1/3}, \quad (1)$$

where

P = specific power, kw/liter,
ρ_{avg} = average density of reactor core, lb/ft^3,
ρ_l = density of liquid, lb/ft^3,
Y = height of boiling liquid, ft,
h_{fg} = latent heat, Btu/lb,
U_{fg} = specific volume change in evaporation, ft^3/lb,
h_b = heat transfer coefficient to bubble, Btu/hr·ft^2·°F,
Δ = liquid superheat, °F,
f_D = drag coefficient of bubble, dimensionless.

In Fig. 16, experimental results are compared with values predicted by Eq. 1

[6] R. V. Bailey, E. N. Lawson, H. A. MacColl, and P. C. Zmola, *HRP Quar. Prog. Rep. Oct. 1, 1952*, ORNL-1424, p. 15. Equation 6 as given in ORNL-1424 should have a numerical coefficient of 0.04 instead of 0.01, and Figs. 6 and 7 should be changed accordingly.

Fig. 12. Atmospheric-Pressure Volume Boiling at 0.65 Kilowatts per Liter.

Total power	86 kw
Initial liquid height	19 in.
Boiling height	22.5 in.
Average vapor fraction	0.15
Average vapor velocity above liquid level	0.9 fps

Fig. 13. Atmospheric-Pressure Volume Boiling at 2105 Kilowatts per Liter.

Total power	34 kw
Initial liquid height	19 in.
Boiling height	28 in.
Average vapor fraction	0.32
Average vapor velocity above liquid level	3.5 fps

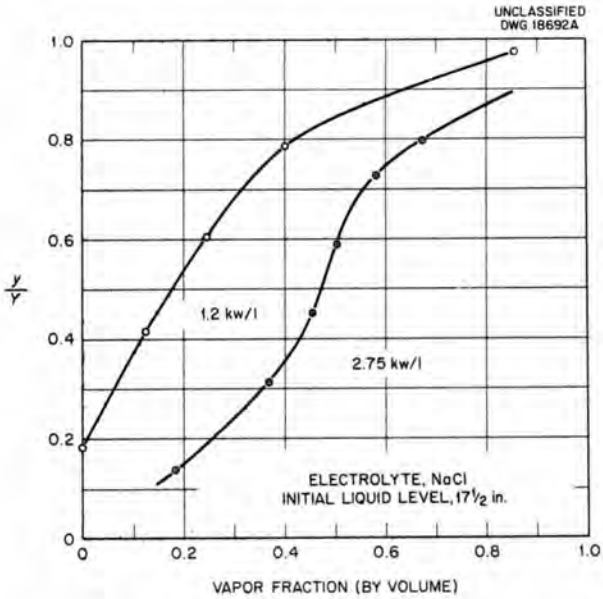

Fig. 14. Vertical Density Distribution in Atmospheric-Pressure Volume Boiling.

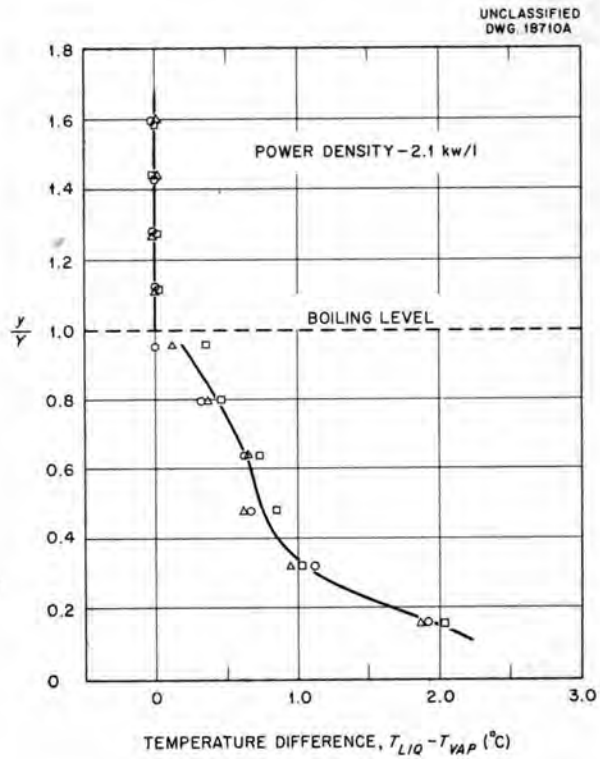

Fig. 15. Temperature Distribution in Atmospheric-Pressure Volume Boiling.

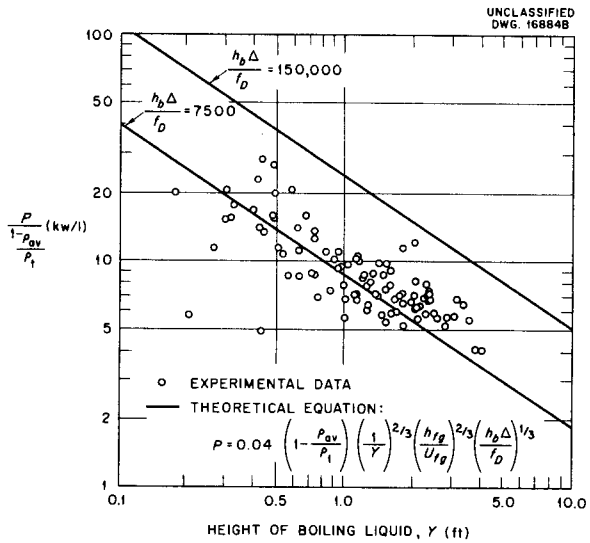

Fig. 16. Comparison of Theoretical and Experimental Values for Atmospheric-Pressure Volume Boiling.

At the time the equation was evolved, it was believed that values of 150,000 and 7,500 Btu/hr·ft^2 represented reasonable upper and lower limits of the parameter $h_b\Delta/f_D$. These were based on published values of h_b,[7] Δ,[7] and f_D.[8] In comparing the actual boiling conditions with the analytical model, there is an inclination to give little credence to the theoretical basis of the equation. In the actual system, the identity of the bubbles is lost even at moderate specific power. However, it appears that Eq. 1 can be used with some confidence in evaluating power removal for systems in which natural vapor rise predominates, provided an experimental value of $h_b\Delta/f_D$ obtained from a similar system is employed. In this case, the parameter rather than the individual factors would have significance.

It is planned to extend the present work to a higher pressure and to determine the splashing limits, that is, the conditions under which appreciable quantities of liquid are ejected from the violently agitated surface.

Mockup of Large-Scale Systems. A 6-ft-dia tank 12 ft high and open at the top has been set up so that it can be filled with water to various depths and so that air can be bubbled through canvas sheeting on the tank bottom to simulate boiling. The objectives of the experiment were outlined in the last quarterly report.[9] Some preliminary runs have been made. Values of mean density decrease of up to 0.3 were attained. Some circulation was evident, but it was not clear whether the circulation was characteristic of a unit of this size or simply peculiar to this system.

Controlled Vapor Separation in Large-Scale Units. It appears that circulation in large-size units will permit a noticeable specific power increase for a given mean density decrease, as compared with the specific power attainable by natural vapor rise only if a large fraction of the entrained vapor can be removed at every pass of the fluid mixture near the top surface of the reactor. At present, little information is available on the behavior of steam separation devices in the range of liquid-to-vapor ratios that are necessary for reactor application. The Babcock and Wilcox Co. was visited for a discussion of the possibility of obtaining their assistance in determining whether centrifugal separators are usable in a homogeneous boiling-reactor system.[10] A preliminary study indicated that there is an economic advantage to a boiling reactor that operates with circulation and separators as compared with a boiling reactor dependent only on natural vapor rise.

(7) M. Jakob, *Heat Transfer*, Vol. 1, Chap. 29, p. 620-635, Wiley, New York, 1949.

(8) L. Hopf, *Handbuch der Physik*, Vol. 7, p. 168, Springer, Berlin, 1927.

(9) P. C. Zmola, W. S. Brown, H. A. MacColl, and M. Richardson, *HRP Quar. Prog. Rep. Jan. 1, 1953*, ORNL-1478, p. 16-17.

(10) R. N. Lyon and P. C. Zmola, *Centrifugal Vapor Separators at Babcock and Wilcox-A Trip Report*, ORNL CF-53-2-67 (Feb. 7, 1953).

TEAPOT MOCKUP

J. R. McWherter R. L. Cauble

The 150-psi core tank for the Teapot mockup has been constructed, and the designs for a recombiner, an after condenser, and a supporting framework have been completed. Construction of these components has been delayed, however, pending a decision on the most practical condenser-recombiner arrangement.

The mockup of the core-condenser-recombiner system, as currently designed and partly constructed, is shown in Fig. 17. Many of the tests on this system will be meaningless, however, if liquid blanketing or iodine poisoning reduces or obliterates the effectiveness of the catalytic recombiner in operation as a reactor.

Several other arrangements are being considered, one of which is a succession of partial condensers with recombiners in the limited space between each condenser. One such arrangement, which will be tested during the coming quarter, is a unit designed for flame-recombination tests, which if favorable, will indicate considerable revision of the present mockup design. It is believed that steam dilution up to the coil just below any burning region will prevent serious flashbacks. A similar system with catalytic recombiners between condenser stages is also being designed for study.

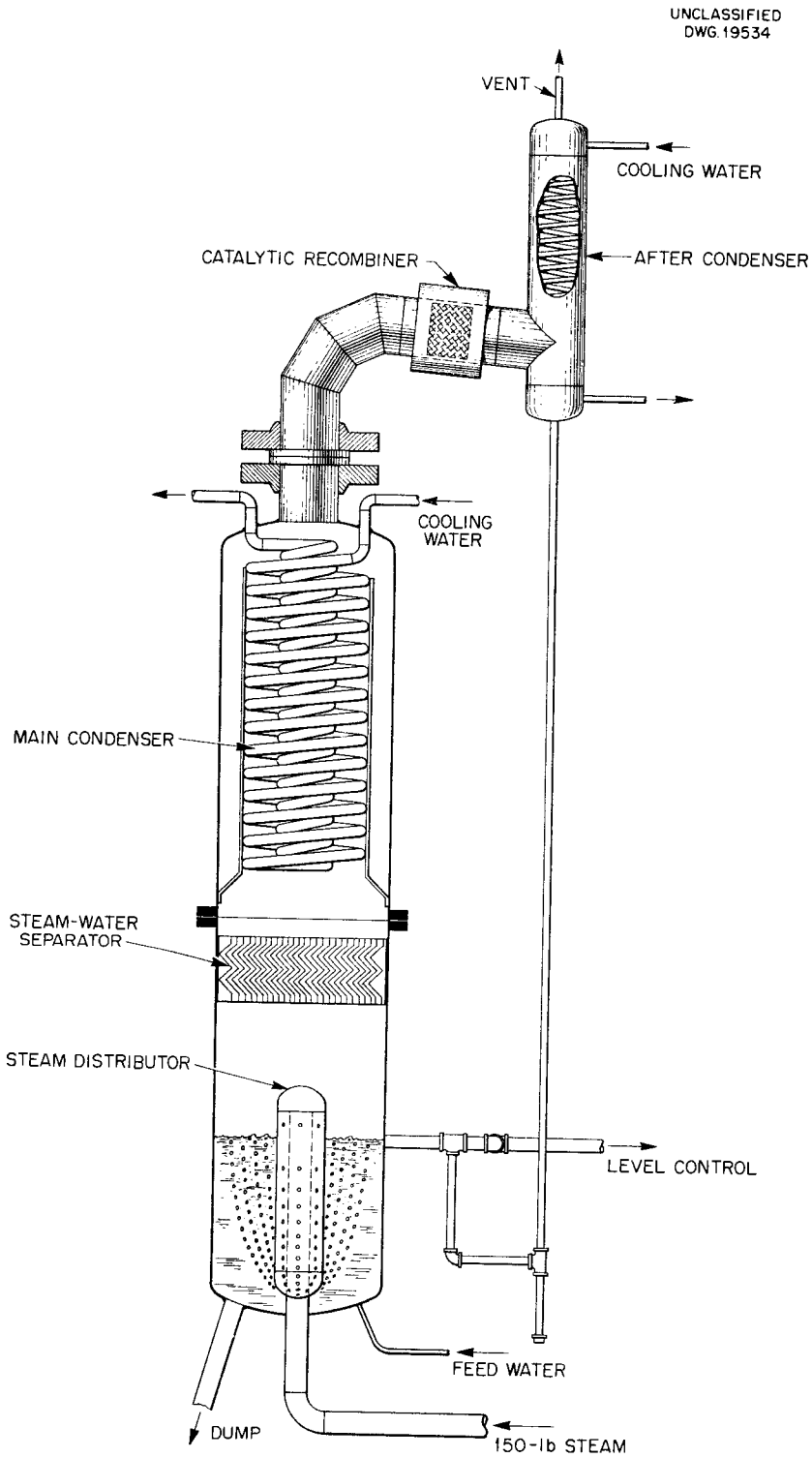

Fig. 17. Mockup of Core-Condenser-Recombiner System.

Part III

GENERAL HOMOGENEOUS REACTOR STUDIES

INTERMEDIATE-SCALE HOMOGENEOUS REACTOR DESIGN

R. B. Briggs, Section Chief

W. R. Gall, R. H. Chapman, M. Tobias, W. Terry
C. L. Segaser, D. K. Taylor, R. E. Aven, J. P. Sanders
F. C. Zapp, P. N. Haubenreich, L. Cooper

INTERNAL RECOMBINATION CATALYST

It has been shown that cupric ions in a fuel solution effectively catalyze the recombination of hydrogen and oxygen. The use of copper as an internal recombination catalyst in the ISHR has obvious advantages. Sufficient copper would prevent formation of gas bubbles in the core, eliminate any explosion hazard, and make a gas separator and external recombiner system unnecessary during normal operation. Disadvantages of copper in the system include parasitic absorption of neutrons, possible accelerated corrosion, and the rapid decrease in efficiency in effecting recombination as the temperature is reduced.

In order to estimate the effect of copper in the ISHR, calculations have been made to determine the amount of copper required and its effect on critical concentration and conversion ratio. If a homogeneous catalyst is used, the maximum concentration of hydrogen would occur at the core outlet. The hydrogen concentration at this point has been calculated as a function of copper concentration by a method which takes into account the changing temperature of the solution as it moves around the circulating system. Figure 18 shows the total pressure required to keep the gas in solution at 250°C, if a 1-to-2 ratio of oxygen to hydrogen is assumed. Also shown is the mole fraction of hydrogen and oxygen (in stoichiometric ratio) in the vapor phase at the corresponding pressure and 250°C. In order that the mixture be nonexplosive, this fraction must certainly be less than 0.3 and probably less than 0.2. Because the effectiveness of copper is quite sensitive to temperature, the results are dependent upon the assumed distribution of temperature in the core. Uncertainty as to the actual temperature distribution accounts for the band in the figure. Nuclear effects were calculated for two copper concentrations: 0.2 and 0.4 mole/liter. Results given below are for the two-region converter with a 1/4-in.-thick stainless steel core tank and a slurry blanket containing 1000 g of thorium per liter.

NUCLEAR EFFECTS OF COPPER ADDITION IN THE ISHR

Copper concentration, mole/liter	0	0.2	0.4
Critical uranium concentration, g/liter	4.79	4.93	5.50
Conversion ratio, atoms of U^{233} per atom of U^{235}	0.79	0.75	0.72

The effect of copper additions on the conversion ratio has not been determined for the 1/8-in.-thick core tank and for the higher concentrations of thorium in the blanket reported in previous quarterly reports. A qualitative examination of the conditions of interest indicates that the percentage change in conversion ratio should be nearly constant for a given copper concentration.

EVAPORATION OF D_2O IN THE GAS SEPARATOR

In operating the ISHR, it is necessary to evaporate D_2O from the fuel solution in the circulating system to change the fuel concentration, to provide D_2O for feeding

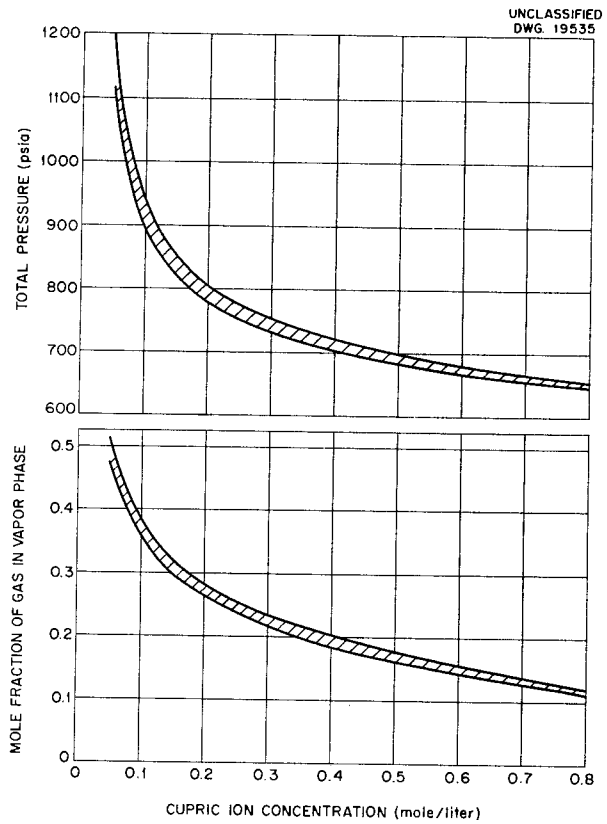

Fig. 18. Effect of Copper on Total Pressure and on Vapor-Phase Composition.

into the bearings of the pumps, and to operate valves or other mechanisms in the system. During normal operation there is a continuous supply of about 9 gpm of D_2O from the recombiner. A high-pressure evaporator has been shown on the flow sheets to supply 1.5 gpm of D_2O when the reactor is operating at very low power. This evaporator presents problems in minimizing holdup and in corrosion and stability of the fuel solution. The evaporator is operated at a temperature of at least 285°C, and the oxygen is rapidly stripped from the boiling solution.

A study has been made to determine whether an equal quantity of D_2O might be obtained by subcooling the gas which is recirculated through the recombiner system so that D_2O would be evaporated into the gas in the gas separator. The necessary heat would be supplied to the fuel solution by supplying steam to the main heat exchanger.

The amount of D_2O that would be evaporated in the gas separator at low power levels (no gas production) was calculated for various temperatures. The calculations were based on the following assumptions:

1. The gas is saturated with D_2O at the entering temperature.
2. The change in the temperature and quantity of the liquid stream in passing through the gas separator is negligible.
3. The flow of gas in the separator is 310 cfm for each calculation.

Two methods of calculation were employed which gave comparable results. Each method involved the calculation of film coefficients based on empirical equations developed for wetted-wall columns. In method I of the calculations, the individual heat and mass transfer coefficients were calculated separately, the total mass and heat transferred were determined, and the resultant temperature and amount of D_2O evaporated were found by trial and error. In method II, coefficients involving an enthalpy driving force were calculated from the same empirical relationships, and the resultant conditions were determined. The results of these calculations are shown in Table 1. It appears that a sufficient quantity of D_2O can be evaporated from the gas separator at temperatures above 150°C.

COOLING-TOWER REACTOR

In considering the evaporation of D_2O in the gas separator, the possibility was suggested that all the heat might be transferred from the fuel solution by evaporation of D_2O into a recirculated gas stream. A preliminary study has been made of a 50-megawatt reactor in which the heat is removed from the fuel solution in a cooling

TABLE 1. CALCULATED CONDITIONS OF OPERATION OF GAS SEPARATOR

	CASE I	CASE II	CASE III	CASE IV
Temperature of liquid, °C	250	250	200	150
Entering gas temperature, °C	230	200	150	100
Pound moles of gas entering per hour	1894	2014	2252	2553
Rate constants:				
k_g, lb-moles/hr·ft^2·atm	0.268	0.242	0.181	0.179
h, Btu/hr·ft^2·°F	64.6	69.6	70.6	76.4
K', Btu/hr·ft^2·Δ enthalpy	286	301	327	369
Method I				
Exit gas temperature, °C	232.9	207.8	155.8	104.9
D_2O evaporated, lb-moles/min	0.714	1.340	0.431	0.120
gpm	1.95	3.67	1.18	0.33
Method II				
Exit gas temperature, °C	233.6	210.0	155.9	104.4
D_2O evaporated, lb-moles/min	0.874	1.721	0.446	0.107
gpm	2.39	4.71	1.22	0.29

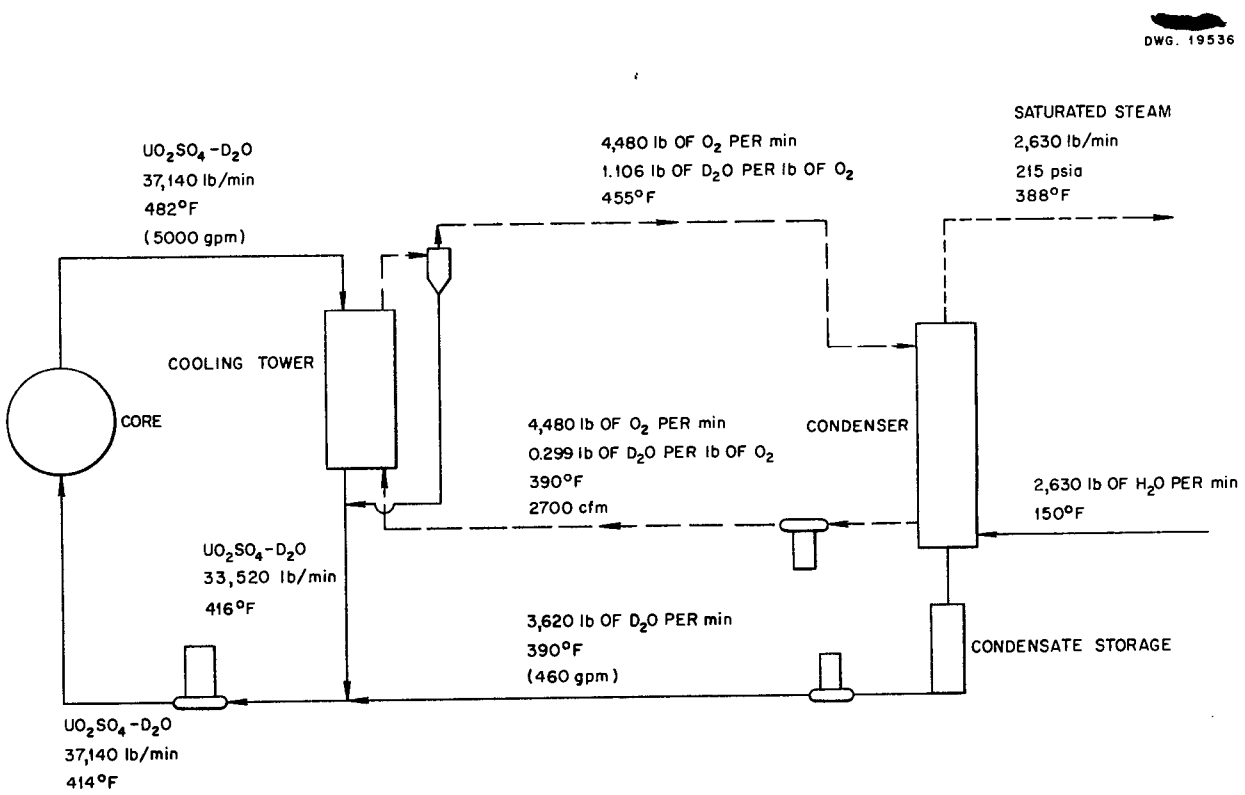

Fig. 19. Flow Sheet for Cooling-Tower Reactor.

tower. The solution is cooled by evaporation of part of the moderator as it passes countercurrently to an oxygen stream in a packed or slatted tower. The gas is cooled, and part of the vapor is condensed in a heat exchanger producing steam. Such a system should reduce corrosion problems in the heat exchanger and eliminate the gas separator, D_2O evaporator, and high-pressure storage tank.

It was found that the required oxygen flow and tower height increase rapidly with system pressure because, primarily, increased pressure reduces the amount of moisture associated with the gas at a given temperature. On the other hand, gas bubbles in the core make higher pressures necessary for reducing their volume. Use of an internal recombination catalyst would prevent excessive bubble formation and permit operation at lower pressures.

Figure 19 represents a system operated at 700 psia. At this pressure, gas bubbles would occupy 7.8% of the core volume unless an internal catalyst were used. Figure 20 shows a possible arrangement in which the core is inside the vessel containing the packing, that is, stacked 3-in. Raschig rings. Designed for the conditions in Fig. 19, the bed is 7 ft wide, 6 ft deep, and about 30 ft long. The condenser, as shown, has 2200 seven-eighths in. tubes 25 ft long. Solution holdup is about 3300 liters. In addition, approximately 1000 kg of D_2O is held up as vapor or in the condensate return line. This holdup compares favorably with the 4000-liter holdup of solution in the present ISHR.

ENGINEERING DEVELOPMENT

C. B. Graham, Section Chief

CORE AND GAS SEPARATOR DEVELOPMENT

J. A. Hafford I. Spiewak
L. B. Lesem R. H. Wilson

ISHR Core. The best flow arrangement for a high power-density core appears to be slug flow, with an equal temperature rise in each stream line. In addition to orderly heat removal, this type of core has other important advantages: low pressure drop, good gas removal, and a low turbulence level.

Slug flow is obtained in the core proposed for the ISHR by means of screens mounted in the entrance section, as shown in Fig. 21. Flow tests on an 18-in. plastic model indicate that this arrangement will be quite satisfactory.[1] Based on the experimental data, the pressure drop through the ISHR core at rated conditions is estimated to be 1.92 psi.

The screen specifications have been reported in an ORNL memorandum[2] that also includes a calculation of the maximum tensile stress caused in the screens by the flow; the calculated value was 5900 psi. It is believed that this is a safe value, especially since the calculation was quite conservative.

Flow tests on a full-scale ISHR core are planned for later this year to confirm the design. These tests will be followed by pressure tests to optimize the mechanical design of the core tank with respect to neutron absorption.

(1) C. B. Graham *et al.*, *HRP Quar. Prog. Rep. Jan. 1, 1953*, ORNL-1478, p. 45-60.

(2) L. B. Lesem, *Specifications and Stress Calculations for ISHR Screens*, ORNL CF-53-2-93 (Feb. 19, 1953).

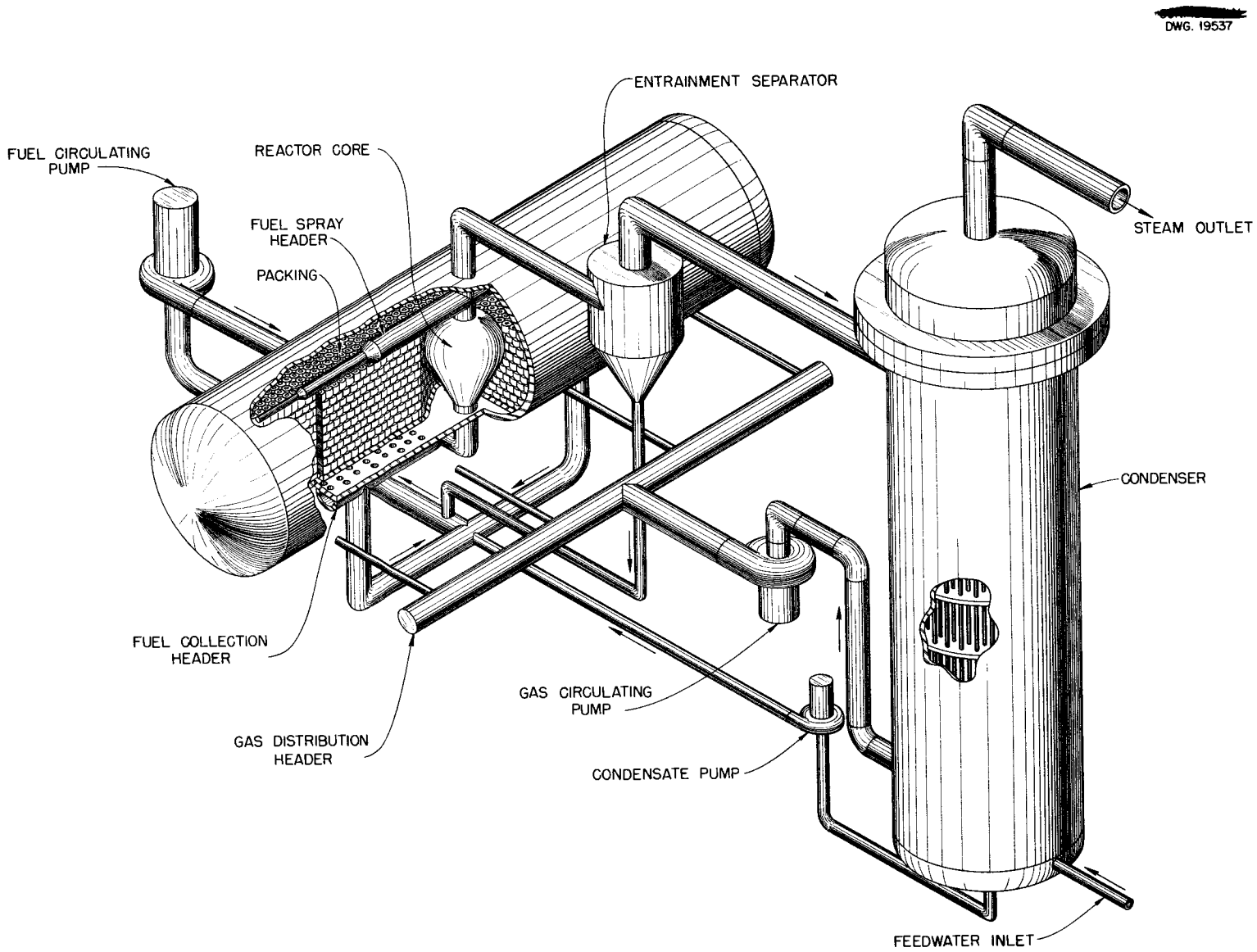

Fig. 20. Cooling-Tower Reactor.

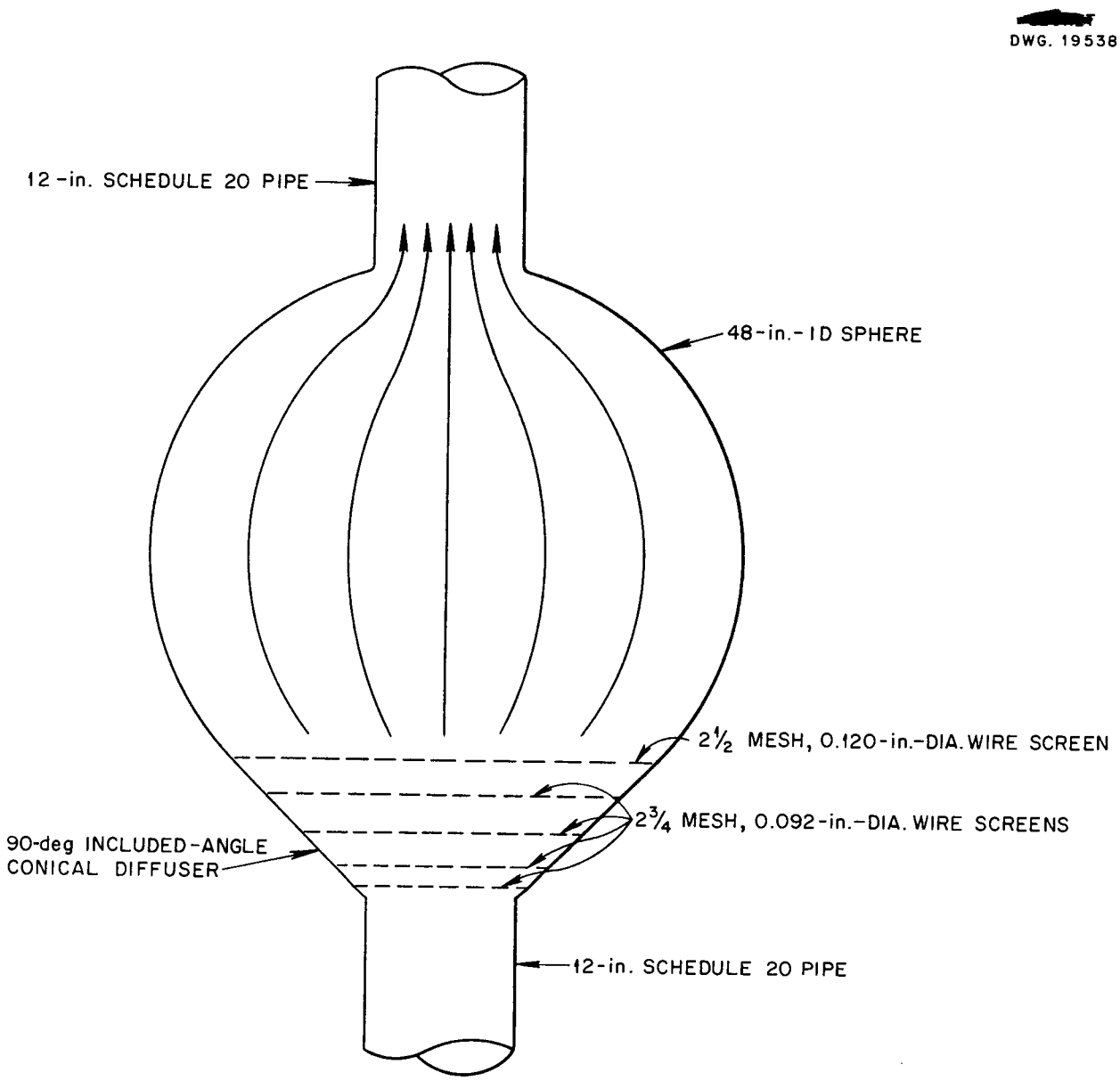

Fig. 21. ISHR Core.

Eight-Foot Rotational-Flow Model. The construction of the 8-ft rotational-flow model described in ORNL-1280[3] has been completed. Operation is expected to begin during the next quarter.

Pipe-Line Gas Separators. The use of straight-through flow in the ISHR core necessitates development of a gas separator for the external circulating system. It is desired to produce high separating efficiency without there being a great sacrifice in pressure drop and liquid holdup.

The system believed to meet these requirements best is a pipe-line

(3) C. B. Graham *et al.*, *HRP Quar. Prog. Rep. Mar. 15, 1952*, ORNL-1280, p. 151.

separator that uses a volute or stationary vanes to give the liquid a rotating component. The rotation centrifuges gas into a central void from which it is removed. Following the gas removal section, most of the remaining rotational energy can be recovered with either vanes or a volute.

Operation of a 5-in. pipe-line separator was described in previous quarterly reports.[4,1] This model has been tested with both vanes and volutes to give rotation and pressure recovery. The following conclusions were drawn from the investigation:

1. Both vanes and volutes provide a gas-separating efficiency of close to 100%, provided the gas takeoff is properly designed.
2. Either vanes or volutes may be used for pressure recovery with about equal success. The estimated efficiency is about 70%.
3. The over-all pressure drop across the separator can be limited to two inlet velocity heads, or 5.4 psi, at an inlet velocity of 20 fps. The over-all pressure drop will be lower when vanes are used to produce rotation than when a volute is used.
4. The length of separator required is about 3 to 6 pipe diameters, depending on design conditions.
5. The gas void produced by a volute is more stable than that produced by vanes, since the wakes produced at the trailing edge of the vanes adversely affect stability. This is particularly true when the void diameter is more than half the pipe diameter.
6. Vanes are much easier to construct than volutes, particularly if the latter must withstand 1000 psi.
7. For most layouts vanes require less holdup of fuel solution, since they fit directly into an existing pipe in the high-pressure circulating system. However, if a layout requires two 90-deg elbows, volutes may be used without there being any sacrifice in holdup.

The relatively high pressure losses in a volute used to impart rotation to the fluid are caused by the increase in rotational velocity as the fluid moves radially inward, as shown in Fig. 22. A modified volute has been built that eliminates this radial velocity, as indicated in Fig. 23. Fluid enters the pipe from a rectangular inlet, which is on a chord of the pipe, and is deflected axially by a helical vane. As a result, there is little radial movement of liquid and minimum pressure loss. Preliminary tests of this modified volute indicate that gas separation is excellent and that the pressure losses are only slightly higher than those for an equivalent set of vanes.

Although development of vanes and volutes appears to be well under way, the ISHR gas separator cannot be specified until a suitable gas takeoff is developed. The gas takeoff can be located at either end of the separator, and its size and shape will determine void size and gas separating efficiency. In principle, it should be sized so that all the gas comes off without liquid entrainment. In practice, some liquid must be withdrawn with the gas as a means of controlling the size of the vortex.

If a small, centrally located takeoff is used, a small void with high gas-separating efficiency is obtained. Applied to the ISHR system, this takeoff would be large enough to remove gas formed in the core but too small to allow dilution to a nonexplosive mixture in the void of the gas separator.

If a large void that will also serve as a pressurizer is desired, some sort of annular takeoff is required to maintain a void large enough to accommodate liquid expansion under all operating conditions.

---

[4] C. B. Graham *et al.*, *HRP Quar. Prog. Rep. Oct. 1, 1952*, ORNL-1424, p. 62.

Although several annular takeoffs have been tested, none have proved satisfactory, since gas removal efficiency has been below 80%. Several new designs will be tested during the next quarter.

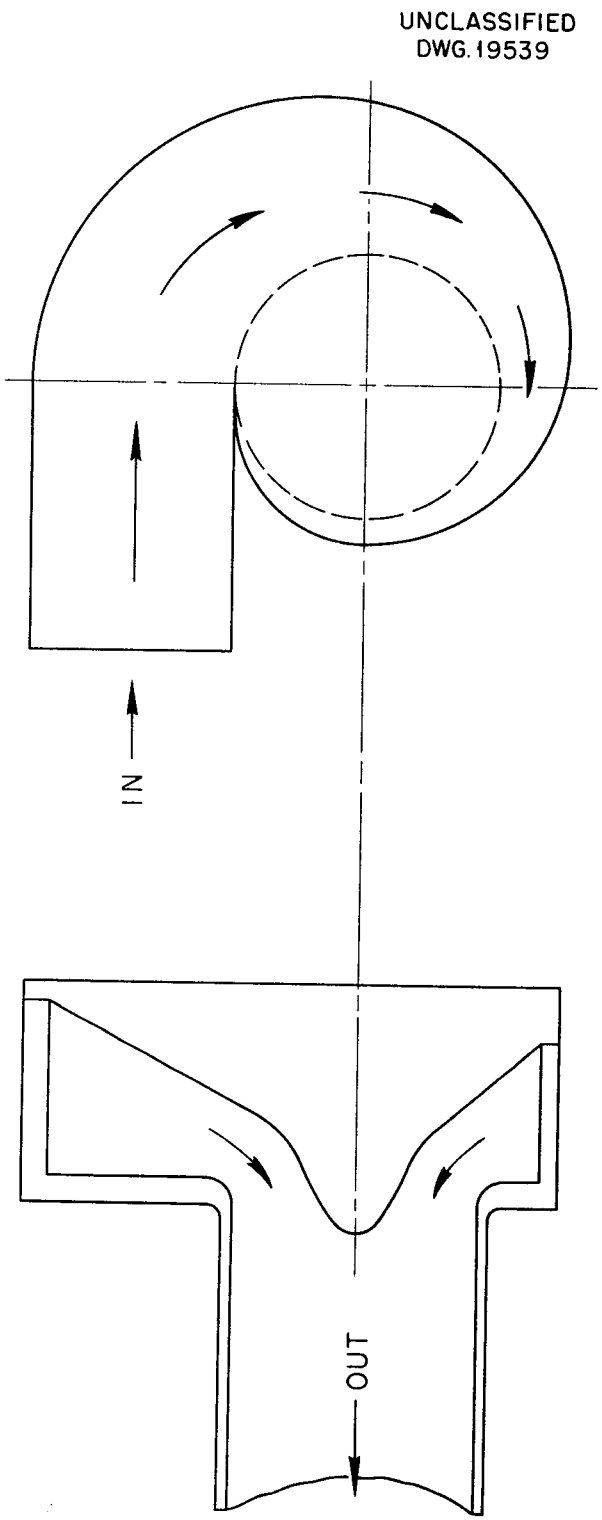

Fig. 22. Volute.

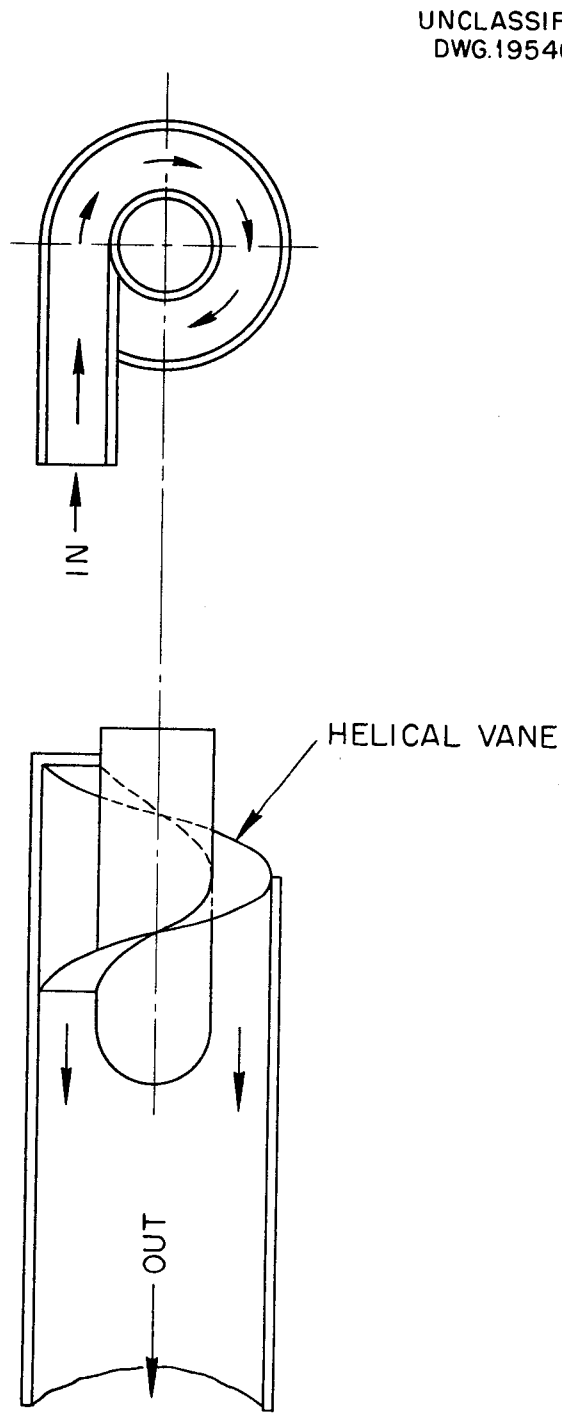

Fig. 23. Helical Volute.

RECOMBINER DEVELOPMENT

J. A. Ransohoff I. Spiewak
S. R. West

Tentative specifications have been prepared for a high-pressure ISHR recombiner. The recombiner consists of platinum deposited on alumina packing arranged in a fixed bed 2 1/2 in. deep and containing 1.75 ft^3 of packing. Since it is desired to operate with a safe, nonexplosive gas, the off-gas from the gas separator is diluted to 2 vol % D_2 before being fed to the recombiner. The pressure drop through the bed under these operating conditions is estimated to be 0.25 psi.

The recombiner design is based on the assumption that deuterium and oxygen diffusion to the catalyst controls the reaction rate. This had been suggested by two MIT Practice School groups[5,6] for the flow range used in the design (630,000 scfh of gas per ft^3 of catalyst). The theoretical efficiency of recombination in the bed is 99.99%; however, practical considerations will probably reduce this.

Since the existing data on catalytic recombiners were obtained at atmospheric pressure in clean beds, further development is required to increase confidence in the proposed design. A recombiner test unit (Fig. 24) has been built that is capable of handling up to 2 scfm of hydrogen. The effects of the following variables will be studied:

1. pressure,
2. hydrogen and oxygen concentration,
3. deuterium behavior as compared with that of hydrogen,
4. traces of iodine,
5. traces of entrained uranyl sulfate.

In addition to being used for evaluating the packed bed, the test

(5) T. W. Costikyan, C. B. Hanford, and D. L. Johnson, *The Catalytic Recombination of Hydrogen and Oxygen*, KT-130 (June 2, 1952).

(6) J. V. Gaven, R. B. Bacastow, and A. C. Herrington, *Catalytic Recombination of H_2 and O_2-II*, KT-134 (Aug. 29, 1952).

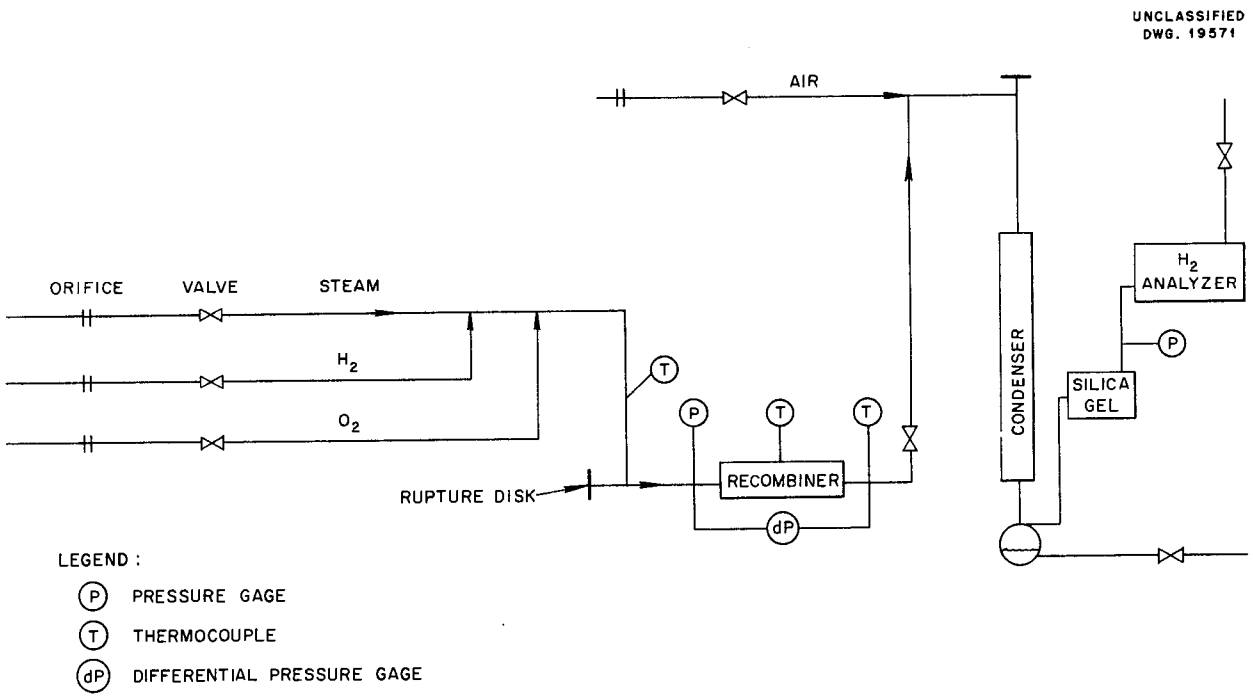

Fig. 24. Flow Diagram of Catalytic Recombiner Test Unit.

unit will be used to evaluate the feasibility of a tube-and-shell recombiner, which utilizes stainless steel tubes with a platinized, porous, stainless steel surface. If this design is feasible, the heat of the reaction would be rapidly removed from the surface where it is generated, and, as a result, less diluent gas would be required.

Some preliminary runs have been made in the test unit with the use of a packed-bed catalyst. Pressures have been varied from 25 to 75 psia, and hydrogen concentrations from 2 to 7% have been used. The low-pressure results thus far obtained appear to be in reasonable agreement with the MIT data referred to above. Raising the pressure increases recombination efficiency, and therefore design of high-pressure recombiners is, apparently, justified on the basis of data obtained at atmospheric pressure.

GAS CIRCULATOR FOR ISHR RECOMBINER SYSTEM

W. L. Ross

Recent calculations[7] have shown that the ISHR will produce at 48-megawatts power approximately 1.0 lb-mole of deuterium per minute, which corresponds to a *G* value of 1.67. Experimental data indicate that this assumed *G* value is conservative. Studies made at Battelle[8] on explosion limits of hydrogen-oxygen-water systems indicate that a gas-vapor mixture which has a hydrogen partial pressure of 2% of the total pressure will probably be nonexplosive at the ISHR design pressure and temperature. Consequently, there must be a gas-vapor circulation rate of about 50 lb-moles/min to render the dissociation gases nonexplosive and to maintain a safe recombiner system.

The gas-vapor mixture is withdrawn from the circulated reactor fuel by a gas separator and it passes through an entrainment gas scrubber which removes entrained moisture. From the scrubber, the mixture is delivered to the catalytic recombiner followed by a gas cooler-condenser. A gas circulator or blower then forces the gas-vapor mixture into the gas separator which again picks up dissociated gases and delivers them through the recombiner system.

Preliminary consideration of a recombiner system which employs a small void gas separator, a gas scrubber, a packed-bed type of catalytic recombiner, a condenser which condenses a small portion of the vapor, and appropriate piping indicates that the pressure drop required to circulate 50 lb-moles/min of gas mixture is in the range of 2.5 to 5 psi. A more accurate calculation of the pressure drop cannot be made at the present time because none of the system components have been designed.

The service requirements of the gas circulator needed to provide sufficient gas-vapor flow under ISHR design conditions can be stated on a tentative and approximate basis, as follows:

Capacity	1250 lb/min (~470 cfm)
Developed head	135 ft at 2.5 psi to 270 ft at 5 psi
Suction pressure	990 psia
Gas temperature	480°F
Gas density	2.7 lb/ft^3
Fluid horsepower	5 hp at 2.5 psi to 10 hp at 5 psi
Gas	Steam and oxygen with radioactive contamination
Leakage	No leakage to atmosphere permissible

There should be no problem in fabricating a circular impeller to meet the requirements because the

(7) J. P. Sanders, *Gas Production in the ISHR*, ORNL CF-53-1-110 (Jan. 6, 1953).

(8) H. A. Pray, C. E. Schweickert, and E. F. Stephan, *Explosion Limits of the Hydrogen-Oxygen-Water System at Elevated Temperatures*, BMI-705 (Nov. 1, 1951).

impeller can be quite similar to the usual pump impeller. The degree of corrosion attack should be small compared with that for a fuel-medium pump. A semistandard canned-rotor-pump motor can probably be used for driving the impeller. The motor will be mounted vertically below the impeller, and condensed D_2O from the gas system will flow through the motor; therefore, water-lubricated bearings can be used in the motor. A water-gas interface would be provided by an overflow below the impeller. Preliminary discussions of this arrangement with prospective manufacturers indicate that a blower designed for operation in this manner will be relatively easy to develop.

PULSAFEEDER PUMP TESTS

P. N. Stevens C. D. Zerby

Diaphragm Endurance Tests. The diaphragm endurance test[1] in which compressed air is used to move the diaphragm was continued until ten million cycles were accumulated. The diaphragm was tested periodically for leaks, and none were detected throughout the duration of the test. Visual examination of the diaphragm showed no obvious cracks; however, some small pits appeared near the outer edge. The Metallography Section is studying the pits and looking for incipient fatigue failure in the diaphragm.

Diaphragm Stress Analysis. The present, calculated value for maximum stress in the diaphragm is 20,000 psi and the experimental value is 24,000 psi. Further work must be done to establish confidence in the results obtained both mathematically and with strain-gage experiments. Tests to date have been run on a diaphragm 0.019 in. thick. The next step will be to study a series of thicker diaphragms.

STELLITE PISTON PUMP TEST

J. S. Culver

The test[1] of the pump with a Stellite No. 3 piston and cylinder has operated a total of 500,000 cycles vertically on distilled water, 500,000 cycles horizontally on distilled water, and 450,000 cycles on uranyl sulfate solution containing 40 g of uranium per liter at room temperature. Visual observation and photographs show no evidence of galling of either the piston or the cylinder. Rubbing surfaces are being polished to a mirror finish.

There was no visible evidence of corrosion after any of the runs; however, a brown, gummy material appeared in the system after operation on uranyl sulfate. This material has not as yet been identified, but it is thought to be merely an accumulation of oil from the air supply. The uranyl sulfate solution is perfectly clear. The total time of operation on uranyl sulfate solution was 504 hours.

TEST LOOP FOR 4000-gpm PUMP

J. S. Culver

Construction of the loop[9] for testing the 4000-gpm pump has been started. Design of the electrical supply for the pump is 50% complete, and material for this work will be ordered immediately. The construction can proceed to completion with little delay, and the proposed completion date is August 1, 1953.

ISHR HEAT EXCHANGER

R. B. Briggs W. L. Ross
W. R. Gall L. F. Goode
C. B. Graham

Recent discussions with prospective fabricators of the ISHR heat exchangers have emphasized the major problems involved in obtaining a suitable exchanger.

---

[9] J. R. McWherter *et al.*, *HRP Quar. Prog. Rep. Nov. 15, 1951*, ORNL-1221, p. 18.

Tube Sheets. Considerable difficulty has been experienced in obtaining large, high-quality, type 347 stainless steel forgings or plate for tube-sheet fabrication. The use of type 304 stainless steel or stainless clad steel for the sheets and other heavy parts may present a possible solution to this difficulty.

Tube and Tube Joints. A small percentage of the stainless steel tubing used, both seamless and welded, has been found to be faulty by heat exchanger manufacturers. Special precautions should therefore be taken to test the tubing adequately. Since no inspection procedures have been established, techniques will have to be developed to cull the faulty tubing. Tube-to-tube-sheet welding techniques require further development to eliminate nonuniformity. The solution to this problem may tie in with the development of an automatic welding machine. The corrosion resistance of rolled or flared tube joints must be investigated.

SMALL CANNED-ROTOR PUMP DEVELOPMENT

Allis-Chalmers 5-gpm Pump (W. L. Ross). As stated in the previous report,[1] some pump parts are subject to corrosion by fuel solution. Therefore, five Allis-Chalmers 5-gpm pumps, similar to the one that has been operated satisfactorily with water, have been ordered for general utility purposes in corrosion programs and in the development of an in-pile loop. Fabrication should not take long because some of the critical construction materials (stainless steel) were supplied to the manufacturer. The five pumps will be constructed so that the pump casing can be closed by either a metal gasket or a seal weld. Otherwise, the pumps are the same as the model which has been tested.

ORNL Small Pump (C. D. Zerby, T. H. Mauney, C. B. Graham). Two, small, canned-rotor pumps (described in the previous quarterly report,[1]) are being fabricated for test purposes. One of the pumps will have a rotor which will be machined from a solid rod of type 410 stainless steel; the other will have a standard rotor which will be canned in type 347 stainless steel. The discharge from one pump will have the normal tangential outlet from the volute; the other will have an axial outlet. The axial discharge is to be used on the pump for the in-pile loop described in the section of this report on "Corrosion."

Development of a stator from a standard 1/2-hp motor to operate the pump is now in progress. Cooling of the stator laminations and coil will be attempted by running water cooling tubes through the cooling holes in the stator iron; an alternate method of air cooling will also be investigated.

CONVERSION OF THE HRE MOCKUP TO OPERATE WITH URANIUM OXIDE SLURRY

C. D. Zerby W. L. Ross

Prior to converting the HRE mockup for operation with uranium oxide slurry, a series of component tests of various parts of the system were planned. The first component test consisted of pumping slurry through a low-pressure loop with a 1-gpm Lapp pulsafeeder pump; the results of this test were reported in the previous quarterly progress report.[1] Subsequent alterations to the low-pressure loop converted it for high-pressure operation, and it now includes a let-down heat exchanger and let-down valve to mockup the let-down system of the HRE.

Considerable difficulty was encountered with the slurry settling in the suction line to the pulsafeeder pump during shutdown; if the suction line was made small, the line would plug; if the line was made large, the slurry would not resuspend upon startup because of low velocities.

This problem has not been solved, but it is believed that continuous circulation to the dump tanks through the suction line of the pulsafeeder pump when it is not in operation may be the solution.

Samples of the mixture being circulated were taken periodically during several days of intermittent operation. A chemical analysis of the samples indicated a variation of approximately 40% in concentration at 200 and at 50 g of uranium per liter of mixture. This variation in concentration is attributed to the poor mixing conditions in the loop dump tank. It is apparent that a recirculation pump loop on the dump tank is necessary to maintain a consistent concentration in the tank and, therefore, in the system.

Helium was injected into the top of the let-down heat exchanger during one run to observe whether unstable flow conditions would be created in the let-down system which would give rise to oscillations in pressure in the system. At room temperature, 800-psig pressure, a solution concentration of 150 g of uranium per liter, and a flow rate of 1.146 gpm from the pulsafeeder pump, a gas-to-liquid volume ratio of 7.076 was achieved with no observable oscillations.

The let-down valve plug and seat were removed and observed for wear. After 95 hr of operation at concentrations of from 50 to 300 g of uranium per liter, only the very slightest indications of the flow pattern were observable on the valve plug. Work has stopped on this program because of time demands of other developmental work.

CORROSION

E. G. Bohlmann, Section Chief

PUMP LOOP OPERATION AND MAINTENANCE

H. C. Savage R. A. Lorenz
D. Schwartz

Loop Status. Ten dynamic corrosion test loops have been in almost continuous operation during the past quarter. Major emphasis has been on operation with solutions of uranyl sulfate under various conditions; only one loop has been in operation with uranyl fluoride solution. Dynamic corrosion tests were conducted, as previously described,[1] on various metals and alloys in the form of round-pin and flat-coupon test specimens.

Loop F was dismantled and cut open for examination of the interior of the pipe. In view of the operating history of this loop (~2100 hr with uranyl sulfate solutions containing 100 to 300 g of uranium per liter at 250°C), the interior surfaces of the 1 1/2-in. type 347 stainless steel pipe were in good condition. The straight sections of pipe were coated with a smooth, black film which is very difficult to remove, and there is no evidence of pitting. The welds in the straight sections of pipe were also in good condition (Fig. 25).

The areas of pitting and corrosion were confined to a few isolated areas where there was high turbulence. As usual in test loops circulating solutions of uranyl sulfate of these concentrations and temperature, the pump impeller and impeller housing were severely pitted and corroded.

[1] H. C. Savage *et al.*, *HRP Quar. Prog. Rep. Mar. 15, 1952*, ORNL-1280, p. 46.

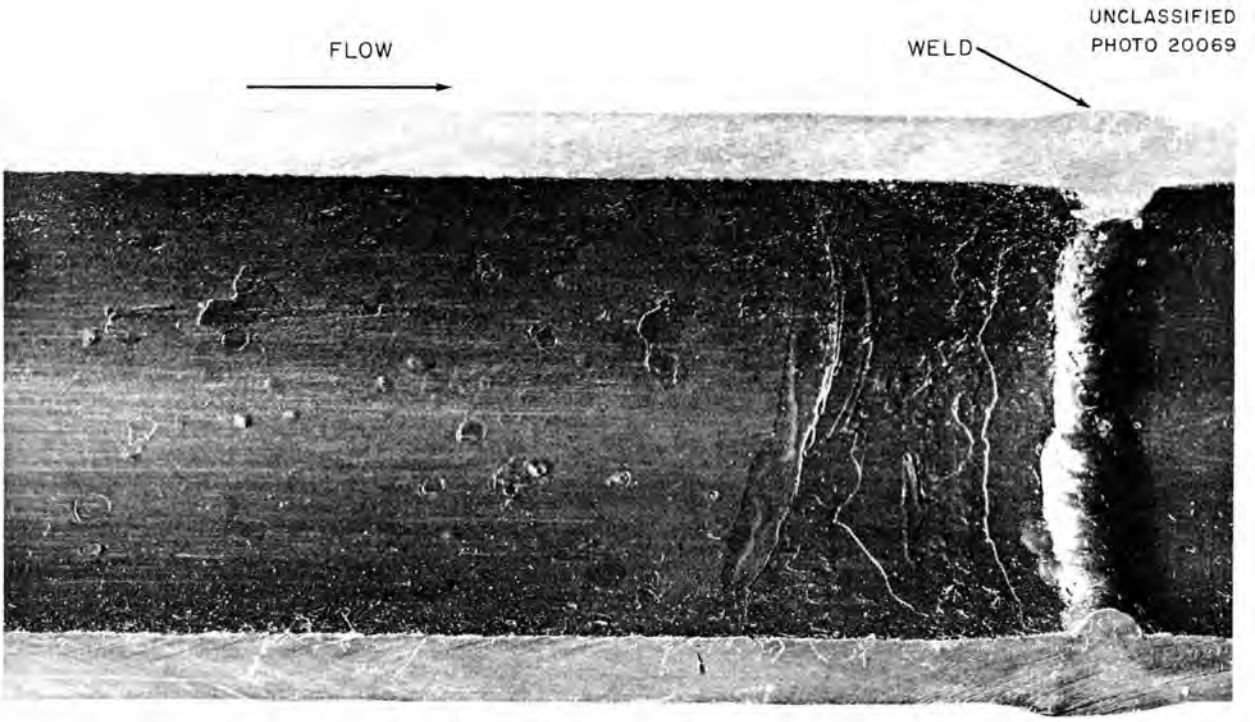

Fig. 25. Straight Pipe Section, Loop F.

In addition, a section of pipe, up to a distance of about 5 in. downstream from a flow restrictor, was pitted and corroded (Fig. 26), as were the butt welds of three, forged, type 347 stainless steel tees downstream from the change in direction of flow (Fig. 27). The bulk flow rate in the loop was about 17 fps. In particular, heavy, localized attack was found at the junction of the 1 1/2-in. pipe and the small 1/4-in. by-pass pipe used to direct solution flow to the pin and coupon test specimens. No serious corrosion was found in the straight sections of the smaller pipes that are more than 1 or 2 in. beyond the take-off point. The bulk velocity in the 1/4-in. pipes was about 45 fps. The entire loop has been cross sectioned and mounted on a plywood board; it is available for inspection.

One new loop, which replaces the dismantled loop F described above, was completed and put in operation during the past quarter. This loop was made with 1 1/2-in., schedule 80, type 347 stainless steel pipe throughout. All welds were made with the inert-gas heliarc method and type 347 stainless steel welding rod. The pressurizer was designed to serve as a gas separator. It contains a tangential inlet and straightening vanes at the outlet (Fig. 28). The two sections designed to contain sample units were placed so that one set of sample units could be exposed to a two-phase (gas and liquid) solution and the other to the solution returned from the gas separator. Loop operation is as follows: The system is filled with liquid to a point above the top sample line entrance to the pressurizer. Gas, usually oxygen, is

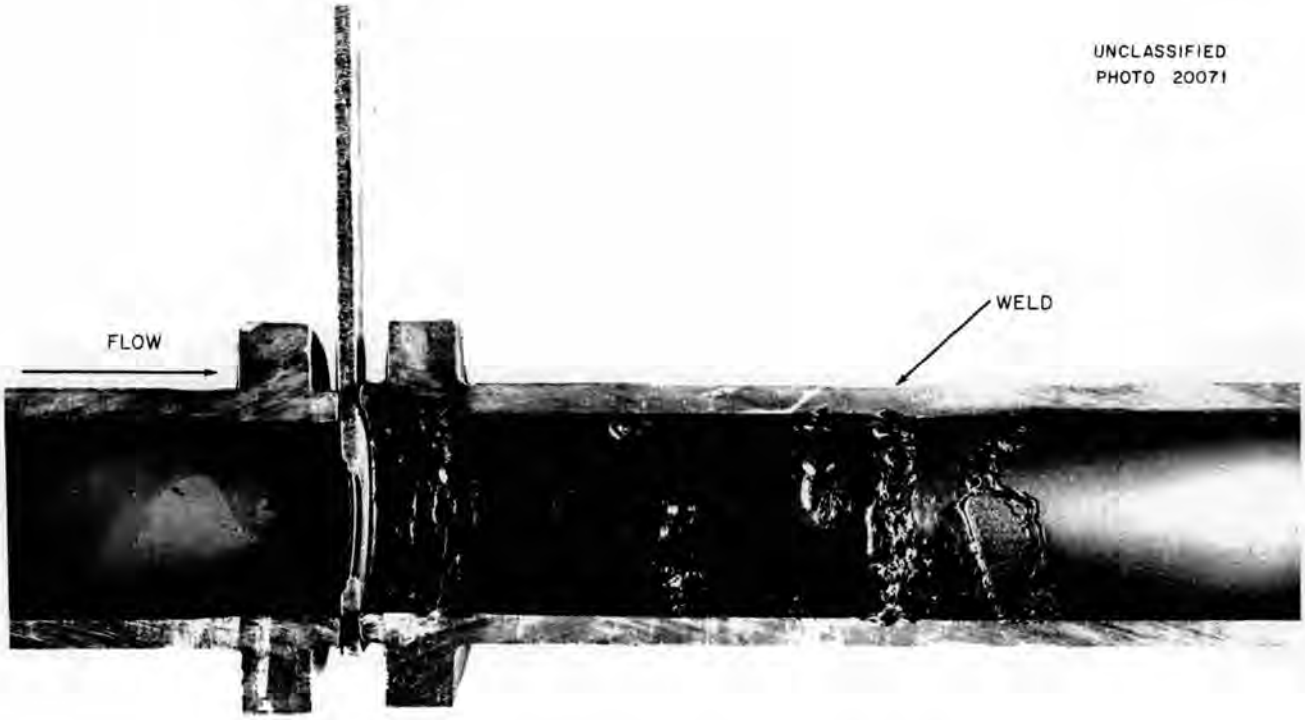

Fig. 26. Orifice Plate Section, Loop F.

then introduced to a pressure of about 200 psig. This is done to supply the oxygen necessary for solution stability and to maintain an excess pressure to prevent boiling of the liquid. With the liquid circulating, some of the excess oxygen (and steam) from the top of the pressurizer is pumped back into the loop ahead of the pressurizer through a 1/4-in. tube connected to a venturi. An orifice plate in the line ahead of the pressurizer provides pressure for the flow through the top sample unit. The circulating solution passes through a second unit after most of the excess gas has been removed. However, this solution still contains gas in excess of that required for saturation.

The purpose of this arrangement is to evaluate the effect on corrosion and/or erosion of uranyl sulfate solution containing oxygen concentrations above saturation. Based on the calculated theoretical values for the solubility of oxygen in water, the solution leaving the gas separating pressurizer contains about 30% more oxygen than that required for saturation, whereas the solution entering the pressurizer and passing through the top sample holder contains three to seven times the amount required for saturation. These values can be varied somewhat by changing the liquid level in the pressurizer and the size of the orifice plates used in the circulating line. However, it has not been possible to obtain perfect separation.

An initial run on this loop is now in progress with a solution of uranyl sulfate containing 300 g of uranium per liter at 250°C. The calculated solubility of oxygen (based on the Henry's law constant for water) at

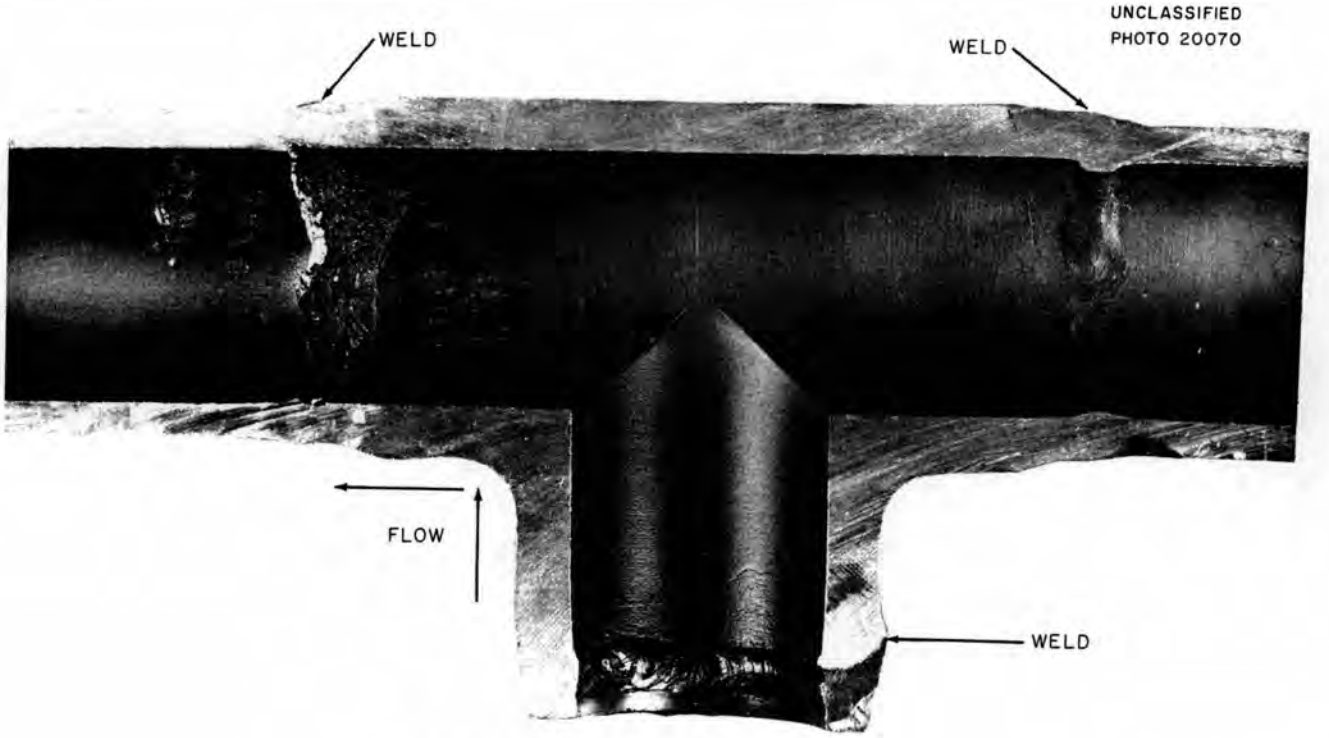

Fig. 27. Forged Tee, Loop F.

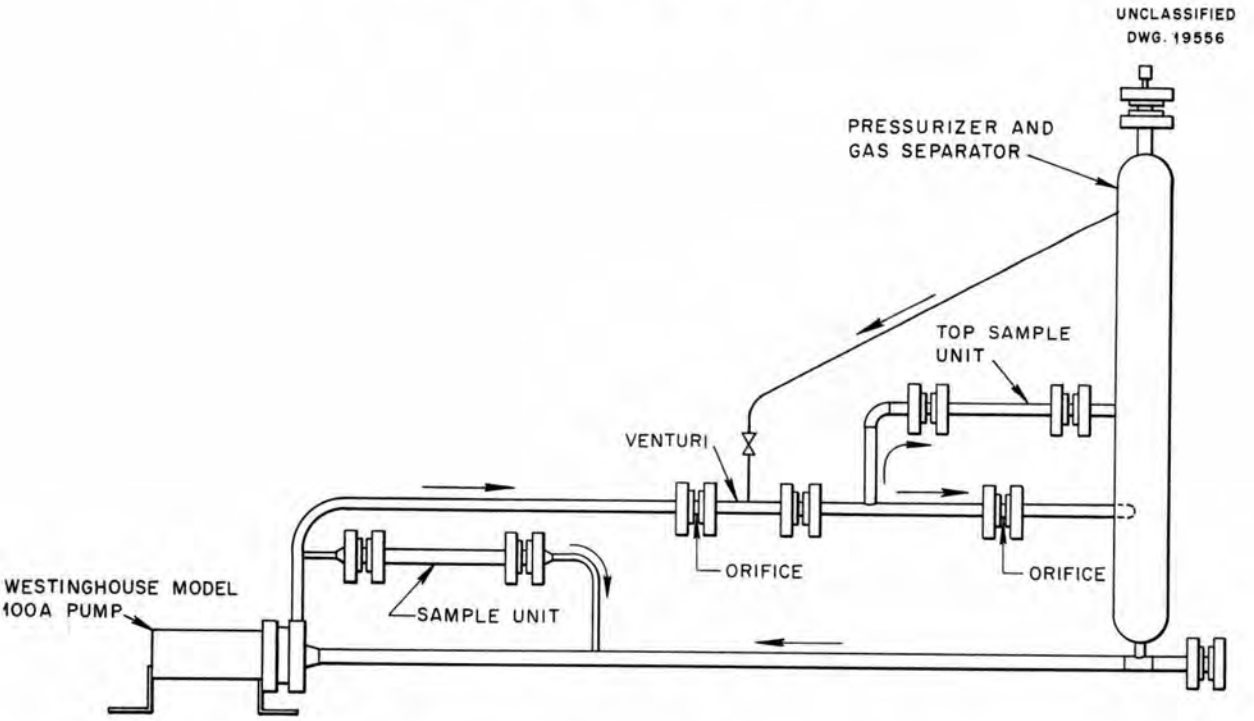

Fig. 28. Loop F with Gas Separator.

operating conditions (250°C and 1050 psig) is approximately 1250 cm^3 (STP) per liter. Analyses of gas samples withdrawn from the loop when it was operating at the above conditions gave the following results:

WITHDRAWAL POINT	OXYGEN CONTENT (cm^3/liter)
Entering pressurizer	4500
Leaving pressurizer	1800
Through top sample unit	7600

Thus it can be seen that all the solution contains excess gas, but the amount of gas obtained through the top sample unit is approximately four times that leaving the pressurizer. Since this run is still under way, no corrosion results have been obtained.

Loop G, an all-titanium loop, has been completed with the exception of one piece of 1/4-in. tubing for the by-pass line. This tubing has been shipped by the vendor. The system has been pressure tested at 1500 psig and is ready for operation as soon as the tubing is received and installed. The only section exposed to the circulating liquid in this system that is not titanium is the stainless steel pump stator diaphragm and rotor can. However, the solution temperature in this region is probably less than 125°C. All other sections, including the rotor stub shaft, impeller, impeller housing, and sample valves, are of titanium. In addition, the system contains a number of titanium welds of varying complexity. Thus the mechanical feasibility of fabricating such a system of titanium is an important consideration that must be considered along with the study of the corrosion resistance of the titanium and its effect on solution stability.

Two new circulating loops, identified as D and M, have been under construction during the past quarter. Loop D is designed for small volume (~4 liters) operation so that special solutions or uranyl sulfate solutions with additives of limited availability may be used for dynamic corrosion tests.

Loop M is a type 347 stainless steel system and differs from test loops previously described[1] in the location of the holders for corrosion test specimens (Fig. 29). The eight specimen holders[2] provided give two to four times the capacity of the present systems. In addition, the liquid flow rate through each specimen holder has been increased by the elimination of the small (1/4 to 3/8 in.) by-pass lines previously used. Thus corrosion rates at wider ranges of flow rates may be studied under identical environmental conditions.

Westinghouse Model 100A Pumps. The Westinghouse model 100A pumps used in the dynamic corrosion test loops continue to give good service. No pump failures occurred in ten pumps that were in almost continuous operation during the quarter. However, one pump was removed from service after approximately 11,000 hr of operation. A routine Dy-Chek of the Inconel diaphragm gave indications of a small leak that could not be found by visual inspection. A new stainless steel diaphragm will be installed before this pump is reused. Six pumps with stainless steel diaphragms have accumulated an operating time of approximately 14,000 hr with no failures.

Corrosion of the front hubs of stainless steel impellers, along with the resulting loss of pump thrust balance, continues to be the major source of concern. When the uranyl sulfate concentrations used are above 100 g of uranium per liter and the operating temperature is 250°C, frequent pump thrust balance inspections and adjustments are necessary. Roughly 300 to 500 hr is required before excessive corrosion of the front hub

(2) *Ibid.*, p. 41.

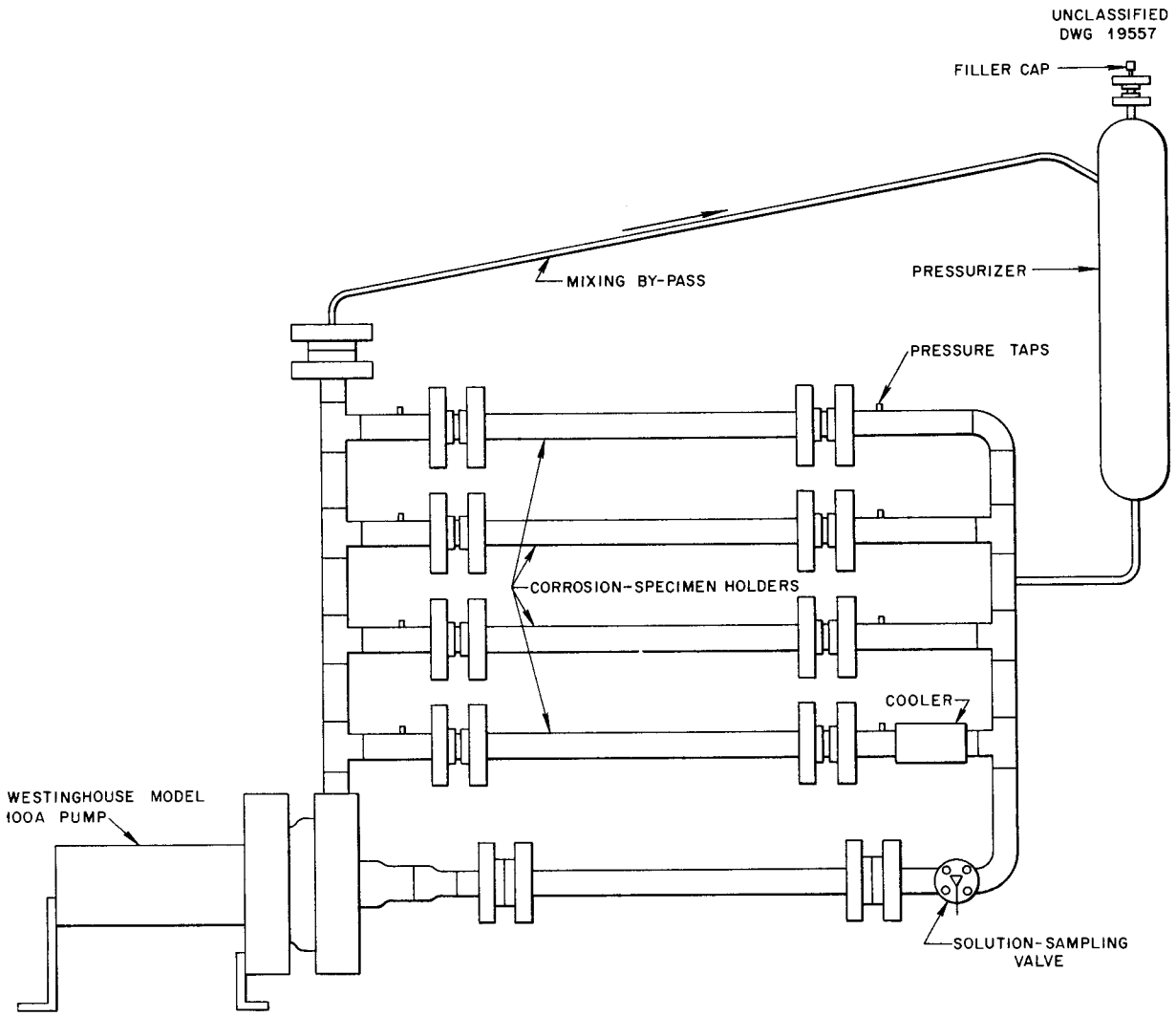

Fig. 29. Dynamic Corrosion Test Loop M.

results in the loss of thrust balance under the above conditions. A solution concentration of 40 g of uranium per liter and a temperature of 250°C may require 2000 to 3000 hr to produce excessive corrosion of the impeller hub, whereas at 15 g of uranium per liter and 250°C somewhat more than 4000 hr are required. In one loop, more than 7500 hr of operation at 250°C with uranyl sulfate solution containing 5 g of uranium per liter have been accumulated without excess corrosion of the impeller hub. Of course, the above-mentioned times will vary with individual pumps, depending on the initial clearance between the impeller hub and seal rings (usually 0.010 to 0.020 in.) and the distance the rotor must move forward before contacting the front thrust bearing.

The problem of corrosion of the impeller hub is being corrected by the use of a titanium impeller or by installation of titanium bushings on the front hubs of all stainless steel impellers after corrosion has occurred and by the use of either titanium or tantalum seal rings. To date, no

appreciable corrosion of titanium impellers has been observed at uranyl sulfate concentrations of up to 300 g of uranium per liter and temperatures of up to 250°C.

Heat Exchanger Tests. Operation of the heat exchanger test assembly[3] is continuing. To date, approximately 2000 hr of operating time with uranyl sulfate solutions (5 and 40 g of uranium per liter) at 250°C has been accumulated on two heat exchanger tubes (approximately 1000 hr on each tube). Flow through the tubes has been approximately 18 fps.

Inspection of the assembly showed that all parts exposed to uranyl sulfate solution, including the inlet and exit welds, became covered with a smooth, black film. No pitting type of corrosion was observed. The outside of the tube (steam side) was covered with a brownish translucent film. Distilled water was used in the steam jacket.

Reproducibility of the heat transfer measurements has not been good. The pulse-welded thermocouples used to measure the temperature drop across the exchanger have given some erratic readings. Heliarc-welded junctions will be used in an effort to improve temperature measurements. Several experiments are being planned for determining the over-all heat transfer coefficient as accurately as the existing apparatus will permit.

LOOP TEST RESULTS

J. C. Griess R. E. Wacker

The objective of the loop test program continues to be that of obtaining a better understanding of the nature of the corrosion processes occurring in uranyl sulfate (and uranyl fluoride)-steel systems. In this regard, studies have been initiated which should ultimately give information on the effect of such variables as temperature, velocity, acidity, and time on the corrosion rate of several alloys. Some of the preliminary data are given here. Long-term testing of promising systems has been continued, and the results obtained from several such systems are given in the following sections. Preliminary data on the stability of thorium dioxide pellets in a dilute, circulating, uranyl sulfate solution are presented.

Solution Stability and Corrosion Damage in Dilute Uranyl Solutions. The fact that dilute uranyl sulfate and fluoride solutions (5 to 15 g of uranium per liter) undergo substantial hydrolysis in the loops at 250°C has been reported previously.[3] All such systems investigated to date have shown that 10 to 25% of the total uranium precipitated as hydrated uranium trioxide, with a corresponding increase in the acidity of the system.

It has been demonstrated that the addition of 25 eq. % of the corresponding acid to the uranyl salt solution at the start of a run completely stabilizes the solutions, allows no precipitation of the uranium at 250°C, and, at the same time, does not greatly increase corrosion. Table 2 shows the weight losses of corrosion specimens in runs with and without added acid.

One loop, run L-13, has been operated for approximately 1000 hr with a starting solution containing 0.02 *M* UO_2SO_4 and 0.05 *M* $CuSO_4$ and having a pH of 3.35. The first solution sample removed from the loop after it had reached a temperature of 250°C had a pH of 1.8, a copper concentration of 0.027 *M*, and the original uranium concentration. These concentrations remained constant for the remainder of the run, except for a slight increase in nickel concentration. At the conclusion of the run, a green precipitate with the formula $3CuO \cdot SO_3 \cdot 2H_2O$ was found in

[3] E. G. Bohlmann *et al.*, *HRP Quar. Prog. Rep. Jan. 1, 1953*, ORNL-1478, p. 62-63.

TABLE 2. EFFECT OF COPPER SULFATE AND ADDED ACID ON THE CORROSION RATE OF SEVERAL STAINLESS STEELS AT 250°C

RUN NO.	TIME (hr)	SALT SOLUTIONS	TYPE OF STAINLESS STEEL					
			347	321	304	304 ELC	316	309 SCb
			CORROSION RATE (mpy)					
B-24	787	0.02 *M* UO_2SO_4 and 0.005 *M* H_2SO_4	0.54 0.48 0.46 0.46	0.32 0.37	0.35 0.37 0.32 0.39		1.00 0.46	0.43 0.48
L-12	1017	0.02 *M* UO_2SO_4	0.39 0.25 0.32	0.27 0.25	0.32 0.32		0.29 0.30	0.25 0.40
L-13	1017	0.02 *M* UO_2SO_4 and 0.05 *M* $CuSO_4$	0.59 0.40 0.42	0.28 0.37	1.90 0.44		0.47 0.42	1.3 0.54
J-20	1102	0.02 *M* UO_2F_2	0.02 0.15 0.09 0.12 0.08	0.15 0.34	0.06 0.05 0.08 0.06	0.03 0.05	0.19 0.19	0.14 0.17
J-21	1031	0.02 *M* UO_2F_2 and 0.01 *M* HF	0.18 0.18 0.20 0.12 0.08	1.0 0.13	0.13 0.21 0.18 0.20	0.12 0.17	0.18 0.18	0.26 0.30

the loop. The following final concentrations were calculated from the analytical data: 0.02 *M* UO_2SO_4, 0.027 *M* $CuSO_4$, and 0.015 *M* H_2SO_4. The weight loss data, given in Table 2, for the corrosion specimens in the loop show that even with the relatively large amount of additional sulfuric acid the corrosion damage was not much more than that occurring without added acid.

General Corrosion Rates. In the last quarterly report,[3] a listing of all data obtained from pin-type corrosion specimens was included. Additional information collected during the past quarter is given in Table 3. As in the previous report, the corrosion rates are reported in mils of penetration per year (mpy). For runs that contained more than two pins of a given alloy, only the minimum, maximum, and average rates are listed. As will be discussed in a later section, the corrosion rates vary with time; and when one run is compared with another, it should be remembered that only runs of similar duration are directly comparable. All corrosion rates are based on the actual amount of metal oxidized, since all specimens were defilmed before the final weighing.

In addition to the pins described in Table 3, some pins containing welds in the center have been exposed to loop solutions. To date, only a limited number of such pins has been examined, and the duration of the tests has been short. However, in

TABLE 3. RESULTS OF PIN CORROSION TESTS

RUN NO.	TEST CONDITIONS						PIN MATERIAL	NO. OF PINS	CORROSION RATE (mpy)		
	Solution	Uranium Concentration (g/l)	Temperature (°C)	Time (hr)	Additions	Flow Rate (fps ± 10%)			Minimum	Average	Maximum
K-12	UO_2SO_4	5	250	2100	200 psi O_2	11	Zirconium-2.5% tin	8[a]			
K-11 and K-12	UO_2SO_4	5	250	2915	200 psi O_2	11	Zirconium-2.5% tin	1[a]			
							Zirconium-5% tin	1[a]			
							Zirconium, crystal bar	1[a]			
K-10 through K-12	UO_2SO_4	5	250	4328	200 psi O_2	11	Titanium (RC-70)	3[b]	0	0.01	0.02
K-5 through K-12	UO_2SO_4	5	250	6334	200 psi O_2	11	Type 347 stainless steel	3	0.02	0.03	0.05
							Type 304 stainless steel	2	0.04	0.05	0.05
							Type 309 SCb stainless steel	2	0.03	0.04	0.04
							Type 316 stainless steel	2	0.03	0.04	0.05
							Type 321 stainless steel	2	0.02	0.03	0.03
							Worthite steel	1		0.11	
							Carpenter-20 steel	2	0.13	0.14	0.14
L-12	UO_2SO_4	5	250	1017	200 psi O_2	17	Type 347 stainless steel	3	0.25	0.3[illegible]	0.39
							Type 304 stainless steel	2	0.32	0.32	0.32
							Type 309 SCb stainless steel	2	0.25	0.33	0.40
							Type 316 stainless steel	2	0.29	0.30	0.30
							Type 321 stainless steel	2	0.25	0.26	0.27
							Worthite steel	3	1.7	1.8	1.9
L-13	UO_2SO_4	5	250	1022	200 psi O_2, 0.05 *M* $CuSO_4$[c]	19	Type 347 stainless steel	3	0.40	0.48	0.59
							Type 304 stainless steel	2	0.44	1.2	1.9
							Type 309 SCb stainless steel	2	0.42	0.86	1.3
							Type 316 stainless steel	2	0.42	0.45	0.47
							Type 321 stainless steel	2	0.28	0.33	0.37
							Worthite steel	1		1.4	
B-25	UO_2SO_4	5	250	1038	200 psi O_2, 0.005 *M* H_2SO_4	11	Type 347 stainless steel	2	0.74	0.76	0.77
							Type 304 stainless steel	1		0.56	
							Type 321 stainless steel	1		0.53	
							Zirconium-2.5% tin	2[a]			
B-24	UO_2SO_4	5	250	787	200 psi O_2, 0.005 *M* H_2SO_4	14	Type 347 stainless steel	6	0.46	0.71	1.6
							Type 347 stainless steel, cast	2	0.63	0.71	0.78
							Type 304 stainless steel	2	0.32	0.34	0.35
							Type 304 stainless steel, cast	2	0.67	0.94	1.2
							Type 309 SCb stainless steel	2	0.43	0.46	0.48
							Type 309 SCb stainless steel	2	1.1	1.1	1.1
							Type 316 stainless steel, cast	2	0.46	0.73	1.0
							Type 316 stainless steel, cast	2	0.69	0.85	1.0
							Type 321 stainless steel	2	0.32	0.34	0.37
							Worthite steel, cast	2	2.7	2.8	2.9
							FA-20 steel, cast	2	1.5	1.5	1.5
							Type 304 M stainless steel[d]	2	0.37	0.38	0.39

TABLE 3. (continued)

RUN NO.	TEST CONDITIONS						PIN MATERIAL	NO. OF PINS	CORROSION RATE (mpy)		
	Solution	Uranium Concentration (g/l)	Temperature (°C)	Time (hr)	Additions	Flow Rate (fps ± 10%)			Minimum	Average	Maximum
J-20	UO_2F_2	5	250	1102	200 psi O_2	11	Type 347 stainless steel	5	0.02	0.09	0.15
							Type 304 stainless steel	2	0.06	0.07	0.08
							Type 304 ELC stainless steel	2	0.03	0.04	0.05
							Type 309 SCb stainless steel	2	0.14	0.16	0.17
							Type 316 stainless steel	2	0.19	0.19	0.19
							Type 321 stainless steel	2	0.15	0.25	0.34
							Type 310 S stainless steel	2	0.09	0.15	0.20
							Type 304 M stainless steel[d]	2	0.05	0.06	0.06
							Type 310 SM stainless steel[e]	2	0.12	0.15	0.17
							Type 430 stainless steel	2	0.40	0.49	0.57
							Type 443 stainless steel	2	0.05	0.31	0.56
							Titanium (RC-70)	3[f]	0	0	0
J-21	UO_2F_2	5	25	1031	200 psi O_2, 0.01 *M* HF	11	Type 347 stainless steel	5	0.08	0.15	0.20
							Type 304 stainless steel	2	0.13	0.17	0.21
							Type 304 ELC stainless steel	2	0.12	0.15	0.17
							Type 309 SCb stainless steel	2	0.26	0.28	0.30
							Type 316 stainless steel	2	0.18	0.18	0.18
							Type 321 stainless steel	2	0.13	0.57	1.0
							Type 310 S stainless steel	2	0.25	0.28	0.31
							Type 304 M stainless steel[d]	2	0.18	0.19	0.20
							Type 310 SM stainless steel[d]	2	0.38	0.39	0.40
							Type 430 stainless steel	2	0.64	0.64	0.64
							Titanium (RC-70)	3[g]	0	0.04	0.10
							Titanium (Ti-150A)	1[g]		0.07	
							Titanium (Ti-100A)	1[g]		0.07	
E-8	UO_2SO_4	15	250	2548	200 psi O_2	12 to 16	Type 347 stainless steel	7	0.08	0.39	0.72
							Type 347 stainless steel, cast	2	0.09	0.24	0.38
							Type 304 stainless steel	3	0.26	0.40	0.67
							Type 304 stainless steel, cast	2	0.28	0.32	0.35
							Type 304 ELC stainless steel	4	0.13	0.25	0.32
							Type 304 ELC stainless steel, cast	2	0.23	0.24	0.25
							Type 309 SCb stainless steel	2	0.41	0.48	0.54
							Type 309 SCb stainless steel, cast	2	0.67	0.68	0.68
							Type 321 stainless steel	2	0.20	0.25	0.29
							Zirconium, crystal bar	2[a]			
							Zirconium, arc-melted sponge	2[h]			
							Zirconium-2.5% tin	2[a]			
							Zirconium-5% tin	2[a]			
H-10[i]	UO_2SO_4	40	250	351	200 psi O_2	17	Type 347 stainless steel	3	4.2	4.3	4.5
							Type 321 stainless steel	3	3.0	3.3	4.4
H-11 and H-12	UO_2SO_4	40	250	1364	200 psi O_2	10	Type 347 stainless steel	3	0.85	2.1	3.3
							Type 321 stainless steel	3	0.50	0.88	1.4
H-10 through H-12	UO_2SO_4	40	250	1715	200 psi O_2	10	Type 347 stainless steel	4	0.94	1.4	2.0
							Type 321 stainless steel	4	0.58	0.71	0.91

TABLE 3. (continued)

RUN NO.	TEST CONDITIONS						PIN MATERIAL	NO. OF PINS	CORROSION RATE (mpy)		
	Solution	Uranium Concentration (g/l)	Temperature (°C)	Time (hr)	Additions	Flow Rate (fps ± 10%)			Minimum	Average	Maximum
I-2	UO_2SO_4	40	250	90	200 psi O_2, 0.04 *M* H_2SO_4	12 to 14	Type 347 stainless steel	4	99	100	110
							Type 304 stainless steel	2	120	130	140
							Type 304 ELC stainless steel	2	70	100	130
							Type 309 SCb stainless steel	2	140	190	230
							Type 321 stainless steel	3	69	76	88
							Type 329 stainless steel	2	95	110	130
							Experimental alloy, R-328[j]	2	99	110	120
							Titanium (RC-70)	2	0	0	0
							Titanium (Ti-75A)	1		0	
							Titanium (Ti-100A)	1		0	
							Titanium (Ti-150A)	1		0	
							Zirconium-2.5% tin	2[a]			
I-1	UO_2SO_4	40	250	599	200 psi O_2, 0.04 *M* H_2SO_4	20	Type 347 stainless steel	4	14	16	18
							Type 304 stainless steel	2	25	25	25
							Type 309 SCb stainless steel	2	25	73	120
							Type 316 stainless steel	2	37	48	58
							Type 321 stainless steel	2	14	31	48
I-3	UO_2SO_4	40	250	1036	200 psi O_2, 0.04 *M* H_2SO_4	15 to 17	Type 347 stainless steel	6	9.5	11	14
							Type 304 stainless steel	2	11	15	19
							Type 304 ELC stainless steel	6	7.3	21	32
							Type 309 SCb stainless steel	2	66	88	110
							Type 316 stainless steel	2	31	41	50
							Type 316 ELC stainless steel	2	20	21	21
							Type 321 stainless steel	5	8.0	9.2	11
							Titanium (RC-70)	2	0	0	0
							Titanium (Ti-75A)	2	0	0	0
							Titanium (Ti-100A)	2	0	0	0
							Zirconium-2.5% tin	2[a]			
A-31	UO_2SO_4	40	250	117	100 psi O_2, O_2 added during run[k,l]	16	Type 347 stainless steel	2	53	57	60
							Type 304 ELC stainless steel	2	68	68	68
							Type 329 stainless steel	2	71	78	84
A-32	UO_2SO_4	40	250	234	100 psi O_2, O_2 added during run[k,l]	16	Type 347 stainless steel	2	25	26	26
							Type 304 ELC stainless steel	2	27	28	29
							Type 329 stainless steel	2	16	46	76
A-31 and A-32	UO_2SO_4	40	250	351	100 psi O_2, O_2 added during run[k,l]	16	Type 347 stainless steel	1		11	
							Type 304 ELC stainless steel	2	25	27	29
							Type 329 stainless steel	2	23	24	25
							Experimental alloy, R-328	2	11	15	18
							Zirconium-2.5% tin	2[a]			
A-33	UO_2SO_4	40	250	97	100 psi O_2, O_2 added during run[k,l]	16	Type 347 stainless steel	2	46	48	49
							Type 304 ELC stainless steel	2	46	48	49
							Type 321 stainless steel	2	11	23	35
							Titanium (RC-70)	2	0	0.09	0.17
							Zirconium-2.5% tin	2[a]			

TABLE 3. (continued)

RUN NO.	TEST CONDITIONS						PIN MATERIAL	NO. OF PINS	CORROSION RATE (mpy)		
	Solution	Uranium Concentration (g/l)	Temperature (°C)	Time (hr)	Additions	Flow Rate (fps ± 10%)			Minimum	Average	Maximum
A-33	UO_2SO_4	40	250	97	100 psi O_2, O_2 added during run[k,l]	100	Type 347 stainless steel	2	180	190	190
							Type 304 ELC stainless steel	2	160	170	180
							Type 321 stainless steel	1		160	
							Titanium (RC-70)	2	0.18	0.36	0.53
							Zirconium-2.5% tin	2[a]			
A-34	UO_2SO_4	40	250	97	200 psi O_2[l]	16	Type 347 stainless steel	2	10	19	27
							Type 304 ELC stainless steel	2	5.3	15	24
							Type 321 stainless steel	2	4.7	7.4	10
							Titanium (RC-70)	2	0	0	0
							Zirconium-2.5% tin	2[a]			
A-34	UO_2SO_4	40	250	97	200 psi O_2[l]	100	Type 347 stainless steel	2	150	160	160
							Type 304 ELC stainless steel	1		140	
							Type 321 stainless steel	2	120	140	150
							Titanium (RC-70)	2	0.18	0.27	0.35
							Zirconium-2.5% tin	2[a]			
A-35	UO_2SO_4	40	250	94	200 psi O_2, 50 ppm Cl as KCl	17	Type 347 stainless steel	4	22	28	39
							Type 321 stainless steel	2	27	35	42
							Titanium (RC-70)	2	0	0	0
							Zirconium-2.5% tin	2[a]			
A-35	UO_2SO_4	40	250	94	200 psi O_2, 50 ppm Cl as KCl	100	Type 347 stainless steel	3	140	150	160
							Type 321 stainless steel	2	130	150	170
							Titanium (RC-70)	2	0	0	0
							Zirconium-2.5% tin	2[a]			
A-36	UO_2SO_4	40	250	12	200 psi O_2[l]	15	Type 347 stainless steel	4	31	45	62
							Type 304 stainless steel	2	68	78	88
							Type 304 ELC stainless steel	2	68	80	91
							Type 309 SCb stainless steel	3	27	35	45
							Type 321 stainless steel	3	86	95	105
A-36	UO_2SO_4	40	250	12	200 psi O_2[l]	100	Type 347 stainless steel	4	47	49	51
							Type 304 stainless steel	2	70	70	70
							Type 304 ELC stainless steel	2	67	87	107
							Type 309 SCb stainless steel	3	30	39	51
							Type 321 stainless steel	3	51	70	88
A-37	UO_2SO_4	40	250	44	200 psi O_2[l]	15	Type 347 stainless steel	4	59	68	81
							Type 304 stainless steel	2	86	87	87
							Type 304 ELC stainless steel	2	65	78	91
							Type 309 SCb stainless steel	3	67	84	100
							Type 321 stainless steel	3	49	71	87
A-37	UO_2SO_4	40	250	44	200 psi O_2[l]	100	Type 347 stainless steel	4	62	81	120
							Type 304 stainless steel	2	91	94	97
							Type 304 ELC stainless steel	2	97	120	140
							Type 309 SCb stainless steel	3	62	85	110
							Type 321 stainless steel	3	110	120	120

TABLE 3. (continued

RUN NO.	TEST CONDITIONS						PIN MATERIAL	NO. OF PINS	CORROSION RATE (mpy)		
	Solution	Uranium Concentration (g/l)	Temperature (°C)	Time (hr)	Additions	Flow Rate (fps ± 10%)			Minimum	Average	Maximum
A-38	UO_2SO_4	40	250	98	200 psi O_2 (l)	15	Type 347 stainless steel	4	48	53	60
							Type 304 stainless steel	2	52	67	82
							Type 304 ELC stainless steel	2	10	47	84
							Type 309 SCb stainless steel	3	37	55	66
							Type 321 stainless steel	3	15	30	40
A-38	UO_2SO_4	40	250	98	200 psi O_2 (l)	100	Type 347 stainless steel	4	110	150	160
							Type 304 stainless steel	2	110	120	120
							Type 304 ELC stainless steel	2	120	120	120
							Type 309 SCb stainless steel	3	170	180	190
							Type 321 stainless steel	3	140	160	200
A-39	UO_2SO_4	40	250	209	200 psi O_2 (l)	15	Type 347 stainless steel	4	17	22	26
							Type 304 stainless steel	2	5.6	15	25
							Type 304 ELC stainless steel	2	4.5	22	39
							Type 309 SCb stainless steel	3	12	25	36
							Type 321 stainless steel	3	7	16	25
A-39	UO_2SO_4	40	250	209	200 psi O_2 (l)	100	Type 347 stainless steel	4	140	150	160
							Type 304 stainless steel	2	150	160	170
							Type 304 ELC stainless steel	2	140	140	140
							Type 309 SCb stainless steel	3	160	180	220
							Type 321 stainless steel	3	140	190	210
A-40	UO_2SO_4	40	250	397	200 psi O_2 (l)	15	Type 347 stainless steel	4	2.4	5.1	7.4
							Type 304 stainless steel	2	1.5	1.6	1.6
							Type 304 ELC stainless steel	2	3.5	3.9	4.2
							Type 309 SCb stainless steel	3	2.5	6.6	8.9
							Type 321 stainless steel	3	2.3	5.7	8.8
A-40	UO_2SO_4	40	250	397	200 psi O_2 (l)	100	Type 347 stainless steel	4	140	170	180
							Type 304 stainless steel	2	170	180	180
							Type 304 ELC stainless steel	2	160	200	230
							Type 309 SCb stainless steel	3	180	180	190
							Type 321 stainless steel	3	140	170	230
C-15	UO_2SO_4	300	150	997	200 psi O_2	16 to 20	Type 347 stainless steel	9	2.0	2.8	3.8
							Type 347 stainless steel, cast	2	3.4	3.7	3.9
							Type 304 stainless steel	6	3.6	4.9	6.4
							Type 304 stainless steel, cast	2	4.4	4.9	5.4
							Type 304 ELC stainless steel	4	4.5	4.6	4.8
							Type 304 ELC stainless steel, cast	2	4.0	4.6	5.2
							Type 309 SCb stainless steel	2	0.62	0.65	0.68
							Type 309 SCb stainless steel, cast	2	0.56	0.62	0.67
							Type 321 stainless steel	2	3.9	4.5	5.0
							Stellite 25	2	5.8	5.9	6.0

TABLE 3. (continued)

RUN NO.	TEST CONDITIONS						PIN MATERIAL	NO. OF PINS	CORROSION RATE (mpy)		
	Solution	Uranium Concentration (g/l)	Temperature (°C)	Time (hr)	Additions	Flow Rate (fps ± 10%)			Minimum	Average	Maximum
C-16	UO_2SO_4	300	175	308	200 psi O_2	16 to 22	Type 347 stainless steel	9	16	18	23
							Type 347 stainless steel, cast	2	19	20	21
							Type 304 stainless steel	6	11	17	19
							Type 304 stainless steel, cast	2	19	20	20
							Type 304 ELC stainless steel	4	10	18	25
							Type 304 ELC stainless steel, cast	2	11	13	14
							Type 309 SCb stainless steel	2	3.2	5.1	7.0
							Type 309 SCb stainless steel, cast	2	6.0	7.3	8.5
							Type 321 stainless steel	2	14	15	16
							Stellite 25	2	28	29	29
C-17	UO_2SO_4	300	150	100	300 to 500 ppm O_2	16 to 20	Type 347 stainless steel	8	2.4	3.7	5.3
							Type 304 stainless steel	6	5.6	6.5	7.3
							Type 304 ELC stainless steel	6	3.6	5.9	7.5
							Type 309 SCb stainless steel	7	1.7	2.1	2.6
							Type 316 stainless steel	4	5.3	6.4	7.5
							Type 316 ELC stainless steel	4	4.3	4.7	5.3
							Type 321 stainless steel	6	5.6	6.5	7.3
C-18	UO_2SO_4	300	175	100	300 to 500 ppm O_2	16 to 20	Type 347 stainless steel	8	16	22	25
							Type 304 stainless steel	6	24	29	33
							Type 304 ELC stainless steel	6	24	26	28
							Type 309 SCb stainless steel	7	9.1	12	15
							Type 316 stainless steel	4	18	21	25
							Type 316 ELC stainless steel	4	20	23	28
							Type 321 stainless steel	7	29	38	43
C-19	UO_2SO_4	300	200	99	300 to 500 ppm O_2	16 to 20	Type 347 stainless steel	8	83	100	110
							Type 304 stainless steel	6	64	78	100
							Type 304 ELC stainless steel	6	72	120	180
							Type 309 SCb stainless steel	6	27	36	43
							Type 316 stainless steel	4	68	71	78
							Type 316 ELC stainless steel	4	58	61	69
							Type 321 stainless steel	6	140	170	220
							Stellite 25	2	100	110	110
C-20	UO_2SO_4	300	225	101	300 to 500 ppm O_2	16 to 20	Type 347 stainless steel	7	100	130	150
							Type 304 stainless steel	6	120	140	190
							Type 304 ELC stainless steel	6	110	140	190
							Type 309 SCb stainless steel	6	66	110	170
							Type 316 stainless steel	4	110	130	140
							Type 316 ELC stainless steel	4	100	120	140
							Type 321 stainless steel	6	110	130	150
							Stellite 25	2	210	220	220
C-21	UO_2SO_4	300	250	101	300 to 500 ppm O_2	16 to 20	Type 347 stainless steel	8	94	240	320
							Type 304 stainless steel	6	140	270	370
							Type 304 ELC stainless steel	6	120	270	430
							Type 309 SCb stainless steel	6	240	350	480
							Type 316 stainless steel	4	210	280	320
							Type 316 ELC stainless steel	4	180	260	320
							Type 321 stainless steel	6	130	150	170
							Stellite 25	1		730	

Footnotes for Table 3

(a) To date, attempts to defilm these pins have been unsuccessful. The deposit of Fe_2O_3 and Cr_2O_3 on the surface exposed to the solution could not be removed by the electrolytic defilming technique.

(b) These pins showed dark, purple films after the Fe_2O_3 and Cr_2O_3 scales had been removed.

(c) After attaining a temperature of 250°C, approximately half the copper precipitated as $3CuO \cdot SO_3 \cdot 2H_2O$ and left the solution with a pH of 1.8 for the remainder of the run.

(d) Type 304 M stainless steel is a standard melt of type 304 stainless steel which includes small additions of misch metal.

(e) Type 310 SM stainless steel is a standard melt of type 310 S stainless steel which includes a small amount of misch metal.

(f) After removing the Fe_2O_3 and Cr_2O_3 film the titanium pins showed very dark, purple films. These films indicated that if the run had been continued for a longer period, corrosion damage might have been apparent from the weight-loss data.

(g) All pins in run J-21, except the Ti-100A and Ti-150A pins, had deep-purple films. The Ti-100A pin had a somewhat less intense purple color, and the color of the Ti-150A pin was intermediate between straw color and purple.

(h) These two pins developed the Fe_2O_3 and Cr_2O_3 deposit but, in addition, each pin was intensively attacked along its longitudinal axis. The attack appeared to be due to an inclusion in the zirconium.

(i) This run was summarized in the last quarterly report, but it is included here for comparative purposes.

(j) This is an experimental, low-nickel, ferritic stainless steel.

(k) The oxygen was added through the rear of the pump at a rate 5 to 15 STP cm^3/min. The purpose in adding the oxygen was to check the effect of excess gas on bearing wear in the Ti-100A pump, in connection with HRE pump operation.

(l) A titanium impeller was used in this run.

most cases, these tests, have shown no adverse effects directly attributable to the welds.

A rather extensive investigation of welding techniques and methods and of the corrosive attack on the welds is being carried out in conjunction with the Metallurgy Group, and a more complete discussion of corrosion damage of welds will be given after this investigation has been completed.

Corrosion Rate vs. Time and Velocity. It has been known for some time that corrosion rates of stainless steels in uranyl sulfate solutions at 250°C are not constant but that, in general, the corrosion rates decrease as the exposure time increases. The comparison of the various loop I and loop H runs listed in Table 3 clearly shows that the longer the duration of the run, the lower the corrosion rate. To further emphasize this point, some of the data collected from loop K, in which 0.02 *M* UO_2SO_4 was circulated at 250°C, are shown in Table 4. It can be seen that within rather wide limits the weight losses of all specimens are unchanged from 1000 to 6000 hr of exposure. Since there were no weight

TABLE 4. WEIGHT LOSSES OF STAINLESS STEEL SPECIMENS EXPOSED TO 0.02 *M* UO_2SO_4

Temperature, 250°C
Velocity, 12 to 17 fps

TIME (hr)	TYPE OF STAINLESS STEEL				
	347	304	316	309 SCb	321
	WEIGHT LOSS (mg)*				
1001	1.9	1.3	0.9	1.3	0.7
	1.4	1.2	0.6	1.0	0.6
	1.3				
	1.6				
1017	2.3	1.9	1.7	1.5	1.6
	1.5	1.9	1.8	2.4	1.5
	1.9				
1023	1.5	1.6	2.5	2.5	1.6
	2.6	1.6	2.2	2.5	1.4
	1.7				
1413		2.5	2.3	4.7	1.7
		2.2	4.8	3.3	1.8
2005	1.4				
	1.3				
	0.9				
	1.0				
2229	3.0				
	3.2				
6334	0.9	1.8	1.2	1.6	1.0
	1.0	1.6	1.9	1.3	0.8

*Corrosion rate, mpy $= \frac{\text{mg loss} \times 170}{\text{hours}}$.

losses between 1000 and 6000 hr, it is obvious that during this period the corrosion rate was zero.

To investigate the corrosion damage of several alloys as a function of time and velocity, loop A has been operated at 250°C with 0.17 *M* UO_2SO_4 (40 g of uranium per liter) for various periods of time. In this particular series of runs, one pin-type sample holder was placed in the main stream of the loop and one in a by-pass line. A tapered coupon holder was also included in the by-pass. Each pin holder contained 14 stainless steel pins, including the following alloys: four type 347, three type 321, three type 309 SCb, two type 304, and two type 304 ELC. The coupon holder contained ten type 347 stainless steel coupons. The solution flowed past the pins in the main line at a rate of 100 fps and in the by-pass line at 16 fps. The flow past the coupons varied from 8.5 fps at the entrance end to 77 fps at the exit end. At the end of each run, all specimens were removed, defilmed, and weighed. Then, new specimens of the same types were inserted in the loop and the next run started. The results of the pin tests are shown in Fig. 30 and the results of the coupon tests in Fig. 31. The lengths of the

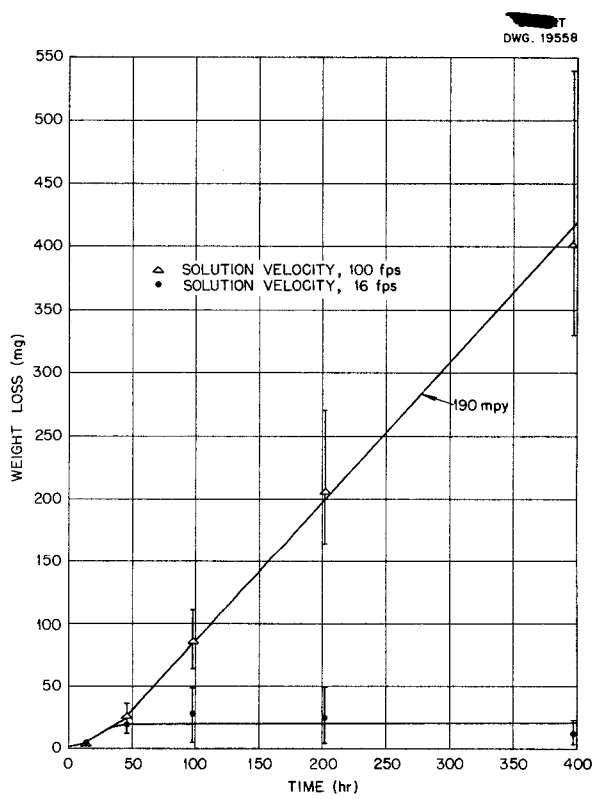

Fig. 30. Weight Loss of Pin-Type Corrosion Specimens in 0.17 *M* UO_2SO_4. Each point represents the average weight loss of all the following 14 stainless steel pins: 4 type 347, 3 type 309 columbium-stabilized, 3 type 321, 2 type 304, 2 type 304 ELC.

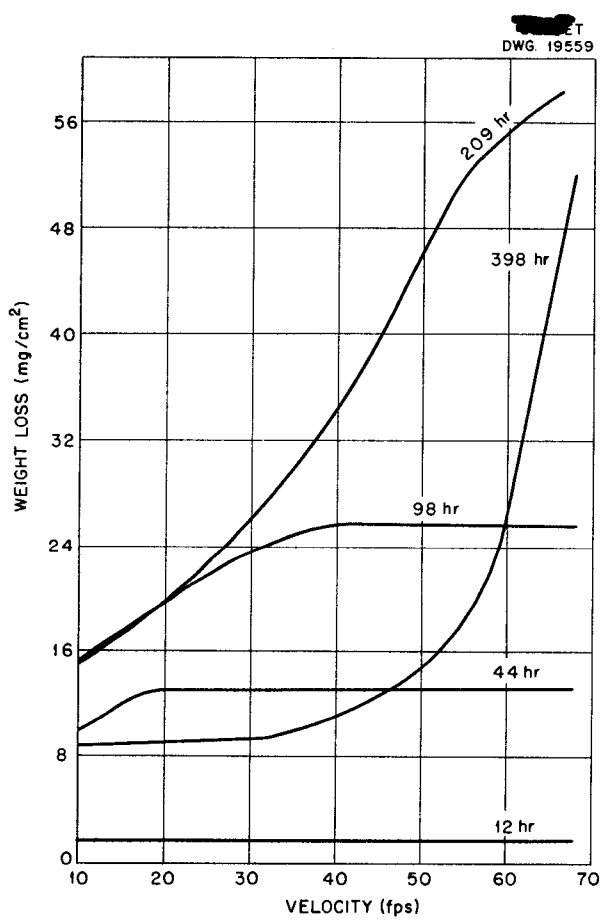

Fig. 31. Effect of Time and Velocity on the Corrosion Damage to Type 347 Stainless Steel in 0.17 *M* UO_2SO_4 at 250°C.

vertical lines in Fig. 30 represent the maximum spread of the data for fourteen pins, whereas the symbols represent the average of the data for fourteen pins. Since there appeared to be no consistent differences in the steels tested, it seemed justifiable to plot the data as a unit; however, the individual pin data for these runs are presented in Table 3, runs A-36 through A-40.

It is evident from Fig. 30 that after a short induction period the corrosion rate was high and constant in solution flowing at a rate of 100 fps, whereas with a flow rate of 16 fps, the corrosion rate was approximately zero after the first 50 hours. The pins exposed at 100 fps developed only very thin films, whereas those exposed at 16 fps were covered with the characteristic, heavy, black coatings. In Fig. 31, the coupon data are represented by a series of curves. To obtain these curves, the best line was drawn through the individual coupon datum for each run. The ordinate is expressed in weight loss per square centimeter.

Other loops have contained coupons identical to those used in the above series of tests. Figure 32 shows a plot of the data from runs E-7 and E-8 in which the uranyl sulfate concentration was 0.06 *M* but the test periods were different by a factor of 2.5. Figure 33 shows the weight loss of type 347 stainless steel coupons as a function of velocity of the solution, which contained 0.02 *M* UO_2SO_4 with and without added sulfuric acid or copper sulfate. Figure 34 shows the effect on the corrosion of type 347 stainless steel of adding sulfuric acid to 0.17 *M* UO_2SO_4 and of varying the solution flow rate. In Figs. 32, 33, and 34, the weight losses of the individual

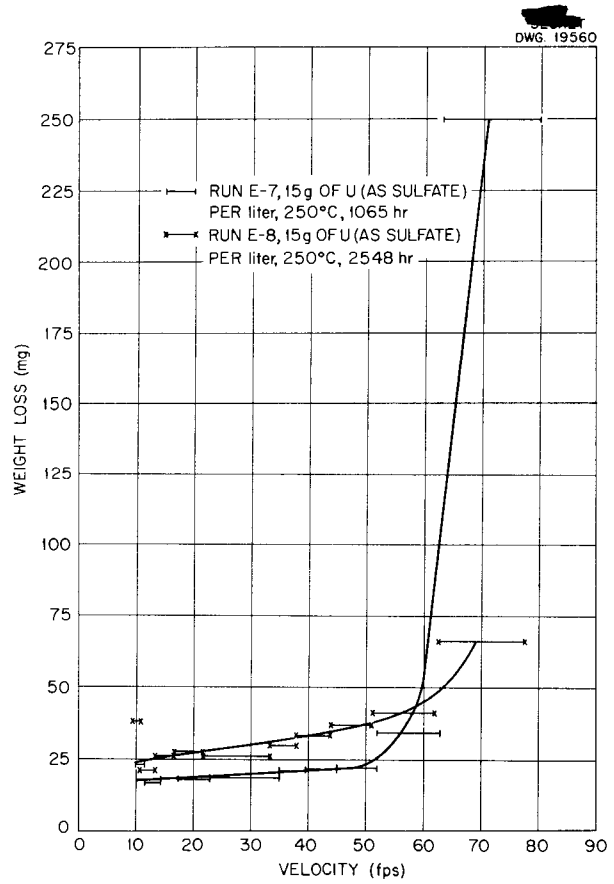

Fig. 32. Effect of Velocity on the Corrosion of Type 347 Stainless Steel in 0.06 *M* UO_2SO_4.

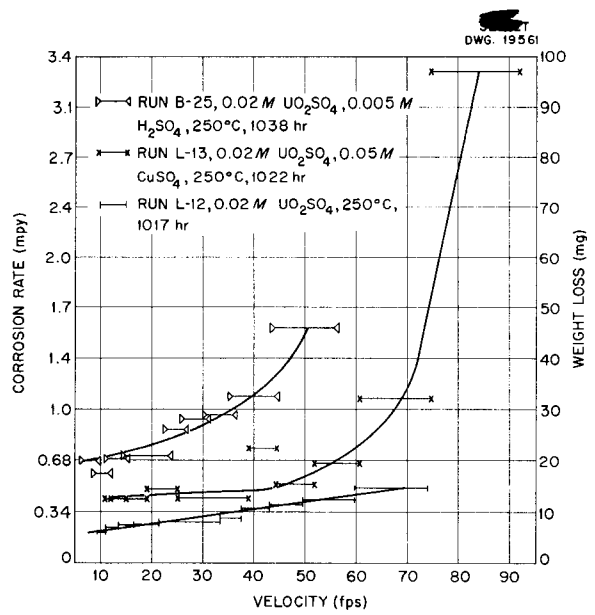

Fig. 33. Effect of Velocity on the Corrosion of Type 347 Stainless Steel in 0.02 *M* UO_2SO_4.

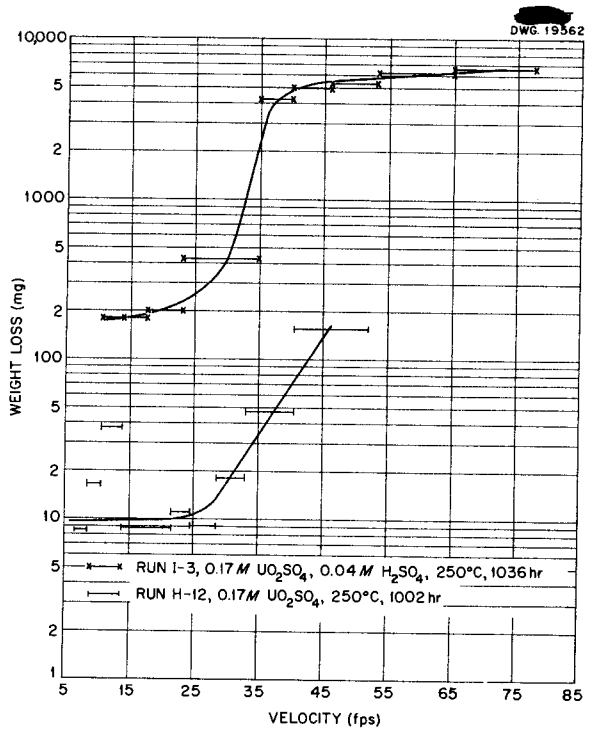

Fig. 34. Effect of Velocity on the Corrosion of Type 347 Stainless Steel in 0.17 *M* UO_2SO_4.

coupons are plotted on the ordinate, and the lengths of the horizontal lines represent the range of solution velocity over a given coupon. The surface area of the coupons exposed to the solution was 12.5 cm^2.

Corrosion Rates as a Function of Temperature. Until recently, only a limited amount of corrosion data at temperatures other than 250°C had been collected. During the past quarter, however, loop C was used to investigate the effect of temperature on corrosion rates. For this study, a 1.26 *M* uranyl sulfate solution and an exposure time of 100 hr were arbitrarily chosen. The first run was made at 150°C, and each run thereafter has been made at a temperature 25°C higher than the previous temperature. The results of the pin tests are shown in Table 3, runs C-17 through C-21. Since the experiment is still in progress and the temperature range is being extended beyond 250°C, no analysis of the data from the steel pins will be made at this time; a complete summary of the experiment will be included in the next quarterly report. Similarily, the results of the coupon tests will be withheld until all the data have been collected.

As was indicated previously, a complication arises in the interpretation of corrosion rates of steel specimens because of the formation of protective oxide films which prevent the corrosion rates under most conditions from being constant. However, one alloy, Haynes alloy 25, has been investigated rather extensively, and under all conditions examined, no film of visible thickness has been observed. As might be expected, runs of different duration have shown that the corrosion rate is constant. The results obtained to date from the data on all tests on this alloy are shown in Fig. 35, where the log of the corrosion rate is plotted against the reciprocal of the absolute temperature. From the slope of the line obtained, an activation energy of 19,500 calories has been calculated. Of the four points at a temperature of 250°C ($1/T = 1.91 \times 10^{-3}$), two were obtained in 0.06 *M* UO_2SO_4 and the other two in 1.26 *M* UO_2SO_4. All the other points were obtained in 1.26 *M* uranyl sulfate. From Fig. 35 it can be shown that the corrosion rate of Haynes alloy 25 is related to the absolute temperature *T* by the following equation:

$$\text{mpy} = 10\left(\frac{10.94T - 4260}{T}\right).$$

Stability of Thorium Dioxide Pellets in Dilute Uranyl Sulfate Solutions. At the request of R. B. Briggs, some thorium dioxide pellets were exposed in a circulating uranyl sulfate solution because of the interest in the possibility of either thorium pellets being put into the core or

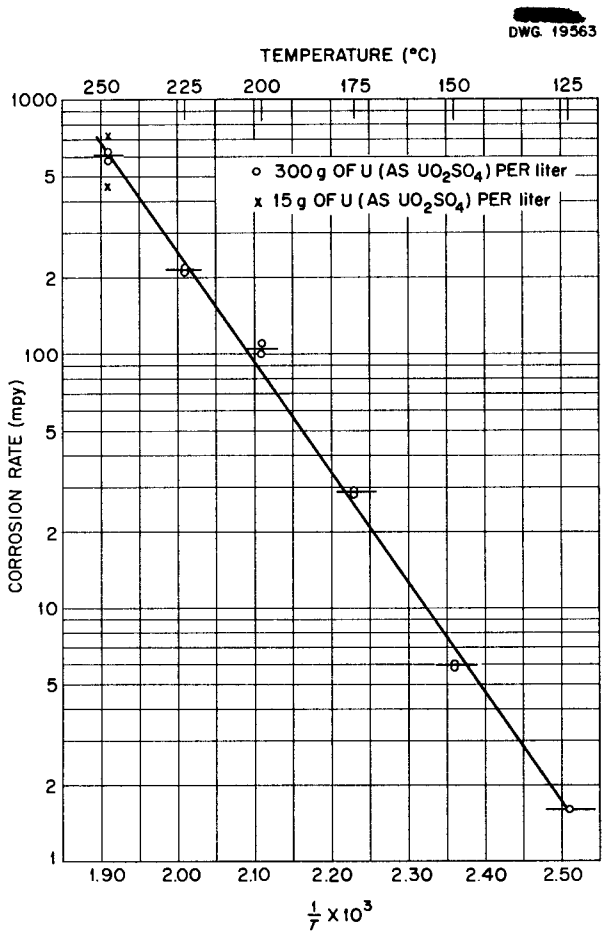

Fig. 35. Corrosion Rate of Haynes Alloy 25 in UO_2SO_4 Solutions.

the fuel solution being allowed to flow through the blanket. A number of nearly spherical pellets, which ranged in diameter from 1/16 to 3/8 in. and weighed 75 g, was placed in a cylinder made of stainless steel screen and the cylinder was inserted in a by-pass line of a loop. The flow rate through the line was 1 to 2 fps, but since the cylinder fit snugly into the line, the flow rate past the pellets was somewhat greater than the normal flow through the line. The pellets were exposed for 209 hr at 250°C to 0.02 *M* UO_2SO_4 that was 0.005 *M* in sulfuric acid.

After the pellets had been removed from the loop, they were washed in water, rinsed in acetone, and dried at 100°C for 2 hours. When reweighed, the pellets showed a weight gain of 2 grams. Visual examination revealed that some residue had been precipitated on the surfaces of the pellets. This precipitate, along with absorbed solution in the pellets, probably accounts for the observed weight gain. Only one pellet cracked, and it was one of the smallest pellets. The break seemed to be clean, judging from what appeared to be two pieces of the pellet that were found in the screen. At present, most of the pellets are being retained so that they can be reinserted in a loop in a future run.

Discussion. The stabilization of dilute uranyl sulfate or uranyl fluoride solutions at 250°C by the addition of either sulfuric or hydrofluoric acid has been demonstrated. Although the addition of acid lowers the room temperature pH of the solutions considerably, corrosion is not significantly increased. This is perhaps not surprising since, in reality, the addition of acid prior to the beginning of a run probably produces a solution not greatly different from an unacidified solution that has undergone partial hydrolysis in a loop operated at 250°C.

A comparison of the corrosion data from different solutions has clearly shown that the corrosiveness of a solution is not dependent alone on the room temperature pH of the solution. For example, all runs made with 0.02 *M* UO_2SO_4 solution and 25 mole % acid have had a pH lower than the pH of a 0.17 *M* UO_2SO_4 solution; however, it is evident that the extent of corrosion was considerably greater in the latter solutions. In run L-13 in which the original solution was 0.02 *M* UO_2SO_4 containing 0.05 *M* $CuSO_4$, approximately one half the copper precipitated, with the formation of 0.015 *M* H_2SO_4. Even with this large excess of sulfuric acid, the corrosion damage was very

small; however, the effect of the presence of the cupric ions must be evaluated.

On the other hand, the addition of 25 mole % H_2SO_4 to a uranyl sulfate solution containing 40 g of uranium per liter greatly increased the extent of corrosion over that observed in the same solution without acid (see runs H-10 to H-12 vs. runs I-1 to I-3, Table 3). With the added acid, the pH of the solution was approximately 1.2, which was considerably lower than that of the 0.02 *M* solution with added acid. Further studies on the effect of acidity on corrosion by UO_2SO_4 solutions of various concentrations are contemplated.

The corrosion resistance of all steels, and even titanium, to 0.02 *M* UO_2F_2 solutions with and without added hydrofluoric acid was surprising (see runs J-20 and J-21, Table 3). Although the titanium corrosion specimens showed little or no weight change, they had developed films, probably of titanium dioxide, that were thicker than those formed in uranyl sulfate solutions during a similar exposure. Unfortunately, zirconium and all its alloys tested to date have shown a complete lack of resistance to all concentrations of uranyl fluoride at 250°C.

The corrosion data presented in Table 3 are, in most cases, sufficiently clear that discussion of them is unnecessary. However, in runs A-31 through A-33 in which oxygen was added through the rear of the pump, it appeared that the corrosion damage was greater than that in the runs in which the solution was initially saturated with oxygen. When gas was added to the system continuously, some gas bubbles that were circulated with the solution may have been responsible for the increased corrosion. To investigate this effect further, a new loop which contains a gas entrainer and separator has been constructed and will be ready for use in the near future (cf., previous section on "Pump Loop Operation and Maintenance," this chapter).

In the previous quarterly report,[3] it was noted that the data at the 40 g of uranium per liter level were discordant, but no explanation was offered. It now appears that three factors can be used to partly clarify the data. First, the data represented by the lower curve in Fig. 30 show the misleading impressions that can be conveyed by reporting all corrosion damage as a constant rate process (at low solution velocities). Although the data in Fig. 30 are for a test of only 400-hr duration, the data from runs H-10 through H-12 in Table 3 are directly comparable. In these runs, the weight losses of the specimens were, within rather wide limits, the same after 1700 hr as they were after 50 hr in the A runs. The data in Table 4 show that the effect of time is not confined to the 40-g level but is the same at the 5-g level. Similarly, the old loop, loop F, which was used to circulate 1.26 *M* UO_2SO_4 and UO_2F_2, demonstrated that in areas where the velocity was low the corrosion damage, even at the 300-g level, was very low after the protective oxide film had formed (see section on "Pump Loop Operation and Maintenance" for description of loop).

Second, it can be observed from Table 3 that, even with the same type of steel specimens in a run, wide variations in weight losses are both possible and probable. The reasons for the large differences in different specimens machined from the same piece of steel are not readily apparent, but the differences may be related to heterogeneities of the steel and/or differences in the degree of cold work as a result of slight differences in the machining methods. Preparations for evaluating such factors are being made.

Third, there have been indications that the corrosion behavior of the

loop itself can influence the extent of attack on the specimens. If some part of the loop system, such as the pump impeller, undergoes severe attack, the corrosion products originating at that point are rather uniformily spread throughout the system, and iron and chromium oxides are deposited on the specimens, as well as on the rest of the loop surface exposed to the solution. Because of the oxide deposits, the specimens can possibly form protective films faster if the loop contains some part which corrodes at a high rate. Hence the data presented in the previous quarterly report[3] can be at least partly reconciled by consideration of the following factors: time, variation in "identical" specimens, and the corrosion behavior of the system as a whole.

The effect of velocity on the corrosion of several systems has been demonstrated, if not clearly evaluated. From the upper curve in Fig. 30, it is evident that if the flow of the solution past the specimens is sufficiently fast, the corrosion rate, after a short induction period, is constant and high. At present, no explanation can be offered for the relatively low corrosion rate at the high velocity used during the induction period, but it appears to be real. A visual comparison of the pin-type corrosion specimens tested with solution velocities of 16 and 100 fps revealed that at the lower velocity the pins developed heavy, black films, whereas those tested in the higher-velocity solution had only very thin films. It thus appeared that in the high-velocity solution the black, oxide film could not form on the surface of the steel and that in the absence of this protective barrier the steel corroded at a very high, constant rate. The same phenomenon could be responsible for the usual high corrosion rate of impellers and other parts exposed to high-velocity solution and/or turbulence in systems containing 40 g (or more) of uranium per liter.

Coupons contained in tapered holders have been exposed to a number of different solutions, and Figs. 31 through 34 represent some of the data that have been collected. Although the data are not always self-consistent, two generalizations can be made: the velocity effect is time dependent, and the more corrosive the solution, the greater the effect of velocity and the lower the velocity at which it becomes apparent. Experience has shown that when a pronounced velocity effect is observed, the coupons that show large weight losses are covered with very thin films instead of black films. Hence, as was the case with pins tested with high-velocity solution, the corrosion resistance of coupons seemed closely related to the stability of the bulk oxide film.

In Fig. 32 it is seen that the velocity effects in dilute uranyl sulfate solutions with and without acid are not excessive. In this connection, it is interesting to note that in these systems there was no damage to impellers, except a slight damage to the hubs (cf., section on "Pump Loop Operation and Maintenance" for a discussion of this effect), and that the loop suffered very little attack elsewhere.

Figure 31 demonstrates how the shape of the velocity curves varies with time in runs A-36 through A-40. There appeared to be a rather uniform pattern in all the runs except A-40. It is hoped that further investigation and experience will clarify the inconsistencies noted in run A-40.

The corrosion data as a whole, and particularly the data represented by Fig. 30 and Tables 3 and 4, rather clearly indicate that the austenitic stainless steels investigated in the wrought condition do not sufficiently differ in their corrosion resistances to uranyl sulfate or fluoride solutions

at 250°C so that it can be said that one is attacked less than the others. It appears that at low solution velocities (perhaps up to 20 fps) the austenitic stainless steels show extremely low corrosion rates in uranyl sulfate solutions at 250°C after a protective film has been formed.

Although the corrosion data presented in this report are probably more optimistic than those reported previously, a number of variables (exclusive of radiation effects) remains to be investigated. Any one of these variables could be a critical factor. Among the variables to be investigated are the effect of gas bubbles on corrosion damage, the ability of welds to resist corrosion, the effect of the presence of fission products, and the effect of copper and added acid on corrosion rates. In addition, various metallurgical factors must be investigated. Additional work will also be directed toward determining the suitability of zirconium and titanium for container materials. Included in the titanium investigation will be the operation of the all-titanium loop.

SMALL-SCALE, DYNAMIC CORROSION TEST PROGRAM

D. Schwartz G. E. Moore

Progress on the small-scale, dynamic corrosion test program continues at a very slow pace because of diversion of the effort of the personnel involved to higher priority problems. A relatively simple mechanism having the required motion to move a slug of liquid around a toroid was operated sporadically during the latter part of this quarter. No corrosion results have, as yet, been obtained from this mechanism.

The Design Group has considered another mechanism (described in the following) which will also give the desired motion to an assembly of toroids, and preliminary drawings have been made.

Torus Rotator (W. L. DeRieux, J. R. McWherter). A preliminary design has been made of a machine to circulate hot liquids in a pipe without the use of a conventional pumping unit. This machine has been designed on the same principle as that used for circulation apparatus described in NACA RME51D12.[4]

When a torus less than half full of liquid is rotated about a vertical axis other than its own, centrifugal force causes formation of a slug of liquid which tends to seek the portion of the torus farthest from the center of rotation, as shown in Fig. 36. If the torus is simultaneously rotated

[4] L. G. Desmon and D. R. Mosher, *Preliminary Study of Circulation in an Apparatus Suitable for Determining Corrosive Effects of Hot Flowing Liquids*, NACA RME51D12 (June 1951).

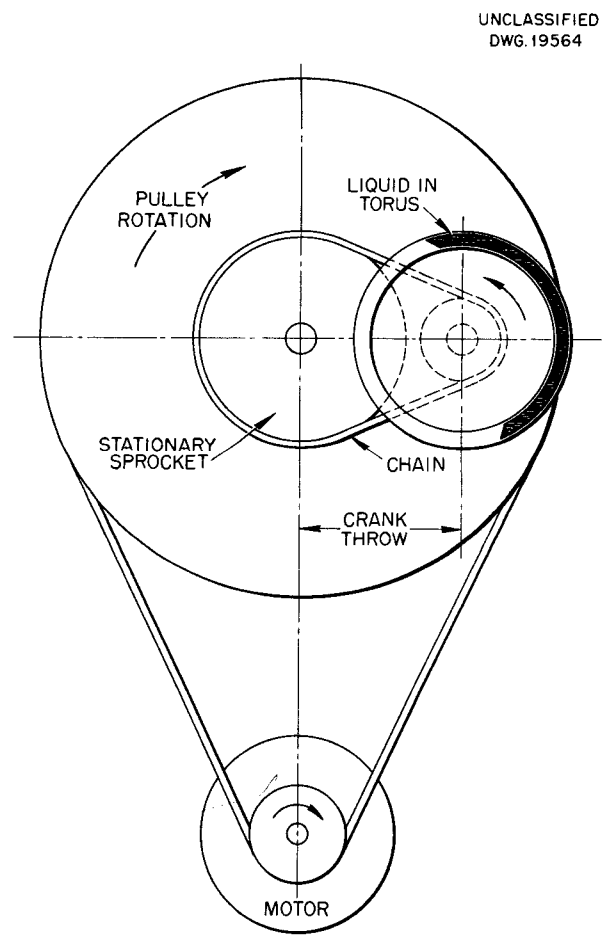

Fig. 36. Liquid Flow in Torus.

about its own vertical axis, flow of the liquid with respect to the pipe wall will occur, provided the centrifugal force on the liquid due to the crank throw is sufficient to overcome frictional resistance to flow.

The proposed machine is shown in Fig. 37. Ten 6-in.-dia tori fabricated from 3/8-in. pipe are mounted on each of two diametrically opposed, rotating shafts, which are, in turn, mounted on a large rotating pulley. Rotation of the shafts is accomplished by using a chain drive that runs on a stationary sprocket on the central support pedestal. Velocities of liquid relative to the wall of from 0 to 25 fps can be obtained by using appropriate pulley speeds and sprocket sizes. A stationary furnace built around the tori will be capable of maintaining the samples at 250°C.

Four openings sealed off with tube fittings will be spaced symmetrically on each torus to permit insertion of solution and sample pins.

IN-PILE LOOP

G. H. Jenks	W. L. Ross
C. B. Graham	C. D. Zerby
R. J. Kedl	D. T. Jones
T. H. Mauney	R. A. Rosenberg

As pointed out previously, one of the most difficult problems associated with the operation of an in-pile test system is that of safely controlling the pressures of hydrogen and oxygen formed in the decomposition of water under irradiation. Originally, it was proposed to control these pressures by the recombination of the gases over a dry catalyst at the pressure of the system. A venturi type of pump, together with a liquid-gas separator, was to be used to effect circulation of gases over the catalyst. Careful analysis of the operation of the proposed system shows that it would be extremely difficult, if not impossible, to prevent the formation of explosive gas mixtures if the recombiner partly or completely failed. An explosive hazard would thus be inherent in this design. Primarily because of this hazard, the attempt to develop a system of this type has been abandoned, at least for the present.

The work is now being directed toward the development of a system that uses $CuSO_4$ in solution as the recombination catalyst. The studies made to date indicate that, with respect to explosion hazards, safe operation of this system can be accomplished. Corrosion information obtained with the loop will be affected by the presence of copper ion; but, even so, it is believed that a measure of the effect of irradiation on corrosion in homogeneous reactor systems can be obtained.

Loop Development and Design. The in-pile loop design has been modified to accommodate the addition of copper sulfate as an internal, homogeneous catalyst for the recombination of hydrogen and oxygen. The major components of the loop will be a centrifugal pump, a steam pressurizer, a loop-temperature control system, a "core," and corrosion sample holders. The loop will operate at 250°C and 1000 psi.

There will be two corrosion sample holders in each loop. One sample holder will be held in the center of the core of the loop in the highest flux region. Arrangements will be made so that the solution leaving the core will pass through the holder and subject the corrosion specimen to the highest possible short-lived fission-product concentration. The other sample holder will be placed in the circulating system so that it will be removed from the high flux region. The two sample holders will be identical with respect to provisions for holding the samples. Considerable effort has been made to pattern the design of these sample holders after the tapered ones used in the critical corrosion-velocity investigations in the out-of-pile dynamic corrosion

UNCLASSIFIED
DWG.19565

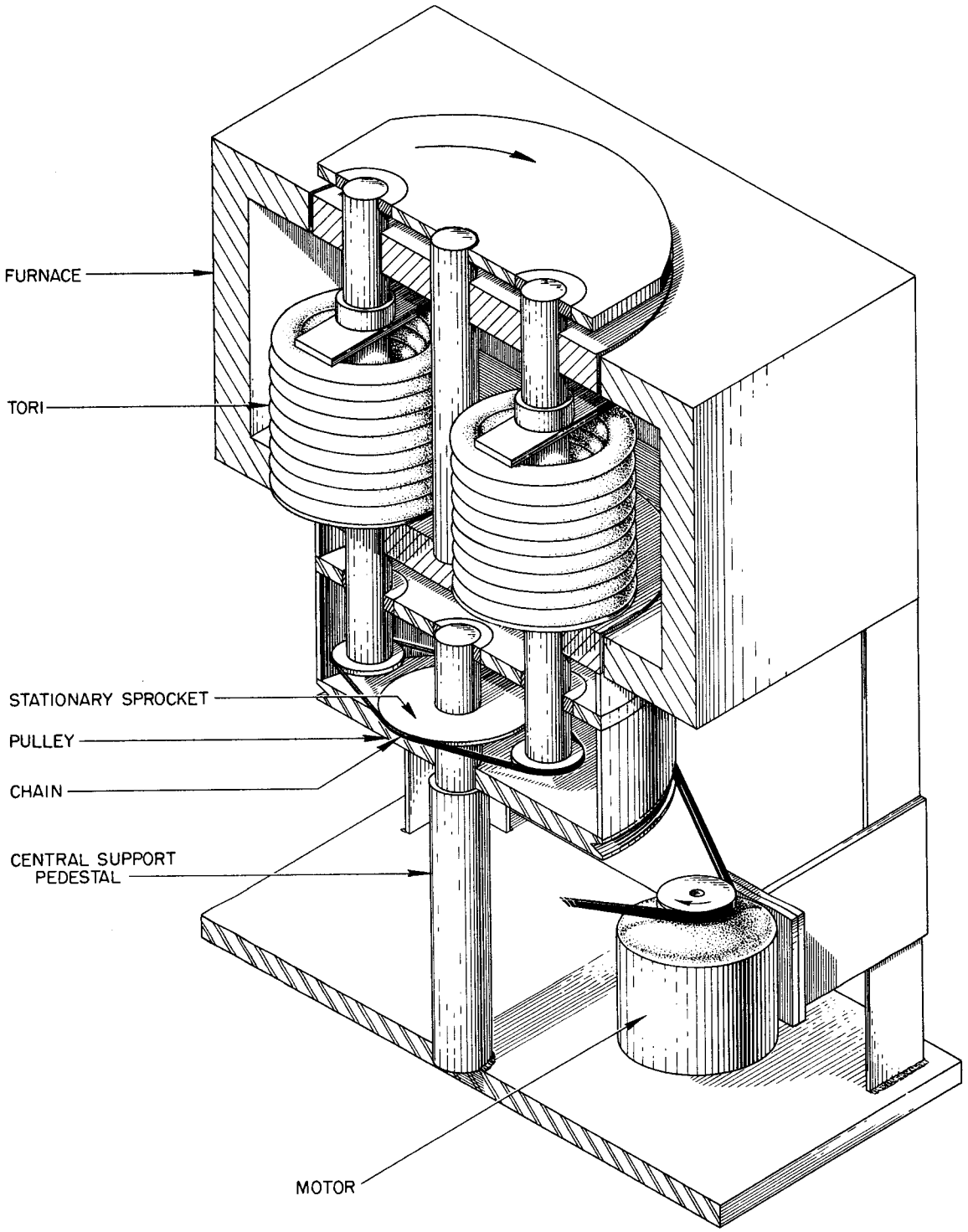

Fig. 37. Torus Rotator.

studies to provide the best possible correlation between data from the two programs. The new sample holder is designed to accommodate an anticipated flow of 50 fps, and it differs in size from the older design. The design is essentially complete, and models will be fabricated and tested in the dynamic corrosion test loops.

The progress on the centrifugal pump for the loop is described in the section of this report on "Small Canned-Rotor Pump Development." Design of the instrumentation to control the loop is nearing completion and orders will be placed for the necessary equipment in the near future. Effort is under way to develop operating methods and equipment and for handling the system after irradiation. Preliminary considerations of this problem have been made, and detailed design has been started.

The use of steam pressurization in the loop has several advantages. First, the main stream can operate with a dissolved gas pressure well below the saturation pressure so that no bubble formation will take place. The absence of bubbles reduces the possibility of explosion in the system and eliminates a possible source of corrosion acceleration. Second, the pressure of hydrogen and oxygen in the pressurizer can be maintained well below the explosion limit. An increase in pressure from these gases can be detected, and corrective measures can be taken before the explosion limit is reached.

Operating Characteristics. The approximate operating conditions of the loop as presently visualized are listed below:

Volume of liquid in pressurizer	200 ml
Volume of gas space in pressurizer	200 ml
Temperature of pressurizer	280°C
Excess oxygen pressure in pressurizer	70 psi
Flow rate through pressurizer	3 ml/sec
Total volume in main stream	1000 ml
Volume in core	300 ml
Power density in core (from fission)	5 watts/ml
Power density in other portions of loop (from fission)	0
Temperature of main stream	250°C
Pressure of excess oxygen dissolved in main stream at startup	100 psi
Steady-state pressure of dissolved stoichiometric gas in main stream	100 psi

The excess oxygen is introduced into the pressurizer at startup, and the concentration of the excess oxygen in the main stream is maintained by circulating a portion of the stream through the pressurizer. The indicated circulation rate is more than ample to maintain a steady-state distribution of oxygen between the pressurizer and the main stream, even at the highest corrosion rates which can be foreseen. Of course, the excess oxygen pressure will decrease as corrosion proceeds, and additional oxygen will have to be introduced from time to time. The pressure of the oxygen in the pressurizer will be recorded during operation, and the data will be used as a measure of the over-all corrosion rate, as well as an indication of when additional oxygen is needed.

Sufficient $CuSO_4$ will be added to the fuel solution to hold the steady-state pressure of stoichiometric gas at the desired value. It is estimated that a copper concentration of 0.01 *M* will result in a steady-state pressure of 100 psi.

The steady-state pressure of stoichiometric gas in the pressurizer will be about 12 psi under the specified operating conditions. Since the excess oxygen pressure will not exceed 70 psi, the partial pressures of oxygen and hydrogen together will normally not exceed 82 psi, or 8% of the total pressure. It is probable that in gas mixtures such as those which exist in the pressurizer, hydrogen and oxygen must supply more than 18% of the total pressure before explosions will take

place. (Note: Determinations of the explosive limits in these mixtures are being made at Battelle.)

A failure of the copper catalyst would be followed by an increase in the pressures of hydrogen and oxygen; some increase can be tolerated before the explosive limit is reached. It is planned that corrective measures will be taken when the total pressure of the system becomes 120 psi greater than steam pressure. Attainment of the 120-psi value corresponds to an increase in the stoichiometric gas pressure of 50 psi if no excess oxygen has been consumed or to an increase of 120 psi if all excess oxygen has been consumed. In either case, the partial pressures of hydrogen and oxygen will, together, comprise about 12% of the total pressure, and the mixture will be below the explosive limit.

STATIC CORROSION STUDIES

J. L. English

Static corrosion data are summarized here for the following four projects which were completed during this quarter:

1. An examination was made of the corrosion behavior of synthetic gems and spinels in oxygenated uranyl sulfate solutions containing 40 and 300 g of uranium per liter at 250°C. Included in this study was the effect of synthetic fission-product additions on corrosion resistance at 250°C.

2. A study was made of the corrosion resistance of type 347 stainless steel and the stability of uranyl sulfate solutions at 125°C in the absence of excess quantities of dissolved oxygen. Corrosion resistance and solution stability were examined as a function of uranium concentration.

3. An investigation was made to determine the susceptibility of type 347 stainless steel to crevice and stress corrosion as a function of temperature, uranium concentration, type of solution aeration, and magnitude of applied stress.

4. A study was made to determine whether commercial-grade titanium metal was subject to crevice and stress corrosion attack in uranyl sulfate solutions containing 5, 40, 100, and 300 g of uranium per liter at 95°C.

The pertinent data from each of these projects are presented in the following sections.

Corrosion Resistance of Synthetic Gems and Spinels. At the request of R. H. Powell, an investigation was undertaken to determine the corrosion resistance of synthetic titania, synthetic sapphire, and magnesium oxide spinel in oxygenated uranyl sulfate solutions at 250°C. The purpose of the investigation was to find a corrosion-resistant, transparent material which could be used for windows in a cell developed for the determination of uranium concentrations in uranyl sulfate solutions[5] by adsorption measurements.

The specimens for the tests were supplied by the Guardian Manufacture and Supply Co. in the form of small, unpolished stones. The average density of the stones was 4.3 g/cm^3. The first set of tests was run in uranyl sulfate solutions containing 40 g of uranium per liter at 250°C with an oxygen partial pressure of about 150 psia. The oxygen partial pressure was produced from the thermal decomposition of hydrogen peroxide that was added to the test solutions at room temperature. The solutions and specimens were contained in type 347 stainless steel autoclaves of 225-ml total capacity. Weight losses and calculated corrosion rates for the specimens are presented in Table 5.

It was apparent from the data in Table 5 that the fused synthetic titania exhibited the best over-all corrosion resistance; the final corrosion rate was 0.3 mpy. The magnesium

(5) W. H. Davenport, Jr. and R. H. Powell, *HRP Quar. Prog. Rep. Mar. 15, 1952*, ORNL-1280, p. 74-80.

TABLE 5. CORROSION RESISTANCE OF SYNTHETIC GEMS AND SPINEL IN URANYL SULFATE SOLUTIONS CONTAINING 40 g OF URANIUM PER LITER AND PRESSURIZED WITH 150 psia OF OXYGEN AT 250°C

EXPOSURE TIME (days)	WEIGHT LOSSES AND CALCULATED CORROSION RATES					
	Titania		Sapphire		MgO Spinel	
	mg/cm^2	mpy	mg/cm^2	mpy	mg/cm^2	mpy
7	-0.05	0.2	-0.50	2.2	-2.13	10.5
14	0.03	< 0.1	0.55	1.3	2.77	6.8
21	0.15	0.2	0.80	1.3	3.38	5.5
28	0.16	0.2	0.98	1.2	3.70	4.5
35	0.19	0.2	1.06	1.0	4.38	4.3
42	0.26	0.2	1.11	0.9	5.02	4.1
49	0.40	0.3	1.19	0.8	5.50	3.8
56	0.48	0.3	1.22	0.8	6.03	3.7
63	0.50	0.3	1.27	0.7	6.60	3.6

oxide spinel exhibited the poorest corrosion resistance, with a final corrosion rate of 3.6 mpy after 63 days. The specimens, except for the magnesium oxide spinel, showed no signs of corrosion damage. The surfaces of the spinel were somewhat etched and generally roughened in texture.

The same specimens were also subjected to exposure in uranyl sulfate solutions containing 300 g of uranium per liter and pressurized with about 150 psia of oxygen at 250°C. The corrosion data after 63 days are shown in Table 6. The corrosion resistance of the titania was little affected by the increase in uranium concentration from 40 to 300 g per liter; the steady-state corrosion rate was similar to that obtained in the solutions containing 40 g of uranium per liter, that is, 0.2 mpy. Corrosion of the sapphire and magnesium oxide spinel was greatly increased, however, by the increase in uranium concentration. Corrosion rates for these materials were more than four times greater than the values obtained in solutions containing 40 g of uranium per liter.

As a final check on the corrosion behavior of the three materials, they were exposed in uranyl sulfate solution containing 40 g of uranium per liter and synthetic fission-product additions. The fission products were added to the original test solutions as sulfates. Not all the additives were completely soluble in the uranyl sulfate; however, sufficient quantities were added to give the following concentrations, in ppm: Ce, 43; Ba, 5; Zr, 15; Sr, 6; Ru, 9; Te, 4; Mo, 12; and I, 3. Weight losses and corrosion rates are presented in Table 7 for 56 days of operation at 250°C. The uranyl sulfate solutions were pressurized with about 150 psia of oxygen in a manner similar to that used in the previously described tests. No adverse effect on the corrosion resistance of the three materials was observed upon the addition of simulated fission products to the corrosion environment. The final corrosion rates obtained after 56 days were nearly identical to the values obtained for a similar

TABLE 6. CORROSION RESISTANCE OF SYNTHETIC GEMS AND SPINEL IN URANYL SULFATE SOLUTIONS CONTAINING 300 g OF URANIUM PER LITER AND PRESSURIZED WITH 150 psia OF OXYGEN AT 250°C

EXPOSURE TIME (days)	WEIGHT LOSSES AND CALCULATED CORROSION RATES					
	Titania		Sapphire		MgO Spinel	
	mg/cm^2	mpy	mg/cm^2	mpy	mg/cm^2	mpy
7	-0.07	0.3	-1.73	8.5	-9.77	47.9
14	0.07	0.2	2.30	5.7	14.70	36.0
21	0.16	0.3	2.92	4.8	17.82	29.1
28	0.16	0.2	3.41	4.2	20.23	24.8
35	0.21	0.2	3.68	3.6	22.00	21.6
42	0.25	0.2	3.98	3.3	23.82	19.4
49	0.27	0.2	4.23	3.0	25.19	17.6
56			4.54	2.8	26.87	16.5
63			4.84	2.6	28.45	15.5

TABLE 7. CORROSION RESISTANCE OF SYNTHETIC GEMS AND SPINEL IN OXYGENATED URANYL SULFATE SOLUTIONS CONTAINING 40 g OF URANIUM PER LITER AND SIMULATED FISSION-PRODUCT ADDITIONS AT 250°C

EXPOSURE TIME (days)	WEIGHT LOSSES AND CALCULATED CORROSION RATES					
	Titania		Sapphire		MgO Spinel	
	mg/cm^2	mpy	mg/cm^2	mpy	mg/cm^2	mpy
7	-0.09	0.4	-0.32	1.6	-1.02	5.0
14	0.12	0.3	0.31	0.8	1.73	4.3
21	0.12	0.2	0.55	0.9	2.58	4.2
28	0.49	0.6	0.69	0.8	3.25	4.0
35	0.51	0.5	0.82	0.8	3.67	3.6
42	0.51	0.4	0.93	0.8	4.42	3.6
49	0.47	0.3	0.96	0.7	5.05	3.5
56	0.53	0.3	1.04	0.6	5.45	3.4

period in fission-product-free solutions containing 40 g of uranium per liter.

The synthetic fused titania offered the best corrosion resistance in all media tested. The synthetic sapphire exhibited the second best corrosion behavior, whereas the magnesium oxide spinel was the poorest. A summary of the data is presented in Table 8.

Corrosion and Solution Stability Studies in Uranyl Sulfate at 125°C. An investigation was completed to determine the corrosion resistance of type 347 stainless steel as a function of uranium concentration in uranyl

TABLE 8. SUMMARY OF CORROSION DATA FOR SYNTHETIC GEMS AND SPINEL IN URANYL SULFATE SOLUTIONS PRESSURIZED WITH 150 psia OF OXYGEN AT 250°C

MATERIAL	URANIUM CONCENTRATION (g/liter)	FISSION PRODUCTS	TIME (days)	CORROSION RATE (mpy)
Titania	40	Absent	63	0.3
Sapphire	40	Absent	63	0.7
MgO Spinel	40	Absent	63	3.6
Titania	40	Present	56	0.3
Sapphire	40	Present	56	0.6
MgO Spinel	40	Present	56	3.4
Titania	300	Absent	49	0.2
Sapphire	300	Absent	63	2.6
MgO Spinel	300	Absent	63	15.5

sulfate solutions at 125°C. Stability of the uranyl sulfate solutions was of interest because the tests were operated in the absence of the excess dissolved oxygen required for assuring solution stability at elevated temperatures; the stability was studied by making total uranium analyses. The available oxygen per test, 27 mg, was the amount dissolved in the test solution at room temperature and the amount of oxygen present in the air space of the test autoclave. Based upon the solubility of oxygen in water, the dissolved oxygen content at 125°C was estimated to be somewhat less than 25 ppm.

The corrosion tests were run in type 347 stainless steel autoclaves of 225-ml capacity which had been used previously for corrosion testing at 250°C. Prior to use, the autoclaves were cleaned with HNO_3-H_2O_2 solution and then pickled for 20 to 30 min at 60°C in 10 vol % HNO_3, 4 vol % HF. The test wafers were machined from type 347 stainless steel bar stock and tested in a machined condition.

The uranyl sulfate test solutions contained uranium concentrations of 40.9, 101.4, 193.1, and 300.5 g/liter, respectively. The tests were stopped at weekly intervals for examining and weighing the specimens. The solutions were analyzed for final total uranium and dissolved nickel contents. The cumulative as-removed weight losses and final electrolytically defilmed weight losses are reported in Table 9 as a function of time and uranium concentration.

The physical appearance of the specimens differed markedly as the uranium concentration was increased from 40 to 300 g/liter. In all cases, the corrosion films appeared to be thin but the colors ranged from the original lustrous, metallic gray in the solution containing 40 g of uranium per liter to a very dark, brown-colored film in the solution containing 300 g of uranium per liter. The final total uranium and dissolved nickel contents in the test solutions are shown in Table 10.

The final uranium analyses showed a reduction of 6 to 9 mole % in total uranium content for all solutions. Whether these reductions were due to the hydrolysis of the uranyl ion to form a hydrated UO_3 precipitate or due

TABLE 9. CORROSION OF TYPE 347 STAINLESS STEEL IN UNOXYGENATED URANYL SULFATE SOLUTIONS AT 125°C

EXPOSURE TIME (days)	URANIUM CONCENTRATION (g/liter)							
	40.9		101.4		193.1		300.5	
	WEIGHT LOSSES AND CALCULATED CORROSION RATES							
	mg/cm^2	mpy	mg/cm^2	mpy	mg/cm^2	mpy	mg/cm^2	mpy
7	-0.08	0.19	-0.01	0.02	-0.12	0.30	-0.13	0.34
14	0.14	0.20	0.16	0.21	0.15	0.19	0.22	0.29
21	0.17	0.14	0.16	0.14	0.26	0.22	0.40	0.34
28	0.16	0.10	0.15	0.09	0.23	0.15	0.50	0.32
35	0.15	0.08	0.18	0.09	0.19	0.09	0.53	0.27
42	0.17	0.07	0.21	0.09	0.23	0.10	0.63	0.27
49	0.19	0.07	0.27	0.10	0.31	0.11	0.75	0.28
Defilmed	0.16	0.06	0.28	0.10	0.42	0.16	0.75	0.28

TABLE 10. FINAL TOTAL URANIUM AND DISSOLVED NICKEL CONTENTS IN URANYL SULFATE TEST SOLUTIONS AT 125°C

URANIUM CONCENTRATION (g/liter)		DISSOLVED NICKEL (mg/ml)
Initial	Final	
40.9	36.9	10
101.4	93.1	17
193.1	182.8	54
300.5	280.5	79

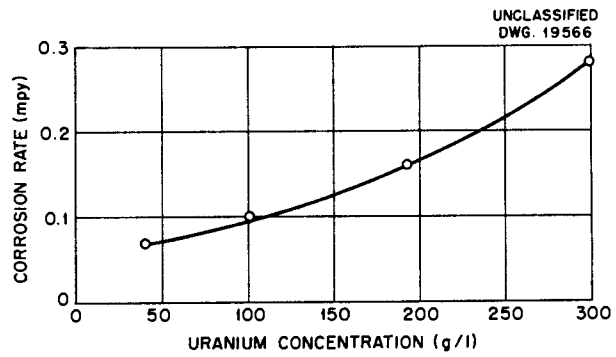

Fig. 38. Corrosion Behavior of Type 347 Stainless Steel as Affected by Uranium Solutions After 49 Days at 125°C.

to an actual reduction of the uranyl ion to UO_2 and/or U_3O_8 is not known. There were no visual indications of deposited $UO_3 \cdot xH_2O$ during operation of the tests, and the final solution pH measurements were steady at values of 0.2 to 0.3 unit higher than the initial pH values.

Corrosion attack on the type 347 stainless steel specimens increased with an increase in total uranium concentration in the solutions. The magnitude of attack as a function of the uranium concentration is shown in Fig. 38. At a concentration of 40.9 g of uranium per liter, the corrosion rate was 0.06 mpy after 49 days; the rate increased to 0.28 mpy as the uranium content was increased to 300.5 g/liter. Microscopic examination of the defilmed specimens disclosed corrosion attack to be generalized and of a uniform nature; no evidences of pitting attack were observed.

The final dissolved nickel values were used to calculate corrosion rates over the surfaces of the type 347 stainless steel autoclaves wetted by

the uranyl sulfate solutions at 125°C. Including the surface area of the specimen in each autoclave, the total immersed area was approximately 245 cm^2. A comparison between the defilmed corrosion rates on the specimens and the corrosion rates calculated from the dissolved nickel contents appears in Table 11. This comparison actually distinguishes between the corrosion behavior of newly machined stainless steel specimen surfaces and the pickled stainless steel surfaces of the autoclave walls. The agreement in values obtained by the two methods was quite good.

TABLE 11. COMPARISON OF CORROSION RATES OBTAINED FROM DEFILMED WEIGHT LOSSES AND FROM DISSOLVED NICKEL CONTENTS IN URANYL SULFATE SOLUTIONS AT 125°C AFTER 49 DAYS

INITIAL URANIUM CONCENTRATION (g/liter)	CORROSION RATE (mpy)	
	Weight Loss Method	Dissolved Nickel Method
40.9	0.07	0.03
101.4	0.10	0.05
193.1	0.16	0.17
300.5	0.28	0.24

Stress and Crevice Corrosion Studies with Type 347 Stainless Steel. Considerable effort was expended on a series of investigations to determine whether type 347 stainless steel was subject to crevice and stress corrosion attack under a wide range of exposure conditions. The susceptibility to these two types of corrosion attack was examined as a function of temperature, uranium concentration, type of solution aeration or deaeration, and magnitude of applied stress.

The results of studies made with the following solutions and conditions are reported:

1. uranyl sulfate solutions containing 5, 40, 100, and 300 g of uranium per liter at 95°C; natural deaeration employed;
2. uranyl sulfate solutions containing 200 g of uranium per liter at 95°C; helium and oxygen aeration employed;
3. uranyl sulfate solutions containing 300 g of uranium per liter at 95°C; natural deaeration, helium aeration, and oxygen aeration employed;
4. uranyl sulfate solutions containing 300 g of uranium per liter at 95°C; pressurized with 1000 psi oxygen;
5. uranyl sulfate solutions containing 40 g of uranium per liter at 250°C; pressurized with 150 psia oxygen.

Studies with Uranyl Sulfate Solutions Containing 5, 40, 100, and 300 g of Uranium per Liter. The stress specimens used in this investigation were of a type recommended by F. LaQue of the International Nickel Co. for qualitative examination of the susceptibility of a material to stress corrosion attack. The specimens, 8 cm in length, were cut from 0.95-cm-dia type 347 stainless steel welded tubing. One end of each tube was pinched together tightly in a vise; the opposite end was then bent at an angle of 90 deg to the central axis of the tube. Thus, a graduation in stresses up to and exceeding the elastic limit of the stainless steel was incorporated into the specimens. The validity of the LaQue-style specimen for determining the susceptibility of type 347 stainless steel to stress corrosion attack was established initially by exposing specimens in 42% $MgCl_2$ solution at 152°C. Within 2 hr, severe cracking occurred at the highly stressed areas.

The stress specimens, along with unpinched and unbent control specimens, were exposed in uranyl sulfate solutions containing 5, 40, 100, and 300 g of uranium per liter, respectively. The solutions were essentially oxygen-free at 95°C, and the test was operated for a period of 79 days. Specimens were examined and weighed at weekly intervals. At completion of the tests, the

specimens were electrolytically treated for removal of the corrosion films. The final defilmed corrosion data are presented in Table 12.

There were no marked differences between the corrosion rates for the control and stress specimens in their respective environments. In fact, the corrosion behavior of type 347 stainless steel, stressed or otherwise, was little affected by an increase in uranium concentration from 5 to 300 g/liter. The specimens were carefully cut in half, longitudinally, and the interior and the mating surfaces were examined microscopically at 100X for indications of stress and/or crevice corrosion attack. No signs of such attack were disclosed by the examination. The surfaces were light gray in color, with uniform distribution of corrosion damage.

Studies with Uranyl Sulfate Solutions Containing 200 g of Uranium per Liter. An examination was made of the corrosion resistance of type 347 stainless steel stress specimens at 95°C in uranyl sulfate solutions containing 200 g of uranium per liter. The specimens were of the LaQue style described in the previous section, and they were prepared from 0.6-cm-dia welded tubing. One slight modification was made in the specimen geometry, however. The 90-deg bend was made on the end which was pinched together so that the opposite end of the specimen was entirely unstressed.

Two types of aeration were employed for the tests. One solution was aerated by the introduction of oxygen at a rapid rate; the second solution was made oxygen-free by the passage through it of helium gas. The tests were run for a period of 95 days, with frequent examination and weighing of the specimens. At the completion of the run, the specimens were defilmed electrolytically for measurement of actual weight losses.

The results showed that the type of aeration used in the solutions had very little effect on the corrosion behavior of the type 347 stainless steel specimens. The defilmed weight loss on the helium-aerated specimen was 0.12 mg/cm^2 as compared with a 0.13-mg/cm^2 loss on the oxygen-aerated specimen. These losses were equivalent to a corrosion rate of 0.03 mpy for the 95-day period.

The specimens were cut in half, longitudinally, and the interior wall and the mating surfaces were examined microscopically. The stressed metal areas were completely free of any signs

TABLE 12. DEFILMED CORROSION DATA ON TYPE 347 STAINLESS STEEL STRESS AND CONTROL SPECIMENS AFTER 79 DAYS IN DEAERATED URANYL SULFATE SOLUTIONS AT 95°C

INITIAL URANIUM CONCENTRATION (g/liter)	SPECIMEN TYPE	WEIGHT LOSS (mg/cm^2)	CORROSION RATE (mpy)
4.9	Stress	0.09	0.02
	Control	0.06	0.01
39.8	Stress	0.07	0.02
	Control	0.07	0.02
101.0	Stress	0.12	0.03
	Control	0.09	0.02
300.0	Stress	0.15	0.03
	Control	0.23	0.05

of localized corrosion attack or cracking. The pinched ends were spread apart, and it was found that these areas of direct metal-to-metal contact were equally free from indications of crevice corrosion attack.

Studies with Uranyl Sulfate Solutions Containing 300 g of Uranium per Liter. Stress and crevice corrosion studies were continued with type 347 stainless steel in uranyl sulfate solutions containing 300 g of uranium per liter at 95°C. Three types of solution aeration and deaeration were used for these tests: natural deaeration, helium aeration, and oxygen aeration. The test specimens were of two types: a modified LaQue-style and a type that is referred to as the Heinkel loop test specimen.[6]

The modified LaQue-style specimens consisted of various lengths of 0.6-cm-dia type 347 stainless steel welded tubing; one end of each specimen was pinched together tightly. No bends were formed in these tubes. The Heinkel loop test specimens were prepared by forming 0.2-cm-thick by 1.9-cm-wide by 12.7-cm-long type 347 stainless steel strips into a U shape. The ends of the U were then bolted together with type 347 stainless steel studs and nuts to subject the specimen to an elastic stress. Unstressed control specimens for each material were tested simultaneously with the stress specimens.

The tests were operated for 76 to 82 days, and then the specimens were defilmed electrolytically and examined microscopically for signs of stress and crevice corrosion attack. The final defilmed corrosion data are summarized in Tables 13 and 14 for the two types of specimens.

The stressed-tube type of specimens were bisected longitudinally and examined for indications of accelerated corrosion attack. As observed in previous tests, the interior surfaces were semidull and whitish-gray in color; there were no signs of localized corrosion attack in the stressed zones, and no contact corrosion attack was visible on the mating surfaces of

[6] F. A. Champion, *Corrosion Testing Procedures*, p. 146-147, Wiley, New York, 1952.

TABLE 13. DEFILMED CORROSION DATA FOR MODIFIED LaQUE-STYLE, TYPE 347 STAINLESS STEEL, STRESS SPECIMENS AFTER 82 DAYS AT 95°C IN URANYL SULFATE SOLUTIONS CONTAINING 300 g OF URANIUM PER LITER

AERATION TYPE	SPECIMEN TYPE	SPECIMEN LENGTH (cm)	WEIGHT LOSS (mg/cm^2)	CORROSION RATE (mpy)
None	Stress	4.0	0.17	0.04
None	Stress	6.5	0.14	0.03
None	Stress	9.0	0.12	0.03
None	Control	5.0	0.16	0.04
Helium	Stress	4.0	0.16	0.04
Helium	Stress	6.5	0.16	0.04
Helium	Stress	9.0	0.11	0.03
Helium	Control	5.0	0.14	0.03
Oxygen	Stress	4.0	0.17	0.04
Oxygen	Stress	6.5	0.14	0.03
Oxygen	Stress	9.0	0.11	0.03
Oxygen	Control	5.0	0.14	0.03

the pinched ends. Similarly, an examination of stress and contact areas on the Heinkel loop specimens disclosed no evidences of localized corrosion attack.

Studies with Uranyl Sulfate Solutions Containing 300 g of Uranium per Liter. LaQue- and Heinkel-type stress specimens of type 347 stainless steel were exposed at 95°C in uranyl sulfate solution containing 300 g of uranium per liter, and an oxygen partial pressure of 1000 psig was maintained. Unstressed control specimens were tested along with each type of stress specimen.

The specimens and solution were contained in a type 347 stainless steel autoclave which was pressurized with 1000 psig of oxygen at room temperature. The test was operated for 76 days, and the specimens were periodically inspected. The defilmed corrosion data are presented in Table 15.

The defilmed corrosion rates were not indicative of accelerated corrosion attack due to either stress or crevice corrosion. The corrosion rates for the stressed specimens were of similar magnitude to the values obtained in previous tests of exposure in uranyl sulfate solution containing 300 g of uranium per liter at 95°C.

Microscopic examination was made of the interior surfaces of the bisected tubing; again, corrosion attack was of

TABLE 14. DEFILMED CORROSION DATA FOR HEINKEL LOOP, TYPE 347 STAINLESS STEEL, STRESS SPECIMENS AFTER 76 DAYS AT 95°C IN URANYL SULFATE SOLUTIONS CONTAINING 300 g OF URANIUM PER LITER

AERATION TYPE	SPECIMEN TYPE	WEIGHT LOSS (mg/cm^2)	CORROSION RATE (mpy)
None	Stress	0.23	0.05
None	Control	0.25	0.06
Helium	Stress	0.17	0.04
Helium	Control	0.18	0.04
Oxygen	Stress	0.24	0.06
Oxygen	Control	0.22	0.05

TABLE 15. DEFILMED CORROSION DATA FOR LaQUE- AND HEINKEL-TYPE STRESS SPECIMENS OF TYPE 347 STAINLESS STEEL EXPOSED IN URANYL SULFATE SOLUTION CONTAINING 300 g OF URANIUM PER LITER AND PRESSURIZED WITH 1000 psig OF OXYGEN AT 95°C

SPECIMEN TYPE	EXPOSURE TIME (days)	WEIGHT LOSS (mg/cm^2)	CORROSION RATE (mpy)
LaQue	76	0.13	0.03
LaQue	76	0.17	0.04
LaQue	76	0.18	0.04
Control	76	0.15	0.04
Heinkel	76	0.27	0.06
Control	76	0.62	0.15

a generalized nature and there was complete absence of pitting or cracking in the regions of stress and metal-to-metal contact. The Heinkel-loop specimens exhibited the usual, slightly roughened surfaces that are representative of generalized corrosion. The contact faces were stained somewhat at junctions with the nuts and studs used to draw the ends of the U tubes together, but, otherwise, they were unchanged.

Studies with Uranyl Sulfate Solutions Containing 40 g of Uranium per Liter. The last series of tests for determining the susceptibility of type 347 stainless steel to crevice and stress corrosion was concerned with exposure at 250°C in oxygenated uranyl sulfate solutions containing 40 g of uranium per liter. In these tests, a stress was applied by three-point loading of beam-type specimen assemblies, and the stress was measured with an SR-4 strain gage. Briefly, the test assembly consisted of a 0.3-cm-thick specimen centrally mounted on a fulcrum and base plate. A load was applied to the specimen by tightening the nuts on the studs positioned in each end of the assembly. The applied load, in turn, was measured with a strain gage cemented to the center of the test specimen. The values of stress used in this investigation represent values for the maximum outer fiber stress on the specimen surface directly above the fulcrum. The applied stresses included in the study were 7,000, 15,000, 30,000, and 75,000 psi.

The test specimens, 0.3 cm thick by 1.6 cm wide by 8.8 cm long, were annealed in air at 1010°C for 1 hr, air-cooled, and lightly pickled in warm 10% HNO_3-4% HF solution for 10 min to remove annealing scale. Unstressed control specimens were treated in a similar fashion. The tests were run in type 347 stainless steel autoclaves with an oxygen partial pressure of 85 to 90 psi at 250°C. The autoclaves were pressurized with 150 psig of oxygen at room temperature to produce the partial pressure at 250°C. The dissolved oxygen content at 250°C was estimated to be 500 ppm.

The tests were run for 48 to 63 days at 250°C, and the specimens were examined frequently. During the tests, the specimens developed heavy, dark-colored corrosion films which obscured corrosion damage effects on the underlying metal surfaces. At the completion of the tests, the specimens were defilmed electrolytically. The results are shown in Table 16.

TABLE 16. DEFILMED CORROSION DATA FOR BEAM-TYPE STRESS SPECIMENS OF TYPE 347 STAINLESS STEEL EXPOSED IN OXYGENATED URANYL SULFATE CONTAINING 40 g OF URANIUM PER LITER AT 250°C

APPLIED MAXIMUM STRESS (psi)	EXPOSURE TIME (days)	WEIGHT LOSS (mg/cm^2)	CORROSION RATE (mpy)
7,000	48	0.69	0.26
15,000	48	0.69	0.26
30,000	48	0.65	0.24
None	48	0.63	0.24
75,000	63	0.71	0.21
75,000	63	0.77	0.22
None	63	0.69	0.20

The corrosion rates for the stressed specimens were completely independent of the magnitude of the applied stress and were in excellent agreement with the rate values for the unstressed control specimens. No signs of accelerated corrosion attack resulting from stress were found by microscopic examination. Definite indications of crevice corrosion were observed, however, on two of the specimen assemblies. In both cases, the localized corrosion took place on the specimen area contacted by the stainless steel nut used to apply the desired load. The maximum pit depth, measured microscopically, ranged from 3 to 5 mils in these areas.

In summarizing the results of the complete investigation to determine whether type 347 stainless steel was subject to stress and crevice corrosion attack under a wide range of exposure conditions, it may be stated that, under the specific test conditions included in the investigation, there was no evidence of corrosion attack which could be attributed directly to the effects of stress at temperatures of 95 to 250°C. Also, no indications of crevice or contact corrosion attack were observed at temperatures of 95°C, but there were positive signs of such type of attack in the 250°C tests.

Stress and Crevice Corrosion Studies with Commerical-Grade Titanium. A study was made to determine whether commercial-grade titanium metal was subject to stress and/or crevice corrosion attack in oxygen-free, quiescent uranyl sulfate solutions containing 5, 40, 100, and 300 g of uranium per liter at 95°C. Stresses of 50,000 psi were obtained by three-point bending of beam-type specimens mounted on rigid base plates. Unstressed control specimens were tested simultaneously with the stressed specimens. A total exposure time of 86 days was accumulated in the tests. The stress specimens were fabricated from commercial-grade titanium metal designated as RC-70. This material was supplied by Rem-Cru Titanium, Inc., in the form of annealed, 0.32-cm-thick sheet. Other components of the stress assembly, such as the fulcrum, studs, and nuts, were machined from similar material. The base plates were prepared from 0.64-cm-thick, annealed, sheet TI-75A, supplied by Titanium Metals Corp.

The applied stress on the specimens was measured in terms of microinches of strain with an SR-4, type A-7, strain gage and a Baldwin SR-4 strain indicator. The stud-nut combination mounted in each end of the stress assembly was tightened to apply a load to the test specimen centrally supported on the fulcrum. The resulting strain was indicated by the gage cemented directly above the fulcrum. The 50,000-psi stress obtained was the maximum outer fiber stress on the specimen at the point directly above the fulcrum.

At the completion of the 86-day tests, the stress assemblies were dismantled, and the specimens were examined and defilmed electrolytically. The final corrosion data for the control and stress specimens appear in Table 17.

Microscopic examination of the stressed surfaces at frequent intervals during the tests disclosed no signs of stress corrosion attack. The final appearance of the stress specimen was the same as that of the control specimen; all surfaces were covered with very thin, adherent, golden-brown-colored films. After the assemblies were dismantled, the areas contacted by the fulcrums and nuts were inspected closely for indications of contact corrosion attack; none were found.

TABLE 17. CORROSION OF TITANIUM STRESS AND CONTROL SPECIMENS AFTER 86 DAYS AT 95°C IN OXYGEN-FREE URANYL SULFATE SOLUTIONS

URANIUM CONCENTRATION (g/liter)	SPECIMEN TYPE	WEIGHT LOSS (mg/cm^2)	CORROSION RATE (mpy)
4.9	Stress	0.03	0.01
	Control	0.03	0.01
39.8	Stress	0.04	0.02
	Control	0.03	0.01
101.0	Stress	0.05	0.02
	Control	0.02	0.01
300.0	Stress	0.04	0.02
	Control	0.05	0.02

METALLURGY

E. C. Miller, Group Leader
W. J. Leonard T. W. Fulton
W. J. Fretague W. O. Harms
Metallurgy Division
A. R. Olsen, Reactor Experimental Engineering Division
F. J. Lambert, Y-12
J. C. Wilson R. G. Berggren
Solid State Division

SERVICE AND MISCELLANEOUS WORK

E. C. Miller T. W. Fulton
W. O. Harms

The service work, described in previous reports, for the Corrosion, Design, Instrument, and Engineering Groups has continued.

Several groups of corrosion test pins have been prepared for the Dynamic Corrosion Group for loop testing. The principal objective of these tests is to evaluate the metallurgical variables, because they may influence attack under dynamic corrosion test conditions.

Previous work indicated that a sensitized type 304 stainless steel specimen holder (which was erroneously introduced into the system in a sensitized condition) underwent serious intergranular disintegration in contact with stagnant uranyl sulfate solution trapped underneath a type 347 stainless steel band. Since the portion of the sensitized material which was freely exposed to flowing solution did not appear to be attacked, several specimens of type 304 stainless steel have been prepared in the fully annealed, sensitized, machined, and electropolished conditions for controlled dynamic corrosion tests.

Another group of type 347 stainless steel specimens containing various amounts of martensite has been prepared to determine the effect of the presence of martensite on corrosion. To produce the martensite, type 347

austenitic stainless steel was cold worked (bent 90 deg and then straightened) at various temperatures - liquid nitrogen temperature, dry ice temperature, room temperature, boiling water temperature, and approximately 400°F.

Preliminary static corrosion tests were made on type 347 stainless steel specimens in water that had been degassed and to which hydrogen and oxygen had been added. The type 347 stainless steel specimens were tested in the as-machined, the fully annealed, and the commercially descaled conditions. Both sand blasting and a commercial salt bath treatment were used to prepare the descaled specimens. The tests indicated that very substantial differences in appearance and in measured corrosion attack resulted from the differences in the initial conditions of the stainless steel surfaces. This work is being extended to include most of the surface conditions which would be encountered normally or might reasonably be achieved in the commerical preparation of austenitic stainless steels. Finishing operations can produce surfaces which differ appreciably from the interior of the metal in chemical composition, degree of cold work, and the presence and disposition of the various microscopic phases. The surface variations may account for variations in corrosion behavior which are sometimes left unexplained or are attributed to the environment. Specimens prepared by various methods are being tested under static and under dynamic conditions. A particular effort will be made to test specimens that have been succesively machined, fully annealed, descaled, and then electropolished so that they have fully austenitic surfaces, are free from cold work, and have the same chemical composition as that of the interior of the specimen.

Another group of specimens is being prepared to determine the corrosion behavior under dynamic corrosion test conditions of weld metal containing up to 10% ferrite. In the fabrication of heat exchangers and other equipment from austenitic stainless steels, a question regarding the amount of cold work permissible in the fabrication is raised. It is known that stress corrosion cracking sometimes occurs in tube sheets, as well as in tubes; the cracking cannot be reproduced consistently in laboratory tests nor can the causes for it be precisely defined.

Specimens are being prepared for evaluating and comparing the effects of cold working at various temperatures (from liquid nitrogen temperature to approximately 400°F), particularly with respect to the resultant variations in martensite content, the partial stress relief and full annealing of these cold-worked materials, and the superimposition of elastic stresses on the residual stresses which result from cold work. Specimens of fully annealed stainless steel tubing are crimped, twisted, and bent at the desired temperatures and are subsequently stress relieved and annealed or left in the cold-worked condition, as desired. The specimens will be exposed to the environments which will probably be encountered in homogeneous reactors and environments which are known to be capable of causing stress corrosion cracking.

RADIATION DAMAGE STUDIES

R. G. Berggren A. R. Olsen
N. E. Hinkle

Impact specimens of type 304 stainless steel, type 347 stainless steel, commercial-purity titanium (Ti-75A), and iodide titanium have been irradiated in the ORNL graphite reactor, and impact tests will be completed shortly. An impact tester has been installed in the hot cell designated for this work, and the test work is now in progress.

WELDING OF TYPE 347 STAINLESS STEEL

W. J. Leonard

Welds of 1-in. type 347 stainless steel plate to type 347 stainless steel plate and to a 30% carbon steel plate were made with type 347, lime-coated, stainless steel filler rod and type 307 (Mn), lime-coated, stainless steel filler rod over type 347 stainless steel, bare-rod, heliarc root passes. Other welds were made with the exclusive use of the two lime-coated rods for the root and the filler passes in the welding of carbon steel plate to stainless steel plate. The plates were cut into standard test specimens for tensile and bend tests.

The tensile strengths of the welds made of type 347 stainless steel exceeded the yield strengths and tensile strengths of the base metals. The per cent elongation in the weld metal was usually lower than that (35%) of the type 347 stainless steel base plate because of the work-hardening by peening during the welding process. Specimens usually broke in the base metal adjacent to the weld metal. All these welds were considered as satisfactory. The tensile strengths of welds made of carbon steel to stainless steel were lower than all-stainless steel welds, since the stainless steel base plate and weld metal were both stronger than the carbon steel base plate. The specimens usually broke outside the heat-affected zone in the carbon steel plate, about 1/8 to 1/4 in. from the weld-to-carbon steel interface. The average yield strength was 42,000 psi and the tensile strength was 78,000 psi. The welds were all considered to be satisfactory.

Plates of type 347 stainless steel, 2 in. thick, were welded with the use of a type 347 stainless steel bare rod and a type 347, lime-coated, stainless steel electrode. The pertinent features of the welding design are a 20-deg included angle, a $1/16\ ^{+0.015}_{-0.000}$ in. root face, and a 3/8-in. root radius with a U groove. The first four passes of the heliarc process were made with 3/32-in. bare, filler rod. The remaining passes were made with 1/8- and 5/32-in., lime-coated electrodes. Penetration through the base of the root was normal. Radiographs and liquid-penetrant inspection methods showed a normal, sound weld.

Because this design restricted the movement of the welder using the heliarc torch, the second weld was made with a design that allowed greater freedom of manipulation while the root passes were being made. A U groove, with an included angle of 40 deg and a 1/4-in. radius, was used in the second weld. The procedures for welding were identical to those for the first weld, except that 3/16-in., coated rod was used for all the filler passes. Good penetration and a sound weldment were indicated by liquid-penetrant inspection and radiographs. The volume of weld metal was larger than that used in the first weld, but the design gave ample freedom of manipulation for the welder.

This second weld was sectioned into specimens for side bend tests and for macroscopic, microscopic, and soundness tests. A standard, guided-bend-test jig was used to bend specimens to angles of between 140 and 165 degrees. All the bend-test specimens were sound. Macroscopic and microscopic examination also indicated sound, normal welds. A soundness test, which consisted of an etch in a saturated ferric chloride solution to show very small fissures in the weld metal which might have escaped detection by the other methods, indicated normal, sound, weld metal.

Specimens of type 347 stainless steel weld metal, laid under conditions of severe enough restraint to cause cracking in the weld metal, were received from another AEC installation. The cracks in the weld metal are being studied microscopically and by x-ray diffraction methods to determine the

role of the chemical concentration of certain of the elements in type 347 stainless steel in the promotion of cracks and to determine the preferred location and mechanism of cracking.

BRITTLE FRACTURE OF TITANIUM

A. R. Olsen

A literature survey has been started to cover the wide variety of laboratory-scale specimens, procedures, and criteria for an engineering evaluation of ductile-to-brittle transition of titanium. It is hoped that careful screening of the tests will lead to an experimental program that will permit comparison of the present test results with data more easily converted into design specifications.

TITANIUM FOR VALVE TRIM

The actual tests of valves are reported by the groups doing the work; however, the Metallurgical Group has continued to assist in these programs. A study has been made of surface hardening with nitrogen, and, more recently, in cooperation with the Static Corrosion Group, attempts have been made to reduce galling of non-hardened surfaces by pretreatment in oxygen-saturated water at 250°C.

PROPERTIES OF TITANIUM

W. J. Fretague

Commercial Titanium. Twelve finish-machined impact specimens of commercial titanium (Ti-75A, item 24, heat L782), which had been vacuum annealed at 500°C for 1 hr and furnace cooled prior to machining, were vacuum annealed at 600°C for 1 hr and furnace cooled. Four of the specimens will be used to establish the transition temperature of annealed titanium. The eight remaining specimens, four of which were abraded lightly with 400-mesh emery paper, were submitted to the Dynamic Corrosion Group for loop testing in uranyl sulfate solution prior to impact testing to study the effect of cold work on the rate of hydrogen absorption by Ti-75A. A more detailed outline of the test was presented in the previous report.[1]

Since cold working is reported[2] to have a drastic effect on the rate of hydrogen absorption of titanium, corrosion and impact tests will be made on a series of severely cold-worked samples. Titanium bar (Ti-75A, item 24, heat L782), 1 in. in diameter, was swaged to 0.219-in.-dia rod from which 20 specimens have been machined. Four specimens are to be corrosion tested in uranyl sulfate in a loop. Four specimens will be cathodically treated in approximately 1 *M* H_2SO_4 (room temperature) at a current density of approximately 0.2 amp per square inch. Eight specimens will be impact tested without further treatment other than swaging and machining. Four specimens will be kept in reserve for future testing.

Two, 0.032-in.-thick by 1 7/8-in.-wide, Ti-75A sheets were fabricated by pack rolling[1] 1/4-in.-thick Ti-75A plate at 850°C. The sheets were then sheared to suitable lengths for sheet fatigue specimens and surface ground on both sides to a final thickness of 0.027 inch. The 18 specimen blanks prepared were vacuum annealed at 600°C for 1 hr and furnace cooled. Four, sheet, fatigue specimens were machined from annealed specimen blanks and fatigue tested at three different stress levels. The results obtained appear in Table 18 and are plotted in Fig. 39.

Six of the remaining 14 specimen blanks (3 5/8 in. long by 1 7/8 in. wide by 0.027 in. thick) were heliarc welded by placing two specimen blanks together and welding around the periphery of the assembly. One of these assemblies and two, single,

(1) W. J. Fretague, *HRP Quar. Prog. Rep. Jan. 1, 1953*, ORNL-1478, p. 83-88.

(2) D. P. Smith, *Hydrogen in Metals*, p. 5, 21, 24, and 26, Univ. of Chicago Press, Chicago, 1948.

TABLE 18. RESULTS OF FATIGUE TESTS ON ANNEALED SPECIMENS OF Ti-75A

SPECIMEN NO.	STRESS (psi)	NUMBER OF CYCLES BEFORE FAILURE
1	40,500	41×10^6*
2	45,000	16.6×10^4
3	50,000	16.4×10^4
4	50,000	8.0×10^4**

*Specimen did not break; test discontinued.

**By mistake, this specimen was subjected to a preload in the fatigue-testing machine and failed prematurely.

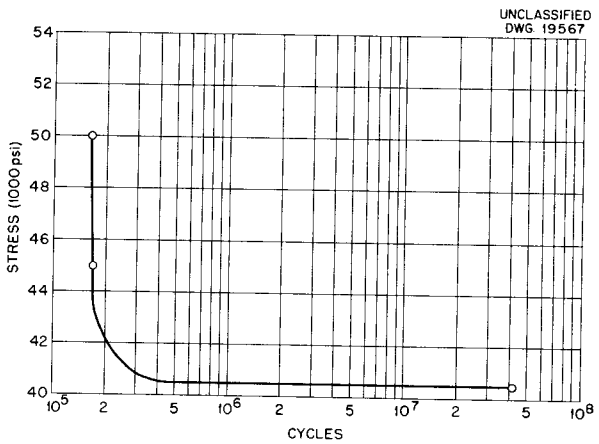

Fig. 39. Fatigue Properties of Ti-75A Hot-Rolled and Annealed Sheet.

specimen blanks were prepared for static exposure to uranyl sulfate solution at approximately 250°C. Another welded assembly and two, single, specimen blanks will be given cathodic treatment in sulfuric acid.

A third set of specimens (one welded assembly and two, single, specimen blanks) was heated at 750°C for 4 1/2 hr in a hydrogen atmosphere. This treatment was somewhat drastic, and the specimens warped badly when moved from the hot zone to the cold zone of the furnace. When an attempt was made to straighten one of the warped specimen blanks by hand, it broke into several smaller pieces. Obviously, the hydrogen absorbed had severely embrittled the material. In an attempt to salvage them, the three remaining pieces that were treated in hydrogen were vacuum annealed at 950°C for 4 hr and furnace cooled. On the assembly made up of two specimen blanks welded together, the hydrogen diffusing from the inner surfaces of the two specimen blanks built up a pressure great enough to actually deform and separate the inner surfaces of the two welded pieces. In an attempt to salvage them, these vacuum-annealed pieces will be cold rolled very slightly. If this is successful, they will be treated again in hydrogen at a lower temperature and for a shorter period of time.

Two sheet specimens machined from 0.027-in.-thick, vacuum-annealed, Ti-75A sheet will be irradiated and then fatigue tested.

The hydrogen content of a number of titanium specimens has been determined by the vacuum-fusion method. A summary of the samples analyzed and the results reported was presented in the previous report. Table 19 lists the previous results plus the results reported during the current quarter.

It has been reported in the literature[3] that the room-temperature solubility of the titanium-hydrogen phase is less than 0.14 at. % H (0.0029 ± 0.0003 wt %), whereas it has been shown that, in titanium-hydrogen alloys, up to at least 4.5 at. % H is soluble in alpha titanium at 200°C. This drastic decrease in the solubility of hydrogen with decreasing temperature suggests that the rapid cooling from above 200°C of titanium-hydrogen alloy containing more than 0.14 at. %H may result in a supersaturated solid solution of hydrogen in titanium at room temperature. Murray and Taylor[4]

(3) C. M. Craighead, G. A. Lenning, and R. I. Jaffee, *J. Metals* 4, 1317 (December 1952).

(4) G. T. Murray and W. E. Taylor, *Effect of Neutron Irradiation on Supersaturated Solid Solution of Beryllium in Copper*, ORNL-1323 (Jan. 30, 1953).

TABLE 19. HYDROGEN CONTENTS OF CORROSION IMPACT SPECIMENS TREATED IN VARIOUS ENVIRONMENTS

MATERIAL	SPECIMEN NO.	TREATMENT PRIOR TO IMPACT TESTING	HYDROGEN CONTENT (wt %)
Ti-75A	1-2	Exposed in UO_2SO_4 solution containing 300 g of U per liter at 250°C for 671 hr in loop A[a]	0.016
	2-1		0.014
	4-1		0.010
	8-1		0.010
	3-1	Exposed in UO_2SO_4 solution containing approximately 300 g of U per liter at 250°C for 99.7 hr in loop A[a]	0.013
	5-1		0.013
	6-1		0.013
	7-1		0.007
	9-3	Exposed in UO_2SO_4 solution containing 40 g of U per liter at 250°C for 10 days[b]	0.010[c]
	10-9		0.012[c]
	11-6		0.011[c] 0.012[d]
	12-3		0.014[c]
	13-1	Cathodically treated in approximately 1 *M* H_2SO_4 at 0.1 amp for 8 hr at 70°F	0.015
	14-8		0.020
	15-9		0.018
	16-9		0.020
	19-10	Cathodically treated as above for 168 hr	0.061
	18-6	Vacuum annealed at 500°C for 1 hr and furnace cooled prior to machining	0.011
	24-6		0.012
	26-1		0.008
	28-8		0.011
Iodide Ti	I-1A1	Arc-melted, swaged, and vacuum annealed at 950°C for 1 hr and furnace cooled prior to machining	0.008
	I-2A1	Arc-melted, swaged, and vacuum annealed at 500°C for 1 hr and furnace cooled prior to machining	0.010
	I-3A		0.014
	I-4A		0.011
	I-5A		0.012
	I-6A		0.008
	I-7A		0.017
	I-8A		0.013

[a] See *HRP Quar. Prog. Rep. Jan. 1, 1953*, ORNL-1478, Table 10, p. 84, for detailed test history.

[b] See *HRP Quar. Prog. Rep. Jan. 1, 1953*, ORNL-1478, Table 11, p. 85, for detailed test history.

[c] Brown corrosion product present on surface of sample.

[d] Sample abraded on surface prior to charging into vacuum-fusion apparatus.

suggest that the course of the decomposition of the supersaturated solid solution of beryllium in copper can be followed by in-pile measurement of electrical resistivity. The similarity with regard to the formation of supersaturated solid solutions of the two alloy systems, copper-beryllium and titanium-hydrogen, suggests that in-pile resistivity measurements be made on commercial titanium specimens (which normally contain from 0.3 to 0.5 at. % H[3]) irradiated at several temperatures within the range of temperature planned for the homogeneous reactor components. Specimens (approximately 1/8-in.-dia rods) will be furnished to the Solid State Division for in-pile resistivity measurements.

The problem of the rate of hydrogen diffusion in commercial titanium has been considered, and it was found that there is some evidence in the literature[5] to support the theory that the oxide layer present on the surface impedes the reaction of hydrogen with titanium until the diffusion of these oxide layers into the base metal permits the hydrogen to enter the metal. Since the proposed operating temperature of the homogeneous reactor (250°C) is fairly low, rapid diffusion of the surface oxide layers would be expected. To test this, a sample of commercial titanium (Ti-75A) sheet, 1/4 in. thick, was charged into the quartz furnace tube of the Seivert's apparatus, the system was evacuated, and the specimen was heated to 250°C; hydrogen (generated by the decomposition of titanium hydride) was then admitted to the system. This specimen will be exposed in a hydrogen atmosphere at 250°C for approximately one month, and it will then be sectioned and examined metallographically for evidences of hydrogen penetration. This test will give information regarding the introduction of molecular hydrogen, but it will not necessarily provide information on the atomic or ionic hydrogen resulting from chemical reaction.

Bureau of Mines Titanium. Three arc melts of Bureau of Mines, high-purity, titanium sponge (lot 1056, R-83A) have been prepared, swaged, vacuum annealed at 600°C for 1 hr, and machined into impact specimens. The three 11 3/4-in.-long impact specimens obtained from melt B-1 will be used to establish the transition temperature of Bureau of Mines, arc-melted, sponge titanium. Three 11 3/4-in.-long specimens from melt B-2 and three specimens of the same length from melt B-3 will be corrosion tested in uranyl sulfate in a loop prior to impact testing. One 9-in.-long specimen from melt B-2 and one 10-in.-long specimen from melt B-3 were retained to compare melts B-2 and B-3 with melt B-1, which will be used to determine the transition temperature of Bureau of Mines titanium.

ZIRCONIUM-TITANIUM ALLOYS

The four zirconium-titanium melts described in the previous report[1] have been arc-melted, swaged, vacuum annealed at 600°C for 1 hr, furnace cooled, and machined into corrosion pins (0.204 in. in diameter by 1.385 in. long) and impact specimens. The pins, four from each alloy, will be corrosion tested and then impact tested.

J. O. Betterton, Jr. of the Metallurgy Division, in the course of his investigation of the zirconium-indium system, has tentatively determined that the beta phase in this system has a face-centered-cubic crystal structure. Since many face-centered-cubic metals are not subject to the transition from the ductile to the brittle type of fracture with decreasing temperature, an attempt was made to produce an arc-melted zirconium-indium alloy

[5] R. W. Dayton *et al.*, *Hydrogen Embrittlement of Zirconium*, BMI-767, p. 27 (Aug. 22, 1952).

(approximately 28 at. % indium) and to fabricate the melt into specimens for corrosion and impact tests. The melt has been prepared (with very little loss in indium, considering the wide difference in the melting point of the two metals), but attempts to swage the alloy were not successful. A metallographic sample of the alloy is being examined to determine whether the alloy is in the all-beta-phase field.

GENERAL

Impact testing of the specimens on hand will be resumed as soon as modifications to facilitate the operation of the tests in a hot cell are completed by the Research Shops.

AQUEOUS SOLUTION AND RADIATION CHEMISTRY

STATIC CORROSION TESTS WITH RADIATION

F. H. Sweeton W. C. Yee

Five tests in the LITR and three tests of out-of-pile blanks have been completed. In all cases, the bombs, which served as the corrosion specimen, were constructed of type 347 stainless steel. The method employed to determine the corrosion rate, which consisted of measurement of the consumption of oxygen, was described previously.[1] Table 20 summarizes the conditions for each of the experiments, and Table 21 gives the corrosion results from the out-of-pile experiments, as calculated from the nickel content of the solution at the conclusion of the experiment, based on the assumption that the corrosion proceeds at a uniform rate throughout the test.

The corrosion results from the in-pile experiments are shown graphically in Figs. 40 through 43 in which the cumulative corrosion is plotted against the square root of time. The corrosion appears to be linear with the square root of time for a period, and then it increases rather sharply. Neither the cause of this break nor the factors determining the time at which it occurs can be definitely specified on the basis of the data from the few experiments completed. Furthermore, attempts to correlate corrosion rates with the variables involved are not yet justified.

[1] C. H. Secoy *et al.*, *HRP Quar. Prog. Rep. Oct. 1, 1952*, ORNL-1424, p. 94-96.

TABLE 20. SUMMARY OF EXPERIMENTAL CONDITIONS FOR STATIC IN-PILE CORROSION TESTS

EXPERIMENT NO.	SOLUTION	TOTAL URANIUM CONCENTRATION (g/liter)	FISSION DENSITY (kw/liter)	BOMB PRETREATMENT	Cu^{++} CONCENTRATION (moles/liter)	INITIAL O_2 PRESSURE (psi)	DURATION OF TEST (days)
H-2	UO_2SO_4	40	4.5 to 6.0	CrO_3	0.01	900	91
H-3	UO_2SO_4	43.9	0	None*	0.01	558	63
H-4	UO_2SO_4	43.9	0	CrO_3	0.01	453	63
H-5	UO_2F_2	40	4.5 to 6.0	None*	0.03	900	63
H-6	UO_2F_2	40	0	None*	0.02	552	6
H-7	UO_2SO_4	40	6.0	None*	0.01	100	18
H-8	UO_2SO_4	5	0.8	None*	0.01	80	18
H-9	UO_2SO_4	40	0.5	None*	0.01	80	40

*Cleaned and etched with 20% HNO_3-3% HF solution.

TABLE 21. CORROSION RESULTS IN OUT-OF-PILE TESTS

EXPERIMENT NO.	SOLUTE	DURATION OF TEST (days)	CUMULATIVE CORROSION (mils)	CORROSION RATE* (mpy)
H-3	UO_2SO_4	63	0.021	0.12
H-4	UO_2SO_4	63	0.0091	0.053
H-6	UO_2F_2	6	0.018	1.09

*Based on the assumption of a uniform rate of corrosion.

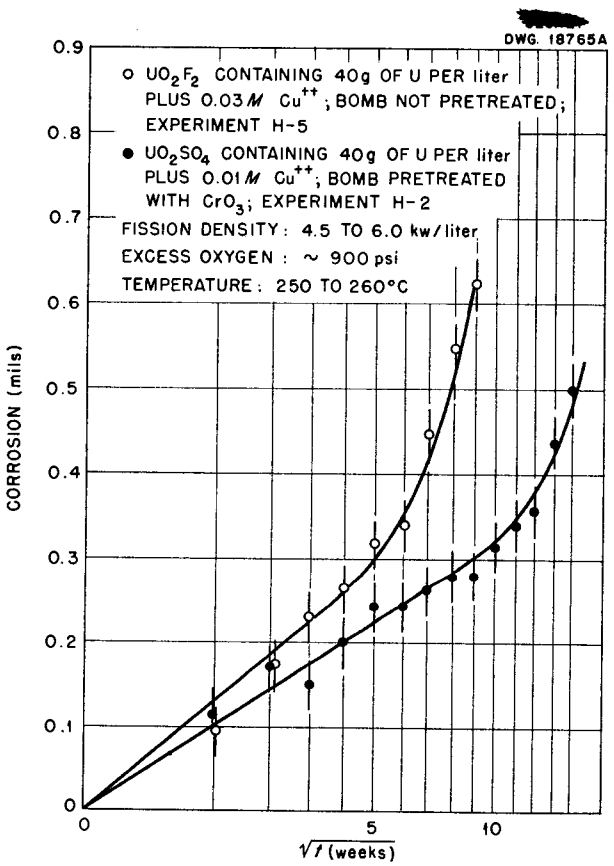

Fig. 40. Corrosion in an In-Pile Irradiation Test of a Type 347 Stainless Steel Bomb Containing Uranyl Sulfate Compared with Corrosion in an Identical Bomb Containing Uranyl Fluoride. Experiments H-2 and H-5.

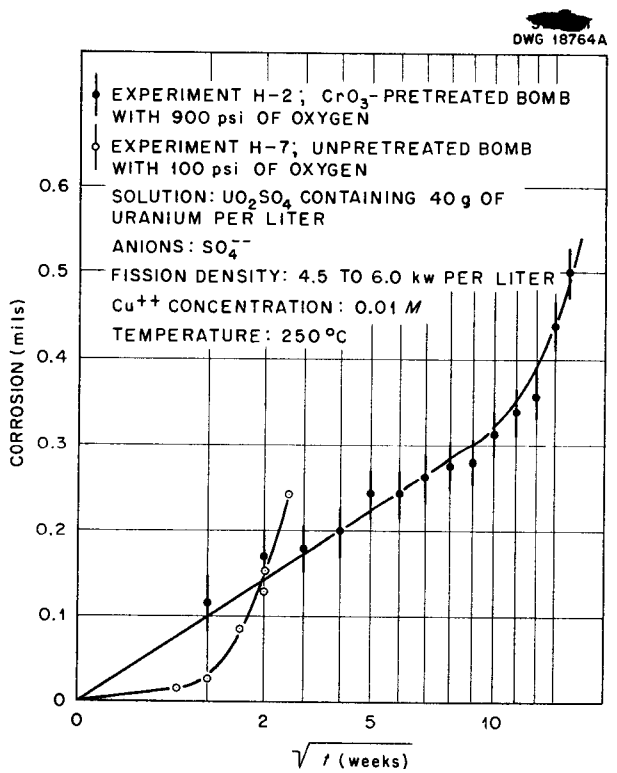

Fig. 41. Effect of Excess Oxygen on Corrosion in In-Pile Irradiation Tests of Type 347 Stainless Steel Bombs Containing Uranyl Sulfate. Experiments H-2 and H-7.

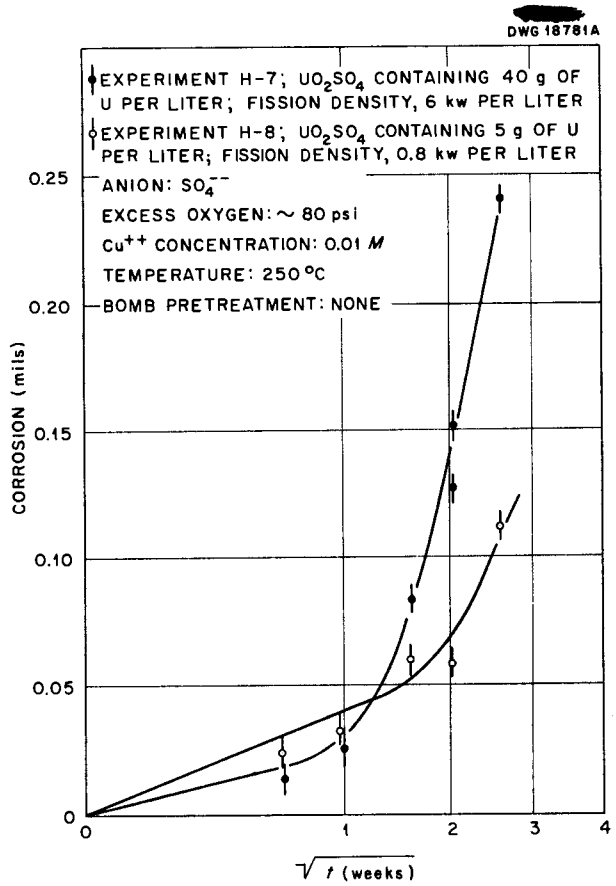

Fig. 42. Effect of Uranium Concentration and Fission Density on Corrosion in In-Pile Irradiation Tests of Type 347 Stainless Steel Bombs Containing Uranyl Sulfate. Experiments H-7 and H-8.

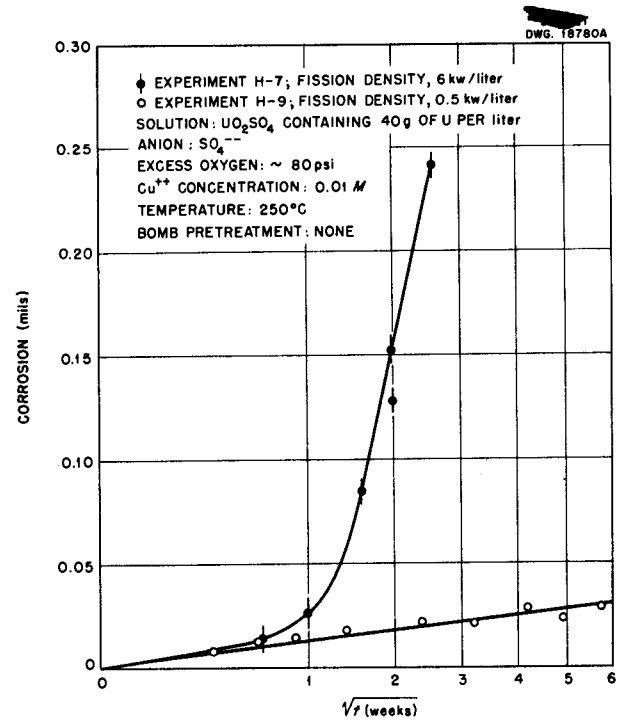

Fig. 43. Effect of Fission Density on Corrosion in In-Pile Irradiation Tests of Type 347 Stainless Steel Bombs Containing Uranyl Sulfate. Experiments H-7 and H-9.

MECHANISM OF THE HYDROGEN-OXYGEN RECOMBINATION REACTION IN SOLUTIONS

H. F. McDuffie L. F. Woo

Additional effort has been made to learn what copper-containing species is [are] the active catalyst[s] responsible for the homogeneous recombination of hydrogen and oxygen in the presence of solutions of cupric compounds at high temperatures.

The significant developments from this work include:

1. the use of cupric perchlorate and perchloric acid to estimate the rate constant for uncomplexed cupric ion and to ascertain the absence of complexing by perchlorate,
2. extension of the previously reported data for copper sulfate plus sulfuric acid to higher concentrations of acid,
3. determination of the effect of uranyl sulfate concentrations of up to 1 *M* upon the rate constant, in both the presence and the absence of added sulfuric acid,
4. the use of rate constant data and direct observation in the Marshall, semimicro, phase-study apparatus to determine the region of hydrolytic precipitation of copper and uranium in dilute solutions of sulfuric acid and uranyl sulfate,
5. evidence that in systems containing sulfate at low concentrations some species appears to exist which has

more activity, catalytically, than uncomplexed cupric ion.

All experiments were carried out at 250°C with solutions which were 0.0010 *M* with respect to copper at room temperature. In this report, all concentrations are expressed as those at room temperature, but all values of k_{Cu}, calculated according to the formulas set forth in a previous report,[2] have been corrected for the expansion in volume and resulting changes in concentration on going to 250°C. It should be noted that all values of k_{Cu} are based on the solubility of hydrogen in water, as reported in BMI-T-25,[3] and that any changes in these solubility values that occur while changes are being made in the nature of the solutions tested will result in different values for the rate constant. In another section of this report, efforts to measure these solubilities are discussed.

Activity of Cupric Perchlorate Plus Perchloric Acid. Perhaps the simplest hypothesis for explaining the recombination of hydrogen and oxygen in the presence of dissolved cupric compounds would involve a reaction of dissolved hydrogen with the cupric ion. Accordingly, it was very desirable to determine the activity of copper under conditions which would tend to minimize any complexing of the cupric ion by anions of the solution. The known usefulness of the perchlorate ion for this purpose at room temperatures for a variety of systems suggested that cupric perchlorate be tested. At a concentration of 0.0010 *M*, precipitation was found to occur at 250°C, but the presence of 0.005 *M* perchloric acid was found to be sufficient to maintain phase stability at this temperature. Recombination experiments were run with perchloric acid concentrations of 0.005, 0.010, and 0.050 *M* in the presence of 0.0010 *M* cupric perchlorate, with the results given in Table 22.

The constancy of k_{Cu} at 5.0 suggests that this may be the value for the activity of uncomplexed cupric ion. The data further indicate that no complexing by perchlorate takes place and that there is no direct participation of hydrogen ions in the reaction (except for the suppression of the hydrolytic precipitation).

All experiments with perchlorate have been limited to short times at high temperatures to avoid excessive corrosion of apparatus by the traces of chloride ion released in the decomposition of perchlorate.

Effect of Sulfuric Acid. Table 23 and Fig. 44 present data showing the

(2) H. F. McDuffie, E. L. Compere, and H. H. Stone, *Chem. Quar. Prog. Rep. Mar. 31, 1952*, ORNL-1285, p. 89-94.

(3) H. A. Pray, C. E. Schweickert, and B. H. Minnick, *The Solubility of Hydrogen, Oxygen, Nitrogen, and Helium in Water at Elevated Temperatures*, BMI-T-25 (May 15, 1950).

TABLE 22. RESULTS OF RECOMBINATION EXPERIMENTS WITH PERCHLORIC ACID IN THE PRESENCE OF CUPRIC PERCHLORATE

EXPERIMENT NO.	EXCESS ACID	$k_{Cu} \times 10^{-3}$ (moles^{-1} hr^{-1} liter^{-1})
B-49	0.000	3.5, phase instability
B-48	0.001	7.1, phase instability
B-151	0.005	5.0
B-152	0.010	5.0
B-153	0.050	5.0

TABLE 23. HOMOGENEOUS RECOMBINATION OF HYDROGEN AND OXYGEN IN THE PRESENCE OF ADDED SULFURIC ACID

H_2SO_4 (moles/liter)	EXPERIMENT NO.	$k_{Cu} \times 10^{-3}$ (moles^{-1} hr^{-1} liter^{-1})	$\sqrt{[H_2SO_4]}$
0.00	B- 1	6.7	
	- 18	6.7	
	- 73	7.7	
	- 74	9.8	
	- 77	9.7	
	- 85	6.1	
	- 89	7.3	
	- 99	8.0	
	-102	6.0	
0.00040	- 47	11.2	0.02
0.0010	- 33	20.6	0.032
	-136	6.4	
	-140	12.7	
	-144	12.3	
0.0020	- 34	19.6	0.045
	-137	12.7	
	-141	12.98	
	-142	11.8	
0.0030	- 35	19.2	0.055
	-138	14.1	
	-139	12.2	
	-143	27.6	
	-145	11.0	
	-146	15.9	
0.0050	-130	14.2	0.071
	-135	14.2	
	-147	14.6	
0.010	-131	12.6	0.10
	-134	12.7	
0.020	-109	10.5	0.141
	-114	10.6	
0.050	-132	7.2	0.223
	-133	6.9	

effect of adding sulfuric acid to solutions of 0.0010 *M* copper sulfate. The complete lack of precision at concentrations of acid below 0.005 *M* was found to be paralleled by the appearance of precipitates when these solutions were heated to 250°C in small glass tubes in the Marshall, semimicro, phase-study apparatus. It is considered that a region of hydrolytic precipitation exists, as discussed in a subsequent section of this chapter on "Exploratory Phase Investigations of Systems Involving $CuSO_4$, UO_2SO_4, H_2SO_4, and H_2O at Uranium Concentrations Below 30 g/liter." The

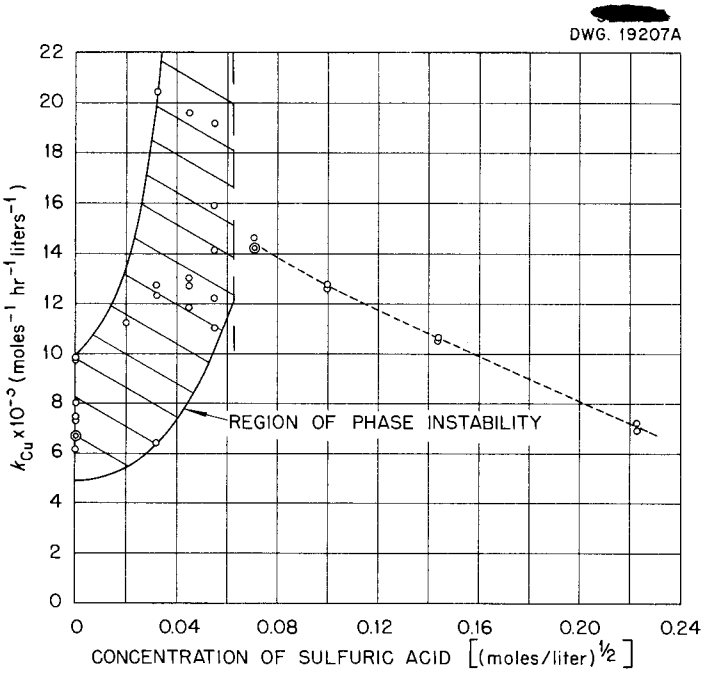

Fig. 44. Effect of Sulfuric Acid Concentration on Hydrogen and Oxygen Recombination in 10^{-3} *M* Cupric Sulfate Solution at 250°C.

precipitation of copper from solution at these temperatures had not been anticipated, since the solubility of copper sulfate in water from 100 to 180°C, as reported by Seidel,[4] was 43 to 45 wt %, with practically no temperature dependence in this region. The suggestion that the precipitation is hydrolytic is supported by the effectiveness of excess acid in preventing its appearance, which is paralleled in this case by the observations on the hydrolytic precipitation of uranium from dilute uranyl solutions. The high precision obtained at concentrations of acid above 0.005 *M* supports the opinion that the experimental technique is not responsible for the scatter observed at lower concentrations. It appears that there is a maximum in the activity at about 0.003 *M* which is hidden by the hydrolytic precipitation. The possibility that the partially hydrolyzed copper precipitate may have heterogeneous catalytic activity has been considered, but at present the emphasis is on learning more about the homogeneous activity.

Effect of Uranyl Sulfate. Table 24 and Fig. 45 illustrate the effect of adding uranyl sulfate of varying concentrations to solutions of 0.0010 *M* copper sulfate. As with the sulfuric acid discussed above, a region of imprecision and phase instability was noted up to a uranyl sulfate concentration of around 10 g of uranium per liter. Also, the activity was lowered at increasing concentrations of uranyl sulfate.

Effect of Uranyl Sulfate Plus Sulfuric Acid. Table 25 and Fig. 46 illustrate the effect of uranyl sulfate concentration on the activity of 0.0010 *M* cupric sulfate plus 0.020 *M* sulfuric acid. It will be noted that these data begin, in a sense, at a place on the curve of Fig. 44 where the activity is already considerably below the maximum and where the addition of more sulfuric acid further depresses the activity. Similarly, the addition of uranyl sulfate depresses the activity. It is also noted that the precision in the concentration region below 10 g of uranium per liter is much better than that observed in the absence of the sulfuric acid. Figure 47 shows the effect of the combination of uranyl sulfate plus 0.020 *M* sulfuric acid superimposed on the effect of sulfuric acid alone.

Plans for Next Quarter. The relatively low activity obtained in the presence of perchlorate as the only anion compared with that obtained in the presence of small amounts of sulfate suggests that catalytic species exists with higher activity than that of uncomplexed cupric ion. The presence of the region of hydrolytic precipitation interferes seriously with the determination of the maximum activity of this species and with the determination of exact conditions for achieving

(4) A. Seidel, *Solubilities of Inorganic and Metal Organic Compounds*, 3d ed., Vol. 1, p. 497, Von Nostrand, New York, 1940.

TABLE 24. HOMOGENEOUS RECOMBINATION OF HYDROGEN AND OXYGEN IN THE PRESENCE OF ADDED URANYL SULFATE

URANYL SULFATE CONCENTRATION (g of U per liter)	EXPERIMENT NO.	$k_{Cu} \times 10^{-3}$ (moles^{-1} hr^{-1} liter^{-1})	$\sqrt{\text{g of U per liter}}$
0	B- 1	6.7	0
	- 18	6.7	
	- 73	7.7	
	- 74	9.8	
	- 77	9.7	
	- 85	6.1	
	- 89	7.3	
	- 99	8.0	
	-102	6.0	
0.25	- 78	8.5	0.5
	- 84	10.1	
	- 92	11.1	
	-100	9.9	
1.0	- 72	6.7	1.0
	- 75	8.3	
	- 79	6.3	
	- 88	10.1	
	- 93	6.6	
2.25	- 80	10.2	1.5
	- 87	6.8	
	- 94	7.1	
2.62	- 62	8.9	1.62
	- 66	8.0	
4.0	- 81	9.45	2.0
	- 86	10.5	
	- 96	6.4	
6.25	- 82	9.8	2.5
	- 90	8.4	
	- 97	8.2	
9.0	- 83	8.1	3.0
	- 91	7.8	
	- 98	14.2	
10.0	- 71	8.3	3.16
	- 76	9.3	
26.2	- 63	6.8	5.1
	- 67	6.9	
83	- 68	4.6	8.2
142.5	- 69	3.3	11.9
205	- 70	3.3	14.3
262	- 64	2.7	16.2
	- 65	3.0	
	-106	3.2	
	-107	4.3	
	-108	2.9	
	-119	3.8	
	-120	3.0	

TABLE 25. HOMOGENEOUS RECOMBINATION OF HYDROGEN AND OXYGEN IN THE PRESENCE OF 0.020 *M* SULFURIC ACID AND ADDED URANYL SULFATE

URANYL SULFATE CONCENTRATION			EXPERIMENT NO.	$k_{Cu} \times 10^{-3}$ (moles^{-1} hr^{-1} liter^{-1})	TOTAL SULFATE (moles/liter)	$\sqrt{[\text{Sulfate}]}$
g of U per liter	$\sqrt{\text{g of U per liter}}$	moles/liter				
0	0	0	B-109	10.5	0.021	0.145
			-114	10.6		
1.0	1.0	0.0042	-110	7.0	0.0252	0.158
			-113	7.2		
2.25	1.5	0.0095	-124	8.0*	0.0305	0.175
			-128	6.1		
4.0	2.0	0.0168	-111	5.5	0.0378	0.194
			-115	6.2		
			-116	6.1		
			-118	8.9 to 6.6**		
6.25	2.5	0.026	-125	7.5*	0.047	0.217
			-129	5.9		
9.0	3.0	0.038	-112	7.3	0.059	0.242
			-117	8.1		
12.25	3.5	0.051	-126	6.8	0.072	0.268
			-127	7.1		
25.0	5.0	0.105	-148	7.2	0.126	0.355
100	10.0	0.420	-149	5.6	0.441	0.665
208	14.4	0.873	-150	3.1	0.894	0.945

*Evidence of excess activity due to contamination of reaction vessel in previous runs.

**Poor experimental data.

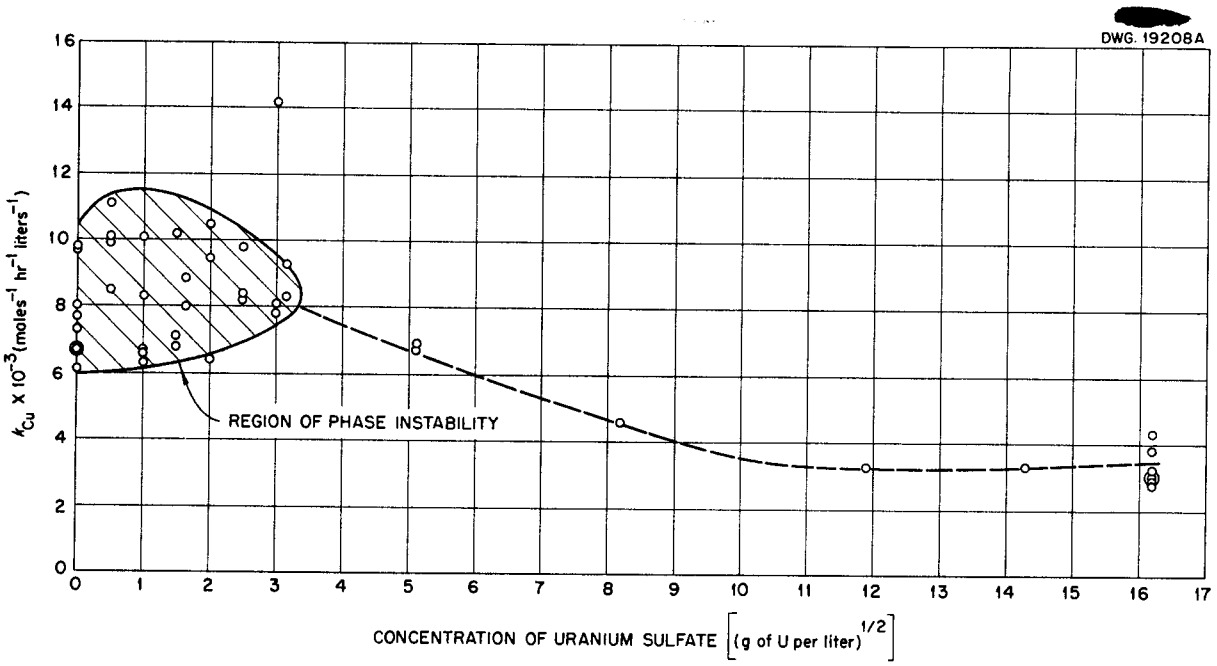

Fig. 45. Effect of Uranyl Sulfate Concentration on Hydrogen and Oxygen Recombination in 10^{-3} *M* Cupric Sulfate Solution at 250°C.

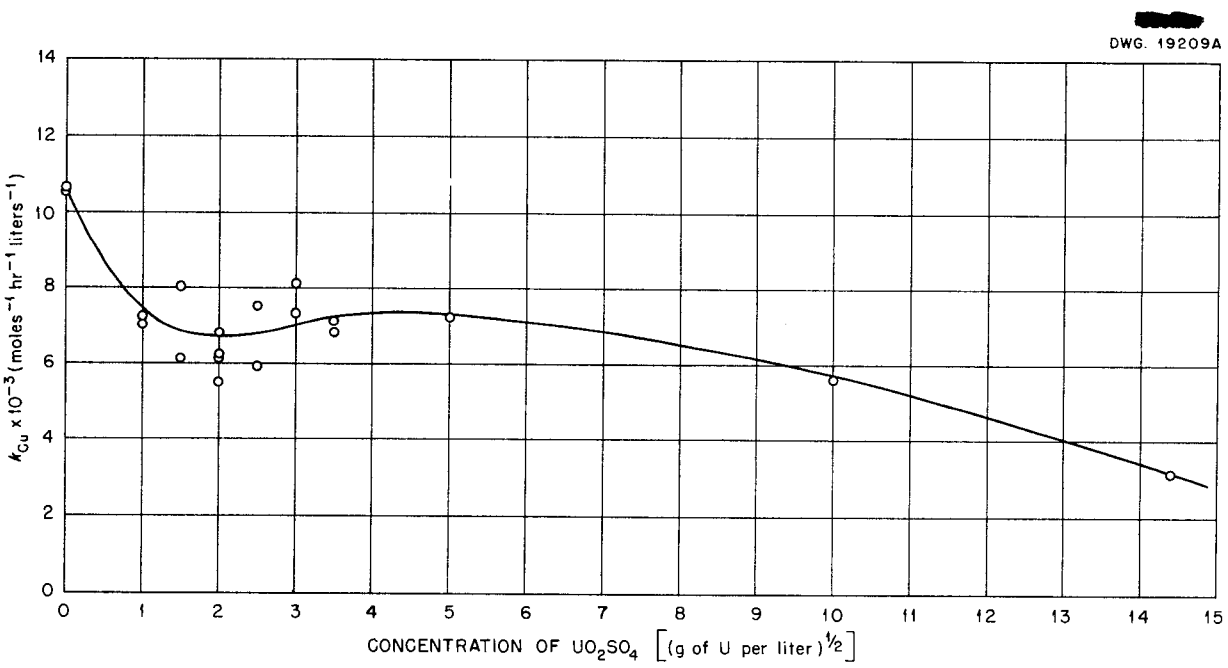

Fig. 46. Effect of Uranyl Sulfate Concentration on Hydrogen and Oxygen Recombination in 10^{-3} *M* Cupric Sulfate Solution at 250°C.

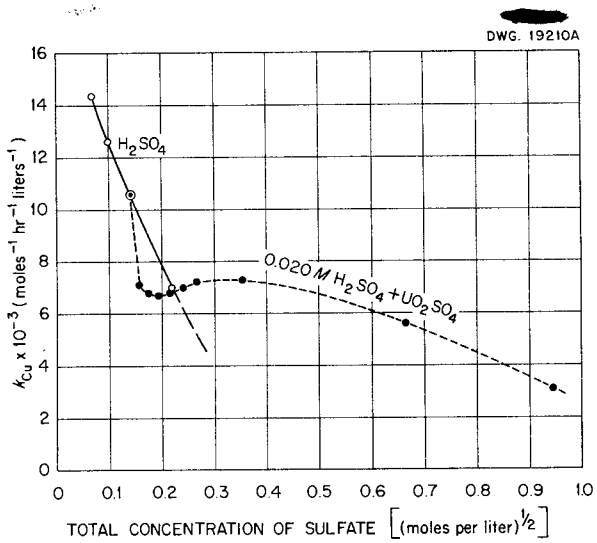

Fig. 47. Effect of Sulfuric Acid and Uranyl Sulfate on Hydrogen and Oxygen Recombination in 10^{-3} *M* Cupric Sulfate at 250°C.

maximum activity. Hence, it is difficult to formulate a network of complexing constants which will adequately describe the various systems studied. However, efforts will be continued to formulate a satisfactory framework, based on experiments in which total sulfate and total acidity are varied independently. Perchloric acid will be used in some cases as a source of excess acidity which is considered not to contribute any complexing anions, and sodium or lithium hydroxide will be used for lowering the acidity while retaining the sulfate concentration. It is contemplated that all solutions will first be tested for phase stability in the Marshall, semimicro, phase-study apparatus, and then recombination studies will be carried out on the stable solutions. As mentioned in the previous report, efforts will be made to use this reaction as a means for determining the relative complexing power of other cations, such as uranyl and zirconyl. It is also of interest that any satisfactory determination of the mechanism of the recombination reaction will probably include a determination of the second ionization constant of sulfuric acid at elevated temperatures. Once a clearer idea of the active species is obtained, it is planned to again test the dependence of the reaction rate upon temperature and upon the concentration of the copper catalyst.

SOLUBILITY OF HYDROGEN AT HIGH TEMPERATURES AND PRESSURES IN SOLUTIONS OF URANYL SULFATE

C. E. Ronneberg

The full elucidation of the reactions involved in the recombination of hydrogen and oxygen in solution as catalyzed by dissolved copper sulfate under the conditions that prevail in the aqueous, homogeneous reactors of interest (high temperatures and pressures) requires a knowledge of the solubility of hydrogen in aqueous solutions of uranyl sulfate. This knowledge will be significant in connection with the operation of the HRE.

The solubility of hydrogen in pure water has been shown to increase with temperature, above a certain minimum temperature (about 200°F[3]). A direct method was used at BMI to determine the solubility, that is, the amount of dissolved hydrogen in a known amount of water, for a range of temperatures and pressures.

The direct determination of the solubility of hydrogen in solutions of uranyl sulfate is impossible because the uranyl ion is reduced by hydrogen at reactor temperatures, with the consequent precipitation of lower oxides of uranium.[5] It is hoped to get around the difficulty mentioned above by the indirect, kinetic method outlined below.

[5] H. F. McDuffie *et al.*, *HRP Quar. Prog. Rep. Aug. 15, 1951*, ORNL-1121, p. 146-148.

Kinetic Method for the Determination of the Solubility of Hydrogen. The recombination of hydrogen and oxygen in solution to form water is catalyzed by even very small amounts of dissolved copper sulfate:

$$H_2 + \tfrac{1}{2}O_2 \xrightarrow{(CuSO_4)} H_2O \ .$$

The rate of the reaction can be conveniently followed by observing the rate of decrease of the pressure of the mixture of gases (principally hydrogen, oxygen, and steam) above a solution of uranyl sulfate, with added copper sulfate, in a suitable bomb that initially contains a known amount of hydrogen and oxygen, measured in terms of their partial pressures. Under these conditions, the uranyl sulfate is not reduced. The recombination reaction is first order with respect to hydrogen and copper sulfate. The rate of decrease in the pressure (dP/dt) of the gaseous mixture in equilibrium with the solutions depends upon the rate of the recombination reaction and the ratio of the volume of the gaseous mixture (V_G) to the volume of the solution (V_L). The following equation can be shown to apply:

$$-\frac{dP}{dt} \cdot \frac{1}{P}\left[\frac{V_G}{V_L} \cdot \frac{\alpha}{RT} + 1\right] = k_{sol}$$

$$= k_{Cu}\ [Cu^{++}] \ . \qquad (1a)$$

Equation 1*a* follows from the basic kinetic equation describing the rate of disappearance of dissolved hydrogen and the basic assumption that the rate of the recombination reaction is directly proportional to the concentrations of dissolved hydrogen and copper, that is,

$$-\frac{d\,[H_2]}{dt} = [H_2]\ [Cu]\ k_{Cu} \ , \qquad (1b)$$

where k_{Cu} is the specific velocity constant due to copper sulfate. The concentration of dissolved hydrogen can be related to the pressure of the hydrogen in the system by Henry's law,

$$[H_2] = \frac{P_{H_2}}{\alpha} \ .$$

Equation 1*b* can be rewritten as

$$-\frac{dP_{H_2}}{dt} = P_{H_2}\ [Cu]\ k_{Cu}$$

$$\times \left[\frac{\text{moles dissolved hydrogen}}{\text{moles hydrogen in system}}\right]$$

$$= P_{H_2}\ [Cu]\ k_{Cu} \cdot F_G \ , \qquad (1c)$$

where F_G is a geometry factor and is equal to the fraction of the total hydrogen in the system which is in the liquid phase.

It has been shown that[6]

$$F_G = \frac{\dfrac{V_L}{V_G}}{\dfrac{V_L}{V_G} + \dfrac{\alpha}{RT}} = \frac{1}{\dfrac{V_G}{V_L} \cdot \dfrac{\alpha}{RT} + 1} \ ,$$

where

V_L = volume of liquid phase,
V_G = volume of gas phase,
R = gas constant,
T = absolute temperature in °K,
α = Henry's law constant for hydrogen.

With the use of the value for F_G given above, Eq. 1*c* can be modified, and it becomes

$$-\frac{dP_{H_2}}{dt} = P_{H_2}\ [Cu]\ k_{Cu} \cdot \frac{1}{\dfrac{V_G}{V_L} \cdot \dfrac{\alpha}{RT} + 1} \ ,$$

which leads directly to Eq. 1*a* above; and P_{H_2} can be replaced by the total

[6] *Chap. 4.8, ENGINEERING DESIGN INFORMATION, from Section 4,* "Aqueous Homogeneous Systems," *Vol. 2 of the Reactor Handbook*, p. 58, ORNL CF-52-12-127 (Feb. 13, 1953).

pressure of 2:1 hydrogen-oxygen (obtained by subtracting the pressure of steam plus excess oxygen from the total observed pressure) for convenience in handling the data.

Equation 1*a* can also be conveniently modified. By letting

$$k_\pi = -\frac{dP}{dt} \cdot \frac{1}{P},$$

and rewriting,

$$\frac{1}{k_\pi} = \left[\frac{\alpha}{RT} \cdot \frac{V_G}{V_L} + 1\right]\left[\frac{1}{k_{sol}}\right]. \qquad (2)$$

The k_π for various V_G/V_L ratios is measured experimentally for a certain solution of uranyl sulfate at suitable temperatures and pressures.

In order to determine the Henry's law constant for hydrogen, a bomb and apparatus are being built to measure k_π, or $(-dP/dt) \cdot (1/P)$, for various solutions of uranyl sulfate at various V_G/V_L ratios. It is proposed to evaluate α by trying various ways of handling the experimental data. It will be noted that Eq. 2 has the general form of a first-degree equation with two variables, $y = mx + b$. Equation 2 can be put in this general form in a number of ways:

Method 1

$$+\frac{k_{sol}}{k_\pi} = \frac{\alpha}{RT} \cdot \frac{V_G}{V_L} + 1,$$

Method 2

$$+\frac{1}{k_\pi} = \left[\frac{\alpha}{RT} \cdot \frac{1}{k_{sol}}\right]\frac{V_G}{V_L} + \frac{1}{k_{sol}},$$

Method 3

$$k_\pi = -\frac{\alpha}{RT}\left[\frac{V_G}{V_L} \cdot k_\pi\right] + k_{sol}.$$

In Method 1, for example, the experimental values for k_{sol}/k_π for various V_G/V_L ratios would be plotted as indicated in Fig. 48. The relationship should be a straight line. The intercept on the y axis should be 1.00 and the slope should be α/RT. Hence, α = experimental slope × (RT), in consistent units. Future experimentation should indicate which of the above-suggested procedures is best for translating k_π and V_G/V_L values into values for α.

Test of the Theory. A rough test of the above theory and methods for the indirect determination of α for hydrogen has been made by determining k_π at 250°C in a small bomb (designed for another purpose) containing uranyl sulfate solution with 262 g of uranium per liter and 0.001 *M* $CuSO_4$. Values for dP/dt and k_π were determined for volume ratios of 3.02, 1.2, and 0.29.

There was no noticeable reduction of the uranyl sulfate by hydrogen. A plot of $1/k_\pi$ vs. V_G/V_L, made as indicated above, gives a slope of 9.1 and an α of 5740 liters·psi·mole^{-1}. This result is sufficiently encouraging to warrant proceeding with the construction of a bomb and furnace designed expressly to measure α kinetically.

Experimental Details. A titanium bomb with capacity of about 55 ml has been built. It was designed to have a very comfortable safety factor at pressures as high as 2500 psi.

An aluminum block furnace with automatic controls to operate at 250°C is being built. It is hoped that

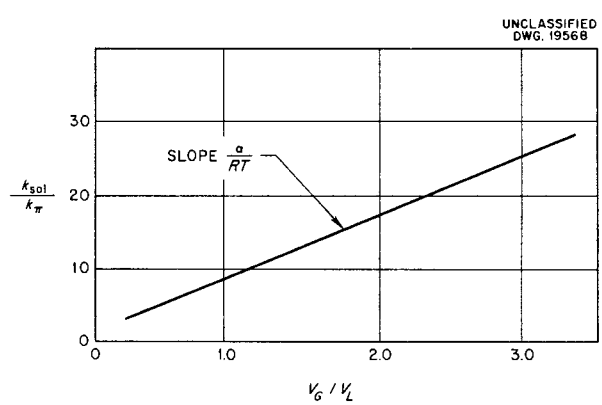

Fig. 48. Plot of k_{sol}/k_π vs. V_G/V_L.

temperature control to 1°C or less can be obtained.

DESCRIPTION OF FILTRATION APPARATUS USED FOR AQUEOUS SOLUBILITY DETERMINATIONS ABOVE 100°C

J. S. Gill E. V. Jones
W. L. Marshall

Experimental data have been obtained during the past year on the solubility of uranium trioxide in aqueous uranyl sulfate and uranyl fluoride solutions above 100°C.[7] Solubility data also have been obtained for the solubility of fission products in aqueous uranyl sulfate and in water by Zemel, Lietzke, Stoughton, Gill, Jones, and Marshall, both cooperatively and independently.[8] One of the experimental methods used in this work has been the filter-bomb technique by which a solution is equilibrated and filtered at the equilibration temperature. The apparatus, designed by Zemel and Stoughton[9] and of the type used by Booth, Bidwell, and previous workers, as reported by Booth and Bidwell,[10] was modified by Gill, Jones, and Marshall and is described for the first time, in detail, to show the modifications.

The purpose of the apparatus is to equilibrate a solution and a solid at a constant temperature and then to filter the solution at that temperature. This objective is accomplished by incorporating a filter unit in the equilibration apparatus. Filtration is carried out by establishing a difference in pressure between the vessel containing the solution in contact with the solid and the collection vessel for the filtrate.

The equilibration bomb is shown in Fig. 49*a*. The titanium filter bomb, which consists of two cells, A, is sealed in the middle with a platinum gasket, B, and there is a modified, Monroe, porous-platinum filter "stick" unit, C, between the two cells. The assembled filter bomb is placed in a stainless steel outer jacket, D, which is sealed in the center by a Teflon gasket, E. After a solution and the excess solid are placed in the lower half of the filter bomb, a titanium-clad soft-iron slug, F, is inserted. This slug, which is used as a magnetic mixer, has Teflon caps on its ends to prevent frictional contact of metallic surfaces. The magnetic slug is activated by means of a solenoid, G, which is controlled with an automatic on-off switch. The solenoid is enclosed in glass to prevent contact and consequent short circuiting by the liquid salt. The assembled unit is placed in a liquid-salt thermostat composed of KNO_3, $LiNO_3$, and $NaNO_3$,[11] and operated with the required temperature accuracy of ±0.5°C at 250°C. After sufficient time has been allowed for equilibration, the unit is inverted *within* the salt bath and set in a cooling unit, H, which consists essentially of a copper coil through which air is blown. Cooling of the lower half of the unit reduces the vapor pressure at that end, and thus filtering of the solution from the solid takes place because of the vapor-pressure difference. The temperature reduction in the lower end is of the order of 6 to 8°C. The solution and the solid are analyzed for their specific components.

Another equilibration apparatus is shown in Fig. 49*b*. In this apparatus, the outer steel jacket is left off the filter bomb and the bomb is inserted into an aluminum heating cylinder. The unit is rocked back and forth through

(7) W. L. Marshall *et al.*, *HRP Quar. Prog. Rep.*, ORNL-1221, p. 99; ORNL-1280, p. 175; ORNL-1318, p. 142.

(8) Data reported in *HRP Quar. Prog. Reps.* for 1950, 1951, 1952.

(9) *HRE Quar. Prog. Rep. Aug. 31, 1950*, ORNL-826, p. 78-79.

(10) H. S. Booth and R. M. Bidwell, *J. Am. Chem. Soc.* **72**, 2567 (1950).

(11) J. A. Beattie, *Rev. Sci. Instr.* **2**, 458 (1931).

UNCLASSIFIED
DWG. 19257A

A — TITANIUM EQUILIBRATION BOMB
B — PLATINUM GASKET
C — MODIFIED MONROE, POROUS-PLATINUM FILTER "STICK" UNIT
D — STAINLESS STEEL OUTER JACKET
E — TEFLON GASKET
F — TITANIUM-CLAD SOFT-IRON SLUG
G — SOLENOID
H — COOLING UNIT

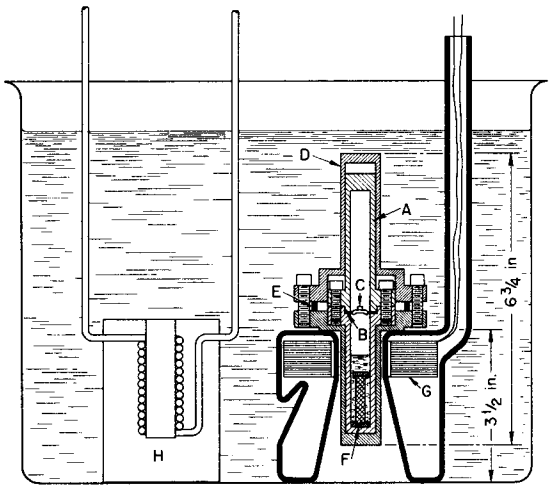

a. LIQUID-SALT THERMOSTAT

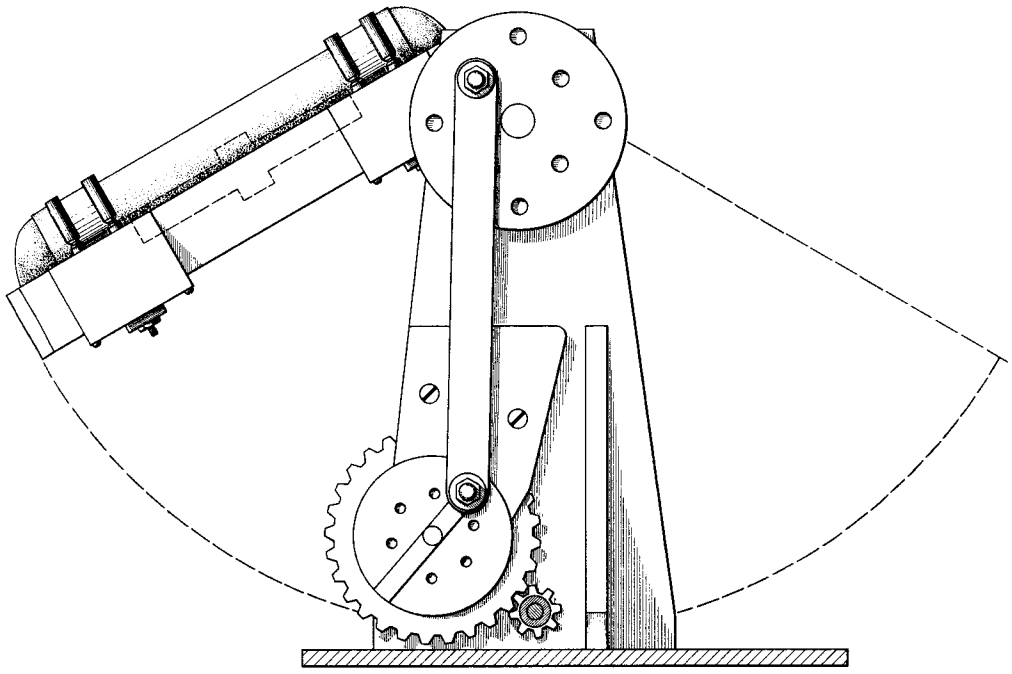

b. ROCKER-HEATER UNIT

Fig. 49. Filtration Apparatus Used for Aqueous Solubility Studies Above 100°C.

an angle of about 120 deg 45 times per minute by means of a series of cams. During equilibration time, both halves of the cylinders are heated uniformly with twin heating coils. After equilibration, a locking device incorporated in the rocker assembly is loosened and the heater unit is inverted. The lower end of the unit is then cooled several degrees by cutting off the current to the heating coils in the lower half of the unit, and filtration occurs. To speed up equilibration with concentrated solutions, a small, long-stemmed titanium cup was introduced into the bomb to hold one-third to one-half the solid phase near the top of the solution.

SOLUBILITY OF UO_3 IN AQUEOUS UO_2SO_4 AT 175°C

E. V. Jones

Investigations of the solubility of uranium trioxide in uranyl sulfate solutions at 175°C, which have been reported in part,[12] have been continued in an effort to determine the behavior of this system in the low concentration region, that is, below 0.1 *M*. As previously stated,[12] "The question is whether the equilibrium [mole] ratio, U to SO_4, drops below 1.00 as concentration is lowered. If the ratio does fall below 1.00, then the data would best be represented by the system UO_3-H_2SO_4-H_2O. On this basis, there is no valid reason why the ratio of U to SO_4 must remain equal to or greater than 1.00. Also, for a given sulfate concentration, the ratio should decrease with temperature because of increased hydrolysis of the uranyl ion."

Data for the solubility of uranium trioxide in uranyl sulfate solutions at 175°C in the low concentration region are given in Table 26 and shown in Fig. 50. The U-to-SO_4 ratio appears

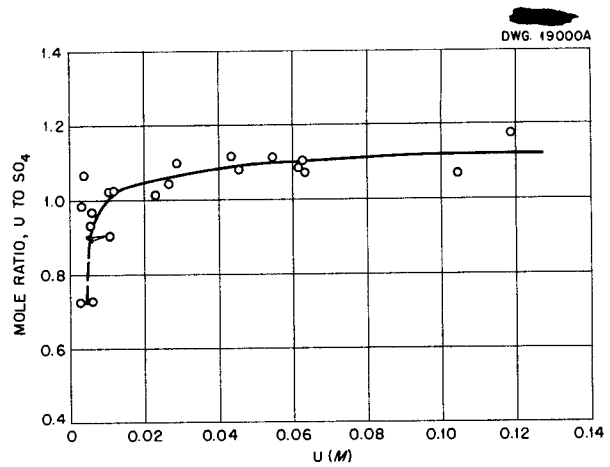

Fig. 50. Solubility Ratio of U to SO_4 in UO_2SO_4 Solutions in low Concentrations at 175°C.

to drop rapidly with decreasing concentration, below approximately 0.01 *M*. Similar studies are being continued at 250°C.

PHASE DIAGRAM FOR THE UO_3-SO_3-H_2O SYSTEM AT 25°C

Work is in progress on the completion of the phase diagram for the UO_3-SO_3-H_2O system at 25°C.

SOLUBILITY OF URANIUM TRIOXIDE IN URANYL FLUORIDE SOLUTIONS AT 25 and 100°C

Three runs at 25°C and three runs at 100°C on the solubility of uranium trioxide in uranyl fluoride solutions of varying concentrations have given very discordant results. These systems seem to be quite unstable, especially in concentrated uranyl fluoride solutions at 25°C. Further investigations are in progress.

EQUILIBRATION TIMES FOR URANIUM TRIOXIDE IN URANYL SULFATE AND URANYL FLUORIDE SOLUTIONS

The results obtained in solubility studies of uranium trioxide in uranyl sulfate and uranyl fluoride solutions make desirable an investigation of

(12) E. V. Jones, J. S. Gill, W. L. Marshall, and C. H. Secoy, *Chem. Quar. Prog. Rep. Sept. 30, 1952*, ORNL-1432, p. 51.

TABLE 26. SOLUBILITY OF UO_3 IN UO_2SO_4-H_2O SOLUTIONS OF LOW CONCENTRATION AT 175°C

Molarities based on room-temperature densities

TOTAL MOLARITY OF URANIUM	MOLARITY OF SO_4	SOLUBILITY-EXCESS MOLARITY OF UO_3	TOTAL MOLE RATIO UO_3 to SO_4	pH (at 25°C)
0.119	0.100	0.0190	1.190	3.25
0.1046	0.0978	0.0067	1.069	3.4
0.0638	0.0568	0.0070	1.070	3.2
0.0630	0.0573	0.0057	1.100	3.6
0.0622	0.0573	0.0049	1.086	3.7
0.0475	0.0428	0.0047	1.110	
0.0458	0.0425	0.0033	1.078	3.5
0.0437	0.0393	0.0044	1.112	3.5
0.0284	0.0258	0.0026	1.101	3.3
0.0271	0.0260	0.0011	1.042	
0.0232	0.0229	0.00033	1.014	3.5
0.01143	0.01114	0.00029	1.026	
0.01109	0.01083	0.00026	1.024	
0.00664	0.00687	-0.00023	0.967	3.7
0.00584	0.00802	-0.00218	0.728	
0.00567	0.00612	-0.00045	0.926	
0.00563	0.00635	-0.00072	0.887	3.5
0.00546	0.00612	-0.00066	0.892	
0.00370	0.00347	+0.00023	1.066	
0.00312	0.00318	-0.00006	0.981	
0.00239	0.00331	-0.00092	0.722	4.2

equilibration times for these systems. Studies are under way for both these systems at 25 and 100°C.

EXPLORATORY PHASE INVESTIGATIONS OF SYSTEMS INVOLVING $CuSO_4$, UO_2SO_4, H_2SO_4, and H_2O AT URANIUM CONCENTRATIONS BELOW 30 g PER LITER

W. L. Marshall

An exploration has been made of the following systems with regard to temperature at which either hydrolytic or true solubility precipitation occurs:

$CuSO_4$-H_2O ,

UO_2SO_4-H_2O ,

UO_2SO_4-$CuSO_4$-H_2O ,

UO_2SO_4-$CuSO_4$-H_2SO_4, H_2O .

The micro phase-study apparatus previously described was utilized for the investigation.[13] About 50 tubes containing the solutions were prepared and tested during the course of the work.

The purpose of the investigation was to define boundaries - not to obtain exact solubility or hydrolytic precipitation temperatures. Accordingly, the temperature was raised slowly, but not slowly enough to determine the precise precipitation temperature. This exact investigation would have delayed attainment of data to a considerable degree. Also, not

[13] H. W. Wright and W. L. Marshall, *HRP Quar. Prog. Rep. Oct. 1, 1952*, ORNL-1424, p. 108.

much emphasis was placed on data obtained below 200°C, the prime interest being in the behavior between 200 and 300°C. The actual phase-stability temperatures at equilibrium may be as much as 10 to 20°C below the values reported. In some systems, namely, UO_2SO_4-$CuSO_4$-H_2O and UO_2SO_4-$CuSO_4$-H_2SO_4-H_2O, the solid phase appeared to dissolve rapidly at room temperature after precipitating at the upper temperature, but it did not dissolve rapidly at temperatures just below the solid-phase appearance temperature. For the other two systems, the precipitations appeared to be irreversible, at least under the experimental conditions.

There is a remote possibility that reaction occurred with the pyrex and silica tubes used in this work. However, some tests were made at 250°C on solutions which had shown precipitation at temperatures between 200 and 240°C. Upon inserting tubes containing these solutions into the furnace at 250°C, precipitation occurred in as little as 5 seconds. It does not seem likely that the solution reacts this fast with the pyrex or silica.

The System $CuSO_4$-H_2O. Hydrolysis data for the system $CuSO_4$-H_2O from 1.0 to 1.0×10^{-3} *M*, as evidenced by precipitation of a bright blue-green solid phase, are given in Table 27. The solid phase must be a hydrolysis product because it appears in the same temperature range over such a wide change of concentration. Further evidence of hydrolysis is given in the rather complete investigation by Posnjak and Tunell,[14,15] from which the data in Table 28 were calculated.

The System UO_2SO_4-H_2O. Temperatures at which hydrolytic precipitation of a yellow solid occurs in the UO_2SO_4-H_2O system are given in Table 29. The data indicate that the minimum concentration of a UO_2SO_4-H_2O solution must be 0.017 *M* to achieve phase stability at 250°C.

TABLE 27. HYDROLYTIC PRECIPITATION OF $CuSO_4$

MOLARITY OF $CuSO_4$	TEMPERATURE AT WHICH PRECIPITATION FIRST OBSERVED (°C)
0.00116	115
0.00402	100
0.0161	115
0.0532	111
0.103	126
0.204	125
1.01	142

The System UO_2SO_4-$CuSO_4$-H_2O. In the work with the system UO_2SO_4-$CuSO_4$-H_2O, UO_2SO_4 is held constant at 0.021 *M* and the $CuSO_4$ concentration is varied. It appears from the data given in Table 30 that a phase-stable system of $CuSO_4$-UO_2SO_4-H_2O with 0.021 *M* UO_2SO_4 and more than 0.0021 *M* $CuSO_4$ could not be maintained at 250°C.

The System UO_2SO_4-$CuSO_4$-H_2SO_4-H_2O. There are four conditions of the system UO_2SO_4-$CuSO_4$-H_2SO_4-H_2O which have been considered. These are the effect of H_2SO_4 on 0.021 *M* UO_2SO_4 containing 0.02 or 0.10 *M* $CuSO_4$ and the effect of H_2SO_4 on 0.126 *M* UO_2SO_4 containing 0.02 or 0.10 *M* $CuSO_4$. The data are given in Table 31. Since 0.126 *M* UO_2SO_4 stabilizes 0.10 *M* $CuSO_4$ at 250°C, the same concentration of UO_2SO_4 should stabilize 0.021 *M* $CuSO_4$. No work was done on this latter system.

General Conclusions. The general conclusions that can be drawn from this work are:

1. Copper sulfate hydrolyzes and subsequently precipitates in the temperature range 90 to 140°C, at least at concentrations from 1.0 to 1.0×10^{-3} *M*.

2. At 250°C, the minimum concentration of UO_2SO_4 possible without

(14) E. Posnjak and G. Tunell, *Am. J. Sci.* **18**, 1 (1929).

(15) G. Tunnel and E. Posnjak, *J. Phys. Chem.* **35**, 929-46 (1931).

TABLE 28. THE SYSTEM $CuO-SO_3-H_2O$

Calculated from data by Posnjak and Tunell[14,15]

Temperature (°C)	CONCENTRATION (moles/1000 g of solution) CuO	SO_3	Mole Ratio of SO_3 to CuO
50	0.0063	0.0062	0.98
	0.016	0.016	1.00
	0.21	0.21	1.00
	0.44	0.45	1.02
100	0.00013	0.00025	1.92
	0.0010	0.0011	1.10
	0.0025	0.0025	1.00
	0.048	0.050	1.04
	0.15	0.15	1.00
	0.46	0.48	1.04
200	0.0025	0.0062	2.48
	0.021	0.037	1.76
	0.30	0.37	1.23
	0.57	0.80	1.40

TABLE 29. HYDROLYTIC PRECIPITATION OF UO_2SO_4

MOLARITY OF UO_2SO_4	TEMPERATURE AT WHICH PRECIPITATION FIRST OBSERVED (°C)
0.00624	225
0.0125	215
0.0150	210
0.0166	255
0.0208	325 to 355
0.0312	No solid phase, two-liquid layer at about 330°C
0.0625	No solid phase, two-liquid layer at about 315°C
0.125	No solid phase, two-liquid layer at about 306°C

TABLE 30. HYDROLYTIC PRECIPITATION IN SYSTEM $UO_2SO_4-CuSO_4-H_2O$ (0.021 *M* UO_2SO_4)

MOLARITY OF $CuSO_4$	TEMPERATURE AT WHICH PRECIPITATION FIRST OBSERVED (°C)	APPROXIMATE COLOR OF CRYSTALS
0.00210	250	Yellow
0.00368	255	Dull blue-green and yellow
0.00525	250	Dull blue-green
0.0101	190 to 215	Dull blue-green

TABLE 31. HYDROLYTIC PRECIPITATION IN SYSTEM UO_2SO_4-$CuSO_4$-H_2SO_4-H_2O

MOLARITY OF UO_2SO_4	MOLARITY OF $CuSO_4$	MOLARITY OF H_2SO_4	TEMPERATURE AT WHICH PRECIPITATION FIRST OBSERVED (°C)	COLOR OF PRECIPITATE
0.0210	0.020	0.00514	240	Questionable yellow
0.0210	0.020	0.0103	236	Questionable yellow
0.0210	0.020	0.0154	260	Questionable yellow
0.0210	0.020	0.0206	285	Questionable yellow
0.0210	0.100	0.0206	196	Bright blue-green
0.0210	0.100	0.0308	244	Bright blue-green
0.0210	0.100	0.0412	280	Bright blue-green
0.0210	0.100	0.0514	No crystals observed, two-liquid layer at about 342°C	Bright blue-green
0.126	0.100	None	240	Bright blue-green
0.126	0.100	0.0103	288 Two-liquid layer at 298°C	Bright blue-green
0.126	0.100	0.0206	None, two-liquid layer at 306°C, raised to 350°C with no solid appearing	

hydrolytic precipitation is approximately 0.017 *M*. Constituents such as $NiSO_4$,[16] other corrosion products, $CuSO_4$, and fission products will alter this value because of the solubility or hydrolysis effects of additional components on phase equilibriums.

3. At 0.021 *M* UO_2SO_4, solutions containing more than 0.0021 *M* $CuSO_4$ will not be phase stable at 250°C.

4. Approximately 0.015 *M* H_2SO_4 will be required to maintain phase stability for the solution which is 0.021 *M* UO_2SO_4 and 0.020 *M* $CuSO_4$. A solution 0.035 *M* in H_2SO_4 will be required to maintain phase stability for 0.021 *M* UO_2SO_4 and 0.10 *M* $CuSO_4$. For 0.126 *M* UO_2SO_4 that is 0.02 *M* in $CuSO_4$, no H_2SO_4 will be needed at 250°C, but approximately 0.005 *M* H_2SO_4 will be required for 0.126 *M* UO_2SO_4 that is 0.10 *M* in $CuSO_4$.

[16] J. S. Gill and C. H. Secoy, private communication.

COMMENT ON THE SYSTEM URANYL DICHROMATE-WATER

W. L. Marshall

In earlier studies, the apparent solubility of uranyl dichromate in the supercritical fluid that exists at above the critical temperature for mixtures of UO_3-CrO_3-H_2O which are soluble at room temperature was observed by Gill, Secoy, and Marshall. There was some doubt at that time as to whether uranium actually was dissolved in the fluid. With the advent of the semimicro phase-study apparatus, tube explosions were eliminated, and thus an easy method of investigation of this system was afforded.

In the present work, solutions of chromium trioxide, from 1.0 to 4.0 molar, in water were observed in silica tubes in the semimicro apparatus. Decomposition of dichromic acid to refractory Cr_2O_3 occurred between 325 and 370°C. No orange-red color was

observed in the supercritical fluid; however, vision was obstructed somewhat by the deposit of Cr_2O_3 on the tube surfaces. It is concluded that the orange-red color previously observed by Gill, Secoy, and Marshall was not due entirely to a chromium compound in the supercritical fluid.

Further investigations were made on stoichiometric $UO_2Cr_2O_7$ from 0.50 to 0.050 molar and on solutions containing 20% excess and 20% deficient UO_2^{++} in the same concentration range. In all experiments the supercritical fluid had an orange-red color. There were always deep-red crystals present above the critical temperature of the system.

This investigation is of interest because B. J. Thamer, R. M. Bidwell, and R. P. Hammond of the Los Alamos Scientific Laboratory recently showed that uranium oxide dissolves in the supercritical fluid of the system UO_3-H_3PO_4 at certain compositions of UO_3 and H_3PO_4.[17]

AN APPARATUS FOR PHASE-STABILITY STUDIES AND CORROSION TESTS ON 2-ml SOLUTION VOLUMES

W. L. Marshall

In August and September of 1952, exploratory investigations were made of aqueous uranyl fluoride solutions containing dissolved fluorides and hydroxides of alkali and alkaline earth metals.[18] Similar explorations were made of sulfate systems. Some of the solutions containing 300 g of uranium per liter which had pH values of 5.00 to 6.00 showed phase stability up to and above 300°C. However, it was not possible to make accurate observations in silica tubes on the high pH solutions because of the reaction of silica with the solutions to form insoluble silicates. As the temperature was raised, the formation of precipitates occurred at about 220°C in all solutions of pH between 5.00 and 6.00. It was necessary to study the phase stability and corrosiveness of these solutions in stainless steel, titanium, or platinum-lined bombs. It was deemed desirable to have a small apparatus in which many solutions could be tested with relative ease, since the large-scale apparatus currently available made this exploratory multitesting procedure impractical. If the apparatus were small and simple in design, many such units could be operated at a minimum of cost. Such an apparatus has been designed.

Description of Apparatus. A schematic drawing of the apparatus is shown in Fig. 51. The thermostat system consists of a 4-liter stainless steel beaker containing a liquid salt mixture of KNO_3, $NaNO_3$, and $LiNO_3$,[11] which melts at about 120°C and is held at the required temperature by suitable heating elements and a stirrer. The container tube for holding the small bombs is fabricated from stainless steel and is heliarc welded at the bottom. The inside dimensions are 5/8 in. in diameter and 8 in. in length. After the unit is loaded with a maximum of three bombs, it is attached to a conventional laboratory motor and rotated in the thermostat at 1800 rpm.

The outside dimensions of the stainless steel or titanium bombs are 1 3/4 in. in length and slightly under 5/8 in. in diameter. The contained volume is 3.2 milliliters. Teflon is used successfully as a gasketing agent. The Teflon ring gasket fits into a groove in the bomb cap, which prevents the ring from extruding from the gasketing surface. Because of the expansion characteristics of Teflon, the bomb cap can be tightened with hand-pressure alone. The expansion of the Teflon when the temperature is raised will seal the bomb. Similarly, upon cooling, only hand-pressure is needed to open

(17) B. J. Thamer, R. M. Bidwell, and R. P. Hammond, private communication.

(18) H. O. Day *et al.*, *HRP Quar. Prog. Rep. Oct. 1, 1952*, ORNL-1424, p. 113.

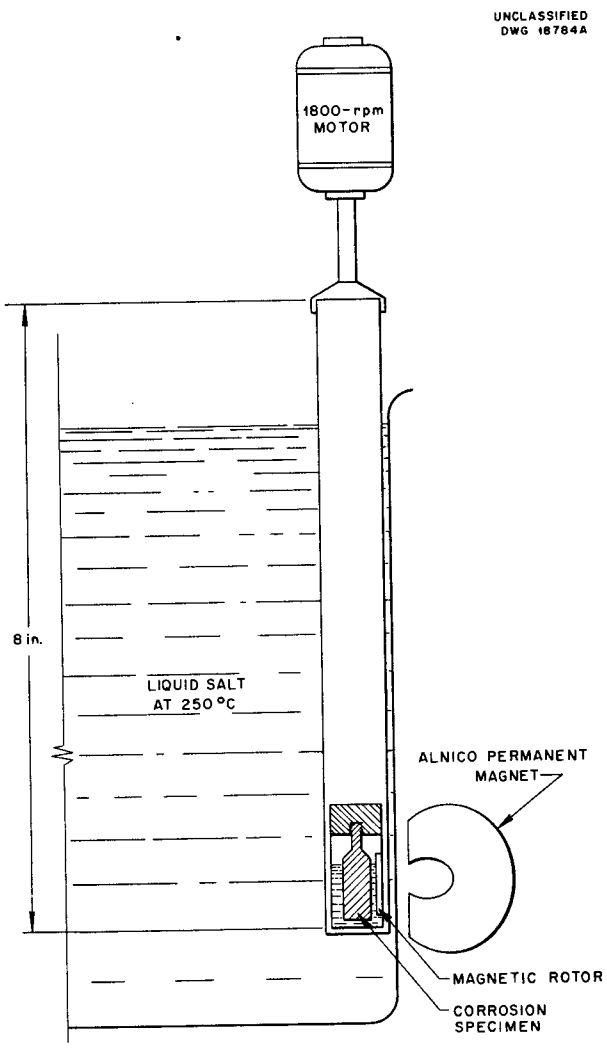

Fig. 51. Experimental Apparatus for Phase Study and Corrosion Experiments.

the bomb. In actual operation, however, a small wrench is used to tighten the bombs. Teflon appears to be a satisfactory seal for aqueous solutions at temperatures up to 325°C, at least for this type of gasket.

The magnetic rotor is prepared by sealing a permanently magnetized metal in either a type 347 stainless steel or a titanium capsule. The ends of the capsule are heliarc welded. No leakage occurs between the magnetized metal and the external system.

Teflon caps placed on the ends of the rotor have been used, in some instances, to eliminate erosion caused by metallic contact between the rotor and the bomb surface.

Corrosion specimens are fabricated from the metal to be tested. A specimen is screwed into the bomb cap and it rotates with the bomb, which, in turn, rotates with the container tube.

Under operating conditions, a container tube is loaded with three bombs, each containing a solution, a corrosion specimen, and a magnetic rotor. The unit is lowered into the thermostat and rotated at 1800 rpm. Three sets of two Alnico permanent magnets are adjusted to fit closely to the sides of the thermostat adjacent to the respective bombs. These magnets cause the rotors within the bombs to revolve around the inside diameter and provide mixing. Three container tubes containing three bombs each can be operated in one 4-liter thermostat bath.

Proposed Use of Apparatus. It is proposed to use this apparatus both for phase-stability studies, in which case the corrosion specimen will be omitted, and for corrosion studies. With respect to phase-stability investigations, the solution being studied will be run at the requisite temperature, the bomb will be cooled and opened, and the solution will be examined. Since cooling and opening of the bomb are completed in 60 sec, during which time there is no mixing, little if any equilibrium reversal should occur.

With regard to corrosion runs, the corrosion test specimen will be included in the bomb and microphotographs will be made of the specimen before and after a run. The specimen can also be weighed, and the solution can be analyzed for corrosion products.

The erosion on the sides of the bomb caused by the revolving rotor is one of the disadvantages of this apparatus. It is anticipated that the

use of titanium bombs, which have not been used up to the present time, and, also, the use of Teflon caps on the ends of the rotors, will eliminate this erosion difficulty.

If oxygen pressure within the bomb is desired, a calculated amount of 30% hydrogen peroxide can be added to each bomb before it is sealed. The peroxide decomposes at temperatures above 100°C and yields oxygen.

EXTENSION OF TWO-LIQUID PHASE STUDIES OF UO_2SO_4

H. W. Wright

An apparatus for more detailed studies of the miscibility break in the system UO_3-SO_3-H_2O has been designed, and fabrication is being completed. Exploratory experiments performed in quartz tubes indicate that both the fission-product activity and the copper ions are largely associated with the heavy, uranium-rich phase. Table 32 summarizes the results of one experiment for which a sample of HRE fuel solution was used.

OXIDATION OF SULFUR DIOXIDE IN URANYL SULFATE SOLUTION

D. W. Sherwood

Present plans for intermittent addition of acid to the inpile loop involve the addition of a mixture of a measured amount of sulfur dioxide and oxygen to react in the presence of the ions of the solution to form sulfuric acid. Experiments are in progress to determine the feasibility of this procedure with reference to the speed of the oxidation and the possible reducing action of the sulfur dioxide with regard to the uranyl ion in solution. Although the analytical data and the experiments are incomplete, present results seem to indicate that there has been no damage to the solution and that the desired oxidation is occurring in 1 hr or less at 200°C. The solution contains 40 g of uranium per liter and small amounts of copper and nickel ions to simulate a uranyl sulfate solution after exposure to loop metal. The desired gases are added to a quartz tube containing the frozen degassed solution. The sealed tubes are then heated in a resistance-wire-wound aluminum block.

TABLE 32. DISTRIBUTION OF FISSION-PRODUCT ACTIVITY

β^- ACTIVITY	ACTIVITY (counts/min/ml)			DISTRIBUTION RATIO	
	Uranium-Rich Phase, H	Water-Rich Phase			
		Aliquot 1, L_1	Aliquot 2, L_2	H/L_1	H/L_2
Gross	2.66×10^9	1.25×10^7	1.58×10^7	213	168
TRE*	2.02×10^9	6.72×10^6	9.14×10^6	301	221
Nb	5.00×10^5	2.44×10^3	2.25×10^3	205	222
Ru	6.00×10^4	2.5×10^3	2.23×10^3	24	27
Zr	3.40×10^5	2.8×10^4	1.15×10^4	12	30
Sr	2.94×10^8	3.86×10^6	4.53×10^6	76	65
Cs	4.22×10^6	6.84×10^4	6.30×10^4	62	67

*Total rare earths.

CHEMISTRY OF CORROSION

G. H. Cartledge R. P. Yaffe

The study of the electrode potential of type 347 stainless steel in 0.1 *F* sulfuric acid exposed to air has shown that the electrode may be made more noble by the addition of small quantities of certain heavy-metal ions. Experiments with radioactive silver showed that the ennobling could be obtained by precipitation on only minute amounts of silver on the electrode. The ennobling is often linear with the logarithm of the added ion concentration and, in certain cases, may amount to as much as 300 mv. Quantitative data are being accumulated in the hope that they may make possible a fuller interpretation of the electrochemical processes related to corrosion. The results may have significance in connection with possible impurities in reactor solutions.

The pertechnetate inhibition studies have been continued chiefly along lines related to the theory of the inhibition process. Details for certain tests may be found in ORNL-1529.[19]

VAPOR PRESSURES OF AQUEOUS URANYL SULFATE SOLUTIONS

H. O. Day, Jr.

Some vapor pressures of uranyl sulfate solutions at various concentrations and temperatures were reported previously.[20] In moving to new quarters in Building 4500, part of the differential pressure apparatus was accidentally broken, and it was necessary to construct an entirely new apparatus, similar to the one previously described; however, several small but important changes were made. The manometer tubes were made longer so that greater pressure differences could be accurately determined. A constriction of capillary tubing was placed in the U of the manometer to damp, as much as possible, any pressure fluctuations.

The tubing connecting the pressure vessels with the manometer was constructed of thick-walled, glass, capillary tubing. The thickness of the walls caused temperature variations in the vapor to be drastically reduced. At the same time, the volume of water vapor was also greatly lowered, and therefore the corrections which must be applied in calculating concentrations of uranyl sulfate were reduced. The capillary tubes were wrapped with nichrome wire so that they could be heated to prevent condensation.

The thermostat in which the pressure vessels were located was filled with dibutylphthalate instead of with the glycerol-water mixture used previously. Temperature control thereafter was much better at elevated temperatures. Loss of dibutylphthalate was much smaller than the glycerol loss at these temperatures. Dibutylphthalate was preferred over mineral oil, since it is easier to stir at lower temperatures and is easier to remove from the pressure vessels.

Considerable mechanical difficulty was experienced with the capillary tubing in that breaks resulting from strains introduced in heating and cooling the connecting tubing were frequent.

Two series of determinations of vapor pressure have been completed recently. *m*-Diphenyl benzene was the manometer fluid. Data for the first series of measurements are given in Table 33. Data from the last series are not reported at this time because the concentration of the uranyl sulfate has not yet been determined. Uncertainties in the concentrations as a result of analysis errors are ±0.0004 in molality and $\pm 0.000006_6$ in mole fraction.

(19) *Oak Ridge National Laboratory Status and Progress Report March 1953*, ORNL-1529, p. 22.

(20) H. O. Day, Jr., *HRP Quar. Prog. Rep. July 1, 1952*, ORNL-1318, p. 138; and H. O. Day, Jr. and W. L. Marshall, *HRP Quar. Prog. Rep. Oct. 1, 1952*, ORNL-1424, p. 104-105.

TABLE 33. VAPOR PRESSURE LOWERING IN URANYL SULFATE SOLUTIONS

TEMPERATURE (°C)	MOLALITY OF UO_2SO_4	MOLE FRACTION OF UO_2SO_4	ΔP (mm Hg)
25	3.1722 ± 0.0004	0.054061 ± 0.000006_6	2.110
30	3.1723	0.054062	2.764
35	3.1724	0.054064	3.696
40	3.1726	0.054066	4.731
45	3.1727	0.054069	5.886
50	3.1729	0.054072	7.390
60	3.1735	0.054082	10.762
70	3.1743	0.054094	16.166
80	3.1753	0.054110	23.272
90	3.1765	0.054129	32.848

SLURRY CHEMISTRY

F. R. Bruce, Section Chief

URANIUM TRIOXIDE CHEMISTRY

Preparation of UO_3 (L. E. Morse). In the previous report, preliminary experiments indicated that UO_3 of a quality suitable for use in fluid-fuel reactors which employ slurries containing 250 g of uranium per liter and are operated at 250°C could be prepared by either of the following methods:

1. a methathesis process in which ammonium diuranate is precipitated from a uranyl nitrate solution and converted to an ammonium uranyl carbonate, which is subsequently decomposed to anhydrous UO_3,
2. an ion-exchange method in which UO_2^{++} is adsorbed on a cation-exchange resin and eluted with $(NH_4)_2CO_3$ solution, and the resulting ammonium uranyl carbonate solution is decomposed to anhydrous UO_3.

The metathesis process has been investigated more thoroughly with the preparation of kilogram quantities of UO_3. The several steps in the process are discussed below.

Preparation of Uranyl Nitrate Solutions. A stock solution of 2.0 *M* $UO_2(NO_3)_2$ was prepared and diluted to the desired concentration for precipitation of $(NH_4)_2U_2O_7$. After the solution was allowed to stand for several days, a brown precipitate settled out, which was subsequently identified by spectroscopic analysis to be mainly an iron compound. In much of the previous work, the use of fresh uranyl nitrate solutions resulted in iron contamination. Therefore it may be necessary in the future to treat the uranyl nitrate solutions to remove iron.

Precipitation of Ammonium Diuranate

$$2\ UO_2(NO_3)_2 + 6\ NH_4OH \longrightarrow (NH_4)_2U_2O_7 + 4\ NH_4NO_3 + 3\ H_2O$$

Excess NH_4OH diluted 1:1 with H_2O was added over a period of 1 hr to a stirred solution of 0.5 *M* $UO_2(NO_3)_2$

at 85°C. Completion of the precipitation was indicated when a pH of 8 was obtained.

The $(NH_4)_2U_2O_7$ obtained by this procedure is a granular precipitate which settles and filters rapidly, and it may be easily washed. Since the precipitation is carried out in alkaline media, the iron originally present will also be carried. In this respect, the process is at a disadvantage compared with a uranyl peroxide precipitation, which affords some separation from iron.

The $(NH_4)_2U_2O_7$ may be filtered and washed free of nitrate with dilute NH_4OH. However, since the nitrate is present mainly as NH_4NO_3, which is decomposed at the temperature used to decompose $(NH_4)_4UO_2(CO_3)_3$, the precipitate and the supernatant could be carried through the metathesis step without the additional treatment that was required in the present test.

Methathesis of $(NH_4)_2U_2O_7$ to $(NH_4)_4UO_2(CO_3)_3$

$$(NH_4)_2U_2O_7 + 6\ (NH_4)_2CO_3 + 3\ H_2O \longrightarrow 2\ (NH_4)_4UO_2(CO_3)_3 + 6\ NH_4OH$$

After the precipitate and the supernatant from the previous operation were allowed to cool below 40°C, 15% excess $(NH_4)_2CO_3$ was added, and the mixture was stirred until metathesis was complete (about 1 hr). The most reliable test for complete metathesis is made by slowly decomposing a sample of the product at 280 to 300°C and heating at 375°C for about 15 minutes. The resulting product should be deep red in color, and there should be no green or black material to indicate the formation of U_3O_8 from the decomposition of unreacted $(NH_4)_2U_2O_7$. Failure of the decomposed carbonate to dissolve completely in HCl would also indicate the presence of U_3O_8 in the oxide product and, hence, of unreacted $(NH_4)_2U_2O_7$ in the carbonate preparation being treated. Experience with kilogram batches indicates that metathesis does not offer any difficulty. The ammonium uranyl carbonate produced by this method settles and filters rapidly.

Since $(NH_4)_4UO_2(CO_3)_3$ is somewhat water-soluble, there is a uranium loss associated with the metathesis step. In five batches carried out on a kilogram scale, the average loss was 2.2% U; however, this uranium is in a form suitable for recycling.

Decomposition of Ammonium Uranyl Carbonate

$$(NH_4)_4UO_2(CO_3)_3 \longrightarrow UO_3 + 4\ NH_3 + 3\ CO_2 + 2\ H_2O$$

The decomposition was carried out in an open porcelain dish in a muffle furnace with the temperature being raised stepwise from 200 to 350°C over a period of about 8 hours. Even though the decomposition appeared to be essentially complete, the heating at 350°C was continued overnight. The resulting product was an amorphous oxide of low bulk density.

When large amounts of material are handled, the stepwise heating procedure is especially necessary to minimize the possibility of uneven heating and consequent reduction of UO_3 by NH_3. In the furnaces employed in this work, the top strata of solids were decomposed first and formed UO_3 on the undecomposed remainder. If the temperature is too high, ammonia evolved from the lower layers may reduce the oxide. This reduction was, in fact, observed to occur when $(NH_4)_4UO_2(CO_3)_3$ was placed in a furnace at about 370°C and allowed to heat rapidly.

Preparation of $UO_3 \cdot H_2O$

$$UO_3 + H_2O \xrightarrow[\text{1 to 2 hr}]{85°C} UO_3 \cdot 2H_2O$$

$$UO_3 \cdot 2H_2O \xrightarrow[\text{16 hr}]{350°C} UO_3$$

$$UO_3 + H_2O \xrightarrow[\text{8 to 16 hr}]{250°C} UO_3 \cdot H_2O$$

The anhydrous oxide from the decomposition step was hydrated for about 12 hr at 85°C. Less than 0.1% of the uranium dissolved in the supernatant. After the supernatant was filtered, the resulting hydrate was decomposed to the anhydrous oxide by heating at 350°C for 16 hours. Rehydration at 250°C yielded monohydrate platelets of suitable purity. An oxide preparation is considered to be satisfactory if, after being hydrated overnight at 250°C, the supernatant contains less than 10 ppm of uranium for a slurry concentration of 250 g of uranium per liter.

Crystallography of $UO_3 \cdot H_2O$ (J. O. Blomeke). The crystal structure of $UO_3 \cdot H_2O$ has been investigated over the temperature range of 150 to 250°C, and crystals have been prepared which exhibit the same x-ray diffraction patterns[1] as the α-$UO_3 \cdot H_2O$ and β-$UO_3 \cdot H_2O$ reported by Zachariasen.[2] A transition from the low-temperature alpha rods to the high-temperature beta platelets occurs at approximately 200°C. This transition may not occur, however, if the alpha form is annealed by heating in water at 150 to 180°C for several hours before the temperature is raised past the transition point. The transition from the beta form back to the alpha form does not occur when the monohydrate is cooled past the transition point at a rate of about 2°C per minute. Revision to the alpha form occurs when the β-$UO_3 \cdot H_2O$ is ground at room temperature in a fluid-energy mill.

The importance of crystal structure studies in the development of an aqueous slurry fuel is emphasized by the definite relationship that can exist between the crystal structure and other properties of the solids, such as crystal habit, density, heat capacity, and hardness. Aside from this, a thorough knowledge of the crystal structure could be used to interpret any changes that might occur in the characteristics of the slurry during reactor operation.

The crystal structure of $UO_3 \cdot H_2O$ has been investigated by Vier,[3] as well as by Zachariasen.[2] Vier reported the existence of four different structures that are dependent on temperature and on the mode of preparation. These structures can be represented by the following schematic equations:

$$UO_4 \cdot xH_2O \xrightarrow[H_2O]{77 \text{ to } 185°C} \alpha\text{-}UO_3 \cdot H_2O \xrightarrow[-H_2O]{185 \text{ to } 300°C} \gamma\text{-}UO_3 \cdot H_2O$$

$$UO_2(NO_3)_2 \xrightarrow{\Delta} \text{Mallinckrodt } UO_3 \xrightarrow[H_2O]{77 \text{ to } 185°C} \beta\text{-}UO_3 \cdot H_2O \xrightarrow[H_2O]{185 \text{ to } 300°C} \alpha\text{-}UO_3 \cdot H_2O$$

Vier reported the alpha, beta, and gamma structures to be orthorhombic and the delta structure to be triclinic. Unfortunately, cell dimensions were not given, and it has been impossible to establish the reproducibility of this work.

Zachariasen reported the cell dimensions of two different $UO_3 \cdot H_2O$ crystals but gave no information concerning the chemical history of his samples. He indexed both these

(1) X-ray diffraction analyses performed by R. D. Ellison of the ORNL Chemistry Division.

(2) W. H. Zachariasen, *Report from July 1 to December 31, 1946 of Mass Spectroscopy and Crystal Structure Division*, p. 20, CP-3774 (Feb. 20, 1947).

(3) D. Vier, *Thermal Stability of Certain Oxide Hydrates in H_2O*, A-1277 (May 26, 1944).

structures as orthorhombic and called them α-$UO_3 \cdot H_2O$ and β-$UO_3 \cdot H_2O$, independently of Vier's nomenclature. By use of the cell dimensions given, the positions of all possible lines in the x-ray diffraction patterns were calculated, and thus a comparison could be made with material prepared in this laboratory.

In the course of the present slurry development work, three well-defined crystal habits have been reported to exist at 250°C in water: $UO_3 \cdot H_2O$ prepared from $UO_4 \cdot xH_2O$ by heating in water at 250°C assumes the crystal habit of hexagonal rods, 1 to 5 μ in diameter by 5 to 30 μ long; $UO_3 \cdot H_2O$ prepared at 250°C from well-washed Mallinckrodt UO_3 or from rods which have been calcined and rehydrated several times assumes a platelet habit of seldom more than 40 to 50 μ across the face; and when Mallinckrodt UO_3 is heated at 250°C in dilute $UO_2(NO_3)_2$ solutions, a larger crystal, several hundred microns on edge, that resembles a truncated bipyramid is formed. X-ray diffraction studies have shown that the rods conform to the pattern of the α-$UO_3 \cdot H_2O$, whereas the platelets possess the same pattern as is found in the beta form in Zachariasen's work. The study of a single crystal with the use of a precision camera indicated that the bipyramids also had the beta structure and were probably platelets in an advanced state of growth.

As suspensions containing 250 g of uranium per liter, the rods and the platelets had sufficiently different slurry properties to justify a study for establishing which of the two forms was more likely to be stable under the conditions of reactor operation. Heating of the rods and platelets in water at 250°C, in the absence of agitation, for as long as 70 hr produced no detectable change in the structure of either. In a dynamic reactor system, however, the crystals would be expected to be fractured both by abrasion and by the fission process. Hence, specimens of both rods and platelets were dried, pulverized in a fluid-energy mill, and then put back into water at 250°C. Platelet crystals were reformed from both samples. Pumping tests carried out in the Reactor Experimental Engineering Division also indicated that conversion from rods to platelets would occur after only a few hours of turbulent circulation at 250°C.[4] Static radiation tests carried out at 250°C in the ORNL graphite reactor with slurries of rods showed a marked tendency for platelets to be formed as the rods were fractionated by fission recoils.[5] It has been concluded from this evidence that the platelets exhibiting the same x-ray diffraction pattern as that of Zachariasen's β-$UO_3 \cdot H_2O$ are the stable form of $UO_3 \cdot H_2O$ in water at 250°C and that they are the crystal form most likely to be present at this temperature in a reactor fuel.

During the past quarter, further evidence was obtained to indicate that platelets are the stable crystal form of $UO_3 \cdot H_2O$ in water at 250°C. Also, the existence of a temperature-crystal structure relationship was demonstrated. The experiments performed are presented schematically in Fig. 52. Initially, it was found that a transition from β-$UO_3 \cdot H_2O$ to α-$UO_3 \cdot H_2O$ occurs as a result of grinding platelets at room temperature. Although such a transition from a "frozen-in" high-temperature form to a low-temperature form is not rare among inorganic salts, it has been known to occur much less frequently with hydrates.

The micronized platelets were then divided into four parts and heated in water for 16 hr at 150, 180, 215, and 250°C, respectively. The samples heated at 150 and 180°C retained the α-$UO_3 \cdot H_2O$ structure, with the fragments

(4) A. S. Kitzes *et al.*, *HRP Quar. Prog. Rep. Jan. 1, 1953*, ORNL-1478, p. 110.

(5) F. R. Bruce *et al.*, *HRP Quar. Prog. Rep. Mar. 15, 1952*, ORNL-1280, p. 107.

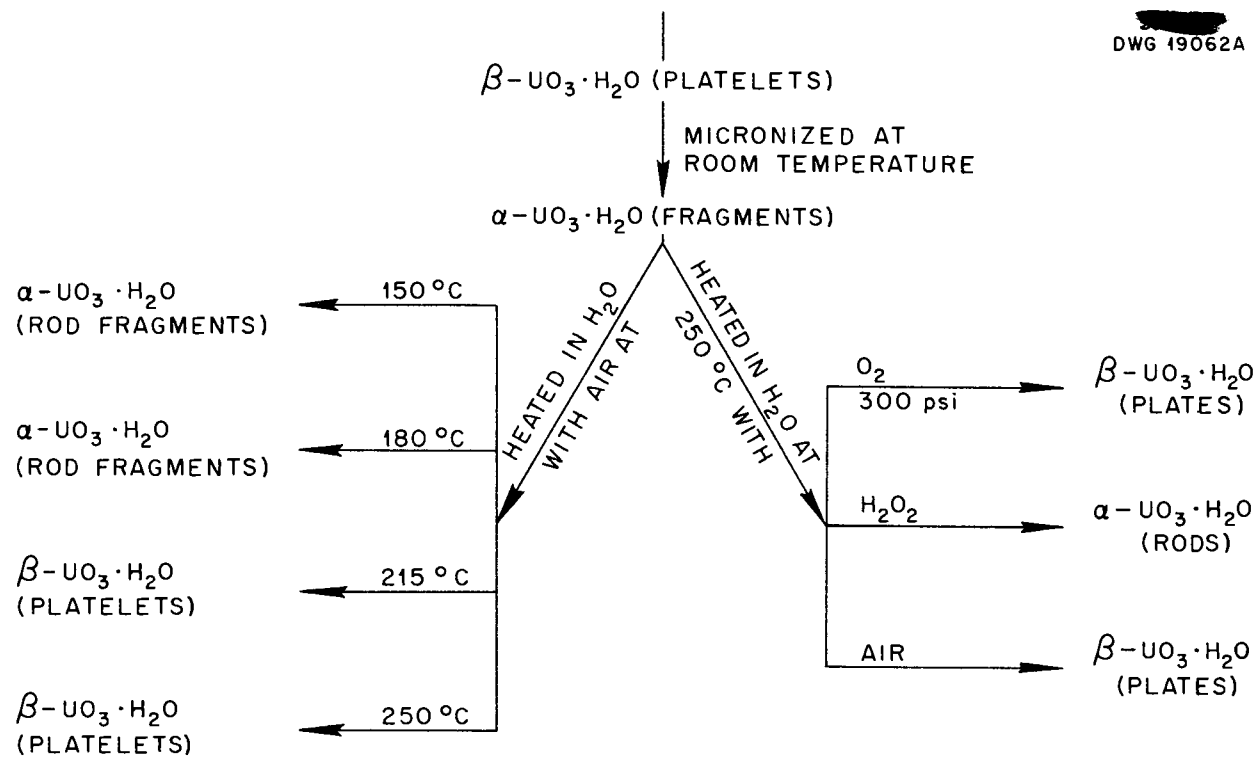

Fig. 52. Structure Stability of $UO_3 \cdot H_2O$.

growing in size and assuming a rod-like habit. The samples heated at 215 and 250°C were converted to platelets and they possessed the β-$UO_3 \cdot H_2O$ structure. These experiments indicate that the transition temperature from the alpha to the beta form must lie in the neighborhood of 200°C.

The question of what induces the formation of rods from $UO_4 \cdot xH_2O$ at 250°C may be partly answered by the remaining three experiments noted in Fig. 52. Samples of micronized platelets were heated in water at 250°C under atmospheres of oxygen that were introduced in two different ways. In one case, the oxygen was introduced as the gas to a pressure of 300 psi at 250°C. In the second case, 30% H_2O_2 was added in a quantity that would produce an oxygen pressure of 300 psi upon decomposition at 250°C. After being heated for 16 hr, the micronized rods had been converted to platelets in the first case, but they had retained their alpha structure and regained the rod crystal habit in the second case. As before, the customary conversion to platelets occurred at 250°C when only air was present. These experiments seem to indicate that the presence of peroxidic oxygen intimately associated with the fragmented crystals promotes the formation of α-$UO_3 \cdot H_2O$, even at temperatures in excess of the transition point.

It is to be noted from these studies that only two structures of $UO_3 \cdot H_2O$ were ever found and that these conformed to those reported by Zachariasen. The existence of a third, orthorhombic structure or of a triclinic pattern, as reported by Vier, was not substantiated.

CHEMISTRY OF UO_2CO_3

Preparation of UO_2CO_3 Slurries (J. P. McBride, W. L. Pattison). Interest in the possible use of UO_2CO_3 as a slurry fuel has been increased

because, as reported in the previous report, the reaction of CO_2 with a slurry of oxide platelets yielded a carbonate that exhibited excellent slurry properties. Investigation of this reaction has continued in an effort to determine the conditions of temperature and pressure which produce the most desirable product. Reactions at room temperature and CO_2 pressures of 225 to 840 psi were found to yield much better slurries than were obtained at higher temperatures (200 to 250°C). The addition of 0.005 *M* Na_2CO_3 to the oxide before reaction at room temperature served to essentially stabilize the resulting slurry against sedimentation so that only a small fraction of the solid separated in one week. Slurries prepared in the absence of added electrolyte, although not free of sedimentation, showed little settling in 24 hr and complete dispersion of the unsedimented material in the slurry phase in contact with the separated solid.

Table 34 summarizes the data on the preparation of UO_2CO_3. It is apparent that the best reaction is obtained with very pure oxide platelets of low soluble uranium content.

Hydrolytic Decomposition of UO_2CO_3 Slurries (J. P. McBride, W. L. Pattison). The effects of temperature and of adding dilute solutions of electrolytes on the hydrolytic decomposition of UO_2CO_3 slurries has been studied.

Effect of Temperature. Although no detailed study of the effect of temperature on the hydrolytic decomposition of UO_2CO_3 slurries has been made, it has been observed that they are hydrolized by prolonged boiling, but the process is slow. At 250°C, however, in a closed system and in the absence of CO_2 pressure, a carbonate slurry is decomposed almost completely to oxide in 2 to 3 hr (Table 35).

Effect of Electrolytes. The hydrolytic decomposition of a UO_2CO_3 slurry at 250°C generally yields an oxide in the form of large rods that are 10 to 20 μ in length. The fact that the original carbonate is prepared in the form of elongated platelets that are much less than 1 μ in average size makes the relatively large oxide particles produced by the decomposition disappointing. It was of interest, therefore, to investigate the effect of adding dilute solutions of electrolytes to the carbonate slurries before hydrolysis in the hope that crystal growth might be inhibited by the adsorption of the ions on the oxide as it is formed.

The effects of Na_2CO_3, NaOH, Na_2SiO_3, Na_3PO_4, $Na_4V_2O_7$, and H_3PO_4 were investigated. Table 35 gives the data for these experiments. The first three promoted the growth of large rods and platelets. Sodium phosphate induced the formation of small, thin, uniform platelets, whereas the vanadate yielded small agglomerates (5 to 10 μ) composed of small particles of approximately the same size as that of the original carbonate particles. The effect of phosphoric acid was similar to that of the sodium salt. In all cases, the presence of the electrolyte apparently caused a rather high dissolution of uranium (500 to 3000 ppm). Since some of the supernatants lost their yellow color upon being allowed to stand, because of the separation of the yellow oxide, the uranium in the supernatants was probably present in a colloidal state.

Thermal Stability of UO_2CO_3 Slurries Under CO_2 Pressure. The chemical equilibriums associated with the formation of UO_2CO_3 by the reaction of CO_2 with $UO_3 \cdot H_2O$ may be expressed as follows:

$$H_2O + CO_2 \overset{K_1}{\rightleftharpoons} CO_{2(aq)} + H_2CO_3 \ , \qquad \text{I}$$

$$H_2CO_3 \overset{K_2}{\rightleftharpoons} H^+ + HCO_3^- \ , \qquad \text{II}$$

$$UO_2(OH)_2 + 2H^+ \overset{K_3}{\rightleftharpoons} UO_2^{++} + 2H_2O \ , \qquad \text{III}$$

TABLE 34. PREPARATION OF UO_2CO_3

EXPERIMENT NO.	STARTING MATERIAL	ADDED ELECTROLYTE	REACTION TEMPERATURE (°C)	REACTION TIME (hr)	CO_2 PRESSURE, AT ROOM TEMPERATURE* (psi)	URANIUM CONCENTRATION (g/liter)	CO_3^{--}-TO-U RATIO	DESCRIPTION OF RESULTING SLURRY
$R4_1$	$UO_3 \cdot H_2O$ platelets prepared from rods by 3 cycles; calcination at 400°C, hydration at 250°C	None	200	48	950	121	0.96	Pale yellow; large agglomerates; rapid settling; no packing
$R4_2$	Dilute portion of slurry produced in R4	None	250	18	500	163	0.97	Smaller particles than $R4_1$; lower bulk density
$R4_3$	Portion of slurry produced in $R4_3$	0.004 *M* Na_2CO_3	250	18	500	135	0.99	Smaller particles than $R4_1$ and $R4_2$; low settling rate
$R5_1$	$UO_3 \cdot H_2O$ platelets (same as $R4_1$)	0.004 *M* Na_2CO_3	250	18	500	224	0.96	Almost white slurry with very small, uniform, regularly shaped particles; average particle size 0.6 μ; 25% settling in 17 hr
$R6_1$	Anhydrous UO_3 produced from UO_4 calcination: 3 hr at 325°C	0.005 *M* Na_2CO_3	250	14	500			Approximately 40% reaction
$RR7_1$	Enriched $UO_3 \cdot H_2O$ platelets prepared from rods by calcination-hydration	0.005 *M* Na_2CO_3	250	20	820			Similar to $R5_1$
$R8_1$	$UO_3 \cdot H_2O$ platelets (same as $R4_1$)	0.005 *M* Na_2CO_3	250	48	500			Similar to $R5_1$
$R8_2$	$UO_3 \cdot H_2O$ platelets (same as $R4_1$)	0.01 *M* Na_2CO_3	250	48	500			High soluble uranium in supernatant, slurry settled slowly but packed badly
$R9_1$	$UO_3 \cdot H_2O$ platelets prepared from rods by 5 cycles; calcinatibn at 400°C, hydration at 250°C	None	250	40	374 psi added at 250°C	240	0.91	Large yellow particles which settled rapidly and packed badly; even upon being allowed to stand for only a short time
$R10_1$	$UO_3 \cdot H_2O$ platelets (same as $R9_1$)	None	250	48	440	213	1.02	Viscous slurry; low bulk density; water-white supernatant
$R11_1$	$UO_3 \cdot H_2O$ platelets (same as $R9_1$)	None	45	90	850	262	1.02	Very white, slow-settling slurry; some tendency to agglomerate and become thixotropic in 24 hr
$R12_1$	$UO_3 \cdot H_2O$ platelets (same as $R9_1$)	0.005 *M* Na_2CO_3	40	20	740	224	1.01	Excellent slurry; virtually stable; less than 5% aettling of solids in one week
$R14_1$	$UO_3 \cdot H_2O$ rods; prepared from pure, micronized platelets by hydration at < 200°C	None	25	18	840			Slow-settling slurry
$R15_1$	$UO_3 \cdot H_2O$ platelets (50 to 100 ppm of soluble uranium)	None	25	25	600	202	0.94	Very little settling in 24 hr
$R16_1$	$UO_3 \cdot H_2O$ platelets similar to $R15_1$	None	25	40	225	210	0.95	Similar to $R15_1$
$R17_1$	$UO_3 \cdot H_2O$ rods prepared at Y-12; high concentration of soluble uranium	None	25	23	400			Incomplete reaction

*In two experiments with similar gas and solution volumes and CO_2 pressures, the partial pressure of CO_2 at 250°C over a carbonate slurry was found to be 1.4 and 1.5 times the pressure added at room temperature.

TABLE 35. HYDROLYTIC DECOMPOSITION OF UO_2CO_3 SLURRIES AT 250°C; EFFECT OF ELECTROLYTES

EXPERIMENT NO.	SLURRY PREPARATION (see Table 34)	REACTION TIME (hr)	ELECTROLYTE	CONDITION OF OXIDE	FINAL URANIUM CONCENTRATION IN SUPERNATANT (ppm)
$R5_6$	$R5_1$	20	0.005 *M* Na_2CO_3	Needles and rods with good slurry properties	500 to 1000
$R10_2$	$R10_1$ (washed and reslurried)	18	0.005 *M* Na_2SiO_3	Large rods; considerable agglomeration and packing	390
$R10_3$	$R10_1$ (washed and reslurried)	18	0.01 *M* NaOH	Large rods and fragments; some agglomeration and slight tendency to pack	540
$R10_4$	$R10_1$ (washed and reslurried)	18	None	Agglomerated and caked rods	274
$R10_5$	$R10_1$ (washed and reslurried)	18	0.004 *M* Na_2CO_3	Not completely decomposed to rods; difficult to slurry	1080
$R10_6$	$R10_1$ (washed and reslurried)	18	0.005 *M* Na_3PO_4	Small, thin, square platelets of uniform sizes; very easily reslurried	3270
$R10_7$	$R10_1$ (washed and reslurried)	18	0.005 *M* $Na_4V_2O_7$	Very fine oxide resembling the original carbonate; easily reslurried	1430
$R10_8$	$R10_1$ (washed and reslurried)	64	0.005 *M* H_3PO_4	Thin square platelets; some tendency to pack	900
$R10_9$	$R10_1$ (boiled for 3 hr)	68	None	Large platelets; rapid settling	144
$R11_2$	$R11_1$	20	None	Rods; nearly complete decomposition	300
$R11_3$	Recarbonated $R11_2$	48	None	Same as $R11_2$	189
$R11_4$	Recarbonated $R11_3$	2.5	None	Same as $R11_2$	111
$R14_2$	$R14_1$	2.5	None	Rods	110

$$UO_2^{++} + HCO_3^- \overset{K_4}{\rightleftharpoons} UO_2CO_3\downarrow + H^+ , \qquad \text{IV}$$

where the K_i are the equilibrium constants.

Since K_1K_2 is equal to 3×10^{-7} and the fraction of the uranium converted to oxide is proportional to the ratio $(HCO_3^-)/(H^+)$, it is apparent that the rate and completion of the reaction will depend not only on the CO_2 pressure and the temperature but also on the pH of the original oxide slurry and the concentration of acid impurities released from the oxide on reaction.

Experiments indicate that the partial pressure of CO_2 required to stabilize pure UO_2CO_3 in a slurry at 250°C and in the presence of 0.005 *N* Na_2CO_3 will be less than 500 psi (see experiments $R9_1$, Table 34; $R5_7$ and $R12_5$, Table 36). Data on the thermal stability of UO_2CO_3 slurries are presented in Table 36.

THORIUM CHEMISTRY

J. O. Blomeke L. E. Morse
J. P. McBride W. L. Pattison

A study of thorium compounds suitable for use in a breeder blanket has been initiated. This work has been divided into two parts:

1. the preparation of pure ThO_2 and a study of its slurry properties,
2. an investigation of other thorium compounds and blanket systems which would be suitable for use in a breeder.

URANYL OXIDE SLURRY IRRADIATIONS

J. P. McBride W. L. Pattison

The investigation of the effect of neutron irradiation on the properties of uranium oxide slurries has continued with another experiment carried out in hole 11 of the ORNL graphite reactor. A slurry of 93% enriched $UO_3 \cdot H_2O$ platelets containing 40 g of uranium per liter was irradiated in type 347 stainless steel for four weeks (600 hr of irradiation) at maximum flux (7×10^{11} neutrons/cm^2·sec) and at temperatures of 250 to 295°C.

The gas production rate was much less than that in a sulfate solution of the same concentration, the value for *G* (molecules of water decomposed per 100 ev of energy absorbed) being about 0.4 at 250°C. The calculated steady-state pressures during the first four days of the run were much higher than those in a solution that indicated a much slower rate of recombination of the hydrogen and oxygen produced by the decomposition of water. The steady-state gas pressure was found to decrease, however, as the irradiation progressed; therefore, at the end of the run, steady-state pressures (including steam) of less than 4000 psi at 250°C and less than 2500 psi at 295°C were observed. With the exception of the values obtained during the first three days of irradiation, the gas production and recombination at any one temperature could be correlated by using the kinetic expression already developed for solutions; that is, a plot of $\Delta P/\Delta t$ vs. P yielded a straight line.[6] The values for the gas production rate found by extrapolating the $\Delta P/\Delta t$ plot to steam pressure were found to decrease by at least a factor of 2 as the slurry temperature was increased from 250 to 295°C.

The experiment was carried out with only 10 ml of slurry, or a total of 400 mg of uranium, as the oxide. Only 30% of the slurry was readily transferred from the radiation bomb. Visual examination of the bomb interior showed the bulk of the material to have plated out on the walls of the container. It was possible to recover this material by adding 1/4-in. steel balls to the bomb, closing it, and shaking it vigorously for several

[6] C. H. Secoy, *HRP Quar. Prog. Rep. Mar. 15, 1952*, ORNL-1280, p. 164.

TABLE 36. STABILITY OF UO_2CO_3 SLURRIES AT 250°C UNDER CO_2 PRESSURE

EXPERIMENT NO.	SLURRY PREPARATION (see Table 34)	ELECTROLYTE CONCENTRATION	CO_2 PRESSURE, AT ROOM TEMPERATURE* (psi)	REACTION TIME (hr)	CONDITION OF SLURRY	FINAL pH (degassed)
$R5_7$	$R5_1$	0.005 *M* Na_2CO_3	150	168	No apparent decomposition to oxide; complete settling within 24 hr	
$R12_2$	$R12_1$	0.005 *M* Na_2CO_3	None	64	Went to partial dryness; nearly complete decomposition to large rods (about 20 μ)	6.4
$R12_3$	$R12_1$	0.005 *M* Na_2CO_3	48	64	Same as $R12_2$	6.7
$R12_4$	$R12_1$	0.005 *M* Na_2CO_3	100	88	More than 50% decomposition to rods; remaining carbonate well dispersed	6.6
$R12_5$	$R12_1$	0.005 *M* Na_2CO_3	300	88	No apparent decomposition or particle growth; complete settling within 24 hr	7.4
$R16_2$	$R16_1$	None	225	164	Decomposed	5.2
$R16_3$	$R16_1$	None	390	48	Decomposed	6.1

*In two experiments with similar gas and solution volumes and CO_2 pressures, the partial pressure of CO_2 at 250°C over a carbonate slurry was found to be 1.4 and 1.5 times the pressure added at room temperature.

hours. Plating appeared to be much more pronounced above the surface of the slurry than below, but no quantitative determination was made.

The portion of the slurry that was readily transferred showed no impairment of slurry properties. Photomicrographs showed that irradiated oxide had undergone considerable degradation to fragments and fines. Only a very small fraction of the material appeared in the form of recognizable platelets, which comprised the bulk of the original material (less than 10 μ average size). In addition, there were many large flakes (20 to 40 μ in size) of irregular shape; the flakes exhibited no definite crystalline form. Since the soluble uranium content at the end of the run was less than 8 ppm, crystal growth should not have occurred. The flakes were probably loosened portions of the film formed on the interior surfaces of the bomb by the plating out described above. In contrast to the slurries previously irradiated, the recovered slurry was brownish in color rather than dark green and no reduced uranium was found.

PHYSICAL STUDIES OF SLURRIES

R. N. Lyon, Section Chief
A. S. Kitzes P. R. Crowley
R. B. Gallaher W. Q. Hullings
C. A. Gifford

THORIUM SLURRIES

Thorium Oxide Studies. Thorium oxide prepared by calcination of thorium oxalate at temperatures above 600°C is extremely abrasive to stainless steel. The reported hardness of this material is approximately 7.5 on the Moh scale, while the hardnesses of stainless steels and titanium on the same scale are 6 to 6.5. These data conform with the results obtained with the abrasion tester described in ORNL-1121,[1] in which the abrasive action of thorium oxide was qualitatively determined by pumping slurry through a 0.008-in. gap between the rim of a rotating wheel and a polished test-plate parallel to the axle of the wheel.

Studies of the possibility of producing a thorium oxide with a scratch hardness of less than 6 on the Moh scale have been initiated. In these studies, thorium oxalate has been calcined at various temperatures between 300 and 500°C, and the indications, so far, are that oxide prepared by calcining the oxalate at 300°C is less abrasive than the corresponding material calcined at 800°C. Calcining at the lower temperatures produces a more chemically reactive oxide which is expected, because of its possibly porous structure, to be less hard than an unreactive form. These tests are being continued to obtain more quantitative data.

The particle shapes and sizes were determined from electron-microscope photomicrographs of three types of thorium oxide. The data, shown in Table 37, were abstracted from ORNL CF-53-1-240.[2]

Thorium Fluoride Studies. Thorium fluoride is another possible material for use as a circulating-type of thorium blanket. Thorium fluoride, obtained from Ames Laboratory in a

(1) A. S. Kitzes *et al.*, *HRP Quar. Prog. Rep. Aug. 15, 1951*, ORNL-1121, p. 156-160.

(2) F. D. McNeer, *Electron Micrographs of ThO_2 Samples*, ORNL CF-53-1-240 (Jan. 22, 1953).

TABLE 37. ELECTRON MICROGRAPHS OF ThO_2

PREPARATION OF ThO_2	PARTICLE SHAPE	PARTICLE SIZE (μ)	
		Average	Range
High-temperature calcination at 800°C from oxalate	Irregular	0.2	0.02 to 2
Low-temperature calcination at 300°C from oxalate	Plate-like crystals	0.5	0.02 to 2
Low-temperature calcination at 300°C from carbonate	Irregular	0.2	0.02 to 2

freshly prepared slurry, abraded type 347 stainless steel in the abrasion tester at 12 times the rate for abrasion by oxide calcined at low temperature. However, thorium fluoride which had been allowed to remain under water for seven to ten days prior to testing abraded the stainless steel specimen only slightly in 24 hr and possible hydration of the fluoride to produce a softer material was indicated. Therefore thorium fluoride prepared by precipitation from $Th(NO_3)_4$ with HF may be nonabrasive, since it will be fully hydrated. No tests have been performed with this material, as yet.

Slurries of thorium fluoride have one disadvantage which may limit their use as a breeder blanket. Because of the low bulk density of the fluoride, it may not be possible to obtain as high a thorium concentration as is desired for some reactor configurations.

Thorium Carbonate. A slurry of thorium carbonate, when autoclaved at 250°C for 24 hr, decomposed to give CO_2 and ThO_2. Consequently, this material is not being considered further as a breeding material for use at 250°C.

Thorium Hydroxide Peptized with Thorium Nitrate. To alleviate the abrasion problem associated with most thorium compounds, colloidal thorium hydroxide was prepared by precipitation from $Th(NO_3)_4$ with concentrated ammonium hydroxide. Normally, the metal hydroxides, if stable, are softer than the corresponding oxides. In addition, abrasion would probably be minimized because of the extremely fine particles in the colloidal solution. To produce the thorium hydroxide suspension, a slurry was peptized with thorium nitrate at 65°C to give a stable mixture that on visual examination was hardly distinguishable from a solution. Prior to peptization with thorium nitrate, the thorium hydroxide was washed by decantation to remove most of the ammonium salts and then electrodialyzed until essentially free of all extraneous ions.

The stable suspension, the composition of which is still unknown, was concentrated by evaporating water at 65°C until a product that was very viscous at room temperature was obtained. The density of this fluid was approximately 3.4 g/cm^3, and it contained about 2300 g of thorium per liter, calculated as ThO_2. Additional quantities of this material are being prepared so that the compound can be identified, the thermal stability at 250°C can be ascertained, and the stability to reactor radiation can be studied.

Thorium Oxide Circulating Loops. During this quarter, the loop for circulating thorium oxide slurries at a temperature of 150°C was put into operation. The loop described in

ORNL-1121[1] was modified by substituting a Richardson-Frithsen, fluid-bearing, canned-rotor pump for the original, conventional, centrifugal pump. The pump, previously tested for its operating characteristics with slurries, circulated a thorium oxide slurry continuously and with no apparent difficulty in an auxiliary testing loop at room temperature for 168 hr before it was installed in the loop. Within 24 hr of operation at 150°C with a slurry containing 300 g of thorium (as the oxide) per liter, the pump failed. Examination of the disassembled pump showed that the stator cans of 0.010-in.-thick, stainless steel had been perforated because of abrasion by the oxide. The total operating time of the pump with thorium oxide slurries in various runs was 264 hours.

Modified stator cans are being designed to prevent accumulation of solids in stagnant corners of the cans. This type of accumulation was a secondary problem in previous tests, since the pump shaft was vertical. The thorium circulating systems will be reserved in the future for slurries of particles less hard than stainless steel.

Design of the thorium loop for operation at 250°C and 1000 psi has been temporarily suspended until a suitable slurry material is developed. The over-all design for the loop described in ORNL-1478[3] has been completed, and some detailed drawings are available.

URANIUM SLURRY LOOPS

Loop S. Loop S has been in operation at 250°C and 1000 psi with uranium oxide slurries for over 2500 hr with no evidence of corrosion or erosion in the loop. However, solids still tend to accumulate in the pressurizer, but they no longer plate out on the walls of the main stream pipes. Various attempts were made to eliminate the accumulation of solids in the pressurizer by changing the level of liquid in the pressurizer and by introducing auxiliary flow through the pressurizer to create turbulence, but none of the attempts were successful. Electron micrographs and x-ray diffraction of the material collected in the pressurizer always showed the oxide to be of the beta or the platelet form.

Alpha-to-Beta Transformation. To eliminate the possibility that the transformation of the alpha oxide (rods) to the beta (platelets) form was the cause for the accumulation of solids in the pressurizer, beta oxide obtained from previous runs was circulated, initially, at 250°C. Within 24 hr, the solids collected in the pressurizer. The temperature of the loop was then dropped to 150°C, since previous experience with another loop[4] had shown that alpha oxide could be circulated at 150°C without difficulty. Within 24 hr after the loop reached equilibrium at 150°C, the beta oxide was being converted to the alpha form, as shown by x-ray diffraction patterns.

By cycling the loop temperature between 250 to 150°C and then to 200°C, the temperature dependence of the oxide form was established. At temperatures above 200°C, the beta oxide is apparently the stable form, and below 200°C, the alpha oxide is more stable. Results of subsequent runs proved that the alpha oxide is the more stable and that it can be circulated at 150°C for long periods of time without accumulation of solids in any part of the loop or pressurizer.

It was also found that accumulations of beta or platelet form which occur at 250°C can be redispersed by lowering

[3] A. S. Kitzes *et al.*, *HRP Quar. Prog. Rep. Jan. 1, 1953*, ORNL-1478, p. 105.

[4] R. N. Lyon *et al.*, *HRP Quar. Prog. Rep. Mar. 15, 1952*, ORNL-1280, p. 83.

the temperature to 150°C, if the accumulations have not existed for more than about 24 hours. Older accumulations are dispersed slowly, if at all, by lowering the temperature. These findings reinforce the belief that alpha, or rod-type, slurries do not plate out in a circulating system. The investigation of the reason for accumulation of the beta oxide (platelet) form at 250°C is being continued.

UO_2CO_3 Slurries. McBride has reported[5] that UO_2CO_3 slurries are thermally stable at 250°C. Interest in circulating this material at 250°C is warranted, not only because of the understanding it may give of the behavior of rod-like particles circulating at this temperature, but also because the UO_2CO_3 itself may be useful as a slurry fuel.

The carbonate was prepared by circulating beta oxide in the loop at 150°C under a pressure of 600 to 800 psi of CO_2 for 65 hours. After bleeding off some of the gas, the loop was heated to 250°C and, within 24 hr after equilibrium was established, solids accumulated in the pressurizer. Microscopic examination of these solids showed them to be predominantly of platelet form. Apparently, the UO_2CO_3 decomposed to $UO_3 \cdot H_2O$, which then promptly took the beta form and plated out in the pressurizer. McBride discusses this reaction in ORNL-1478[5] and reports evidence that 0.005 *M* Na_2CO_3 stabilizes UO_2CO_3 slurries at 250°C. A run is now in progress in which a UO_2CO_3 slurry is being prepared in the presence of 0.02 *M* Na_2CO_3. At 150°C, the pH of the slurry is steadily increasing from 6.4 to 7.0 and approaching the value of 7.4 reported by McBride. No other data are available, as yet.

The System $UO_3 \cdot H_2O$-Na_2HPO_4. The addition of 0.5 *M* Na_2HPO_4 to the loop in which solids were beginning to accumulate in the pressurizer readily dispersed the solids and prevented the plating out of the slurry circulating at 250°C. The pH of the slurry was 10.6.

Phosphates are common and efficient deflocculating agents for the dispersion of solids in water. Their mode of action is probably the following: adsorption of the phosphate ions on the surface of the solids imparts a negative charge that causes repulsion of similar particles and thereby stabilizes the system.

With the addition of oxygen to prevent reduction of U^{+6} to U^{+4}, after 100 hr of operation with uniform concentration of solids throughout the loop, evidence of corrosion was found. The slurry particles turned muddy brown in color, and thus there was indication of the formation of Fe_2O_3; since the supernate became yellow, there was possibly soluble chromate present.

Analysis of the slurry confirmed the presence of iron and chromium. Large quantities of iron compounds were found with the solids, and chromate ions, rather than uranium compounds, were the cause for the yellow color of the supernate.

This run was stopped and the system was inspected for corrosion damage. Most of the system was coated with a heavy, brown layer resembling Fe_2O_3. This layer dissolved only partially in nitric acid and left a fine, reddish precipitate which could be washed from the system. In three parts of the system, smooth, shiny, base metal was exposed. These parts were the 3/4-in. orifice plate, part of the pump casing, and the pump impeller, all of which were exposed to high, surface, shear stresses during operation. The pump impeller was found to have lost 16 g in weight compared with its weight when originally installed; however, in previous runs, it had gained about 5 g, presumably in building up a thin oxide scale. Thus the total weight loss during the

(5) F. R. Bruce *et al.*, *HRP Quar. Prog. Rep. Jan. 1, 1953*, ORNL-1478, p. 101.

phosphate run was 21 g, of which 5 g was probably represented by oxygen in base metal oxide. Since the atomic weights of iron, nickel, and chromium are roughly three and one half times that of oxygen, the major portion of the weight loss can be accounted for as loss of metal by conversion to oxide before the phosphate run began.

Further investigation of the phosphate system is planned to determine whether the base metal is attacked seriously in this medium. In addition, a run will be made with monobasic sodium phosphate.

Other Proposed Additions. Other additions, such as ferric nitrate, nickel nitrate, and possibly some aluminum compound, will be added to uranium slurries to determine the influence of these additives on the stabilization of a particular form of oxide and on the plating-out problem.

In an effort to study the transformation of the various crystal habits of $UO_3 \cdot H_2O$ (alpha and beta) and possibly to discover the mechanism for those transformations, beta $UO_3 \cdot H_2O$ (platelets) was statically autoclaved at 150, 200, and 250°C for as long as 168 hours. Microscopic examination of samples removed at various times showed particle growth but no transformation from the beta form to the alpha allomorph. J. O. Blomeke of the Chemical Technology Group, however, confirmed the dynamic test results when he micronized the beta oxide prior to autoclaving at 150, 175, 225, and 250°C for 24 hr and found that below 200°C the beta form converted to alpha and that no conversion occurred at temperatures above 200°C.

The mechanism and temperature dependence of this transformation are still unknown. Various additives, such as Fe^{+++}, Ni^{++}, PO_4^{---}, are being added to calcined UO_3 prior to hydration to $UO_3 \cdot H_2O$ in an effort to influence the production of one allomorph in preference to the other. Preliminary results indicate that Ni^{++} favors the production of alpha, whereas the beta form is enhanced by the presence of Fe^{+++}.

Loop T. Loop T for circulating uranium slurries at 250°C and 1000 psi will be identical to loop S, except that the pressurizer will not be an integral part of the loop but, rather, it will be isolated and connected to the circulating stream only by means of an S-shaped stainless steel tube to minimize formation of a vortex and the accumulation of solids. The loop is now being fabricated and assembled, and it should be ready for a shakedown test by May 1953.

In this system, the effect of system design on slurry stability will be studied at 250°C. Also, the present studies on the effect of additives on the chemical and physical stability of slurries will be continued.

Glass Loop. The glass loop has been modified to simulate the design of loop T, and it has been operated at above atmospheric pressures to aid in anticipating the effect of the isolated pressurizer on the operation of the rest of the loop. The loop has been intermittently operated for 50 hr with no accumulation of solids in the pressurizer and with no evidence of a vortex. On the basis of these results, no difficulty is expected with the isolated pressurizer for loop T.

CRITICAL EXPERIMENTS

The slurry critical experiments conducted in cooperation with the ORNL Criticality Group should be completed early in May. For these experiments, an aluminum tank with an agitator and a water reflector is fed from a continuously circulating loop that contains the enriched slurry. When enough slurry has been added to make the system almost critical, the feed flow is stopped and the agitator is slowed. For a 12-in. reactor and for a constant reflector height, the results, to date, indicate that for

all concentrations the reactivity increases rapidly to a maximum when the agitator is slowed from any speed above 200 rpm to 200 rpm. The sudden increase in reactivity at 200 rpm is probably due to the peculiar particle distribution at this speed and also to a finite reflector layer being formed on top of the charge as the solids begin to settle out. In very few cases was it necessary to scram the system because of the sudden increase of reactivity at 200 rpm. At all agitator speeds above 200 rpm, the system was unusually stable and predictable.

At the completion of the tests, the data will be compared with predictions based on calculations for the system by P. R. Kasten.[6]

[6] P. R. Kasten, *Prediction of Criticality Behavior of a Slurry Upon Settling*, ORNL CF-53-1-294 (Jan. 26, 1953).

CHEMICAL PROCESSING

F. R. Bruce, Section Chief
D. E. Ferguson W. E. Tomlin
R. G. Mansfield W. B. Howerton
O. K. Tallent

FUEL PROCESSING

Chemical processing of the inner core of a thermal breeder is required because it is necessary to remove fission products and corrosion products which adversely affect the neutron economy of the reactor. In addition, continuous extraction of the fission products to maintain the contained radioactivity at a relatively low level is desirable as a means of decreasing the possibility of a reactor catastrophe. The requirements for this type of fuel processing differ widely from those for the present, heterogeneous reactor fuel. For the aqueous homogeneous reactor, large decontamination factors for fission products are not necessary, because the fuel is returned to the reactor as a solution. Consideration must be given only to removing a large fraction of those fission and corrosion products which contribute to reactor poison. A major factor in all developmental work on fuel processing is that strong emphasis must be placed on economy if the reactor is to produce power at a cost comparable to present power costs.

Fission-Product Poisons. In discussing the fission-product poisons of a reactor, it is convenient to divide the fission products into three classes: the rare gases, the nongaseous fission products with very high cross sections (Sm^{149}, Sm^{151}, Gd^{157}, and Eu^{155}) and combined yield of 0.82% for U^{233} fission, and the remaining nongaseous fission products. It is expected that the rare gases will be removed from an aqueous solution fuel in the gas separator and that their contribution to reactor poison will be small. Therefore, in the chemical processing, only the nongaseous fission products and the corrosion products must be considered.

Figure 53 shows the effect of the chemical cycle on the fission-product poisons in the ISHR if there is continuous processing of the fuel solution. It can be seen that chemical processing cycles of more than ten days will not significantly lower the amount of poison from the very high cross-section fission products.

To obtain the data presented in Fig. 53, a cross section of 40 barns was used for the "other" fission

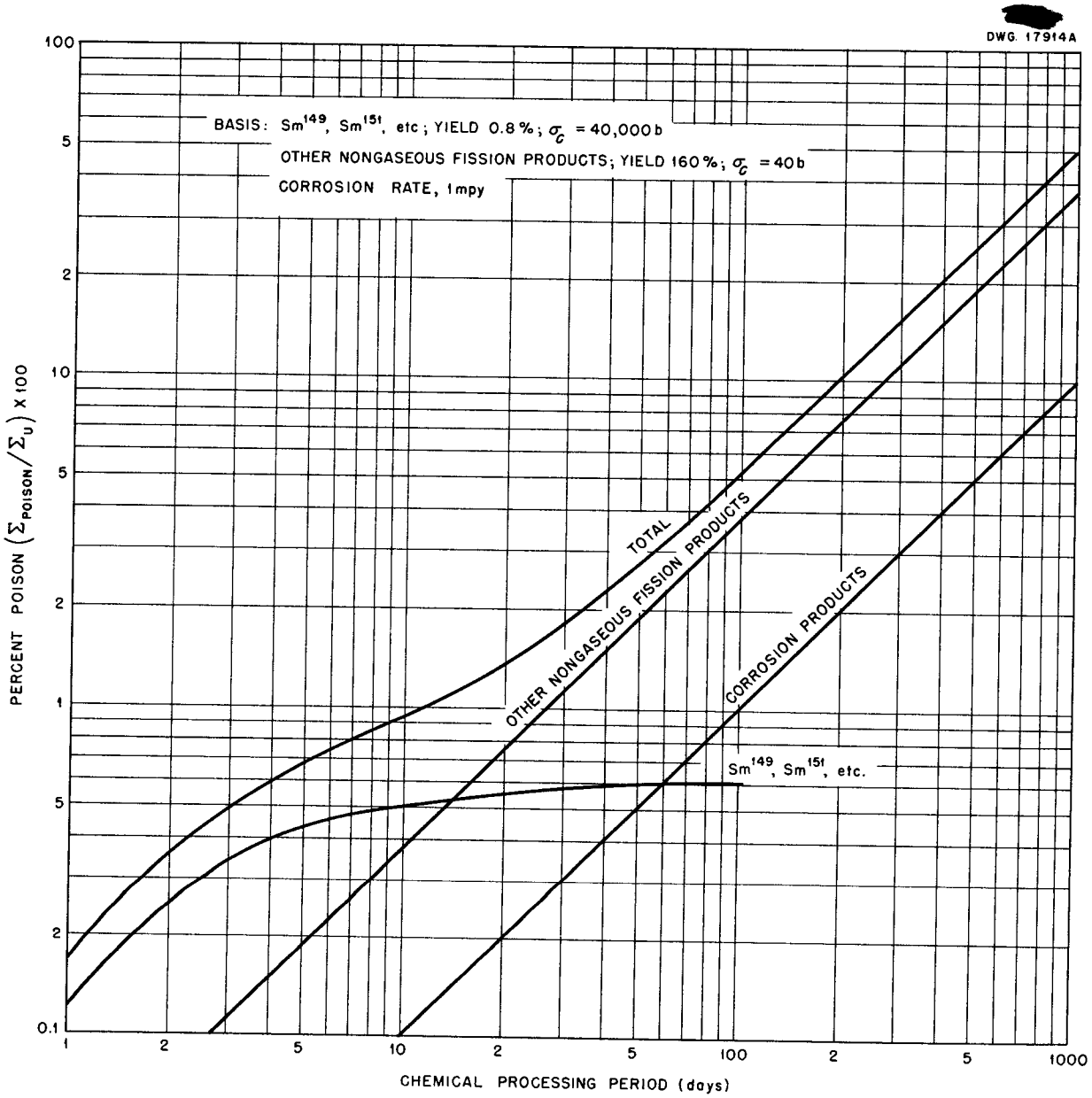

Fig. 53. Poisoning of ISHR When Operated as a Two-Core Thermal Breeder.

products of U^{233}. This value is probably pessimistic when the very high cross-section fission products are excluded.

Corrosion Product Poisons. Based on a generalized corrosion rate of 1 mpy, the poison from nickel and manganese in the fuel solution will build up at the rate of 3% per year (Fig. 53). The rate of dissolution of type 347 stainless steel from the ISHR will be 27 g per liter of fuel solution per year. Of this amount, about 2.7 g of Ni and 0.53 g of Mn per liter of solution will remain dissolved. Iron and chromium can be neglected because of their low solubilities and low cross sections.

Distribution of Fission-Product Poison. A summary of the contributions

to reactor poison of the various fission products, by chemical group, is presented in Table 38. These values are based on the ISHR and include all fission products for which the cross sections are known.[1]

It can be seen from Table 38 that the rare earths contribute about 80% of the nongaseous fission-product poison. For short irradiation periods, only the halogens, primarily I^{131}, contribute significant amounts of poison in addition to that from the rare earths; however, owing to the short half-life of I^{131}, its concentration does not continue to build up, and for irradiation periods of 100 days or longer, molybdenum, cesium, and the noble metals are the most significant of the poisons, except for the rare earths. From these observations, it is possible to list qualitatively the requirements for processing of the fuel solution of a thermal breeder.

The requirements, in the order of their importance, are:

1. to remove rare earths rapidly,
2. to remove cesium, molybdenum, and the noble metals,
3. to remove the corrosion products, nickel and manganese,
4. to remove the halogens.

[1] K. Way, L. Fano, M. R. Scott, and K. Thew, *Nuclear Data*, NBS Circular 499 and Suppl. 1, 2, and 3 (Sept. 1, 1950).

Methods of Processing. Two general types of processing have been considered for the fuel solution of a thermal breeder: complete decontamination of the fuel solution by solvent extraction and partial decontamination of the fuel solution by adsorption. As stated above, complete decontamination of the fuel is not essential. The removal of 75% of the rare earths and 25% of the cesium, molybdenum, noble metals, and corrosion products is sufficient decontamination if the fuel solution, after processing, is suitable for direct return to the reactor.

Complete decontamination of the fuel by solvent extraction would be essentially the same as the present U^{235} recovery process, with metal dissolution replaced by heavy-water recovery. The decontaminated uranyl nitrate product from the process would have to be converted to a heavy water solution of uranyl sulfate for return to the reactor. The cost of this process would be at least $5.00 per gram of uranium if the processing were done at the Idaho Chemical Processing Plant, provided it was operating at full capacity.

An adsorption process could be carried out by using an organic ion-exchange medium, an insoluble inorganic adsorbent, such as CaF_2 (suggested

TABLE 38. DISTRIBUTION OF FISSION-PRODUCT POISON IN ISHR FOR U^{233} FISSION PERIOD OF OPERATION AS INDICATED

CHEMICAL GROUP	PER CENT OF TOTAL FISSION-PRODUCT CROSS SECTION				
	20 Days	50 Days	100 Days	300 Days	900 Days
Rare earths	82	81	80	76	67
Halogens	11	10	7	4	3
Noble metals	2	3	4	6	8
Cesium	2	4	6	8	13
Molybdenum	1	1	3	5	7
Cadmium	2	1	1	< 1	< 1

by Vitro Corp.) or $BaSO_4$, or a combination of adsorbents. A cost of 20 cents per gram of uranium processed seems to be a pessimistic estimate for the simple adsorption process envisioned here.[2] However, the uranium adsorbed along with the fission products would have to be recovered at a cost of at least $5.00 per gram. This would increase the cost of an adsorption process to 45 cents per gram of uranium if 5% of the uranium is retained on the adsorbent and to 25 cents per gram if 1% of the uranium is adsorbed along with the fission products.

Optimum Processing Cycles. Since the main product of this thermal breeder is power, economy must be a prime objective in the design of the reactor system, if power is to be produced at a competitive cost. From the standpoint of chemical processing, this requires minimizing the cost of processing and the losses of fissionable material both in processing and by reactor poisons. The results of an analysis of these requirements, based on the processing of the ISHR fuel solution, are summarized in Table 39. A value of $100 per gram for U^{233} and the chemical processing cost given in the preceding section were used.

These results show that a process costing $5.00 per gram of uranium is impractical for a thermal breeder. Both the cost of processing and the losses from poisons are unreasonable with the optimum process cycle. The results also demonstrate that a processing cost of 45 cents per gram of uranium is reasonable. The cost of processing would then amount to 0.5 mil per kwh of power produced, and U^{233} production lost because of poison would be about 3%. If the U^{233} adsorbed along with the fission products is only 1% of the uranium processed, chemical processing costs would drop to 0.3 mil per kwh, but the optimum process cycle and the poison remain the same as for 5% uranium retention.

Adsorption of Fission Products on Calcium Fluoride. Many adsorbent materials have been tested for removal of fission products from the fuel solution of an aqueous, homogeneous, thermal breeder. Of the materials tested by Vitro Corp., calcium fluoride was recommended as the most suitable for this application.[3] Additional experiments at ORNL have shown that finely divided CaF_2 has a remarkable capacity for removing rare earths from dilute uranyl sulfate solutions; however, it was found that the mechanism of this removal is not adsorption. It appears to be metathesis of the calcium fluoride which yields insoluble rare earth fluorides and soluble calcium sulfate. Since the solubility of calcium sulfate in dilute

(2) D. E. Ferguson, *Fuel Processing of a Homogeneous Thermal Breeder*, ORNL CF-53-1-324 (Jan. 30, 1953).

(3) *January Progress Report for Homogeneous Reactor Processing*, KLX-1609 (Feb. 10, 1953).

TABLE 39. COMPARISON OF METHODS OF FUEL PROCESSING FOR THE ISHR

PROCESSING METHOD	COST OF PROCESSING ($/g of U)	OPTIMUM CHEMICAL PROCESSING CYCLE (days)	POISON FROM FISSION AND CORROSION PRODUCTS (%)	COST OF PROCESSING (mils per kwh)
Complete decontamination by solvent extraction	5	70	4	5
Adsorption (5% U holdup)	0.45	50	3	0.5
Adsorption (1% U holdup)	0.25	50	3	0.3

uranyl sulfate solution at elevated temperatures is not known, it is not yet possible to evaluate the feasibility of using this material for removing rare earths from the fuel solution of a thermal breeder. If uranyl fluoride solution were used as fuel for the reactor, this difficulty would be eliminated and the CaF_2 would serve as an inert filter medium.

Even though the absolute capacity of CaF_2 for removing rare earths from the reactor fuel solution is undoubtedly the stoichiometric amount of rare earths, the practical capacity under continuous contact conditions in a fixed bed was found to depend on temperature. At 25°C, 1.5 liters of CaF_2 per day would be required for removing rare earths from the ISHR; at 75°C only 0.75 liter of CaF_2 would be required.

The solubility of calcium fluoride in 0.02 *M* UO_2SO_4 solution was found to be 0.07 mg/ml at 250°C. At room temperature the solubility was 0.33 mg of CaF_2 per milliliter. This should not contribute a significant amount of calcium or fluoride to the fuel solution.

Other Inorganic Adsorbents. Several inorganic adsorbents other than calcium fluoride were found to be effective in removing fission products from dilute uranyl sulfate solution. In batch tests at room temperature, the following results were obtained by contacting the adsorbents with 0.02 *M* UO_2SO_4 solution containing mixed fission products:

ADSORBENT	PER CENT OF BETA ACTIVITY ADSORBED
CaF_2	77
De Calso	96
Zeo Dur	79
Manganese Zeolite	72
$BaSO_4$ (freshly precipitated)	88

These adsorbent materials will be investigated further if CaF_2 is found to contribute excessive calcium to the fuel solution.

THORIUM OXIDE PELLET STUDIES

Autoclave tests indicated that thorium oxide pellets which had been fired at 1700°C were stable for as long as 150 hr in water at 250°C and for as long as 120 hr in 0.02 *M* UO_2SO_4 solution at 250°C. No dissolved thorium could be detected in either the water or the uranyl sulfate solution at the end of the test period.

The batch of thorium oxide pellets selected for testing was prepared by the Norton Co. The pellets were about 1 cm in diameter, and they had an average specific gravity of 8.8 and a porosity of less than 0.1%. Two general types of pellets could be distinguished by visual observation: smooth-surfaced, white pellets and tan, rough-surfaced pellets. Spectrographic analysis showed no significant differences in the chemical compositions of the two types. The tan pellets were found to be subject to abrasion and chipping when agitated against one another in water.

Autoclave Tests of Thorium Oxide Pellets. The result of heating thorium oxide pellets in water or uranyl sulfate solution was determined by sealing white or tan pellets inside pyrex tubes with 10 ml of distilled water or 0.02 *M* UO_2SO_4 solution and heating the tubes in a rocking autoclave at 250°C for periods of time of up to 150 hours. Two types of tests were carried out: (1) the pellets were immobilized in the glass tube by a coil of platinum wire so that only the liquid was in motion, (2) both pellets and liquid were allowed to move freely back and forth within the tube. The results of these tests are summarized in Table 40. No significant loss in weight occurred during the tests in which the pellets were immobilized. The small weight loss observed in the other test was due to abrasion, since analysis of the liquid phase indicated essentially no dissolved thorium. The pellets heated

TABLE 40. STABILITY OF THORIUM OXIDE PELLETS IN WATER AND URANYL SULFATE SOLUTION

Autoclave tests at 250°C

PELLET	CONDITIONS OF TEST	DURATION OF TEST (hr)	CHANGE IN WEIGHT AS PER CENT OF ORIGINAL WEIGHT
Tan, rough-surfaced	Pellets stationary, water in motion	150	0.02% loss
	Pellets and water in motion	150	1.53% loss
White, smooth-surfaced	Pellets stationary, water in motion	150	0.06% gain
	Pellets and water in motion	150	0.08% loss
	Pellets and water in motion	150	0.00%
	5 g of U per liter UO_2SO_4 solution in motion, pellets stationary	120	0.23% gain
	5 g of U per liter UO_2SO_4 solution in motion, pellets stationary	120	0.29% gain
	5 g of U per liter UO_2SO_4 solution in motion, pellets stationary	72	0.06% gain
	5 g of U per liter UO_2SO_4 solution in motion, pellets stationary	72	0.02% gain

in uranyl sulfate solution actually gained weight as a result of deposition of UO_3 on their surfaces.

Two additional tests were made with immobilized pellets in water at 325°C for 56 hours. At the end of these tests the pellets showed less than 0.1% weight loss, and no thorium was found in the water phase.

DISSOLUTION OF THORIUM OXIDE PELLETS

The thorium oxide pellets were found to dissolve in 60% HNO_3 containing 0.1 *M* fluoride as a catalyst. The dissolution experiments were carried out on a 10-ml scale in glass equipment. It was found that by using a 100% excess of thorium oxide and 60% HNO_3, a dissolver solution containing only 0.6 *M* acid could be obtained in 12 hours. This solution would be a suitable feed for a solvent extraction process.

Since this dissolution study was made with unirradiated pellets, additional studies must be made with irradiated pellets before an acceptable dissolution process can be assured.